Fluid Mechanics for Masters Students

Olivier Cleynen

last edited July 2, 2016
http://fluidmech.ariadacapo.net

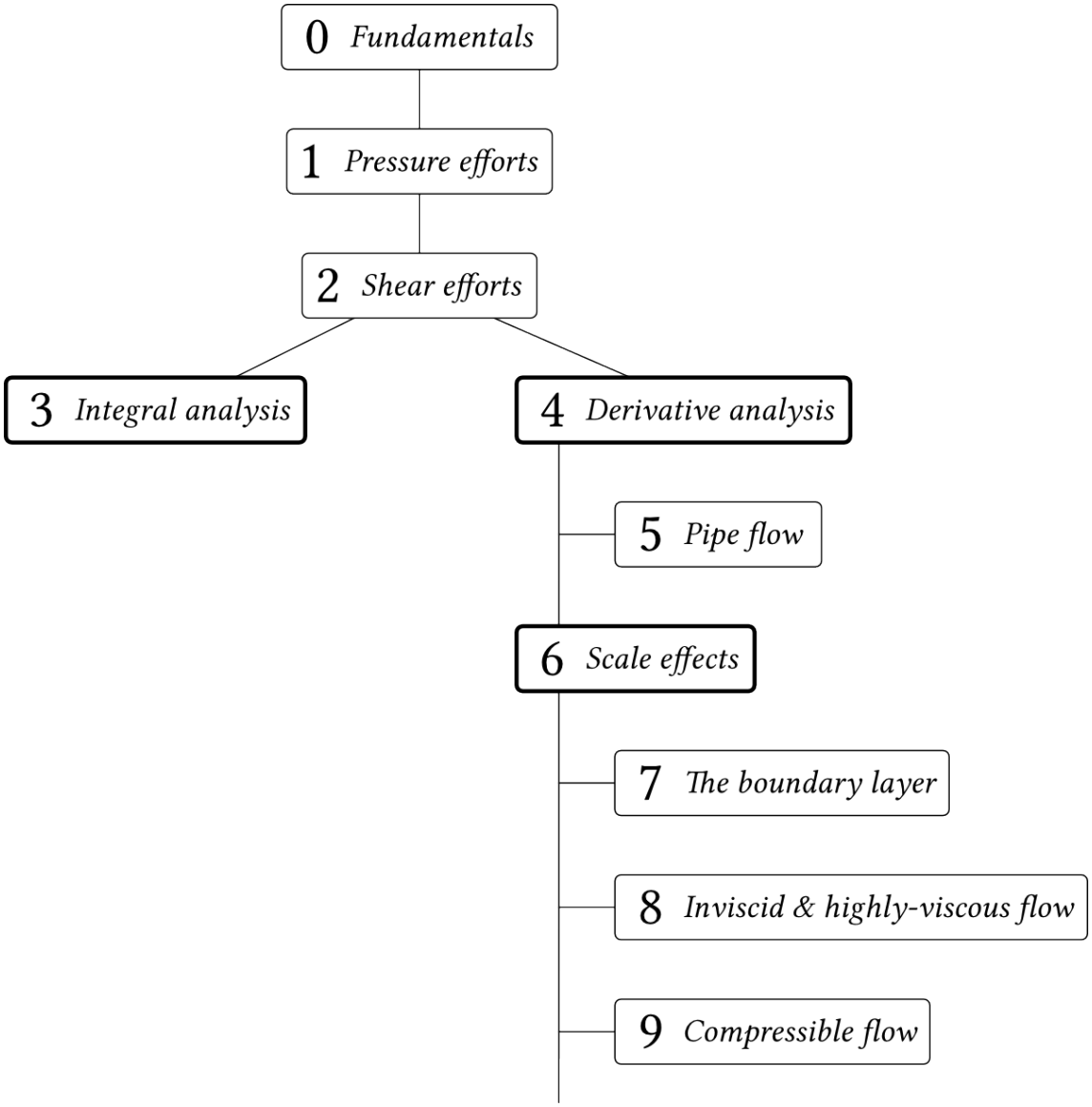
0 Fundamentals
1 Pressure efforts
2 Shear efforts
3 Integral analysis
4 Derivative analysis
5 Pipe flow
6 Scale effects
7 The boundary layer
8 Inviscid & highly-viscous flow
9 Compressible flow

Contents

Fluid Mechanics for Masters Students

42 h – 2016

Olivier Cleynen

Objectives

This course is built for students working towards a Masters in engineering, who have had little or no previous involvement with fluid dynamics. The objectives are simultaneously:

- to provide you with a solid understanding of what can (and can't) be achieved with engineering fluid dynamics, and a strong foundation for the later study of computational fluid dynamics;
- to enable you to solve selected engineering fluid dynamics problems with confidence — yet not over-confidence;
- to request the minimum feasible amount of your time and energy for the above.

Thus, the author attempts to put greater emphasis on the structure, relevance and limitations of the content than over its breadth and depth.

Format

Lectures 14×90 min, covering one chapter per session. Since the content of lectures follows the course script, and that PDF versions of the slides are provided, no note-taking is required.

Exercise sessions 14×90 min, in half-size classes, during which the lecturer(s) assist students with solving given problems.
There is not enough time during the exercise sessions to go through the whole exercise sheets in detail. Thus students are expected to work through them before and after the sessions.

One final exam of 120 min which is the only assessment for the course. The content of the exam consists exclusively of lightly-modified exercise sheet problems.

Key references

The course matches closely the content and level of three mainstream undergraduate textbooks: White [9], Çengel et al. [12], and Munson et al. [14].

[9] Frank M. White. *Fluid Mechanics.* 7th ed. McGraw-Hill, 2008. ISBN: 9780071311212

[12] Yunus A. Çengel and John M. Cimbala. *Fluid Mechanics. Fundamentals and Applications.* 2nd ed. McGraw-Hill, 2010. ISBN: 9780070700345

[14] Bruce R. Munson, Theodore H. Okiishi, Wade W. Huebsch, and Alric P. Rothmayer. *Fluid Mechanics.* 7th ed. Wiley, 2013. ISBN: 9781118318676

Author's notes

I intended these notes as the main support for a short, one-semester introductory (or revision) course. They should be sufficient to get through the course, but they are not meant to replace a good book! All of the topics included here are explored and explained with greater care in popular textbooks, in particular those cited above.

This document will be updated progressively during the summer semester 2016. Ultimately, it will be licensed under a free copyright license. All of the figure source files (which stem from many different authors, not all associated with this course) can already be accessed and re-used by clicking the links in the captions. The LaTeX sources can be downloaded from the git repository accessed from http://fluidmech.ninja/. All types of feedback, including reports of inaccuracies and errors, are welcomed at olivier.cleynen@ariadacapo.net.

I hope you get as much pleasure studying fluid dynamics as I do!

Olivier Cleynen
April 2016

Fluid Mechanics
Chapter 0 – Fundamentals

last edited April 5, 2016

These lecture notes are based on textbooks by White [9], Çengel & al.[12], and Munson & al.[14].

0.1 Concept of a fluid

We call *fluid* a type of matter which is continuously deformable, and which spontaneously tends to adapt its shape to its container by occupying all of the space made available to it.

0.2 Fluid mechanics

0.2.1 Solution of a flow

Fluid mechanics is the study of fluids subjected to given constraints. The most common type of problem in this discipline is the search for a complete description of the fluid flow around or through a solid object. This problem is solved when the entire set of velocities of fluid particles has been described, together with the shear and pressure efforts generated on the surface of the object. These speeds and efforts (either as sets of discrete values, or as mathematical functions) are functions of space, and they often vary with time.

Thus, the *flow solution* we are implicitly searching for in fluid mechanics is a description of speed, pressure, and shear.

0.2.2 Modeling of fluids

Like all matter, fluids are made of discrete, solid molecules. However, within the scope of fluid mechanics we work at the macroscopic scale, in which matter can be treated like a *continuum* within which all physical properties of interest can be continuously differentiable.

There are about $2 \cdot 10^{22}$ molecules in the air within an "empty" 1-liter bottle at ambient temperature and pressure. Even when the air within the bottle is completely still, these molecules are constantly colliding with each other and with the bottle walls; their average velocity is the speed of sound: approximately 1 000 km/h.

Despite the complexity of individual molecule movements, even the most turbulent flows can be accurately described and solved by considering the velocities of *groups* of several millions of molecules collectively, which we name *fluid particles*. By doing so, we never find out the velocity of individual molecules: instead, those are averaged in space and time and result in much simpler and smoother trajectories, which are those we can observe with macroscopic instruments such as video cameras and pressure probes.

Our selection of an appropriate fluid particle size (in effect defining the lower boundary of the *macroscopic scale*), is illustrated in fig. 0.1. We choose to reduce our volume of study to the smallest possible size before the effect of individual molecules becomes meaningful.

Adopting this point of view, which is named the *continuum abstraction*, is not a trivial decision, because the physical laws which determine the behavior of molecules are very different from those which determine the behavior of elements of fluid. For example, in fluid mechanics we never consider any inter-element attraction or repulsion forces; while new forces "appear" due to pressure or shear effects that do not exist at a molecular level.

A direct benefit of the continuum abstraction is that the mathematical complexity of our problems is greatly simplified. Finding the solution for the bottle of "still air" above, for example, requires only a single equation (section 1.3.3 p.27) instead of a system of $2 \cdot 10^{22}$ equations with $2 \cdot 10^{22}$ unknowns (all leading up to $\vec{V}_{\text{average},x,y,z,t} = \vec{0}$!).

Another consequence is that we cannot treat a fluid as if it were a mere set of marbles with no interaction which would hit objects as they move by. Instead we must think of a fluid –even a low-density fluid such as atmospheric air–

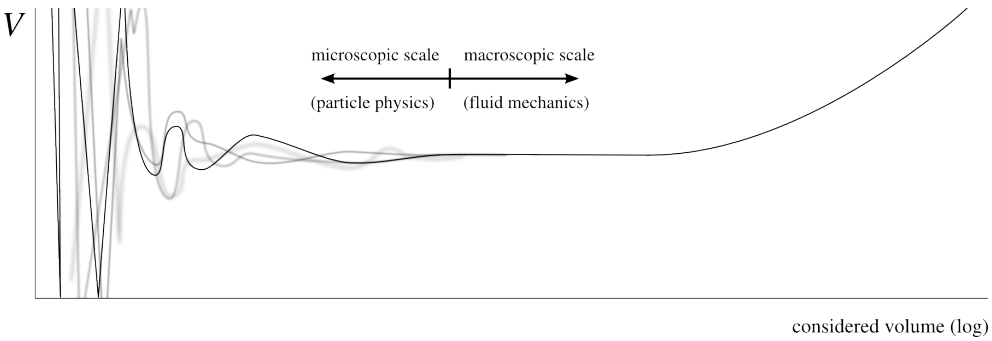

Figure 0.1 – Measurement of the average value of a property (here, velocity V; but it could be pressure, or temperature) inside a given volume. As the volume shrinks towards zero, the fluid can no longer be treated as a continuum; and property measurements will oscillate wildly.

Figure CC-BY-SA O.C.

as an infinitely-flexible medium able to fill in almost instantly all of the space made available to it.

0.2.3 The three pillars of fluid mechanics

Modern fluid mechanics is typically described as the combination of three sub-disciplines:

Analytical fluid mechanics which is the main focus of these lectures and which consists in predicting fluid flows mathematically. As we shall see, it is only able to provide (exact) solutions for very simple flows. Analytical fluid mechanics, however, allows us to gain insight —but not solutions!— about the mechanisms of complex fluid phenomena, describe scale effects, and predict forces associated with given fluid flows;

Numerical fluid mechanics also called *Computational Fluid Dynamics* or CFD, which consists in solving problems using very large amounts of discrete values. Initiated as a research topic in the 1970s, CFD is now omnipresent in the industry; it allows for excellent visualization and parametric studies of very complex flows. Nevertheless, computational solutions obtained within practical time frames are inherently approximate: they need to be challenged using analysis, and calibrated using experimental measurements;

Experimental fluid mechanics which consists in reproducing phenomena of interest within laboratory conditions and observing them using experimental techniques. A very mature branch (it first provided useful results at the end of the 19^{th} century), it is unfortunately associated with high human, equipment and financial costs. Experimental measurements are indispensable for the validation of computational simulations; meanwhile, the design of meaningful experiments necessitates a good understanding of scale effects.

Our study of analytical fluid mechanics should therefore be a useful tool to approach the other two sub-disciplines of fluid mechanics.

0.3 Properties of fluids

We hereby list a few important properties of fluids.

0.3.1 Velocity

We shall represent velocity (speed) within a fluid as a vector $\vec{V}$ which can be expressed with several equivalent notations:

$$\begin{aligned}\vec{V} &= \begin{pmatrix} u \\ v \\ w \end{pmatrix} \\ &= \begin{pmatrix} u_x \\ u_y \\ u_z \end{pmatrix} \\ &= (u_i) \equiv (u_1, u_2, u_3)\end{aligned}$$

We shall soon be describing $\vec{V}$ as a function of space (x, y, z) and time (t).

0.3.2 Phase

Fluids can be broadly classified into *phases*, which are loosely-defined sets of physical behaviors. Typically one distinguishes *liquids* which are fluids with large densities on which surface tension effects play an important role, from *gases* or *vapors* which have low densities and no surface tension effects. Phase changes are often brutal (but under specific conditions can be blurred or smeared-out); they usually involve large energy transfers. The presence of multiple phases in a flow is an added layer of complexity in the description of fluid phenomena.

0.3.3 Density

The density ρ is defined as the inverse of mass-specific volume v,

$$\rho \equiv \frac{1}{v} = \frac{m}{\mathcal{V}} \tag{0/1}$$

where v is the specific volume ($\mathrm{m^3\,kg^{-1}}$);
ρ the density ($\mathrm{kg\,m^{-3}}$);
m is the considered mass (kg);
and $\mathcal{V}$ is the considered volume ($\mathrm{m^3}$).

At ambient conditions air has a density of approximately $\rho_{\text{air}} = 1{,}2\,\mathrm{kg\,m^{-3}}$; that of water is almost a thousand times greater, at $\rho_{\text{water}} = 1\,000\,\mathrm{kg\,m^{-3}}$.

0.3.4 Temperature

Temperature is a scalar property measured in Kelvins (an absolute scale). It represents a body's potential for receiving or providing heat and is defined, in thermodynamics, based on the transformation of heat and work.

Under a specific set of conditions (most particularly at high temperature and low pressure), the absolute temperature T of gases can be modeled as a function of their pressure p with a single, approximately constant parameter $R \equiv pv/T$:

$$pv = RT \tag{0/2}$$

$$\frac{p}{\rho} = RT \tag{0/3}$$

where R depends on the state and nature of the gas ($\mathrm{J\,K^{-1}\,kg^{-1}}$);
and p is the pressure (Pa), defined later on.

This type of model (relating temperature to pressure and density) is called an *equation of state*. Where R remains constant, the fluid is said to behave as a *perfect gas*. Other models exist which predict the properties of gases over larger property ranges, at the cost of increased mathematical complexity.

Many fluids, especially liquids, do not follow this equation and their temperature must be determined in another way, most often with the help of laboratory measurements.

0.3.5 Speed of sound and compressibility

The average speed of molecules within a stationary fluid is called the *speed of sound* a. It is the speed at which pressure changes can travel across a fluid.

We define the *Mach number* [Ma] as the ratio of the local fluid speed V to the local speed of sound a:

$$[\mathrm{Ma}] \equiv \frac{V}{a} \tag{0/4}$$

Since both V and a can be functions of space in a given flow, [Ma] may not be uniform (e.g. the Mach number around an airliner in flight is different at the nose than above the wings). Nevertheless, a representative Mach number can typically be found for any given flow.

It is observed that when fluids flow without energy transfer at [Ma] $< 0{,}3$, their density ρ stays constant. Its variations can be safely neglected below [Ma] $= 0{,}6$. These flows are termed *incompressible*. Above these Mach numbers, it is observed that when subjected to pressure variations, fluids exert work upon themselves, which translates into density changes: these are called *compressibility effects*, and we shall study them in chapter 9.

In most flows, the density of *liquids* is almost invariant – so that water flows are generally entirely incompressible.

Within a perfect gas, we will show in chapter 9 (§9.3 p.184) that a depends only on the absolute temperature:

$$a = \sqrt{\gamma R T} \tag{0/5}$$

in all cases for a perfect gas,
where a is the local speed of sound ($\mathrm{m\,s^{-1}}$);
γ is a gas property, approx. constant (dimensionless);
and T is the local temperature (K).

0.3.6 Pressure

The concept of pressure can be approached with the following conceptual experiment: if a flat solid surface is placed in a fluid at zero relative velocity, the pressure p will be the ratio of the perpendicular force $F_\perp$ to the surface area A:

$$p \equiv \frac{F_\perp}{A} \tag{0/6}$$

where p is the pressure ($\mathrm{N\,m^{-2}}$ or pascals, $1\,\mathrm{Pa} \equiv 1\,\mathrm{N\,m^{-2}}$);
$F_\perp$ is the component of force perpendicular to the surface (N);
and A is the surface area ($\mathrm{m^2}$).

In general the pressure p exerting on an element of fluid can be thought of as the time- and space-average of the perpendicular component of impact force of its molecules on its neighbors. It is strictly a macroscopic property. We accept that in subsonic flows, it is a scalar property, meaning that for a given particle, it is the same in all directions. Pressure effects are explored in further detail in chapter 1.

It is worth noting that in practice pressure is measured in bars, where $1\,\mathrm{bar} \equiv 1 \cdot 10^5\,\mathrm{Pa}$. Ambient atmospheric pressure at normal altitude varies with the weather and is approximately 1 bar.

Pressure variations within fluids are related to their speed distribution according to relations that we will study later. We shall then be looking for a *pressure field* $p_{(x,y,z,t)}$, a function of space an time.

0.3.7 Shear

In the same thought experiment as above, shear τ expresses the efforts of a force *parallel* to a surface of interest:

$$\tau \equiv \frac{F_{\parallel}}{A} \tag{0/7}$$

where τ is the shear ($\mathrm{N\,m^{-2}}$ or Pa);
$F_{\parallel}$ is the component of force parallel to the surface (N);
and A is the surface area ($\mathrm{m^2}$).

Contrary to pressure, shear is not a scalar, i.e. it can (and often does) take different values in different directions: on the flat plate above, it would have two components and could be represented by a vector $\vec{\tau} = \left(\tau_x, \tau_y\right)$. We will explore shear in further detail in chapter 2.

0.3.8 Viscosity

We have accepted that a fluid element can deform continuously under pressure and shear efforts; however this deformation may not always be "for free", i.e. it may require force and energy inputs which are not reversible. Resistance to shear in a fluid is measured with a property named *viscosity*.

Formally, viscosity is defined as the ratio between the time rate of deformation of a fluid, and the shear effort applied to it. For example, if a fluid element is strained uniformly in the x-direction, the velocity u_x will be different everywhere inside the fluid element, and shear τ_{yx} will occur in the x-direction. The viscosity μ is then defined as:

$$\mu = \frac{\tau_{xy}}{\left(\frac{\partial u_x}{\partial y}\right)} \tag{0/8}$$

where μ is the viscosity ($\mathrm{N\,s\,m^{-2}}$ or Pa s);
τ_{xy} is the shear along the $x-z$ plane in the x-direction (Pa);
and u_x is the velocity in the x-direction ($\mathrm{m\,s^{-1}}$).

In less formal terms, viscosity is the "stickiness" of fluids, i.e. their resistance to being sheared: honey and sugar syrups are very viscous while water has low viscosity.

As a first approximation, the viscosity of most fluids may be considered as a constant and uniform property. We shall study the effects of shear and viscosity in chapter 2.

0.4 Basic flow quantities

A few fluid-flow related quantities can be quantified easily and are worth listing here.

Mass flow is noted $\dot{m}$ and represents the amount of mass flowing through a chosen surface per unit time. When the velocity across the surface is uniform, it can be quantified as:

$$\dot{m} = \rho V_{\perp} A \tag{0/9}$$

where $\dot{m}$ is the mass flow ($\mathrm{kg\,s^{-1}}$);

ρ is the fluid density ($\mathrm{kg\,s^{-1}}$);
A is the area of the considered surface ($\mathrm{m^2}$);
and $V_\perp$ is the component of velocity perpendicular to the area ($\mathrm{m\,s^{-1}}$).

Volume flow is noted $\dot{\mathcal{V}}$ and represents the volume of the fluid flowing through a chosen surface per unit time. Much like mass flow, when the velocity is uniform, it is quantified as:

$$\dot{\mathcal{V}} = V_\perp A = \frac{\dot{m}}{\rho} \tag{0/10}$$

where $\dot{\mathcal{V}}$ is the volume flow ($\mathrm{m^3\,s^{-1}}$).

Mechanical power is a time rate of energy transfer. When fluid flows through a fixed volume, the power $\dot{W}$ required to overcome pressure losses can be quantified as:

$$\dot{W} = \vec{F}_{\text{net, pressure}} \cdot \vec{V}_{\text{fluid, average}} = \dot{\mathcal{V}}\ |\Delta p|_{\text{loss}} \tag{0/11}$$

where $\dot{W}$ is the power spent as work (W);
and $|\Delta p|$ is the pressure loss occurring due to fluid flow (Pa).

Power as heat is also a time rate of energy transfer. When fluid flows uniformly and steadily through a fixed volume, its temperature T increases according to the net power as heat $\dot{Q}$:

$$\dot{Q} = \dot{m}\ c_{\text{fluid}} \Delta T \tag{0/12}$$

where $\dot{Q}$ is the power spent as heat (W);
ΔT is the temperature change occurring in the fluid (K);
and c_{fluid} is the specific heat capacity of the fluid ($\mathrm{J\,K^{-1}\,kg^{-1}}$).

The heat capacity of fluids varies strongly according to the amount of work that they are performing. When no work is performed in a steady flow, the heat capacity is termed c_p. In fluids such as liquid water and air, this capacity is almost independent from temperature, and takes very high values ($c_{p\text{air}} = 1\,005\,\mathrm{J\,K^{-1}\,kg^{-1}}$ and $c_{p\text{liquid water}} = 4\,100\,\mathrm{J\,K^{-1}\,kg^{-1}}$).

0.5 Conservation equations

The analytical and numerical resolution of problems in fluid mechanics is arched upon five important physical principles, which are sometimes called *conservation principles*.

1. Mass conservation:
   Without nuclear reactions, the total amount of matter at hand in a given phenomenon must remain constant. This statement can be expressed as:

$$\begin{aligned} m_{\text{system}} &= \text{cst} \\ \frac{\mathrm{d}m_{\text{system}}}{\mathrm{d}t} &= 0 \end{aligned} \tag{0/13}$$

2. Conservation of linear momentum:
   This is a form of Newton's second law, which states that the net force

$\vec{F}_{\text{net}} \equiv \Sigma\vec{F}$ applying to any given system of mass m is equal to the time change of its linear momentum:

$$\vec{F}_{\text{net}} = \frac{\mathrm{d}}{\mathrm{d}t}\left(m\vec{V}\right) \tag{0/14}$$

3. Conservation of angular momentum:
   This is a different form of Newton's second law, which compares the net moment $\vec{M}_{\text{net, X}} \equiv \Sigma\vec{M}_{\text{X}}$ applied on a system about a point X and the variation of its total angular momentum about this same point:

$$\vec{M}_{\text{net, X}} = \frac{\mathrm{d}}{\mathrm{d}t}\left(\vec{r} \wedge m\vec{V}\right) \tag{0/15}$$

4. Conservation of energy:
   This equation, also known as the "first principle of thermodynamics", states that the total amount of energy within an isolated system must remain constant:

$$\frac{\mathrm{d}E_{\text{isolated system}}}{\mathrm{d}t} = 0 \tag{0/16}$$

5. Second principle of thermodynamics:
   By contrast with all four other principles, this is not a conservation statement. Instead this principle states that the total amount of entropy S within a constant-energy system can only increase as time passes; in other words, the entropy change of any system must be greater than the heat transfer Q divided by the temperature T at which it occurs:

$$\mathrm{d}S_{system} \geqslant \frac{\mathrm{d}Q}{T} \tag{0/17}$$

These are the only five equations written in fluid mechanics. We usually apply these statements to our problem in either one of two ways:

- We may wish to calculate the *net* (overall) change in fluid properties over a zone of interest so as to relate them to the net effect (forces, moments, energy transfers) of the fluid flow through the zone's boundaries. This method is called **integral analysis** and we will develop it in chapter 3.
- We may instead wish to describe the flow through our zone of interest in an *extensive* manner, aiming to obtain vector fields for the velocity and pressure everywhere, at all times. This method is called **differential analysis** and we will develop it in chapter 4.

0.6 Classification of fluid flows

For reasons we shall explore progressively, it is extremely difficult to obtain general solutions for fluid flow. Whenever possible or reasonable, simplifying hypothesis are made about the behavior of one particular flow, that allow us to proceed with the analysis and obtain a reasonable, if inexact, solution. It is therefore a habit of fluid dynamicists to *classify* fluid flows in various categories, which are not necessarily incompatible. When approaching a given problem, we typically look out for the following characteristics:

Time dependence Flows which do not vary with time are said to be *steady*. Steadiness is dependent on the chosen point of view: for example, the air flow around an airliner in cruise flight is seen to be steady from within the aircraft, but is obviously highly unsteady from the point of view of the air particles directly in the path of the airliner. Steadiness is also dependent on the selection of a suitable time frame: time-variations in a flow may be negligible if the time window used in the study is short enough.
Mathematically, flows are steady when the total time derivative $\mathrm{D}/\mathrm{D}t$ (a concept we will study in chapter 4) of properties is zero: this considerably eases the search for solutions. It is important not to confuse steadiness (property fields constant in time) with *uniformity* (properties constant in space).

Temperature distribution In a fluid flow, temperature changes (which matter to us since they affect viscosity) can occur due to three phenomena:

- Heat transfer from solid bodies;
- Heat created through internal friction within the fluid;
- Changes in pressure and density due to work being performed on the fluid (by moving solid bodies, or by the fluid itself).

In practice, in most flows where velocities are moderate, temperature changes due to the last two phenomena are negligible because of the high specific heat capacity of fluids.
It is important not to confuse *isothermal* flows (in which the temperature is uniform) from *adiabatic* flows (in which the heat transfer is zero).

Influence of viscosity As we will explore in chapter 8, fluid flow kinematics are very strongly affected by the viscosity of the fluid. High viscous effects tend to attenuate non-uniformities and unsteadiness in fluid flow. We will learn to evaluate these effects in chapter 6 with a parameter named the *Reynolds number*.

Compressibility When the density of the fluid is uniform, the flow is said to be *incompressible*. The term is treacherous, because it refers to density, not pressure (incompressible flows almost always feature non-uniform pressure fields). Compressibility effects are important in flows where the Mach number exceeds 0,3, and in atmospheric dynamics when altitude changes are significant. They are always associated with temperature variations — and with increased mathematical complexity!

Turbulence One last characteristic that we systematically attempt to identify in fluid flows is *turbulence* (or its opposite, *laminarity*). While laminar flows are generally very smooth and steady, turbulent flows feature multiple, chaotic velocity field variations in time and space. We shall first approach the concept of turbulence in chapter 5, and study it more formally in chapter 6.

0.7 Limits of fluid mechanics

Fluid mechanics is a complex discipline.

It is easy to observe that flows as ordinary as sea waves crashing on a reef, water flowing down a river stream, or air blown into one's hands, display tremendous geometrical complexity. Even after choosing to describe only the movement of macroscopic fluid particles instead of individual molecules (and thereby avoiding studying thousands of billions of individual movements), we still need to describe a three-dimensional field of properties (pressure, temperature, etc.), one of which, velocity, is itself three-dimensional.

Thus, even before we begin describing the exact problem and a procedure to obtain its solution, we know that the mere description of a *solution* can have tremendous complexity.

Additionally, we have to admit that in practice much progress can be made in the field of fluid mechanics. For example, our weather forecasts have almost no value beyond one week, and aircraft manufacturers with budgets measured in billions of dollars still make extensive use of wind tunnel models – this despite our staggering continuous rate of progress in computing technology, and many decades of efforts dedicated to analytical fluid mechanics.

In our present study of fluid mechanics, therefore, we shall proceed modestly, and will always take care to show the limits of our analysis.

Fluid Mechanics
Exercise sheet 0 – Fundamentals

last edited April 10, 2016

Except otherwise indicated, we assume that fluids are Newtonian, and that:
$\rho_{\text{water}} = 1\,000\,\text{kg m}^{-3}$; $p_{\text{atm.}} = 1\,\text{bar}$; $\rho_{\text{atm.}} = 1{,}225\,\text{kg m}^{-3}$; $T_{\text{atm.}} = 11{,}3\,^{\circ}\text{C}$; $\mu_{\text{atm.}} = 1{,}5 \cdot 10^{-5}\,\text{N s m}^{-2}$;
$g = 9{,}81\,\text{m s}^{-2}$. Air is modeled as a perfect gas ($R_{\text{air}} = 287\,\text{J K}^{-1}\,\text{kg}^{-1}$; $\gamma_{\text{air}} = 1{,}4$; $c_{p\text{air}} = 1\,005\,\text{J kg}^{-1}\,\text{K}^{-1}$).

0.1 Compressibility effects

An aircraft is flying in air with density $0{,}9\,\text{kg m}^{-3}$ and temperature $-5\,^{\circ}\text{C}$. Above which flight speed would you expect the air flow over the wings to become compressible?

0.2 Pressure-induced force

A 2 m by 2 m flat panel is used as the wall of a swimming pool (fig. 0.2). On the left side, the pressure is uniform at 1 bar.

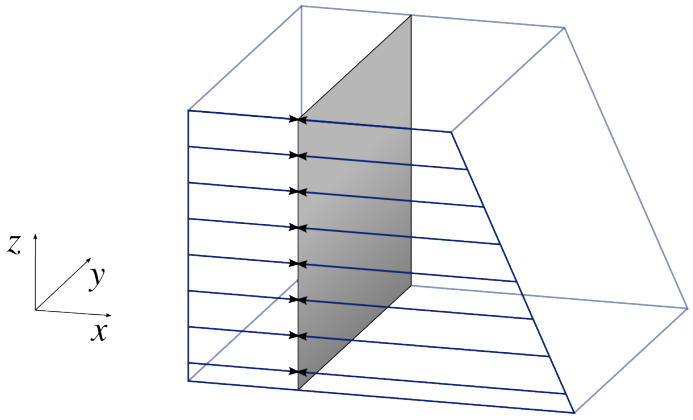

Figure 0.2 – Pressure distribution on a flat plate

Figure CC-0 o.c.

1. What is the pressure force exerted on the left side of the plate?

On the right side of the plate, the water exerts a pressure which is not uniform: it increases with depth. The relation, expressed in pascals, is:

$$p_{\text{water}} = 1{,}3 \cdot 10^{5} - 9{,}81 \cdot 10^{3} \times z \tag{0/18}$$

2. What is the pressure force exerted on the right side of the plate?
   [Hint: we will explore the required expression in chapter 1 as eq. 1/14 p.29]

0.3 Shear-induced force

Fluid flows over a 3 m by 3 m flat plate (fig. 0.3). Because of this flow, the plate is subjected to uniform shear $\tau_{zx} = 1\,650\,\text{Pa}$.

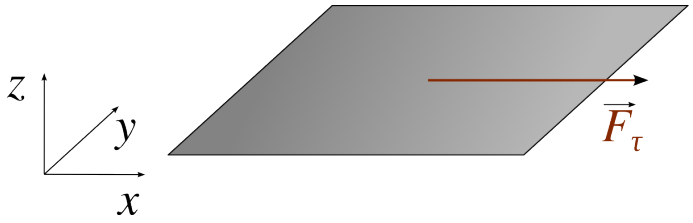

Figure 0.3 – Shear force exerting on a plate

Figure CC-0 o.c.

1. What is the shear force applying on the plate?
2. What would be the shear force if the shear was not uniform, but instead was a function of x expressed (in pascals) as $\tau_{zx} = 1\,650 - 10 \times x^2$?

0.4 Speed of sound

White [9] P1.87

Isaac Newton measured the speed of sound by timing the interval between observing smoke produced by a cannon blast and the perception of the detonation. The cannon is shot 8,4 km away from Newton. What is the air temperature if the measured interval is 24,2 s? What is the temperature if the interval is 25,1 s?

0.5 Power lost to drag

A truck moves with constant speed $\vec{V}$ on a road, with $V = 100\,\text{km}\,\text{h}^{-1}$. Because it experiences cross-wind, it is subjected to a drag $\vec{F}_D$ with $F_D = 5\,\text{kN}$ at an angle $\theta = 20°$, as shown in fig. 0.4.

1. What is the power required to overcome drag?

The drag force $\vec{F}_D$ is applying at a distance 0,8 m behind the center of gravity of the truck.

2. What are the magnitude and the direction of the moment exerted by the drag $\vec{F}_D$ about the center of gravity?

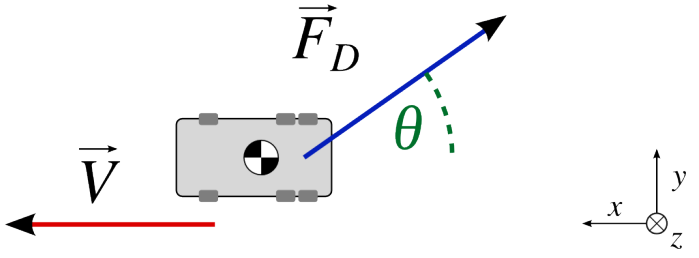

Figure 0.4 – Top view of a truck traveling at velocity $\vec{V}$ and subject to a drag force $\vec{F}_D$

Figure CC-0 o.c.

0.6 Go-faster exhaust pipe

The engine exhaust gases of a student's hot-rod car are flowing quasi-steadily in a cylindrical outlet pipe, whose outlet is slanted at an angle $\theta = 25°$ to improve the good looks of the car and provide the opportunity for an exercise.

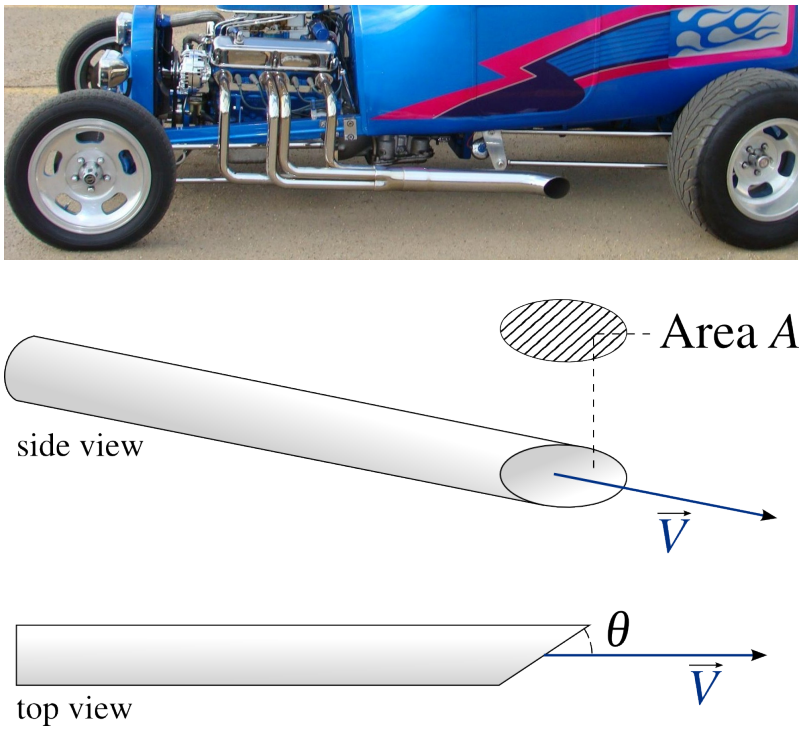

Figure 0.5 – Exhaust gas pipe of a car. The outlet cross-section is at an angle θ relative to the axis of the pipe.

Figure CC-0 o.c.
Photo cropped, mirrored and edited from an original CC-BY-SA *by kazandrew2*

The outlet velocity is measured at $15\,\mathrm{m\,s^{-1}}$, and the exhaust gas density is $1{,}1\,\mathrm{kg\,m^{-3}}$. The slanted outlet section area A is $420\,\mathrm{cm^2}$.

1. What is the mass flow $\dot{m}$ through the pipe?
2. What is the volume flow $\dot{\mathcal{V}}$ of exhaust gases?

Because of the shear within the exhaust gases, the flow through the pipe induces a pressure loss of $21\,\mathrm{Pa}$ (we will learn to quantify this in chapter 5). In these conditions, the specific heat capacity of the exhaust gases is $c_{p\mathrm{gases}} = 1\,100\,\mathrm{J\,kg^{-1}\,K^{-1}}$.

3. What is the power required to carry the exhaust gases through the pipe?
4. What is the gas temperature increase due to the shear in the flow?

0.7 Acceleration of a particle

Inside a complex, turbulent water flow, we are studying the trajectory of a cubic fluid particle of width $0{,}1\,\mathrm{mm}$. The particle is accelerating at a rate of $2{,}5\,\mathrm{m\,s^{-2}}$.

1. What is the net force applying to the particle?
2. In practice, which types of forces could cause it to accelerate?

0.8 Flow classifications

1. Can an inviscid flow also be steady?
2. Can a creeping flow also be inviscid?
3. *[more difficult]* Can a compressible flow also be isothermal?
4. Give an example of an isothermal flow, of an unsteady flow, of a compressible flow, and of an incompressible flow.

Answers

0.1 If you adopt [Ma] = 0,6 as an upper limit, you will obtain $V_{max} = 709\,\mathrm{km\,h^{-1}}$ (eqs. 0/4 & 0/5 p.11). Note that propellers, fan blades etc. will meet compressiblity effects far sooner.

0.2 1) $F_{left} = 400\,\mathrm{kN}$ (eq. 0/6 p.11); 2) $F_{right} = 480\,\mathrm{kN}$ (eq. 1/14 p.29).

0.3 1) $F_1 = 14{,}85\,\mathrm{kN}$ (eq. 0/7 p.12); 2) $F_2 = 14{,}58\,\mathrm{kN}$ (eq. 2/20 p.45). Note these two forces in this exercises are irrealistically high for an ordinary fluid flow.

0.4 26,7 °C & 5,6 °C.

0.5 1) $\dot{W} = \vec{F}_{drag} \cdot \vec{V}_{truck} = 130{,}5\,\mathrm{kW}$;
2) $M = ||\vec{r} \wedge \vec{F}_{drag}|| = 1\,368\,\mathrm{N\,m}$, $\vec{M} = \begin{pmatrix} 0 \\ 0 \\ -1\,368 \end{pmatrix}$ (points vertically upwards).

0.6 1) $\dot{m} = 0{,}2929\,\mathrm{kg\,s^{-1}}$ (eq. 0/9 p.12); 2) $\dot{\mathcal{V}} = 266{,}2\,\mathrm{L\,s^{-1}}$ (eq. 0/10 p.13);
3) $\dot{W} = 5{,}59\,\mathrm{W}$ (eq. 0/11 p.13); 4) $\Delta T = +0{,}0174\,\mathrm{K}$ (eq. 0.7 p.19), an illustration of remarks made in §0.6 p.15 regarding temperature distribution.

0.7 1) $F_{net} = 2{,}5 \cdot 10^{-9}\,\mathrm{N}$, such are the scales at hand in CFD calculations!
2) Only three kinds: forces due pressure, shear, and gravity.

0.8 1) yes, 2) no, 3) yes (in very specific cases such as high pressure changes combined with high heat transfer or high irreversibility, therefore generally no), 4) open the cap of a water bottle and turn it upside down: you have an isothermal, unsteady, incompressible flow. An example of compressible flow could be the expansion in a jet engine nozzle.

Fluid Mechanics
Chapter 1 – Pressure effects

last edited April 17, 2016

These lecture notes are based on textbooks by White [9], Çengel & al.[12], and Munson & al.[14].

1.1 Motivation

In fluid mechanics, only three kinds of force apply to fluid particles: forces due to pressure, shear, and gravity. This chapter focuses on the first type, and should allow us to answer two questions:

- How is the effect of pressure described and quantified?
- What are the pressure forces generated by static fluids?

1.2 Concept of pressure

We approached the concept of pressure in the introductory chapter with the notion that it represented force perpendicular to a given flat surface (eq. 0/6), for example a flat plate of area A:

$$p \equiv \frac{F_\perp}{A} \tag{1/1}$$

To appreciate the concept of pressure in fluid mechanics, we need to go beyond this equation.

1.2.1 The direction of pressure

An important concept is that in continuum mechanics, the flat surface is imaginary. More precisely, a fluid is able to exert pressure on not only on solid surfaces, but also upon and within itself. In this context, we need to

rework eq. 1/1 so that now pressure is defined as perpendicular force per area on an *infinitesimally small* plate:

$$p \equiv \lim_{A \to 0} \frac{F_\perp}{A} \tag{1/2}$$

Equation 1/2 may appear unsettling at first sight, because as A tends to zero, $F_\perp$ also tends to zero; nevertheless, in any continuous medium, the ratio of these two terms tends to a single non-zero value.

This brings us to the second particularity of pressure in fluids: the pressure on both sides of the infinitesimal flat plate are the same regardless of its orientation. In other words, *pressure has no direction*: there is only one (scalar) value for pressure at any one point in space.

Thus, in a fluid, there exists pressure not just on the solid surfaces of its container, but also everywhere within itself. We need to think of pressure as a *scalar property field* $p_{(x,y,z,t)}$.

1.2.2 Pressure on an infinitesimal volume

While pressure has no direction, it may not have the same value everywhere in a fluid, and so the *gradient* (the space rate of change) of pressure may not be null. For example, in a static water pool, pressure is uniform in the two horizontal directions, but it increases along with depth.

Instead of a flat plate, let us now consider an infinitesimally small *cube* within the fluid (fig. 1.1). Because the cube is placed in a scalar field, the pressure exerting on each of its six faces may be different. The net pressure effect will therefore have *three* components: one for each pair of opposing faces. Further down in this chapter, we will express this effect with the help of the gradient of pressure $\vec{\nabla} p$, a vector.

Thus, pressure itself is a (one-dimensional) scalar field, and the pressure effect on a submerged volume is a (three-dimensional) vector field.

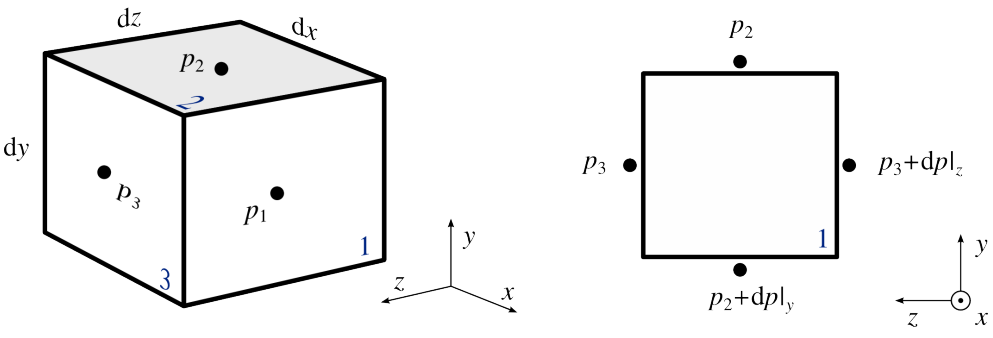

Figure 1.1 – The pressure on each face of an infinitesimal volume may have a different value. The *net* effect of pressure will depend on how the pressure varies in space. These changes are labeled $\mathrm{d}p|_i$ in each of the $i = x, y, z$ directions.

figure CC-0 o.c.

1.3.1 Fluid statics

Fluid statics is the study of fluids at rest, i.e. whose velocity field $\vec{V}$ is everywhere null and constant:

$$\begin{cases} \vec{V} &= \vec{0} \\ \frac{\partial \vec{V}}{\partial t} &= \vec{0} \end{cases} \tag{1/3}$$

We choose to study this type of problem now, because it makes for a conceptually and mathematically simple case with which we can start analyzing fluid flow and calculate fluid-induced forces.

1.3.2 Shear in static fluids

We will see in chapter 2 that shear efforts can be expressed as a function of viscosity and velocity: $\vec{\tau} = \mu \frac{\partial u_i}{\partial x_j} \vec{i}$ (2/16). We will also see that for most ordinary fluids (termed *Newtonian fluids*) the viscosity μ is independent from the speed distribution.

For now, it is enough to accept that in a static fluid (one in which $\frac{\partial u_i}{\partial x_j} = 0$ since $u_{(x,y,z,t)} = 0$), there cannot be any shear $\vec{\tau}$. **Static fluids are unable to generate shear effort**.

This is a critical difference between solids and fluids. For example:

- A static horizontal beam extruding from a wall carries its own weight because it is able to support internal shear; but this is impossible for a static fluid.
- A solid brick resting on the ground exerts pressure on its bottom face, but because of internal shear, the pressure on its sides is zero. On the contrary, a static body of water of the same size and weight cannot exert internal shear. Because pressure has no direction, the body exerts pressure not only on the bottom face, but also laterally on the sides of its container.

1.3.3 Pressure and depth

We now wish to express pressure within a fluid as a function of depth. Let us consider, inside a static fluid reservoir, a small element of fluid. We choose an element with finite horizontal surface S but infinitesimal height $\mathrm{d}z$, as shown in fig. 1.2.

The element's geometry is such that all of the lateral forces (which are due to pressure only) compensate each other. In the vertical direction, we are left with three forces, which cancel out because the element is not accelerating:

$$\vec{F}_{p\ \text{bottom}} + \vec{F}_{p\ \text{top}} + m\vec{g} = \vec{0}$$
$$p_{\text{bottom}} S - p_{\text{top}} S - mg = 0$$

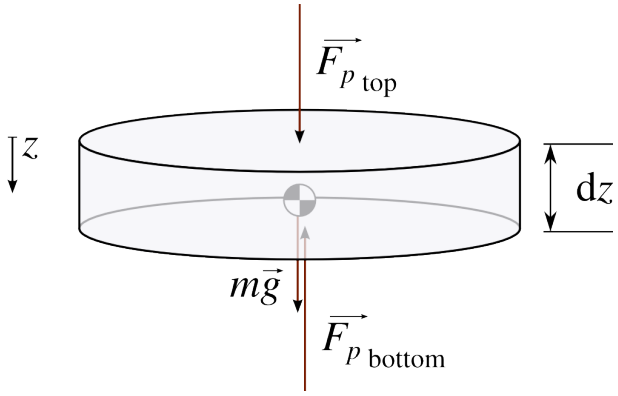

Figure 1.2 – A fluid element of (finite) horizontal surface S and infinitesimal height $\mathrm{d}z$ within a static fluid.

figure CC-0 o.c.

If we now rewrite the bottom pressure as $p_{\text{bottom}} = p_{\text{top}} + \mathrm{d}p$, we obtain:

$$\begin{aligned}(p_{\text{top}} + \mathrm{d}p)S - p_{\text{top}}S - mg &= 0\\ \mathrm{d}p &= \frac{m}{S}g \end{aligned} \tag{1/4}$$

This equation 1/4 expresses the fact that the infinitesimal variation of pressure $\mathrm{d}p$ between the top and bottom surfaces of the element is due only to its own weight. If we evaluate this variation along the infinitesimal height $\mathrm{d}z$, we obtain:

$$\frac{\mathrm{d}p}{\mathrm{d}z} = \frac{m}{S\,\mathrm{d}z}g = \frac{m}{\mathrm{d}\mathcal{V}}g$$

$$\frac{\mathrm{d}p}{\mathrm{d}z} = \rho g \tag{1/5}$$

Thus, equation 1/5, which is obtained from Newton's second law applied to a static fluid, links the *vertical variation in pressure* to the fluid's density ρ and the local gravitational acceleration g. This equation is so useful that it is sometimes called "the fundamental equation of fluid statics".

If our coordinate system is not aligned with the vertical direction (and thus with gravity), we will have to adapt equation 1/5 and obtain a more general relationship:

$$\begin{cases} \frac{\partial p}{\partial x} &= \rho g_x \\ \frac{\partial p}{\partial y} &= \rho g_y \\ \frac{\partial p}{\partial z} &= \rho g_z \end{cases} \tag{1/6}$$

$$\frac{\partial p}{\partial x}\vec{i} + \frac{\partial p}{\partial y}\vec{j} + \frac{\partial p}{\partial z}\vec{k} = \rho\vec{g} \tag{1/7}$$

We can simplify the writing of this last equation by using the mathematical operator *gradient*, defined as so:

$$\vec{\nabla} \equiv \vec{i}\frac{\partial}{\partial x} + \vec{j}\frac{\partial}{\partial y} + \vec{k}\frac{\partial}{\partial z} \tag{1/8}$$

And thus, equation 1/7 is more elegantly re-written as:

$$\vec{\nabla} p = \rho \vec{g} \tag{1/9}$$

This equation is read "the gradient of pressure is equal to the density times the gravitational acceleration vector". It expresses concisely a very important idea: **in a static fluid, the spatial variation of pressure is due solely to the fluid's own weight**.

In chapter 4, we shall see that eq. 1/9 is a special case in a much more potent and complex relation called the *Navier-Stokes equation* (eq. 4/37 p.84). For now, it suffice for us to work with just pressure and gravity.

1.3.4 Pressure distribution

An immediate consequence stemming from equation 1/9 is that in a static fluid (in a glass of water, in a swimming pool, in a calm atmosphere), pressure depends solely on height. Within a static fluid, at a certain altitude, we will measure the same pressure regardless of the surroundings (fig. 1.3).

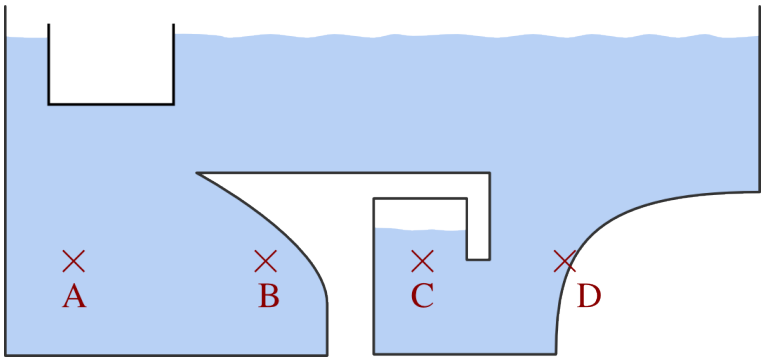

Figure 1.3 – Pressure at a given depth (or height) in a static fluid does not depend on the environment. Here, as long as the fluid remains static, $p_A = p_B = p_C = p_D$.

Figure CC-0 o.c.

1.3.5 Hydrostatic pressure

How is pressure distributed within static liquid water bodies? The density of liquid water is approximately constant: $\rho_{water} = 1\,000\,\mathrm{kg\,m^{-3}}$. In a water reservoir, if we align the z-direction vertically downwards, equation 1/9 becomes:

$$\begin{aligned} \vec{\nabla} p &= \rho \vec{g} \\ \frac{\mathrm{d}p}{\mathrm{d}z} &= \rho g \\ \left(\frac{\mathrm{d}p}{\mathrm{d}z}\right)_{water} &= \rho_{water}\, g \\ \left(\frac{\mathrm{d}p}{\mathrm{d}z}\right)_{water} &= 1\,000 \times 9{,}81 = 9{,}81 \cdot 10^3\,\mathrm{Pa\,m^{-1}} = 9{,}81 \cdot 10^{-2}\,\mathrm{bar\,m^{-1}} \end{aligned} \tag{1/10}$$

Therefore, in static water, pressure increases by approximately 0,1 bar/m as depth increases. For example, at a depth of 3 m, the pressure will be approximately 1,3 bar (which is the atmospheric pressure plus $\Delta z \times \frac{\mathrm{d}p}{\mathrm{d}z}$).

1.3.6 Atmospheric pressure

The density ρ_{air} of atmospheric air is not uniform, since —unlike for water— it depends strongly on temperature and pressure. If we model atmospheric air as a perfect gas, once again orienting z vertically downwards, we can express the pressure gradient as:

$$\left(\frac{\mathrm{d}p}{\mathrm{d}z}\right)_{\text{atm.}} = \rho_{\text{air}}\, g = p \frac{1}{T} \frac{g}{R} \tag{1/11}$$

This time, the space variation of pressure depends on pressure itself (and it is proportional to it). A quick numerical investigation for ambient temperature and pressure (1 bar, 15 °C) yields:

$$\begin{aligned}\left(\frac{\mathrm{d}p}{\mathrm{d}z}\right)_{\text{atm. ambient}} &= 1 \cdot 10^5 \times \frac{1}{288{,}15} \times \frac{9{,}81}{287} \\ &= 11{,}86\ \mathrm{Pa\,m^{-1}} = 1{,}186 \cdot 10^{-4}\ \mathrm{bar\,m^{-1}}\end{aligned}$$

This rate (approximately 0,1 mbar/m) is almost a thousand times smaller than that of water (fig. 1.4).

Since the rate of pressure change depends on pressure, it also varies with altitude, and the calculation of pressure differences in the atmosphere is a little more complicated than for water.

If we focus on a moderate height change, it may be reasonable to consider that temperature T, the gravitational acceleration g and the parameter R (gas constant) are uniform. In this admittedly restrictive case, equation 1/11 can

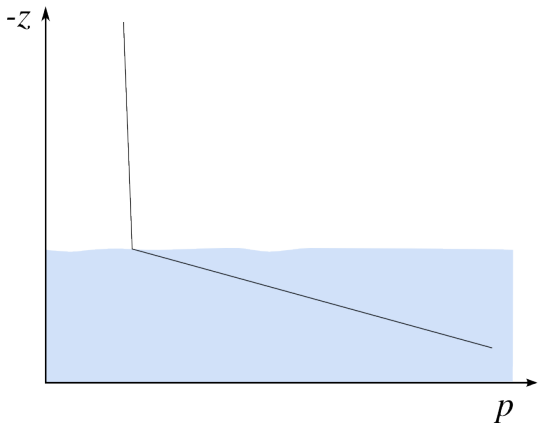

Figure 1.4 – Variation of pressure as a function of altitude for water and air at the surface of a water reservoir. The gradient of pressure with respect to altitude is almost a thousand times larger in water than in air.

Figure CC-0 o.c.

be integrated as so:

$$\begin{aligned}
\frac{\mathrm{d}p}{\mathrm{d}z} &= \frac{g}{RT_{\text{cst.}}}p \\
\int_1^2 \frac{1}{p}\,\mathrm{d}p &= \frac{g}{RT_{\text{cst.}}}\int_1^2 \mathrm{d}z \\
\ln\frac{p_2}{p_1} &= \frac{g}{RT_{\text{cst.}}}\Delta z \\
\frac{p_2}{p_1} &= \exp\left[\frac{g\Delta z}{RT_{\text{cst.}}}\right]
\end{aligned} \tag{1/12}$$

Of course, air temperature varies significantly within the atmosphere (at moderate altitudes the change with altitude is approximately $-6\,\mathrm{K\,km^{-1}}$). Adapting equation 1/12 for a uniform temperature gradient (instead of uniform temperature) is the subject of exercise 1.7 p.35.

In practice, the atmosphere also sees large lateral pressure gradients (which are strongly related to the wind) and its internal fluid mechanics are complex and fascinating. Equation 1/12 is a useful and convenient model, but refinements must be made if precise results are to be obtained.

1.4 Wall pressure forces and buoyancy

1.4.1 Pressure forces on plane surfaces

When the pressure p exerted on a flat surface of area S is uniform, the resulting force F is easily easily calculated ($F = p_{\text{cst.}}S$). In the more general case of a three-dimensional object immersed in a fluid with non-uniform pressure, the force must be expressed as a vector and obtained by integration:

$$\vec{F}_{\text{pressure}} = \int_S \mathrm{d}\vec{F} = \int_S p\,\vec{n}\,\mathrm{d}S \tag{1/13}$$

where the S-integral denotes an integration over the entire surface;
and $\vec{n}$ is a unit vector describing, on each infinitesimal surface element $\mathrm{d}S$, the direction normal to the surface.

Equation 1/13 is easily implemented in software algorithms to obtain numerically, for example, the pressure force resulting from fluid flow around a body such as an aircraft wing. In our academic study of fluid mechanics, however, we will restrict ourselves to the simpler cases where the surface is perfectly flat (and thus $\vec{n}$ is everywhere the same). Equation 1/13 then becomes:

$$F_{\text{pressure}} = \int_S \mathrm{d}F = \int_S p\,\mathrm{d}S \tag{1/14}$$

for a flat surface.

What is required to calculate the scalar F in eq. 1/14 is an expression of p as a function of S. In a static fluid, this expression will be given by eq. 1/9. Typically in two dimensions x and y we re-write $\mathrm{d}S$ as $\mathrm{d}S = \mathrm{d}x\,\mathrm{d}y$ and we may then proceed with the calculation starting from

$$F_{\text{pressure}} = \iint p_{(x,y)}\,\mathrm{d}x\,\mathrm{d}y \tag{1/15}$$

Such a calculation gives us the *magnitude* of the pressure force, but not its position. This position can be evaluated by calculating the magnitude of moment generated by the pressure forces about any chosen point X. This moment $\vec{M}_X$, using notation shown in fig. 1.5, is expressed as:

$$\vec{M}_X = \int_S d\vec{M}_X = \int_S \vec{r}_{XF} \wedge d\vec{F} = \int_S \vec{r}_{XF} \wedge p\, \vec{n}\, dS \qquad (1/16)$$

where $\vec{r}_{XF}$ is a vector expressing the position of each infinitesimal surface relative to point X.

Much like eq. 1/13 above, this eq. 1/16 is easily implemented in software algorithms but not very approachable on paper. In the simple case where we study only a flat surface, and where the reference point X is in the same plane as the surface, eq. 1/16 simplifies greatly and we can calculate the magnitude M_X as:

$$M_X = \int_S dM_X = \int_S r_{XF}\, dF = \int_S r_{XF}\, p\ dS \qquad (1/17)$$

for a flat surface, with X in the plane of the surface.

Once both F_{pressure} and $M_{X\ \text{pressure}}$ have been quantified, the distance R_{XF} between point X and the application point of the net pressure force is easily computed:

$$R_{XF} = \frac{M_{X\ \text{pressure}}}{F_{\text{pressure}}} \qquad (1/18)$$

While we restrict ourselves to simple cases where surfaces are flat, the process above outlines the method used by computational fluid dynamics software packages to determine the position of forces resulting from fluid pressure on any arbitrary solid object.

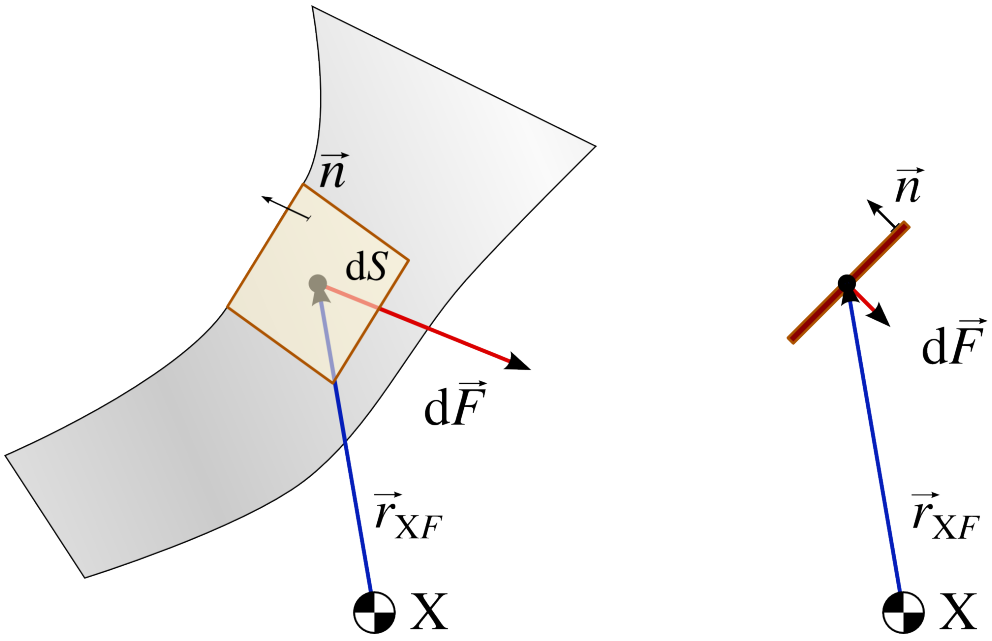

Figure 1.5 – Moment generated about an arbitrary point X by the pressure exerted on an arbitrary surface (left: perspective view; right: side view). The vector $\vec{n}$ is a convention unit vector everywhere perpendicular to the infinitesimal surface dS considered.

Figure CC-0 o.c.

1.4.2 Buoyancy and Archimedes' principle

Any solid body immersed within a fluid is subjected to pressure on its walls. When the pressure is not uniform (for example because the fluid is subjected to gravity, although this may not be the only cause), then the net force due to fluid pressure on the body walls will be non-zero.

When the fluid is purely static, this net pressure force is called *buoyancy*. Since in this case, the only cause for the pressure gradient is gravity, the net pressure force is oriented upwards. The buoyancy force is completely independent from (and may or may not compensate) the object's weight.

Since it comes from equation 1/9 that the variation of pressure within a fluid is caused solely by the fluid's weight, we can see that the force exerted on an immersed body is equal to the weight of the fluid it replaces (that is to say, the weight of the fluid that would occupy its own volume were it not there). This relationship is sometimes named *Archimedes' principle*. The force which results from the static pressure gradient applies to all immersed bodies: a submarine in an ocean, an object in a pressurized container, and of course, the reader of this document as presently immersed in the earth's atmosphere.

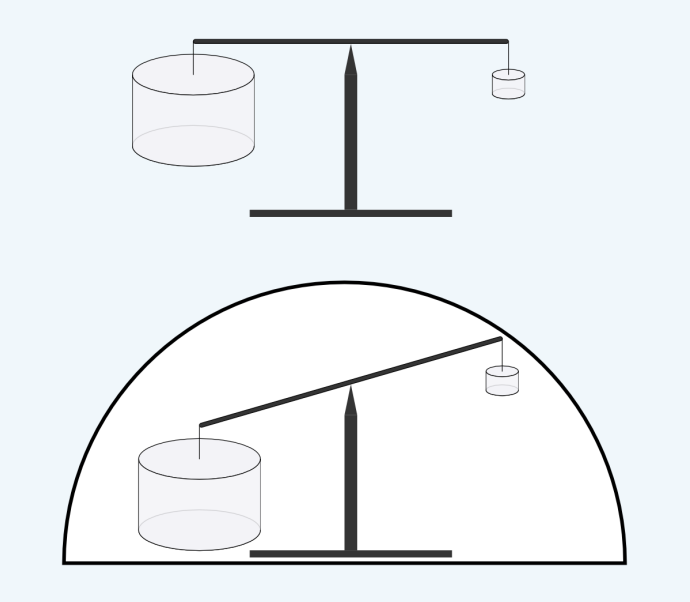

Figure 1.6 – Immersion in a static fluid results in forces that depend on the body's volume. They can evidenced by the removal of the fluid (for example in a depressurized semi-spherical vessel).

Figure CC-0 o.c.

Fluid Mechanics
Exercise sheet 1 – Statics

last edited July 2, 2016

These lecture notes are based on textbooks by White [9], Çengel & al.[12], and Munson & al.[14].

Except otherwise indicated, we assume that fluids are Newtonian, and that:
$\rho_{water} = 1\,000\,\mathrm{kg\,m^{-3}}$; $p_{atm.} = 1\,\mathrm{bar}$; $\rho_{atm.} = 1{,}225\,\mathrm{kg\,m^{-3}}$; $T_{atm.} = 11{,}3\,^{\circ}\mathrm{C}$; $\mu_{atm.} = 1{,}5 \cdot 10^{-5}\,\mathrm{N\,s\,m^{-2}}$;
$g = 9{,}81\,\mathrm{m\,s^{-2}}$. Air is modeled as a perfect gas ($R_{air} = 287\,\mathrm{J\,K^{-1}\,kg^{-1}}$; $\gamma_{air} = 1{,}4$; $c_{pair} = 1\,005\,\mathrm{J\,kg^{-1}\,K^{-1}}$).

1.1 Pressure in a fluid

A small water container whose geometry is described in fig. 1.7 is filled with water. What is the pressure at the bottom of the container?

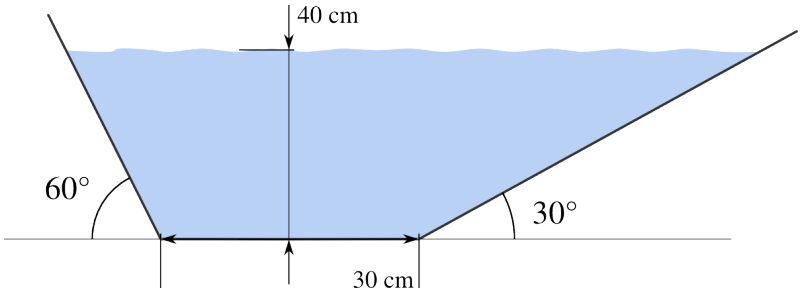

Figure 1.7 – A small water container.

Figure CC-0 o.c.

1.2 Pressure measurement

A tube is connected to a pressurized vessel as shown in fig. 1.8. The U-tube is filled with water. What is the pressure $p_{int.}$ in the vessel?

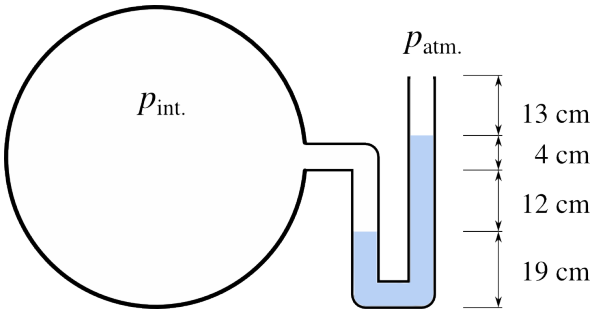

Figure 1.8 – Working principle of a simple liquid tube manometer. The outlet is at atmospheric pressure $p_{atm.}$.

Figure CC-0 o.c.

What would be the height difference shown if mercury ($\rho_{mercury} = 13\,600\,\mathrm{kg\,m^{-3}}$) was used instead of water?

1.3 Water lock

Exam ws*2015/16*

A system of lock doors is set up to allow boats to travel up the side of a hill (figure 1.9).

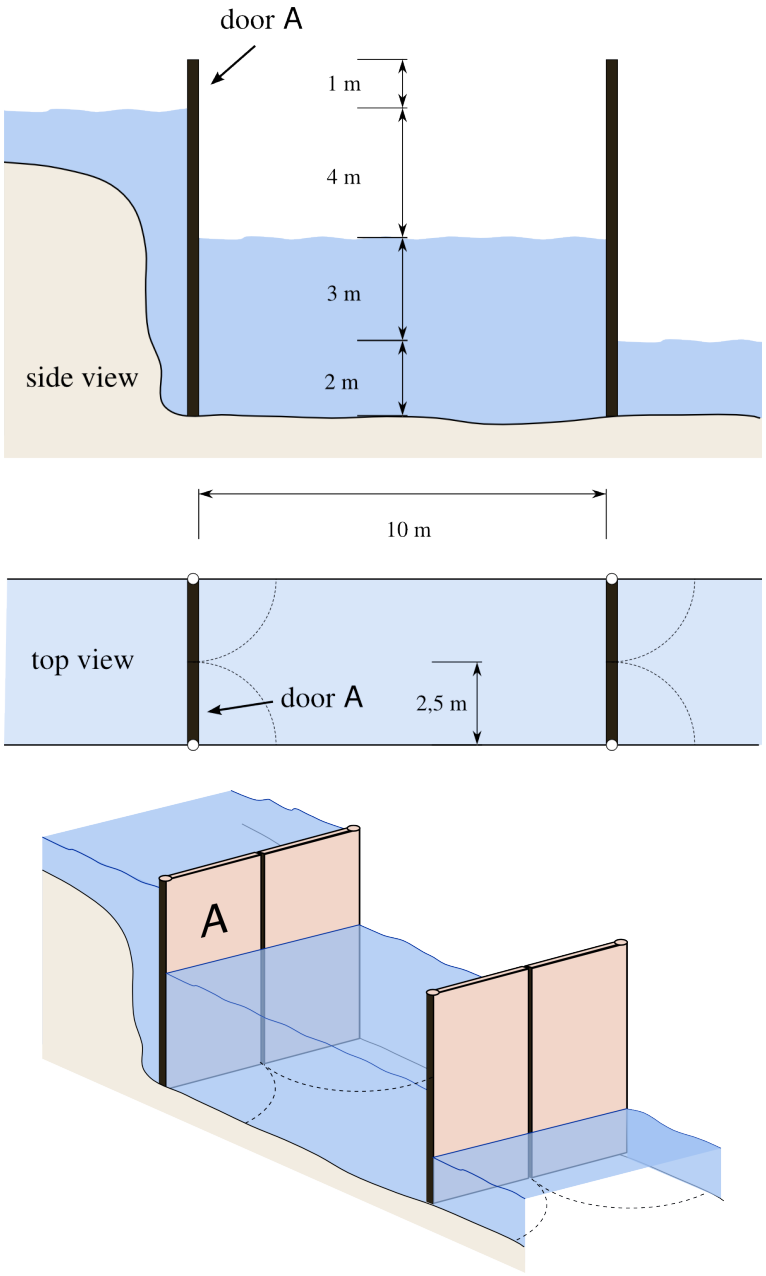

Figure 1.9 – Outline schematic of a water canal lock.

Figure CC-0 o.c.

We are studying the force and moment exerted by the water on the lock door labeled **A**. At this instant, the water levels are as shown in figure 1.9: 2 m in the lower canal, 5 m in the lock, and 9 m in the upper canal. The door is 2,5 metres wide.

1. Sketch the distribution of the pressure exerted by the water and the atmosphere on both sides of door A.
2. What is the net force exerted by the water on door A?

3. What is the net moment exerted by the water about the hinge of door A?
4. If the water level was lowered by 1 m everywhere, would the moment about the hinge be reduced? (briefly justify your answer)

1.4 Buoyancy force on a tin can

A student contemplates a tin can of height 10 cm and diameter 7 cm.

1. If one considers that the atmospheric density is uniform, what is the buoyancy force generated by the atmosphere on the can when it is positioned vertically?
2. What is the force generated when the can is immersed in water at a depth of 20 cm? At a depth of 10 m?
3. What is the buoyancy force generated when the can is immersed in the water in a horizontal position?

Instead of uniform density, we now wish to calculate the atmospheric buoyancy under the hypothesis of uniform temperature (room temperature 20 °C).

4. Starting from equation 1/9: $\vec{\nabla}p = \rho\vec{g}$, show that when the temperature $T_{\text{cst.}}$ is assumed to be uniform, the atmospheric pressure p at two points 1 and 2 separated by a height difference Δz is such that:

$$\frac{p_2}{p_1} = \exp\left[\frac{g\Delta z}{RT_{\text{cst.}}}\right] \tag{1/12}$$

5. What is the buoyancy generated by the room atmosphere?

1.5 Buoyancy of a barge

A barge of very simple geometry is moored in a water reservoir (fig. 1.10).

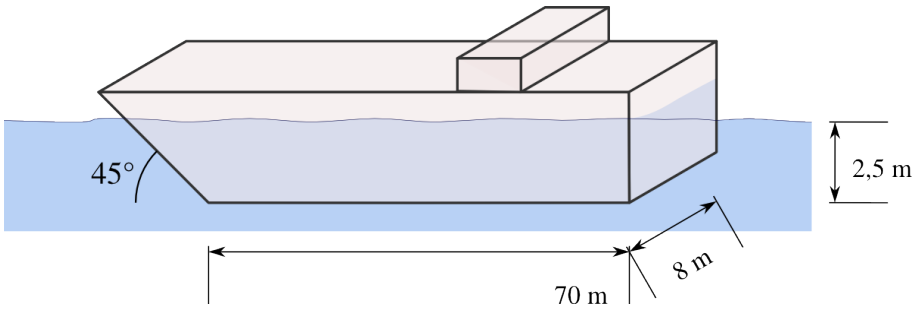

Figure 1.10 – Basic layout of a barge floating in water.

Figure CC-0 o.c.

1. Sketch the distribution of pressure on each of the immersed walls of the barge.
2. What is the force resulting from pressure efforts on each of these walls?
3. What is the weight of the barge?

1.6 Atmospheric buoyancy force

If the atmospheric density is considered uniform, estimate the buoyancy force exerted on an Airbus A380, both on the ground and in cruise flight ($\rho_{\text{cruise}} = 0{,}4\,\text{kg}\,\text{m}^{-3}$, $T_{\text{cruise}} = -40\,^{\circ}\text{C}$).

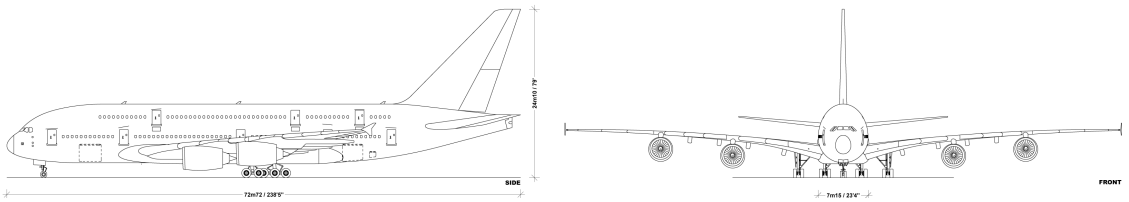

Figure 1.11 – Airbus A380-800

Drawing CC-BY-SA *by Julien Scavini*

Length overall	72,73 m
Wingspan	79,75 m
Height	24,45 m
Wing area	845 m^2
Aspect ratio	7,5
Wing sweep	33,5°
Maximum take-off weight	560 000 kg
Typical operating empty weight	276 800 kg

Table 1.1 – Characteristics of the Airbus A380-800.

1.7 Atmospheric pressure distribution

The integration we carried out in §1.3.6 p.28 to model the pressure distribution in the atmosphere was based on the hypothesis that the temperature was uniform and constant ($T = T_{\text{cst.}}$). In practice, this may not always be the case.

1. If the atmospheric temperature decreases with altitude at a constant rate (e.g. of $-7\,\text{K}\,\text{km}^{-1}$), how can the pressure distribution be expressed analytically?

A successful fluid dynamics lecturer purchases an apartment at the top of the Burj Khalifa tower (800 m above the ground). Inside the tower, the temperature is controlled everywhere at 18,5 °C. Outside, the ground temperature is 30 °C and it decreases linearly with altitude (gradient: $-7\,\text{K}\,\text{km}^{-1}$).

A door is opened at the bottom of the tower, so that at zero altitude the air pressure (1 bar) is identical inside and outside of the tower.
For the purpose of the exercise, we pretend the tower is entirely hermetic (meaning air is prevented from flowing in or out of its windows).

2. What is the pressure difference between each side of the windows in the apartment at the top of the tower?

1.8 Lock with diagonally-mounted doors

The doors of the lock studied in exercise 1.3 p.33 are replaced with diagonally-mounted doors at an angle $\alpha = 20°$, mounted such that no bending moment is sustained by the hinges (fig. 1.12).

What is the force exerted by door "A" on the other door?

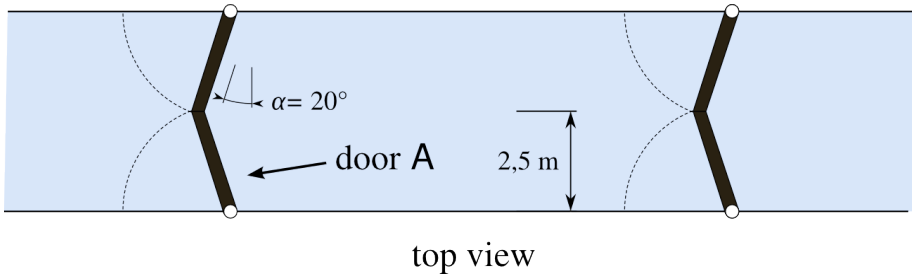

Figure 1.12 – Lock doors mounted with an angle relative one to another. The angle relative to the case in exercise 1.3 is $\alpha = 20°$. The width of the canal is still 5 m.

Figure CC-0 o.c.

1.9 Force on a water lock door

We return one last time to exercise 1.3 p.33. We had calculated the force $F_{\text{pressure}A}$ resulting from the pressure of the water on door "A". At which height is this force exerting?

1.10 Reservoir door

Munson & al. [14] 2.87

A water reservoir has a door of width 3 m which is held in place with a horizontal cable, as shown in fig. 1.13.

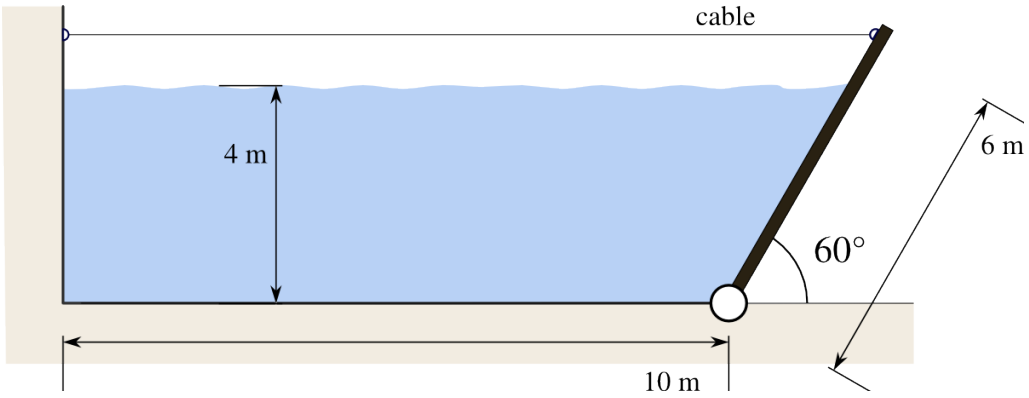

Figure 1.13 – A sealed, hinged door in a water reservoir. The width across the drawing (towards the reader) is 3 m

Figure CC-0 o.c.

The door has a mass of 200 kg and the hinge exerts negligible bending moment. What is the force in the cable?

Answers

1.1 $p_A = p_{atm.} + 0{,}039\,\text{bar} \approx 1{,}039\,\text{bar}$.

1.2 1) $p_{inside} = p_{atm.} + 0{,}0157\,\text{bar} \approx 1{,}0157\,\text{bar}$; 2) $\Delta z_2 = 1{,}1765\,\text{cm}$.

1.3 2) $F_{net} = \rho g L \left[\frac{1}{2}z^2\right]_{5\,\text{m}}^{9\,\text{m}} = 686{,}7\,\text{kN}$ per door; 3) $M = F_{net}\frac{L}{2} = 858{,}3\,\text{kN m}$ per hinge. 4) yes — look at the analytical expression for the moment to find out why.

1.4 1) $F_{vertical} = 4{,}625\,\text{mN}$ upwards; 2) $F_{vertical} = 3{,}775\,\text{N}$ in both cases; 3) There is no change; 4) See §1.3.6; 5) $F_{vertical} = 4{,}487\,\text{mN}$ upwards (and so in question 1 we were off by 3 %).

1.5 2) $F_{rear} = 0{,}2453\,\text{MN}$, $F_{side} = 2{,}1714\,\text{MN}$, $F_{bottom} = 13{,}734\,\text{MN}$, $F_{front} = 0{,}3468\,\text{MN}$; 3) $F_{buoyancy} = 13{,}979\,\text{MN}$ (1 425 t).

1.6 Assuming a volume of approx. $2\,600\,\text{m}^3$, we obtain approx. 30,9 kN on the ground, 10,4 kN during cruise.

1.7 1) $\frac{p_2}{p_1} = \left(1 + \frac{kz_2}{T_1}\right)^{\frac{g}{kR}}$.

1.8 The moment is brought to zero by an inter-door force $F_{sideways} = 1{,}068\,\text{MN}$ (perpendicular to the canal axis).

1.10 $M_{water} = L\left(\frac{\mathrm{d}p}{\mathrm{d}z}\right)_{water}\left[\frac{H}{2}r^2 - \frac{\sin\theta}{3}r^3\right]_2^R = 0{,}4186\,\text{MN m}$; so, $F_{cable} = 81{,}13\,\text{kN}$.

Fluid Mechanics
Chapter 2 – Shear effects

last edited May 10, 2016

These lecture notes are based on textbooks by White [9], Çengel & al.[12], and Munson & al.[14].

2.1 Motivation

In fluid mechanics, only three kinds of force apply to fluid particles: forces due to pressure, shear, and gravity. This chapter focuses on the second type, and should allow us to answer two questions:

- How is the net effect of shear described within fluid flows?
- What are the pressure forces generated by simple flows?

2.2 Concept of shear

We approached the concept of shear in the introductory chapter with the notion that it represented force parallel to a given flat surface (eq. 0/7), for example a flat plate of area A:

$$\tau \equiv \frac{F_{\parallel}}{A} \tag{2/1}$$

Like we did with pressure, to appreciate the concept of shear in fluid mechanics, we need to go beyond this equation.

2.2.1 The direction of shear

Already from the definition in eq. 2/1 we can appreciate that "parallel to a flat plate" can mean a multitude of different directions, and so that we need more than one dimension to represent shear. Furthermore, much in the same way as we did for pressure, we do away with the flat plate and accept that shear is a *field*, i.e. it is an effort applying not only upon solid objects but also

upon and within fluids themselves. We replace eq. 2/1 with a more general definition:

$$\vec{\tau} \equiv \lim_{A \to 0} \frac{\vec{F}_{\parallel}}{A} \tag{2/2}$$

Contrary to pressure, shear is not a scalar, i.e. it can (and often does) take different values in different directions. At a given *point* in space we represent it as a vector $\vec{\tau} = \left(\tau_x, \tau_y, \tau_y\right)$, and in a fluid, there is a shear *vector field*:

$$\vec{\tau}_{(x,y,z,t)} \equiv \begin{pmatrix} \tau_x \\ \tau_y \\ \tau_z \end{pmatrix}_{(x,y,z,t)} \tag{2/3}$$

2.2.2 Shear on an infinitesimal volume

Describing the changes in space of the shear vector field requires another mathematical dimension (called *order*).
Instead of a flat plate, let us consider an infinitesimally small cube within the fluid (fig. 2.1). Because it is placed in a vector field, the shear vector exerting on each of its six faces may be different.

In order to express the efforts on any given face, we express a component of shear with two subscripts, the first indicating the direction normal to the surface of interest, and the second indicating the direction of the effort. For example, $\vec{\tau}_{xy}$ represents the shear in the y-direction on a surface perpendicular to the x-direction. On this face, the shear vector would be:

$$\vec{\tau}_{xj} = \vec{\tau}_{xx} + \vec{\tau}_{xy} + \vec{\tau}_{xz} \tag{2/4}$$

$$= \tau_{xx}\vec{i} + \tau_{xy}\vec{j} + \tau_{xz}\vec{k} \tag{2/5}$$

where the subscript xj indicates all of the directions ($j = x, y, z$) on a face perpendicular to the x-direction.

In eq. 2/4, the reader may be surprised to see the term τ_{xx} appear — a shear effort perpendicular to the surface of interest. This is because the faces of the infinitesimal cube studied here (shown in fig. 2.1) are not solid. They are permeable, and the local velocity on each one may (in fact, must, if there is to be any flow) include a component of velocity through the face of the cube.

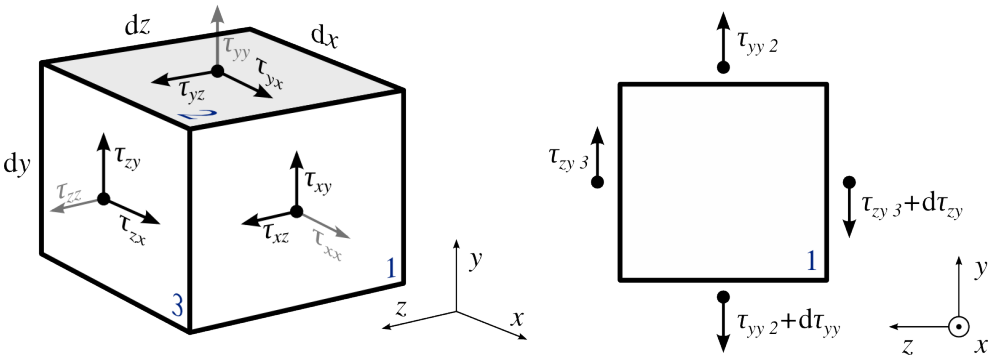

Figure 2.1 – Shear efforts on a cubic fluid particle (with only the efforts on the visible faces 1 to 3 represented). The shear tensor $\vec{\tau}_{ij}$ has six members of three components each.

Figure CC-0 o.c.

Thus, there is no reason for the shear effort, which is three-dimensional, to be aligned along each flat surface. As the fluid travels across any face, it can be sheared (which results in strain) in any arbitrary direction, regardless of the local pressure — and thus shear can and most often does have a component (τ_{ii}) perpendicular to the surface.

Now, the net shear effect on the cube will have *eighteen* components: one tree-dimensional vector for each of the six faces. Each of those components may take a different value. The net shear could perhaps be represented as en entity —a *tensor*— containing six vectors $\vec{\tau}_1, \vec{\tau}_2, \vec{\tau}_3 \ldots \vec{\tau}_6$. By convention, however, shear is notated using only three vector components: one for each pair of faces. Shear efforts on a volume are thus represented with a *tensor field* $\vec{\tau}_{ij}$:

$$\vec{\tau}_{ij} \equiv \begin{pmatrix} \vec{\tau}_{xj} \\ \vec{\tau}_{yj} \\ \vec{\tau}_{zj} \end{pmatrix} \equiv \begin{pmatrix} \vec{\tau}_{xj\ \{1,4\}} \\ \vec{\tau}_{yj\ \{2,5\}} \\ \vec{\tau}_{zj\ \{3,6\}} \end{pmatrix}$$
$$\vec{\tau}_{ij} \equiv \begin{pmatrix} \tau_{xx} & \tau_{xy} & \tau_{xz} \\ \tau_{yx} & \tau_{yy} & \tau_{yz} \\ \tau_{zx} & \tau_{zy} & \tau_{zz} \end{pmatrix} \tag{2/6}$$

In this last equation 2/6 each of the nine components of the tensor acts as the container for two contributions: one for each of the two faces perpendicular to the direction in its first subscript.

So much for the shear *effort* on an element of fluid. What about the net *force* due to shear on the fluid element? Not every element counts: part of the shear will accelerate (change the velocity vector) the particle, while part of it will merely strain (deform) the particle. Quantifying this force thus requires making a careful selection within the eighteen components of $\vec{\tau}_{ij}$. We may start with the x-direction, which consists of the sum of the component of shear in the x-direction on each of the six cube faces:

$$\begin{aligned} \vec{F}_{\text{shear } x} = {} & S_3 \vec{\tau}_{zx\ 3} - S_6 \vec{\tau}_{zx\ 6} \\ & + S_2 \vec{\tau}_{yx\ 2} - S_5 \vec{\tau}_{yx\ 5} \\ & + S_1 \vec{\tau}_{xx\ 1} - S_4 \vec{\tau}_{xx\ 4} \end{aligned} \tag{2/7}$$

Since $S_3 = S_6 = \mathrm{d}x\,\mathrm{d}y$, $S_2 = S_5 = \mathrm{d}x\,\mathrm{d}z$ and $S_1 = S_4 = \mathrm{d}z\,\mathrm{d}y$, this is re-written as:

$$\begin{aligned} \vec{F}_{\text{shear } x} = {} & \mathrm{d}x\,\mathrm{d}y(\vec{\tau}_{zx\ 3} - \vec{\tau}_{zx\ 6}) \\ & + \mathrm{d}x\,\mathrm{d}z(\vec{\tau}_{yx\ 2} - \vec{\tau}_{yx\ 5}) \\ & + \mathrm{d}z\,\mathrm{d}y(\vec{\tau}_{xx\ 1} - \vec{\tau}_{xx\ 4}) \end{aligned} \tag{2/8}$$

In the same way we did with pressure in chapter 2 (§1.3.3 p.25), we express each pair of values as a space derivative multiplied by an infinitesimal distance:

$$\begin{aligned} \vec{F}_{\text{shear } x} &= \mathrm{d}x\,\mathrm{d}y\left(\mathrm{d}z\frac{\partial \vec{\tau}_{zx}}{\partial z}\right) + \mathrm{d}x\,\mathrm{d}z\left(\mathrm{d}y\frac{\partial \vec{\tau}_{yx}}{\partial y}\right) + \mathrm{d}z\,\mathrm{d}y\left(\mathrm{d}x\frac{\partial \vec{\tau}_{xx}}{\partial x}\right) \\ &= \mathrm{d}\mathcal{V}\left(\frac{\partial \vec{\tau}_{zx}}{\partial z} + \frac{\partial \vec{\tau}_{yx}}{\partial y} + \frac{\partial \vec{\tau}_{xx}}{\partial x}\right) \end{aligned} \tag{2/9}$$

If we make use of the operator *divergent* written $\vec{\nabla}\cdot$:

$$\vec{\nabla}\cdot \equiv \frac{\partial}{\partial x}\vec{i}\cdot + \frac{\partial}{\partial y}\vec{j}\cdot + \frac{\partial}{\partial z}\vec{k}\cdot \tag{2/10}$$

$$\vec{\nabla}\cdot\vec{A} \equiv \frac{\partial A_x}{\partial x} + \frac{\partial A_y}{\partial y} + \frac{\partial A_z}{\partial z} \tag{2/11}$$

$$\vec{\nabla}\cdot\vec{A}_{ij} \equiv \begin{pmatrix} \frac{\partial A_{xx}}{\partial x} + \frac{\partial A_{yx}}{\partial y} + \frac{\partial A_{zx}}{\partial z} \\ \frac{\partial A_{xy}}{\partial x} + \frac{\partial A_{yy}}{\partial y} + \frac{\partial A_{zy}}{\partial z} \\ \frac{\partial A_{xz}}{\partial x} + \frac{\partial A_{yz}}{\partial y} + \frac{\partial A_{zz}}{\partial z} \end{pmatrix} = \begin{pmatrix} \vec{\nabla}\cdot\vec{A}_{ix} \\ \vec{\nabla}\cdot\vec{A}_{iy} \\ \vec{\nabla}\cdot\vec{A}_{iz} \end{pmatrix} \tag{2/12}$$

we can re-write eq. 2/9 and see that the net shear force in the x-direction is equal to the particle volume times the divergent of the shear in the x-direction:

$$\vec{F}_{\text{shear } x} = \mathrm{d}\mathcal{V}\ \vec{\nabla}\cdot\vec{\tau}_{ix} \tag{2/13}$$

The y- and z-direction are taken care in the same fashion, so that we can gather up our puzzle pieces and express *the force per volume due to shear as the divergent of the shear tensor*:

$$\vec{F}_{\text{shear}} = \begin{pmatrix} \vec{F}_{\text{shear } x} \\ \vec{F}_{\text{shear } y} \\ \vec{F}_{\text{shear } z} \end{pmatrix} = \mathrm{d}\mathcal{V} \begin{pmatrix} \vec{\nabla}\cdot\vec{\tau}_{ix} \\ \vec{\nabla}\cdot\vec{\tau}_{iy} \\ \vec{\nabla}\cdot\vec{\tau}_{iz} \end{pmatrix} = \mathrm{d}\mathcal{V}\ \vec{\nabla}\cdot\vec{\tau}_{ij} \tag{2/14}$$

This exploration goes beyond the theory required to to through this chapter (we will come back to it when we start concerning ourselves with the dynamics of fluid particles in chapter 4, where the divergent of shear will make part of the glorious *Cauchy equation*). It suffices for now to sum up our findings as follows:

- Shear at a point in space has three components — it is a vector field;
- The effect of shear on a volume of fluid has eighteen components – it is a second-order tensor field;
- The net force due to shear a volume of fluid, expressed using the divergent of the shear tensor, has three components — it is a vector field.

2.3 Slip and viscosity

2.3.1 The no-slip condition

We observe that whenever we measure the velocity of a fluid flow along a solid wall, the speed tends to zero as we approach the wall surface. In other words, the fluid "*sticks*" to the surface regardless of the overall faraway flow velocity. This phenomenon is called the *no-slip condition* and is of paramount importance in fluid mechanics. One consequence of this is that fluid flows near walls are dominated by viscous effects (internal friction) due to the large speed gradients.

2.3.2 Viscosity

When a solid wall is moved longitudinally within a fluid, the fluid generates an opposing friction force through viscous effects (fig. 2.2). We call *viscosity* μ the ratio between the fluid velocity gradient and the shear effort. For example, the norm of the shear $\vec{\tau}_{xy}$ on a surface perpendicular to the x-direction, in the y-direction, can be expressed as:

$$||\vec{\tau}_{xy}|| = \mu \frac{\partial u_y}{\partial x} = \mu \frac{\partial v}{\partial x}$$

In a more general case, viscosity is defined as the (scalar) ratio between norm of shear and the spatial rate of change of velocity in a direction perpendicular to the flow:

$$\mu \equiv \frac{||\vec{\tau}_{ij}||}{\left(\frac{\partial u_j}{\partial i}\right)} \tag{2/15}$$

$$||\vec{\tau}_{ij}|| = \mu \frac{\partial u_j}{\partial i} \tag{2/16}$$

in which the subscript i is an arbitrary direction (x, y or z) and j is the direction following it in order (e.g. $j = z$ when $i = x$);
and where μ is the viscosity (or *dynamic viscosity*) (Pa s).

Viscosity μ is measured in Pa s, which is the same as $\mathrm{N\,s\,m^{-2}}$ or $\mathrm{kg\,m^{-1}\,s^{-1}}$. It has historically been measured in poise (1 poise ≡ 0,1 Pa s).

The concept of *kinematic viscosity* ν (Greek letter *nu*) is sometimes used instead of the dynamic viscosity; it is defined as

$$\nu \equiv \frac{\mu}{\rho} \tag{2/17}$$

where ν is measured in $\mathrm{m^2\,s^{-1}}$.

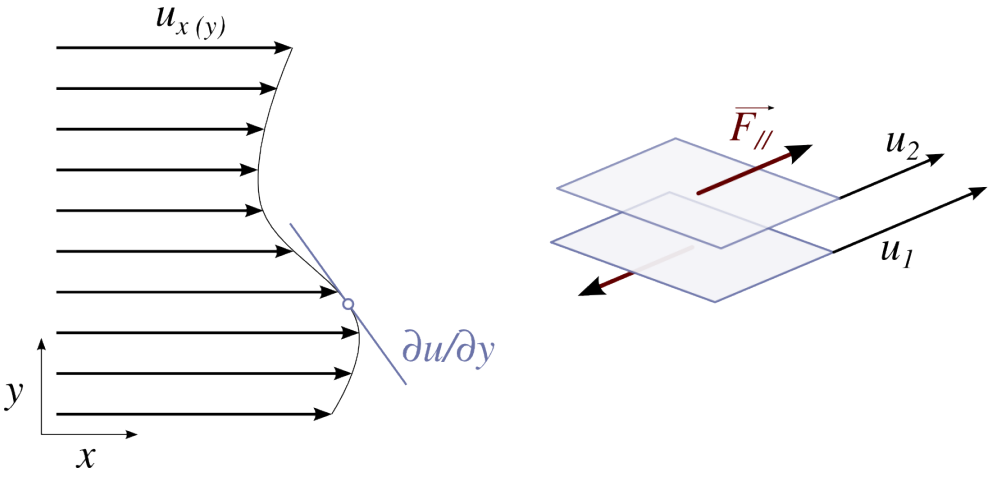

Figure 2.2 – Any velocity gradient $\frac{\partial u_x}{\partial y}$ in the flow results in a shear force $F_{||}$ in the direction x. The ratio between the gradient and the shear is called *viscosity*

Figure CC-0 o.c.

2.3.3 Newtonian Fluid

Fluids for which μ is independent from $\frac{\partial u_j}{\partial i}$ are called *Newtonian fluids*.

Most fluids of interest in engineering fluid mechanics (air, water, exhaust gases, pure gases) can be safely modeled as Newtonian fluids. Their viscosity μ varies slightly with pressure and mildly with temperature – in our study of fluid mechanics, we will not take these dependencies into account.
The values of viscosity vary very strongly from one fluid to another: for example, honey is roughly ten thousand times more viscous than water, which is roughly a hundred times more viscous than ambient air. The viscosities of various fluids is described in fig. 5.11 p.107.

Oil-based paint, blood and jelly-based fluids are strongly non-Newtonian; they require more complex viscosity models (fig. 2.3).

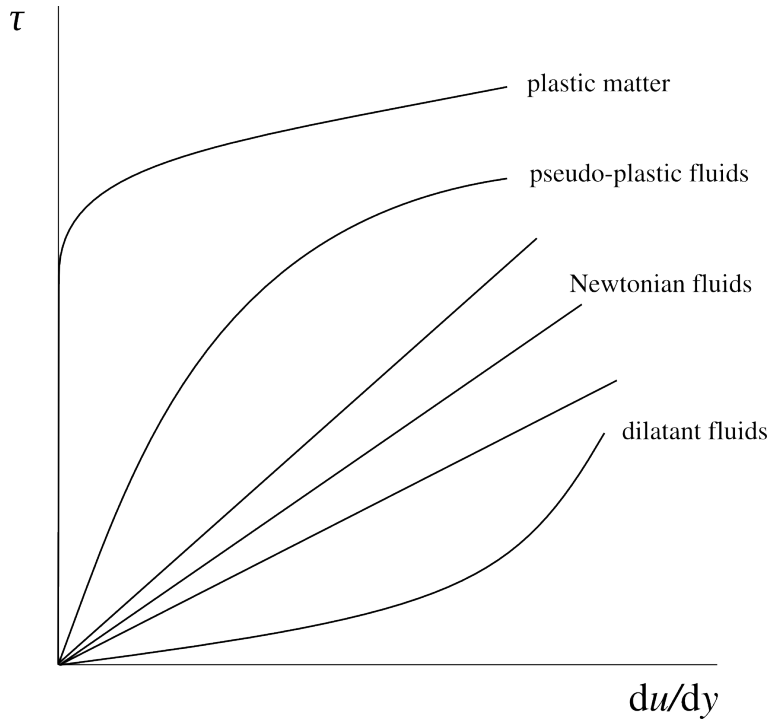

Figure 2.3 – Viscosity characteristics of various fluids. Those for which μ is independent of $\partial u_j / \partial i$ are called *Newtonian*.

Figure CC-0 o.c.

2.4 Wall shear forces

The calculation of forces due to shear is very similar to that which we used in the previous chapter with pressure.

When the shear $\vec{\tau}$ exerted on a flat surface of area S is uniform, the resulting force F is easily easily calculated ($F = \tau_{\text{cst.}} S$). In the more general case of a three-dimensional object immersed in a fluid with non-uniform shear, the force must be expressed as a vector and obtained by integration:

$$\vec{F}_{\text{shear}} = \int_S \mathrm{d}\vec{F} = \int_S \vec{\tau}_{\text{surface}}\, \mathrm{d}S \tag{2/18}$$

Much like equation 1/13 in the previous chapter, eq. 2/18 is easily implemented in software algorithms to obtain numerically, for example, the force resulting from shear due to fluid flow around a body such as an aircraft wing. In our academic study of fluid mechanics, however, we will restrict ourselves to the simpler cases where the surface is perfectly flat and the shear has uniform direction. The force in eq. 2/18, in the i-direction due to shear on a surface perpendicular to the j-direction, then becomes:

$$F_{\text{shear }ji} = \int_S \mathrm{d}F = \int_S ||\vec{\tau}_{ji}||\, \mathrm{d}S \tag{2/19}$$

What is required to calculate the scalar F in eq. 2/19 is an expression of τ as a function of S. We proceed like we did in the previous chapter, splitting $\mathrm{d}S$ as $\mathrm{d}S = \mathrm{d}i\,\mathrm{d}k$ before proceeding with the calculation starting from;

$$F_{\text{shear}ji} = \iint \tau_{ji\ (i,k)}\, \mathrm{d}i\,\mathrm{d}k \tag{2/20}$$

$$= \mu \iint \frac{\partial u_i}{\partial j}\, \mathrm{d}i\,\mathrm{d}k \tag{2/21}$$

where i is the direction of the force;
j is the direction perpendicular to the flat surface;
and k is the third direction.

The above expression 2/21 is perhaps more easily read when developed. For example, the shear force $\vec{F}_{\text{shear}yi}$ exerting on a plate perpendicular to the y-direction is:

$$\vec{F}_{\text{shear}yi} = \begin{pmatrix} F_{\text{shear}yx} \\ 0 \\ F_{\text{shear}yz} \end{pmatrix}$$

with

$$F_{\text{shear}yx} = \mu \iint \frac{\partial u}{\partial y}\, \mathrm{d}x\,\mathrm{d}z$$

$$F_{\text{shear}yz} = \mu \iint \frac{\partial w}{\partial y}\, \mathrm{d}x\,\mathrm{d}z$$

Just like for pressure, the moment $\vec{M}_{\text{X}j}$ generated about a point X by the shear forces in the i-direction on a plane surface perpendicular to the j-direction can be calculated as

$$\vec{M}_{\text{X}j} = \int_S \mathrm{d}\vec{M}_{\text{X}} = \int_S \vec{r}_{\text{X}F} \wedge \mathrm{d}\vec{F} = \int_S \vec{r}_{\text{X}F} \wedge \vec{\tau}_{ij}\, \mathrm{d}S \tag{2/22}$$

If the point X is along the surface this can be expressed as:

$$M_{\mathrm{X}j} = \mu \iint r_{\mathrm{X}F} \frac{\partial u_i}{\partial j} \,\mathrm{d}i \,\mathrm{d}k \tag{2/23}$$

$$M_{\mathrm{X}y} = \mu \iint r_{\mathrm{X}F} \frac{\partial u_x}{\partial y} \,\mathrm{d}x \,\mathrm{d}z \tag{2/24}$$

Fluid Mechanics
Exercise sheet 2 – Shear efforts

last edited April 4, 2016

These lecture notes are based on textbooks by White [9], Çengel & al.[12], and Munson & al.[14].

Except otherwise indicated, we assume that fluids are Newtonian, and that:
$\rho_{water} = 1\,000\,\mathrm{kg\,m^{-3}}$; $p_{atm.} = 1\,\mathrm{bar}$; $\rho_{atm.} = 1{,}225\,\mathrm{kg\,m^{-3}}$; $T_{atm.} = 11{,}3\,^{\circ}\mathrm{C}$; $\mu_{atm.} = 1{,}5 \cdot 10^{-5}\,\mathrm{N\,s\,m^{-2}}$;
$g = 9{,}81\,\mathrm{m\,s^{-2}}$. Air is modeled as a perfect gas ($R_{air} = 287\,\mathrm{J\,K^{-1}\,kg^{-1}}$; $\gamma_{air} = 1{,}4$; $c_{pair} = 1\,005\,\mathrm{J\,kg^{-1}\,K^{-1}}$).

2.1 Flow in between two plates

Munson & al. [14] Ex1.5

A fluid is forced to flow between two stationary plates (fig. 2.4). We observe that the flow is laminar, with a velocity profile in the x-direction $u_x = u = f(y)$ which is linked to the average fluid velocity $V_{average}$ by the relationship:

$$u = \frac{3}{2} V_{average} \left[1 - \left(\frac{y}{H} \right)^2 \right] \tag{2/25}$$

where y is measured from the middle of the gap;
and H is half of the gap length.

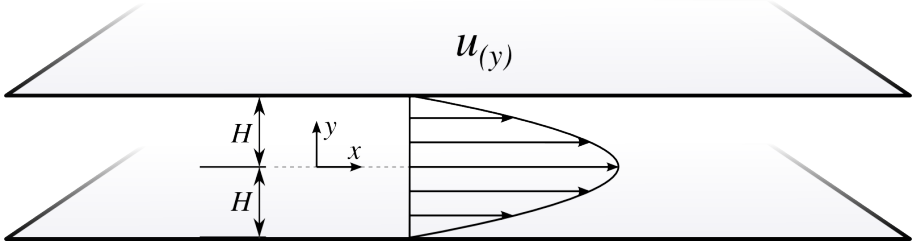

Figure 2.4 – Velocity distribution for laminar flow in between two plates, also known as *Couette flow*.

Figure CC-0 o.c.

The fluid viscosity is $2\,\mathrm{N\,s\,m^{-2}}$, the average velocity is $0{,}6\,\mathrm{m\,s^{-1}}$ and the two plates are $10\,\mathrm{mm}$ apart.

1. What is the shear effort generated on the lower plate?
2. What is the shear effort at the center of the flow?

2.2 Friction on a plate

A plate the size of an A4 sheet of paper (210 mm × 297 mm) is moved horizontally at constant speed above a large flat surface (fig. 2.5). The fluid velocity profile in between the plate and the bottom surface is assumed to be strictly linear everywhere.

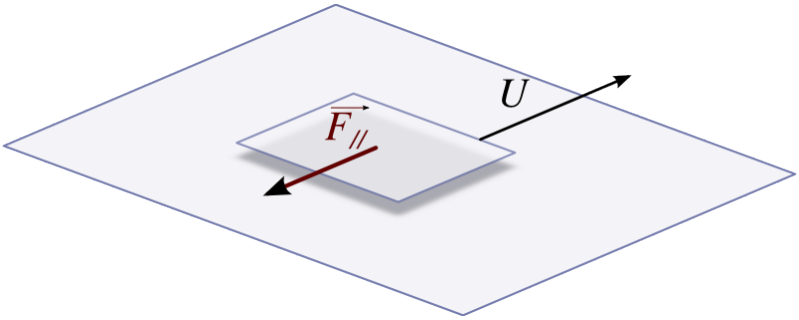

Figure 2.5 – A plate moved horizontally across a flat surface.

Figure CC-0 o.c.

1. Express the shear force on the plate as a function of its velocity U_{plate}, the gap height H, and the properties of the fluid.
2. The plate speed is $1\,\text{m}\,\text{s}^{-1}$ and the gap height is 5 mm. What is the shear force if the fluid is air ($\mu_{\text{atm.}} = 1{,}5 \cdot 10^{-5}\,\text{N}\,\text{s}\,\text{m}^{-2}$), and if the fluid is honey ($\mu_{\text{honey}} = 40\,\text{N}\,\text{s}\,\text{m}^{-2}$)?

2.3 Viscometer

Çengel & al. [12] 2-78

An instrument designed to measure the viscosity of fluids is made of two coaxial cylinders (fig. 2.6). The inner cylinder is immersed in a liquid, and it rotates within the stationary outer cylinder.

The two cylinders are 75 cm tall. The inner cylinder diameter is 15 cm and the spacing is 1 mm.

When the inner cylinder is rotated at 300 rpm, a friction-generated moment of 0,8 N m is measured.

1. If the flow in between the cylinders corresponds to the simplest possible flow case (steady, uniform, fully-laminar), what is the viscosity of the fluid?
2. Would an non-Newtonian fluid induce a higher moment? (briefly justify your answer)

Note: in practice, when the inner cylinder is turned at high speed, the flow displays mesmerizing patterns called Taylor—Couette vortices, the description of which is much more complex!

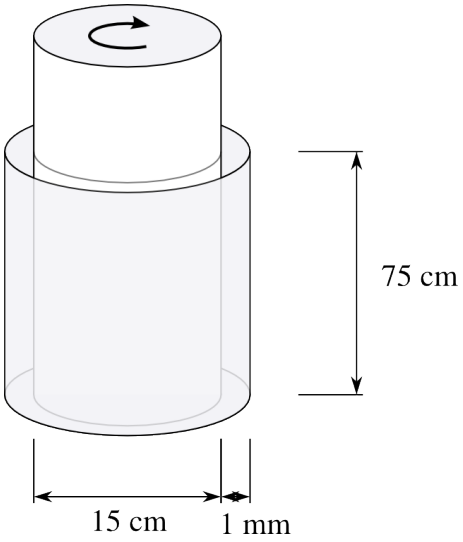

Figure 2.6 – Sketch of a cylinder viscometer. The width of the gap has been greatly exaggerated for clarity.

Figure CC-0 o.c.

2.4 Boundary layer

White [9] P1.56

A laminar fluid flow occurs along a wall (fig. 2.7). Close to the wall ($y < \delta$), we observe that viscous effects dominate the mechanics of the flow. This zone is designated *boundary layer*. The speed $u_{(y)}$ can then be modeled with the relation:

$$u = U \sin\left(\frac{\pi y}{2\delta}\right) \tag{2/26}$$

in which U is the flow speed far away from the wall.

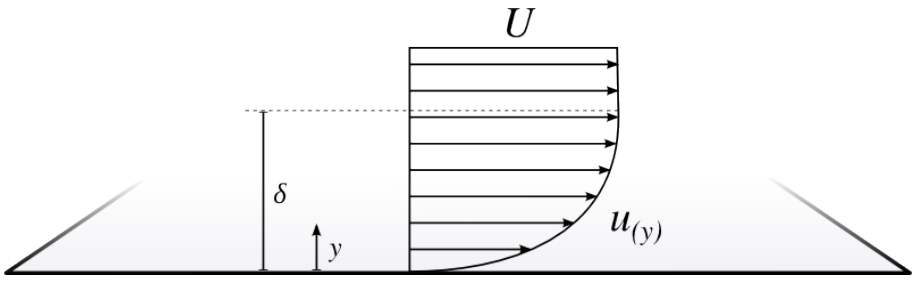

Figure 2.7 – Velocity profile across the boundary layer.

Figure CC-0 o.c.

The fluid is helium at 20 °C and 1 bar ($9 \cdot 10^{-6}$ N s m^{-2}); measurements yield $U = 10{,}8$ m s^{-1} and $\delta = 3$ cm.

1. What is the shear effort on the wall?
2. At which height y will the shear effort be half of this value?
3. What would be the effort if helium was replaced with water ($1 \cdot 10^{-3}$ kg m^{-1} s^{-1})?

2.5 Clutch

Çengel & al. [12] 2-74

Two aligned metal shafts are linked by a clutch, which is made of two disks very close one to another, rotating in the same direction at similar (but not identical) speeds. The disk diameters are both 30 cm and the gap between them is 2 mm ; they are submerged in SAE30W oil with viscosity 0,38 $\mathrm{kg\,m^{-1}\,s^{-1}}$.

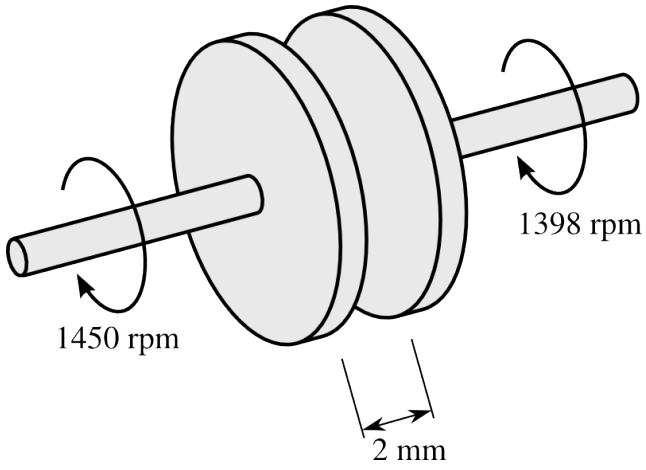

Figure 2.8 – Sketch of the two disks constituting the clutch. The gap width has been exaggerated for clarity.

Figure CC-0 o.c.

The power shaft rotates at 1 450 rpm, while the powered shaft rotates at 1 398 rpm. We consider the simplest possible flow case (steady, laminar) in between the two disks.

1. What is the moment imparted by one disk to the other?
2. What is the transmitted power and the clutch efficiency?
3. What do you think the flow patterns in between the two plates would look like in the real case?

Answers

2.1 1) $\tau_{y=-H} = 720\,\mathrm{N\,m^{-2}}$; 2) $\tau_{y=0} = 0\,\mathrm{N\,m^{-2}}$.

2.2 1) $F_\tau = L_1 L_2 \mu \frac{U}{H} = 1{,}87 \cdot 10^{-4}\,\mathrm{N}$ for air, and 500 N for honey(!).

2.3 $\mu = \frac{hM}{2\pi\omega R_1^3 H} = 1{,}281 \cdot 10^{-2}\,\mathrm{N\,s\,m^{-2}}$.

2.4 1) $\tau_{\text{wall}} = \mu \frac{\pi U}{2\delta} = 5{,}09 \cdot 10^{-3}\,\mathrm{N^2\,m^{-1}}$ for helium;
2) $y_1 = \frac{2}{3}\delta = 2\,\mathrm{cm}$; 3) $\tau_{\text{wall}} = 0{,}565\,\mathrm{N\,m^{-2}}$ for water.

2.5 1) $M = \frac{\pi}{2}\frac{\mu\omega}{h}R^4 = 0{,}8228\,\mathrm{N\,m}$; 2) $\dot{W}_2 = \omega_2 M = 120\,\mathrm{W}$;
3) $\eta_{\text{clutch}} = \frac{\dot{W}_2}{\dot{W}_1} = 96{,}4\,\%$ (remember this is a very low-power, low-relative speed, laminar-flow case).

Fluid Mechanics
Chapter 3 – Integral analysis of fluid flows

last edited May 1, 2016

These lecture notes are based on textbooks by White [9], Çengel & al.[12], and Munson & al.[14].

3.1 Motivation

Our objective for this chapter is to answer the question "what is the *net* effect of a given fluid flow through a given volume?".

Here, we develop a mass, momentum and energy accounting methodology to analyze the flow of continuous medium. This method is not powerful enough to allow us to describe extensively the nature of fluid flow around bodies; nevertheless, it is extremely useful to quantify forces, moments, and energy transfers associated with fluid flow.

3.2 The Reynolds transport theorem

3.2.1 Control volume

Let us begin with the study of a fluid flow described with a velocity field $\vec{V} = (u, v, w)$ which is a function of space and time ($\vec{V} = f(x, y, z, t)$).

Within this flow, we are interested in an arbitrary volume named *control volume* (CV) which is free to move and change shape (fig. 3.1). We are going to measure the properties of the fluid at the borders of this volume —the *control surface*— in order to compute the net effect of the flow through the volume.

At a given time, the control volume contains a certain amount of mass; we name this mass the *system*. Thus the system is a fixed amount of mass transiting through the control volume at the time of our study, and its properties (volume, pressure, velocity etc.) may change in the process.

All along the chapter, we are focusing on the question: based on measured fluid properties at some point in space and time (the properties at the border of the control volume), how can we quantify what is happening to the system (the mass inside the control volume)?

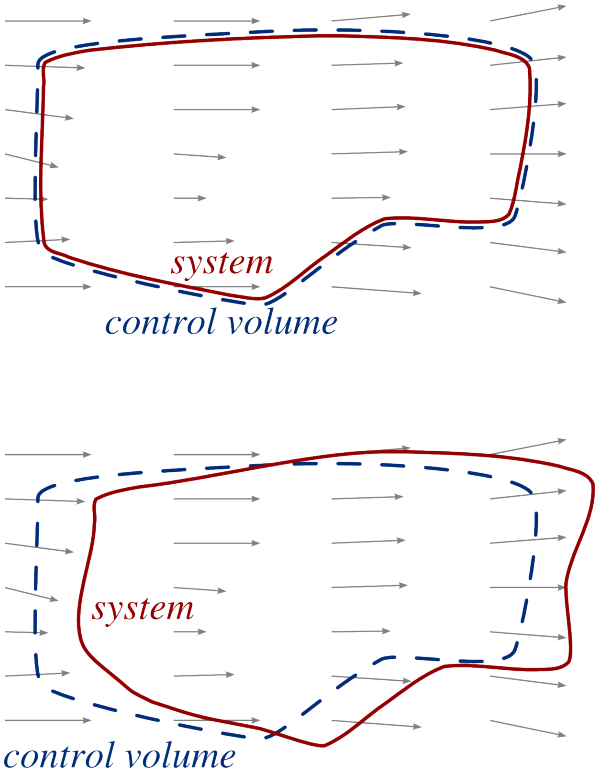

Figure 3.1 – A control volume within a flow. The *system* is the amount of mass included within the control volume at a given time. At a later time, it may have left the control volume, and its shape and properties may have changed. The control volume may also change shape, although this is not represented here.

Figure CC-0 o.c.

3.2.2 Rate of change of an additive property

In order to proceed with our calculations, we need a robust accounting methodology. We start with a "dummy" fluid property B, which we will later replace with physical variables of interest.
Let us thus consider an arbitrary additive property B of the fluid. By the term *additive* property, we mean that the total *amount of property* is divided if the fluid is divided. For instance, this is true of mass, volume, energy, entropy, but not pressure or temperature.
The *specific* (i.e. per unit mass) value of B is designated $b \equiv B/m$.

We now wish to compute the variation of a system's property B based on measurements made at the borders of the control volume.

The time variation of the quantity B within the system is measured with the term $\frac{\mathrm{d}B_{\mathrm{sys}}}{\mathrm{d}t}$. This may represent, for example, the rate of change of the fluid's internal energy as it travels through a jet engine.

Within the control volume, the enclosed quantity B_{CV} can vary by accumulation (for example, mass may be increasing in an air tank fed with compressed air): we measure this with the term $\frac{\mathrm{d}B_{\mathrm{CV}}}{\mathrm{d}t}$. Finally, a mass flux may be flowing through the boundaries of the control volume, carrying with it some amount of B every second: we name that net flow out of the system $\dot{B}_{\mathrm{net}} \equiv \dot{B}_{\mathrm{out}} - \dot{B}_{\mathrm{in}}$.

We can now link these three terms with the simple equation:

$$\frac{\mathrm{d}B_{\mathrm{sys}}}{\mathrm{d}t} = \frac{\mathrm{d}B_{\mathrm{CV}}}{\mathrm{d}t} + \dot{B}_{\mathrm{net}} \qquad (3/1)$$

the rate of change of B for the system = the rate of change of B within the control volume + the net flow of B through the boundaries of the control volume

Since B may not be uniformly distributed within the control volume, we like to express the term $\frac{\mathrm{d}B_{\mathrm{CV}}}{\mathrm{d}t}$ as the integral of the volume density $\frac{B}{\mathcal{V}}$ with respect to volume:

$$\frac{\mathrm{d}B_{\mathrm{CV}}}{\mathrm{d}t} = \frac{\mathrm{d}}{\mathrm{d}t}\iiint_{\mathrm{CV}} \frac{B}{\mathcal{V}}\,\mathrm{d}\mathcal{V} = \frac{\mathrm{d}}{\mathrm{d}t}\iiint_{\mathrm{CV}} \rho b\,\mathrm{d}\mathcal{V} \qquad (3/2)$$

Obtaining a value for this integral may be difficult, especially if the volume CV is itself a function of time.

The term $\dot{B}_{\mathrm{net}}$ can be evaluated by quantifying, for each area element $\mathrm{d}A$ of the control volume's surface, the surface flow rate $\rho b V_\perp$ of property B that flows through it (fig. 3.2). The integral over the entire control volume surface CS of this term is:

$$\dot{B}_{\mathrm{net}} = \iint_{\mathrm{CS}} \rho b V_\perp\,\mathrm{d}A = \iint_{\mathrm{CS}} \rho b\,(\vec{V}_{\mathrm{rel}}\cdot\vec{n})\,\mathrm{d}A \qquad (3/3)$$

where CS denotes the control surface (enclosing the control volume),
flows and velocities are positive outwards and negative inwards by convention,
$\vec{n}$ is a unit vector on each surface element $\mathrm{d}A$ pointing outwards,
$\vec{V}_{\mathrm{rel}}$ is the local velocity of fluid relative to the control surface,
and $V_\perp \equiv \vec{V}_{\mathrm{rel}}\cdot\vec{n}$ is the local cross-surface velocity.

By inserting equations 3/2 and 3/3 into equation 3/1, we obtain:

$$\frac{\mathrm{d}B_{\mathrm{sys}}}{\mathrm{d}t} = \frac{\mathrm{d}}{\mathrm{d}t}\iiint_{\mathrm{CV}} \rho b\,\mathrm{d}\mathcal{V} + \iint_{\mathrm{CS}} \rho b\,(\vec{V}_{\mathrm{rel}}\cdot\vec{n})\,\mathrm{d}A \qquad (3/4)$$

Equation 3/4 is named the *Reynolds' transport theorem*; it stands now as a general, abstract accounting tool, but as we soon replace B by meaningful variables, it will prove extremely useful, allowing us to quantify the *net* effect

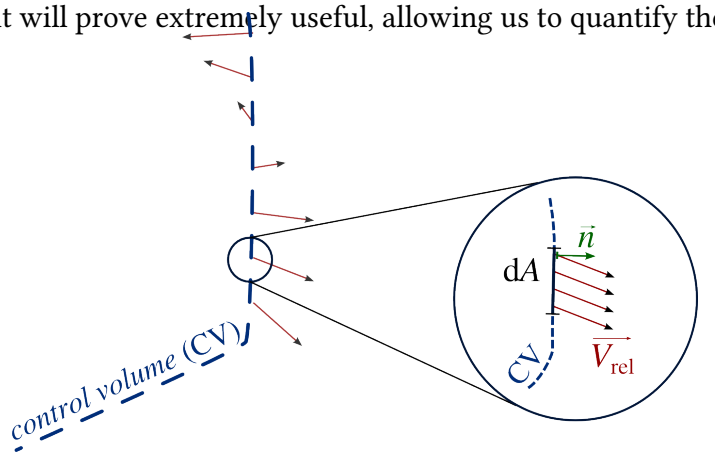

Figure 3.2 – At any arbitrary point on the border of the control volume (which we call *control surface*), some part of the system may be flowing through. The $\vec{n}$ vector defines the orientation of the volume's surface, and by convention is always pointed outwards.

Figure CC-0 o.c.

of the flow of a system through a volume for which border properties are known.

In the following sections we are going to use this equation to assert four key physical principles (§0.5) in order to analyze the flow of fluids:

- mass conservation;
- conservation of linear momentum;
- conservation of angular momentum;
- energy conservation.

3.3 Mass conservation

In this section, we focus on simply asserting that mass is conserved (eq. 0/13 p.13). Our study of the fluid's properties at the borders of the control volume is made by replacing variable B by mass m. Thus $\frac{\mathrm{d}B}{\mathrm{d}t}$ becomes $\frac{\mathrm{d}m_{\text{sys}}}{\mathrm{d}t}$, which by definition is zero.
In a similar fashion, $b \equiv B/m = m/m = 1$ and consequently the Reynolds transport theorem (3/4) becomes:

$$\frac{\mathrm{d}m_{\text{sys}}}{\mathrm{d}t} = 0 = \frac{\mathrm{d}}{\mathrm{d}t}\iiint_{\text{CV}} \rho \,\mathrm{d}\mathcal{V} + \iint_{\text{CS}} \rho\,(\vec{V}_{\text{rel}} \cdot \vec{n})\,\mathrm{d}A \tag{3/5}$$

$$\begin{array}{c}\text{the time change}\\ \text{of the system's mass}\end{array} = 0 = \begin{array}{c}\text{the rate of change}\\ \text{of mass inside}\\ \text{the control volume}\end{array} + \begin{array}{c}\text{the net mass flow}\\ \text{at the borders}\\ \text{of the control volume}\end{array}$$

This equation 3/5 is often called *continuity equation*. It allows us to compare the incoming and outgoing mass flows through the borders of the control volume.

When the control volume has well-defined inlets and outlets through which the term $\rho(\vec{V}_{\text{rel}} \cdot \vec{n})$ can be considered uniform (fig. 3.3), this equation reduces to:

$$0 = \frac{\mathrm{d}}{\mathrm{d}t}\iiint_{\text{CV}} \rho \,\mathrm{d}\mathcal{V} + \sum_{\text{out}} \{\rho V_\perp A\} + \sum_{\text{in}} \{\rho V_\perp A\} \tag{3/6}$$

$$= \frac{\mathrm{d}}{\mathrm{d}t}\iiint_{\text{CV}} \rho \,\mathrm{d}\mathcal{V} + \sum_{\text{out}} \{\rho |V_\perp| A\} - \sum_{\text{in}} \{\rho |V_\perp| A\}$$

$$= \frac{\mathrm{d}}{\mathrm{d}t}\iiint_{\text{CV}} \rho \,\mathrm{d}\mathcal{V} + \sum_{\text{out}} \{\dot{m}\} - \sum_{\text{in}} \{\dot{m}\} \tag{3/7}$$

In equation 3/6, the term $\rho V_\perp A$ at each inlet or outlet corresponds to the local mass flow $\pm\dot{m}$ (positive inwards, negative outwards) through the boundary.

With equation 3/6 we can see that when the flow is steady (§0.6), the last two terms amount to zero, and the integral $\iiint_{\text{CV}} \rho \,\mathrm{d}\mathcal{V}$ (the total amount of mass in the control volume) does not change with time.

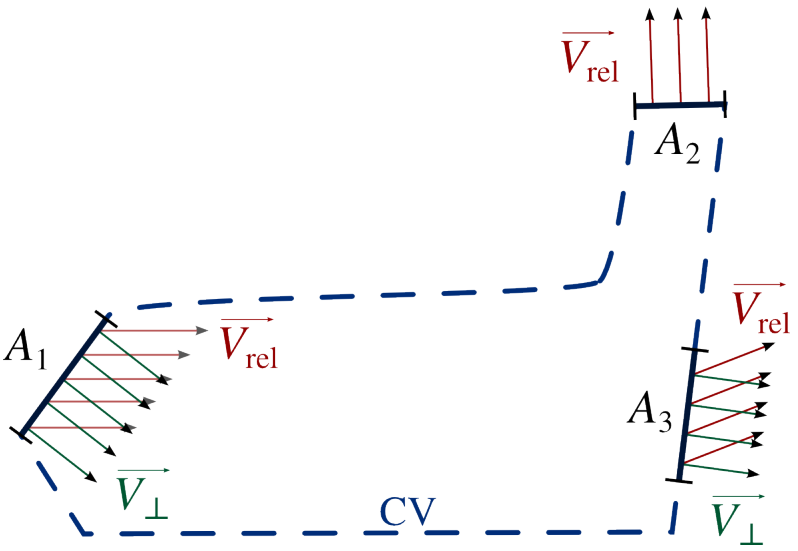

Figure 3.3 – A control volume for which the system's properties are uniform at each inlet and outlet. Here $0 = \frac{\mathrm{d}}{\mathrm{d}t}\iiint_{\mathrm{CV}} \rho \,\mathrm{d}\mathcal{V} + \rho_3|V_{\perp 3}|A_3 + \rho_2|V_{\perp 2}|A_2 - \rho_1|V_{\perp 1}|A_1$.

Figure CC-0 o.c.

3.4 Change of linear momentum

In this section, we apply Newton's second law: we assert that the variation of system's total linear momentum is equal to the net force being applied to it (eq. 0/14 p.14). Our study of the fluid's properties at the borders of the control volume is made by replacing variable B by the quantity $m\vec{V}$: momentum. Thus, $\frac{\mathrm{d}B_{\text{sys}}}{\mathrm{d}t}$ becomes $\frac{\mathrm{d}(m\vec{V}_{\text{sys}})}{\mathrm{d}t}$, which is equal to $\vec{F}_{\text{net}}$, the vector sum of forces applied on the system as it transits the control volume.
In a similar fashion, $b \equiv B/m = \vec{V}$ and equation 3/4, the Reynolds transport theorem, becomes:

$$\frac{\mathrm{d}(m\vec{V}_{sys})}{\mathrm{d}t} = \vec{F}_{\text{net}} = \frac{\mathrm{d}}{\mathrm{d}t}\iiint_{\mathrm{CV}} \rho\vec{V}\,\mathrm{d}\mathcal{V} + \iint_{\mathrm{CS}} \rho\vec{V}\,(\vec{V}_{\text{rel}}\cdot\vec{n})\,\mathrm{d}A \tag{3/8}$$

$$\begin{array}{ccccc} \text{the vector sum of forces on the system} & = & \text{the rate of change of linear momentum within the control volume} & + & \text{the net flow of linear momentum through the boundaries of the control volume} \end{array}$$

When the control volume has well-defined inlets and outlets through which the term $\rho\vec{V}(\vec{V}_{\text{rel}}\cdot\vec{n})$ can be considered uniform (fig. 3.3), this equation reduces to:

$$\vec{F}_{\text{net}} = \frac{\mathrm{d}}{\mathrm{d}t}\iiint_{\mathrm{CV}} \rho\vec{V}\,\mathrm{d}\mathcal{V} + \sum_{\text{out}}\left\{(\rho|V_\perp|A)\vec{V}\right\} - \sum_{\text{in}}\left\{(\rho|V_\perp|A)\vec{V}\right\} \tag{3/9}$$

$$= \frac{\mathrm{d}}{\mathrm{d}t}\iiint_{\mathrm{CV}} \rho\vec{V}\,\mathrm{d}\mathcal{V} + \sum_{\text{out}}\left\{\dot{m}\vec{V}\right\} - \sum_{\text{in}}\left\{\dot{m}\vec{V}\right\} \tag{3/10}$$

Let us observe the four terms of equation 3/9 for a moment, for they are full of subtleties.

First, we notice that even if the flow is steady (an therefore that $\sum_{\text{net}}(\rho V_\perp A) = 0\,\mathrm{kg\,s^{-1}}$), the last two terms do not necessarily cancel each other (i.e. it is possible that $\sum_{\text{net}}\left(\rho V_\perp A\vec{V}\right) \neq \vec{0}$).

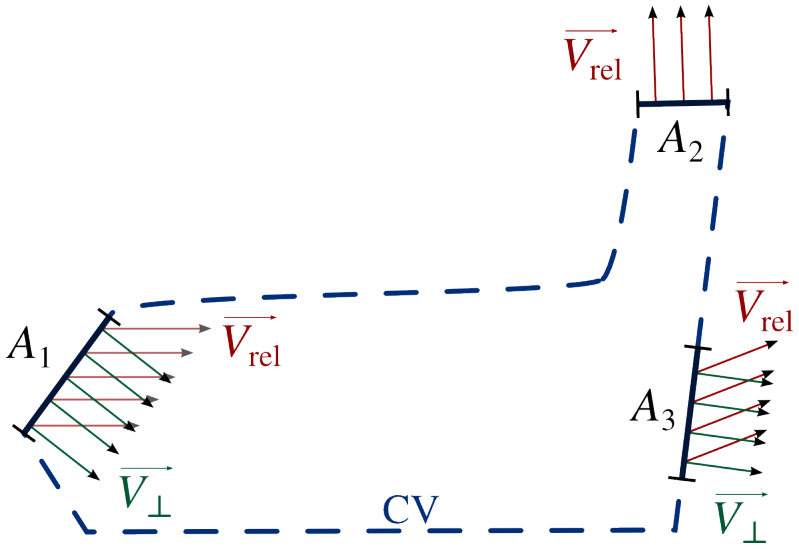

Figure 3.4 – The same control volume as in fig. 3.3. Here, since the system's properties are uniform at each inlet and outlet, $\vec{F}_{net} = \frac{d}{dt}\iiint_{CV} \rho\vec{V}\,d\mathcal{V} + \rho_3|V_{\perp 3}|A_3\vec{V}_3 + \rho_2|V_{\perp 2}|A_2\vec{V}_2 - \rho_1|V_{\perp 1}|A_1\vec{V}_1$.

Figure CC-0 o.c.

Looking further into the equation, we notice that it is quite possible that $\vec{F}_{net} = \vec{0}$ even if the net momentum flow through the boundaries is null (that is, that $\sum_{net}\left(\rho V_\perp A\vec{V}\right) \neq \vec{0}$). This would be the case, if $\iiint_{CV}\rho\,d\mathcal{V}$ (the total amount of momentum within the borders of the control volume) varies with time. Walking forwards and backwards within a rowboat would cause such an effect.

From equation 3/9 therefore, we read that two distinct phenomena can result in a net force on the system:

- A difference between the values of $\dot{m}\vec{V}$ of the fluid at the entrance and exit of the control volume (caused, for example, by a deviation of the flow);
- A change in time of the term $m\vec{V}$ within the control volume (for example, with the acceleration or the variation of the mass of the control volume).

These two factors may cancel each other, so that the system may not require any force to travel through the control volume.

3.5 Change of angular momentum

In this third spin on the Reynolds transport theorem, we assert that the change of the angular momentum of a system about a point X is equal to the net moment applied on the system about this point (eq. 0/15 p.14). Our study of the fluid's properties at the borders of the control volume is made by replacing variable B by the quantity $\vec{r}_{Xm} \wedge m\vec{V}$. Thus, $\frac{dB_{sys}}{dt}$ becomes $\frac{d(\vec{r}_{Xm}\wedge m\vec{V}_{sys})}{dt}$, which is equal to $\vec{M}_{net}$, the vector sum of moments applied on the system about point X as it transits through the control volume.

In a similar fashion, $b \equiv B/m = \vec{r} \wedge \vec{V}$ and equation 3/4, the Reynolds transport theorem, becomes:

$$\frac{\mathrm{d}(\vec{r}_{Xm} \wedge m\vec{V})_{\text{sys}}}{\mathrm{d}t} = \vec{M}_{\text{net,X}} = \frac{\mathrm{d}}{\mathrm{d}t} \iiint_{\text{CV}} \vec{r}_{Xm} \wedge \rho \vec{V} \, \mathrm{d}\mathcal{V} + \iint_{\text{CS}} \vec{r}_{Xm} \wedge \rho \, (\vec{V}_{\text{rel}} \cdot \vec{n}) \vec{V} \, \mathrm{d}A \tag{3/11}$$

the sum of moments applied to the system	=	the rate of change of the angular momentum in the control volume	+	the net flow of angular momentum through the control volume's boundaries

in which $\vec{r}_{Xm}$ is a vector giving the position of any mass m relative to point X.

When the control volume has well-defined inlets and outlets through which the term $\vec{r}_{Xm} \wedge \rho \, (\vec{V}_{\text{rel}} \cdot \vec{n}) \vec{V}$ can be considered uniform (fig. 3.5), this equation reduces to:

$$\vec{M}_{\text{net,X}} = \frac{\mathrm{d}}{\mathrm{d}t} \iiint_{\text{CV}} \vec{r}_{Xm} \wedge \rho \vec{V} \, \mathrm{d}\mathcal{V} + \sum_{\text{out}} \left\{ \vec{r}_{Xm} \wedge \dot{m} \vec{V} \right\} - \sum_{\text{in}} \left\{ \vec{r}_{Xm} \wedge \dot{m} \vec{V} \right\} \tag{3/12}$$

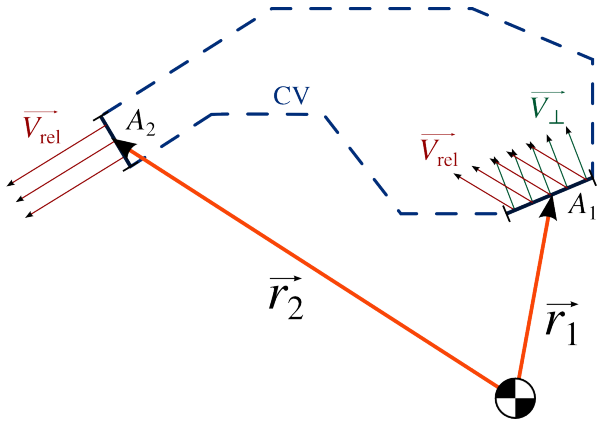

Figure 3.5 – A control volume for which the properties of the system are uniform at each inlet or outlet. Here the moment about point X is $\vec{M}_{\text{net,X}} \approx \frac{\mathrm{d}}{\mathrm{d}t} \iiint_{\text{CV}} \vec{r}_{Xm} \wedge \rho \vec{V} \, \mathrm{d}\mathcal{V} + \vec{r}_2 \wedge |\dot{m}_2| \vec{V}_2 - \vec{r}_1 \wedge |\dot{m}_1| \vec{V}_1$.

Figure CC-0 o.c.

Equation 3/12 allows us to quantify, with relative ease, the moment exerted on a system based on inlet and outlet velocities of a control volume.

3.6 Energy conservation

We conclude our frantic exploration of control volume analysis with the first principle of thermodynamics. We now simply assert that the change in the energy of a system can only be due to well-identified transfers (eq. 0/16 p.14). Our study of the fluid's properties at the borders of the control volume is made by replacing variable B by an amount of energy E_{sys}. Now, $\frac{\mathrm{d}E_{\text{sys}}}{\mathrm{d}t}$ can be attributed to three contributors:

$$\frac{\mathrm{d}E_{\text{sys}}}{\mathrm{d}t} = \dot{Q}_{\text{net in}} + \dot{W}_{\text{shaft, net in}} + \dot{W}_{\text{pressure, net in}} \tag{3/13}$$

where $\dot{Q}_{\text{net in}}$ is the net power transfered as heat;

$\dot{W}_{\text{shaft, net in}}$ is the net power added as work with a shaft;
and $\dot{W}_{\text{pressure, net in}}$ is the net power required to enter and leave the control volume.

It follows that $b \equiv B/m = E/m \equiv e$; and e is broken down into

$$e = i + e_k + e_p \tag{3/14}$$

where i is the specific internal energy ($\mathrm{J\,kg^{-1}}$);
e_k the specific kinetic energy ($\mathrm{J\,kg^{-1}}$);
and e_p the specific potential energy ($\mathrm{J\,kg^{-1}}$).

Now, the Reynolds transport theorem (equation 3/4) becomes:

$$\frac{\mathrm{d}E_{\text{sys}}}{\mathrm{d}t} = \dot{Q}_{\text{net in}} + \dot{W}_{\text{shaft, net in}} + \dot{W}_{\text{pressure, net in}} = \frac{\mathrm{d}}{\mathrm{d}t}\iiint_{\text{CV}} \rho\, e\, \mathrm{d}\mathcal{V} + \iint_{\text{CS}} \rho\, e\, (\vec{V}_{\text{rel}} \cdot \vec{n})\, \mathrm{d}A \tag{3/15}$$

When the control volume has well-defined inlets and outlets through which the term $\rho\, e\, (\vec{V}_{\text{rel}} \cdot \vec{n})$ can be considered uniform, this equation reduces to:

$$\dot{Q}_{\text{net in}} + \dot{W}_{\text{shaft, net in}} + \dot{W}_{\text{pressure, net in}} = \frac{\mathrm{d}}{\mathrm{d}t}\iiint_{\text{CV}} \rho\, e\, \mathrm{d}\mathcal{V} + \sum_{\text{out}} \{\dot{m}\, e\} - \sum_{\text{in}} \{\dot{m}\, e\} \tag{3/16}$$

$$\begin{aligned}
\dot{Q}_{\text{netin}} + \dot{W}_{\text{shaft, net in}} &= \frac{\mathrm{d}}{\mathrm{d}t}\iiint_{\text{CV}} \rho\, e\, \mathrm{d}\mathcal{V} + \sum_{\text{out}} \left\{\dot{m}(i + e_k + e_p)\right\} \\
&\quad - \sum_{\text{in}} \left\{\dot{m}(i + e_k + e_p)\right\} - \dot{W}_{\text{pressure, net in}} \\
&= \frac{\mathrm{d}}{\mathrm{d}t}\iiint_{\text{CV}} \rho\, e\, \mathrm{d}\mathcal{V} + \sum_{\text{out}} \left\{\dot{m}\left(i + \frac{1}{2}V^2 + gz\right)\right\} \\
&\quad - \sum_{\text{in}} \left\{\dot{m}\left(i + \frac{1}{2}V^2 + gz\right)\right\} + \sum_{\text{out}} \left\{\dot{m}\frac{p}{\rho}\right\} - \sum_{\text{in}} \left\{\dot{m}\frac{p}{\rho}\right\}
\end{aligned}$$

Making use of the concept of *enthalpy* defined as $h \equiv i + p/\rho$, we obtain:

$$\dot{Q}_{\text{net in}} + \dot{W}_{\text{shaft, net in}} = \frac{\mathrm{d}}{\mathrm{d}t}\iiint_{\text{CV}} \rho\, e\, \mathrm{d}\mathcal{V} + \sum_{\text{out}} \left\{\dot{m}\left(h + \frac{1}{2}V^2 + gz\right)\right\} - \sum_{\text{in}} \left\{\dot{m}\left(h + \frac{1}{2}V^2 + gz\right)\right\} \tag{3/17}$$

the net power received by the system = the rate of change of energy inside the control volume + the net energy flow rate exiting the control volume boundaries

This equation 3/17 is particularly attractive, but it necessitates the input of a large amount of experimental data to provide useful results. It is indeed very difficult to predict how the terms i and p/ρ will change for a given flow process. For example, a pump with given power $\dot{Q}_{\text{net in}}$ and $\dot{W}_{\text{shaft, net in}}$ will generate large increases of terms p, V and z if it is efficient, or a large increase of terms i and $1/\rho$ if it is inefficient. This equation 3/17, sadly, does not allow us to quantify the net effect of shear and the extent of irreversibilities in a fluid flow.

3.7 The Bernoulli equation

The Bernoulli equation has very little practical use for us; nevertheless it is so widely used that we have to dedicate a brief section to examining it. We will start from equation 3/17 and add five constraints:

1. Steady flow.
   Thus $\frac{\mathrm{d}}{\mathrm{d}t} \iiint_{\mathrm{CV}} \rho\, e\, \mathrm{d}\mathcal{V} = 0$.
   In addition, $\dot{m}$ has the same value at inlet and outlet;

2. Incompressible flow.
   Thus, ρ stays constant;

3. No heat or work transfer.
   Thus, both $\dot{Q}_{\text{net in}}$ and $\dot{W}_{\text{shaft, net in}}$ are zero;

4. No friction.
   Thus, the fluid energy i cannot increase due to an input from the control volume;

5. One-dimensional flow.
   Thus, our control volume has only one known entry and one known exit, all fluid particles move together with the same transit time, and the overall trajectory is already known.

With these five restrictions, equation 3/17 simply becomes:

$$\begin{aligned} 0 &= \sum_{\text{out}} \left\{ \dot{m}(i + \frac{p}{\rho} + e_k + e_p) \right\} - \sum_{\text{in}} \left\{ \dot{m}(i + \frac{p}{\rho} + e_k + e_p) \right\} \\ &= \dot{m} \left[(i + \frac{p_2}{\rho} + \frac{1}{2}V_2^2 + gz_2) - (i + \frac{p_1}{\rho} + \frac{1}{2}V_1^2 + gz_1) \right] \end{aligned}$$

and we here obtain the *Bernoulli equation*:

$$\frac{p_1}{\rho} + \frac{1}{2}V_1^2 + gz_1 = \frac{p_2}{\rho} + \frac{1}{2}V_2^2 + gz_2 \tag{3/18}$$

This equation describes the properties of a fluid particle in a steady, incompressible, friction-less flow with no energy transfer.

Let us insist on the incredibly frustrating restrictions brought by the five conditions above:

1. Steady flow.
   This constrains us to continuous flows with no transition effects, which is a reasonable limit;

2. Incompressible flow.
   We cannot use this equation to describe flow in compressors, turbines, diffusers, nozzles, nor in flows where $M > 0{,}6$.

3. No heat or work transfer.
   We cannot use this equation in a machine (e.g. in pumps, turbines, combustion chambers, coolers).

4. No friction.
   This is a tragic restriction! We cannot use this equation to describe a turbulent or viscous flow, e.g. near a wall or in a wake.

5. One-dimensional flow.
   This equation is only valid if we know precisely the trajectory of the fluid whose properties are being calculated.

Among these, the last is the most severe (and the most often forgotten): **the Bernoulli equation does not allow us to predict the trajectory of fluid particles**. Just like all of the other equations in this chapter, it requires a control volume with a known inlet and a known outlet.

3.8 Limits of integral analysis

Integral analysis is an incredibly useful tool in fluid dynamics: in any given problem, it allows us to rapidly describe and calculate the main fluid phenomena at hand. The net force exerted on the fluid as it is deflected downwards by a helicopter, for example, can be calculated using just a loosely-drawn control volume and a single vector equation.

As we progress through exercise sheet 3, however, the limits of this method slowly become apparent. They are twofold.

- First, we are confined to calculating the *net* effect of fluid flow. The net force, for example, encompasses the integral effect of all forces —due to pressure, shear, and gravity— applied on the fluid as it transits through the control volume. Integral analysis gives us absolutely no way of distinguishing between those sub-components. In order to do that (for example, to calculate which part of a pump's mechanical power is lost to internal viscous effects), we would need to look within the control volume.

- Second, all four of our equations in this chapter only work in one direction. The value $\mathrm{d}B_{\mathrm{sys}}/\,\mathrm{d}t$ of any finite integral cannot be used to find which function $\rho b V_\perp \,\mathrm{d}A$ was integrated over the control surface to obtain it. For example, there are an *infinite* number of velocity profiles which will result in a net force of $-12\,\mathrm{N}$. Knowing the net value of an integral, we cannot deduce the conditions which lead to it.
  In practice, this is a major limitation on the use of integral analysis, because it confines us to working with large swaths of experimental data gathered at the borders of our control volumes. From the wake below the helicopter, we deduce the net force; but the net force tells us nothing about the shape of the wake.

Clearly, in order to overcome these limitations, we are going to need to open up the control volume, and look at the details of the flow within — perhaps by dividing it into a myriad of sub-control volumes. This is what we set ourselves to in chapter 4, with a thundering and formidable methodology we shall call *derivative analysis*.

Fluid Mechanics
Exercise sheet 3 – Integral analysis

last edited July 2, 2016

These lecture notes are based on textbooks by White [9], Çengel & al.[12], and Munson & al.[14].

Except otherwise indicated, we assume that fluids are Newtonian, and that:
$\rho_{water} = 1\,000\,\mathrm{kg\,m^{-3}}$; $p_{atm.} = 1\,\mathrm{bar}$; $\rho_{atm.} = 1{,}225\,\mathrm{kg\,m^{-3}}$; $T_{atm.} = 11{,}3\,^{\circ}\mathrm{C}$; $\mu_{atm.} = 1{,}5 \cdot 10^{-5}\,\mathrm{N\,s\,m^{-2}}$;
$g = 9{,}81\,\mathrm{m\,s^{-2}}$. Air is modeled as a perfect gas ($R_{air} = 287\,\mathrm{J\,K^{-1}\,kg^{-1}}$; $\gamma_{air} = 1{,}4$; $c_{p\,air} = 1\,005\,\mathrm{J\,kg^{-1}\,K^{-1}}$).

Reynolds Transport Theorem:

$$\frac{\mathrm{d}B_{sys}}{\mathrm{d}t} = \frac{\mathrm{d}}{\mathrm{d}t}\iiint_{CV} \rho b \,\mathrm{d}\mathcal{V} + \iint_{CS} \rho b \,(\vec{V}_{rel} \cdot \vec{n})\,\mathrm{d}A \tag{3/4}$$

Mass conservation:

$$\frac{\mathrm{d}m_{sys}}{\mathrm{d}t} = 0 = \frac{\mathrm{d}}{\mathrm{d}t}\iiint_{CV} \rho \,\mathrm{d}\mathcal{V} + \iint_{CS} \rho \,(\vec{V}_{rel} \cdot \vec{n})\,\mathrm{d}A \tag{3/5}$$

Change in linear momentum:

$$\frac{\mathrm{d}(m\vec{V}_{sys})}{\mathrm{d}t} = \vec{F}_{net} = \frac{\mathrm{d}}{\mathrm{d}t}\iiint_{CV} \rho\vec{V} \,\mathrm{d}\mathcal{V} + \iint_{CS} \rho\vec{V} \,(\vec{V}_{rel} \cdot \vec{n})\,\mathrm{d}A \tag{3/8}$$

Change in angular momentum:

$$\frac{\mathrm{d}(\vec{r}_{Xm} \wedge m\vec{V})_{sys}}{\mathrm{d}t} = \vec{M}_{net,X} = \frac{\mathrm{d}}{\mathrm{d}t}\iiint_{CV} \vec{r}_{Xm} \wedge \rho\vec{V} \,\mathrm{d}\mathcal{V} + \iint_{CS} \vec{r}_{Xm} \wedge \rho \,(\vec{V}_{rel} \cdot \vec{n})\vec{V}\,\mathrm{d}A \tag{3/11}$$

3.1 Water jet

White [9] Ex3.9

A horizontal water jet hits a vertical wall and is split in two symmetrical vertical flows (fig. 3.6). The water nozzle has a $3\,\mathrm{cm^2}$ cross-sectional area, and the water speed is $20\,\mathrm{m\,s^{-1}}$.
In this exercise, we consider the simplest possible case, with the effects of gravity and viscosity neglected. In that case, the water is simply deflected on the wall without changing its velocity, and the velocity distribution is always uniform.

1. What is the velocity of each water flow as it leaves the wall?
2. What is the force exerted by the water on the wall?

Now we let the wall move longitudinally with the water jet, with a speed of $15\,\mathrm{m\,s^{-1}}$.

3. What is the force exerted by the water on the wall?

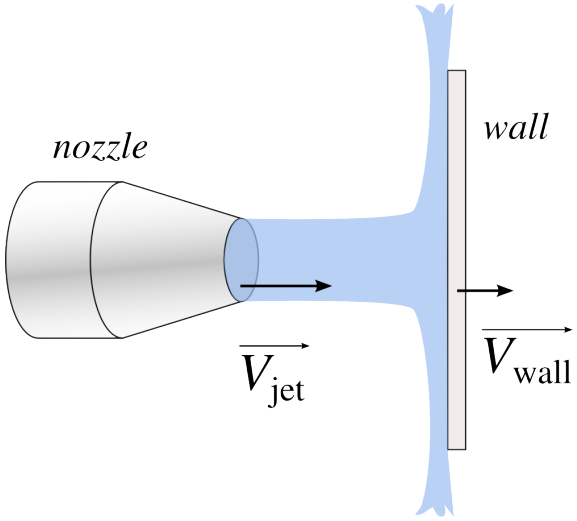

Figure 3.6 – A water jet flowing out of a nozzle (left), and impacting a vertical wall on the right.

Figure CC-0 o.c.

4. What is the velocity of each water jet as it leaves the wall?
5. How would the above results be changed if viscous effects and three-dimensional effects were taken into account?

3.2 Exhaust gas deflector

A deflector is used behind a stationary aircraft during ground testing of a jet engine (fig. 3.7).

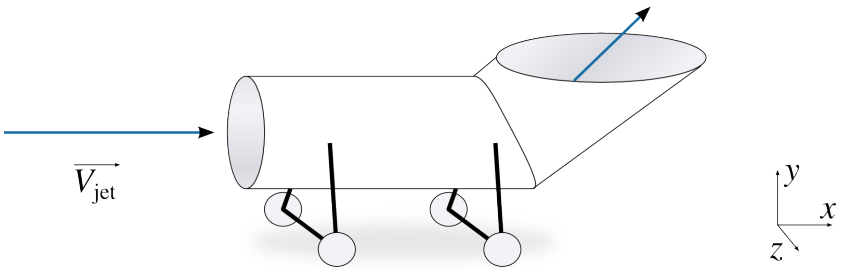

Figure 3.7 – A mobile exhaust gas deflector, used to deflect hot jet engine exhaust gases upwards during ground tests.

Figure CC-0 o.c.

The deflector is fed with a horizontal air jet with a quasi-uniform velocity profile; the speed is 600 $\mathrm{km\,h^{-1}}$, temperature 400 °C and the pressure is atmospheric. As the exhaust gases travel through the pipe, their heat losses are negligible. Gases are rejected with a 40° angle relative to the horizontal.

The inlet diameter is 1 m and the horizontal outlet surface is 6 $\mathrm{m^2}$.

1. What is the force exerted on the ground by the deflection of the exhaust gases?
2. Describe qualitatively a modification to the deflector that would reduce the horizontal component of force.
3. What would the force be if the deflector traveled rearwards (positive x-direction) with a velocity of 10 $\mathrm{m\,s^{-1}}$?

3.3 Pelton water turbine

White [9] P3.56

A water turbine is modeled as the following system: a water jet exiting a stationary nozzle hits a blade which is mounted on a rotor (fig. 3.8). In the ideal case, viscous effects can be neglected, and the water jet is deflected entirely with a 180° angle.

The nozzle has a cross-section diameter of 5 cm and produces a water jet with a speed of 15 $\mathrm{m\,s^{-1}}$. The rotor diameter is 2 m and the blade height is negligibly small.

We first study the case in which the rotor is prevented from rotating, so that the blade is purely stationary.

1. What is the force exerted by the water on the blade?
2. What is the moment exerted by the blade around the rotor axis?
3. What is the power transmitted to the rotor?

We now let the rotor rotate freely. Friction losses are negligible, and it accelerates until it reaches maximum velocity.

4. What is the rotor rotation speed?
5. What is the power transmitted to the rotor?

The rotor is now coupled to an electrical generator.

6. Show that the maximum power that can be transmitted to the generator occurs for $V_{\text{blade}} = \frac{1}{3} V_{\text{water}}$.
7. What is the maximum power that can be transmitted to the generator?
8. How would the above result change if viscous effects were taken into account?

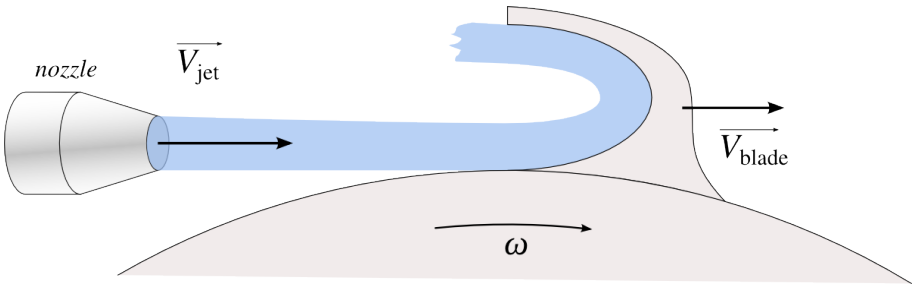

Figure 3.8 – Schematic drawing of a water turbine blade. This type of turbine is called Pelton turbine.

Figure CC-0 o.c.

3.4 Snow plow

derived from Gerhart & Gross [4] Ex5.9

A road-based snow plow (fig. 3.9) is clearing up the snow on a flat surface. We wish to quantify the power required for its operation.

The snow plow is advancing at 25 $\mathrm{km\,h^{-1}}$; its blade has a frontal-view width of 4 m.

The snow on the ground is 30 cm deep and has density 300 $\mathrm{kg\,m^{-3}}$.

The snow is pushed along the blade and is rejected horizontally with a 30° angle to the left of the plow. Its density has then risen to 450 $\mathrm{kg\,m^{-3}}$. The cross-section area A_{outlet} of the outflowing snow in the x-y plane is 1,1 $\mathrm{m^2}$.

1. What is the force exerted on the blade by the deflection of the snow? (Indicate its magnitude and coordinates)
2. What is the power required for the operation of the snow plow?
3. If the plow velocity was increased by 10 %, what would be the increase in power?

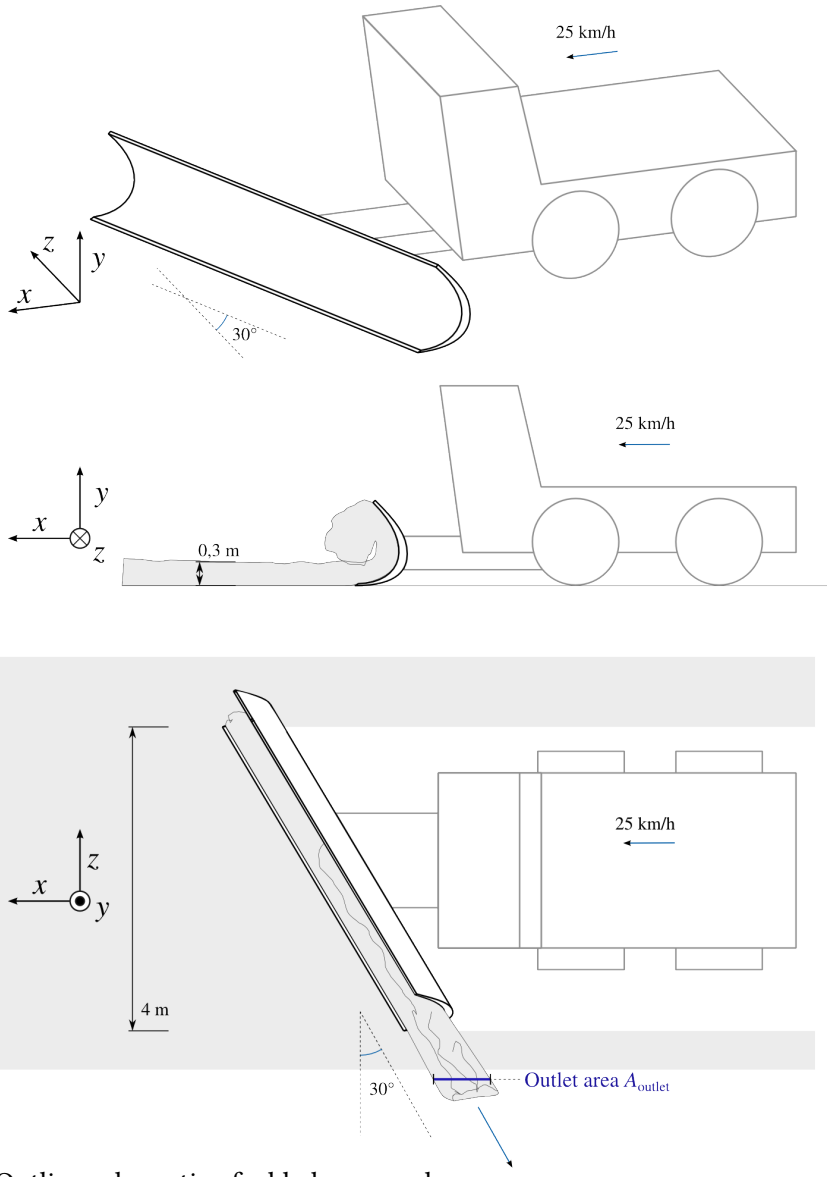

Figure 3.9 – Outline schematic of a blade snow plow.

3.5 Motorized snow plow

non-examinable. Based on a problem from Gerhart & Gross [4]

A different type of snow plow is used on another vehicle. A cylindrical rotor with radius $50\,\mathrm{cm}$ rotates at $800\,\mathrm{rpm}$. The machine travels longitudinally with a speed of $5\,\mathrm{km\,h^{-1}}$ in a $40\,\mathrm{cm}$-deep layer of snow.

The apparatus's width is $2\,\mathrm{m}$ at the entrance and $1\,\mathrm{m}$ at the outlet. The snow density increases from $200\,\mathrm{kg\,m^{-3}}$ at the inlet to $250\,\mathrm{kg\,m^{-3}}$ at the outlet.

The requirements are for the snow to be rejected with a uniform $10\,\mathrm{m\,s^{-1}}$ velocity and a 30° angle relative to the horizontal.

1. What is the net moment generated by the snow movement around the cylinder rotation axis?
2. What is the power required to rotate the cylinder?

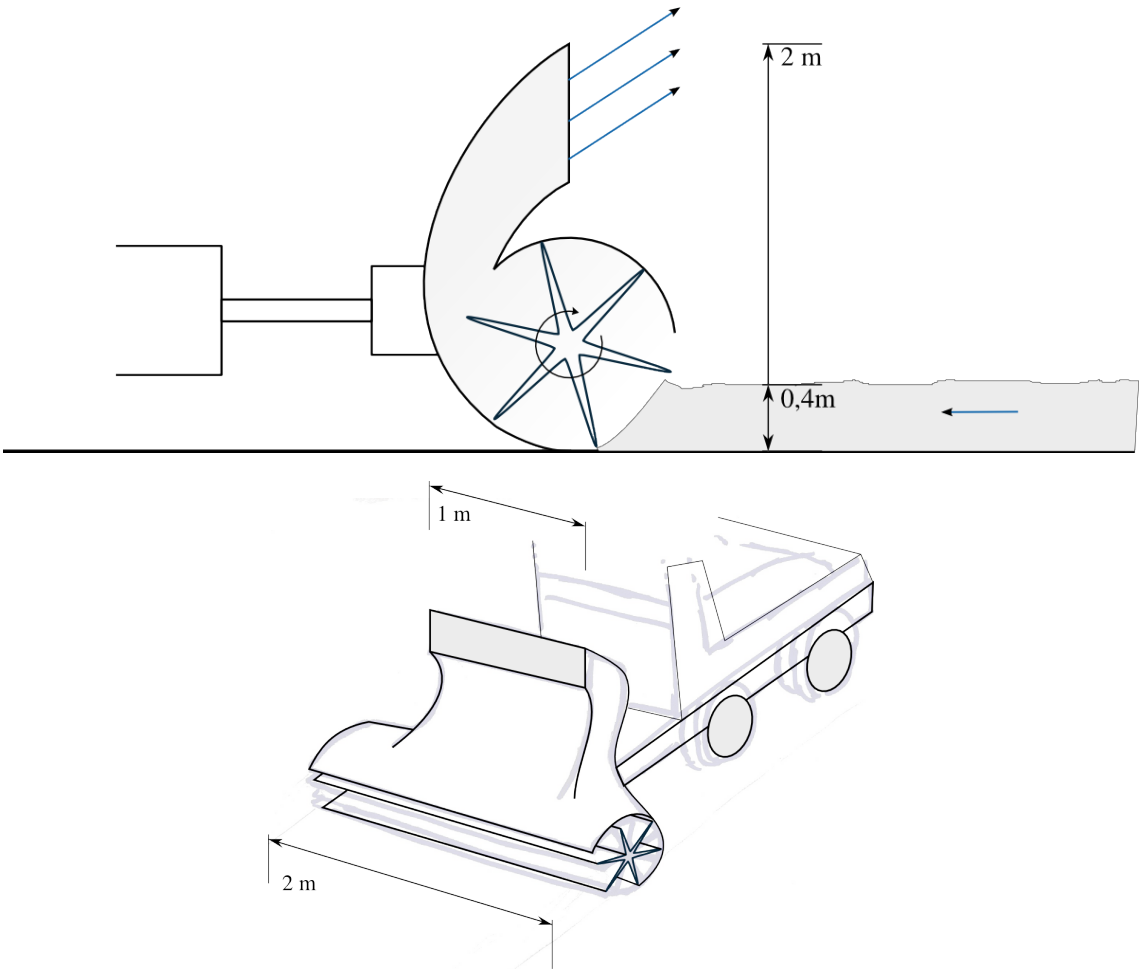

Figure 3.10 – Conceptual sketch of a motorized snow plow.

Figure CC-0 o.c.

3.6 Drag on a cylindrical profile

In order to measure the drag on a cylindrical profile, a cylindrical tube is positioned perpendicular to the air flow in a wind tunnel (fig. 3.11), and the longitudinal component of velocity is measured across the tunnel section.

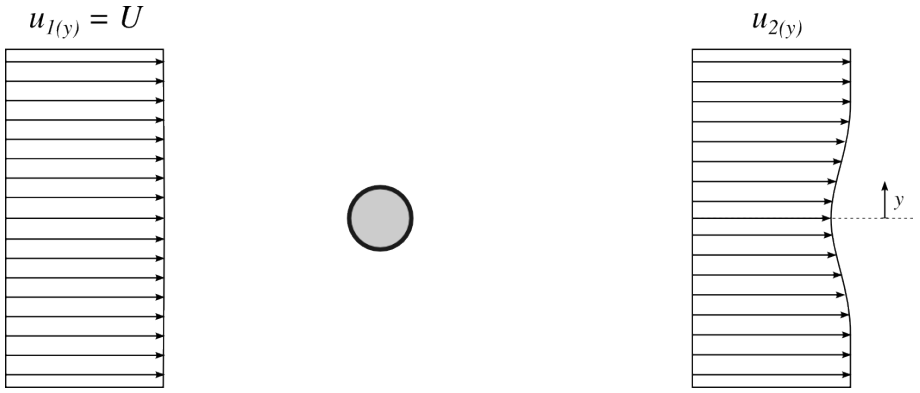

Figure 3.11 – A cylinder profile set up in a wind tunnel, with the air flowing from left to right.

Figure CC-0 o.c.

Upstream of the cylinder, the air flow velocity is uniform ($u_1 = U = 30\,\mathrm{m\,s^{-1}}$).

Downstream of the cylinder, the speed is measured across a $2\,\mathrm{m}$ height interval. Horizontal speed measurements are gathered and modeled with the following relationship:

$$u_{2(y)} = 29 + y^2 \tag{3/19}$$

The width of the cylinder (perpendicular to the flow) is $2\,\mathrm{m}$. The Mach number is very low, and the air density remains constant at $\rho = 1{,}23\,\mathrm{kg\,m^{-3}}$; pressure is uniform all along the measurement field.

- What is the drag force applying on the cylinder?
- How would this value change if the flow in the cylinder wake was turbulent, and the function $u_{2(y)}$ above only modeled *time-averaged values* of the horizontal velocity?

3.7 Drag on a flat plate

We wish to measure the drag applying on a thin plate positioned parallel to an air stream. In order to achieve this, measurements of the horizontal velocity u are made around the plate (fig. 3.12).

At the leading edge of the plate, the horizontal velocity of the air is uniform: $u_1 = U = 10\,\mathrm{m\,s^{-1}}$.

At the trailing edge of the plate, we observe that a thin layer of air has been slowed down by the effect of shear. This layer, called *boundary layer*, has a thickness of $\delta = 1\,\mathrm{cm}$. The horizontal velocity profile can be modeled with the relation:

$$u_{2(y)} = U\left(\frac{y}{\delta}\right)^{\frac{1}{7}} \tag{3/20}$$

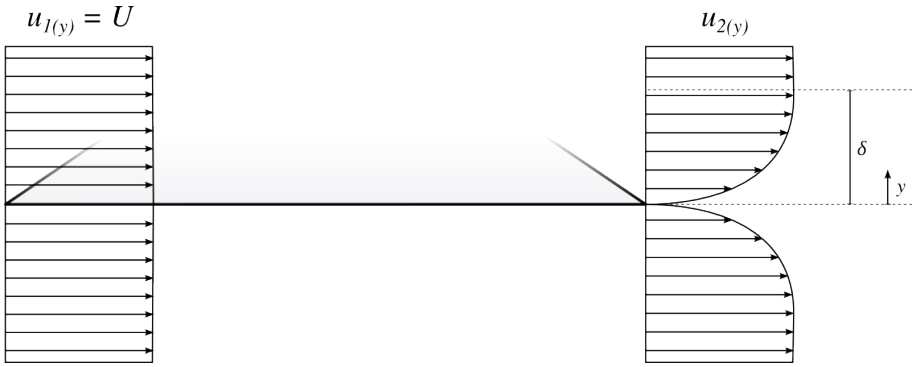

Figure 3.12 – Side view of a plate positioned parallel to the flow.

figure CC-0 o.c.

The width of the plate (perpendicular to the flow) is 30 cm and it has negligible thickness. The flow is incompressible ($\rho = 1{,}23\,\mathrm{kg\,m^{-3}}$) and the pressure is uniform.

- What is the drag force applying on the plate?
- What is the power required to compensate the drag? Under which form is the kinetic energy lost by the flow carried away?

3.8 Drag measurements in a wind tunnel

A group of students proceeds with speed measurements in a wind tunnel. The objective is to measure the drag applying on a wing profile positioned across the tunnel test section (fig. 3.13).

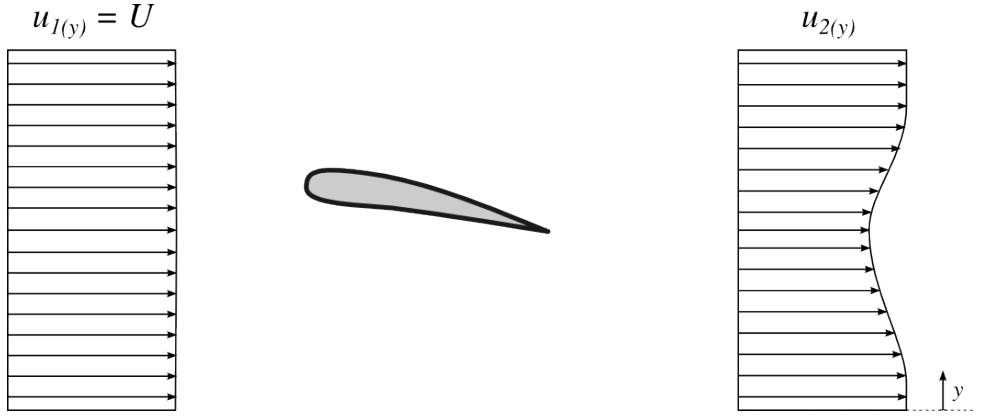

Figure 3.13 – Wing profile positioned across a wind tunnel. The horizontal velocity distributions upstream and downstream of the profile are also shown.

figure CC-0 o.c.

Upstream of the profile, the air flow velocity is uniform ($u_1 = U = 50\,\mathrm{m\,s^{-1}}$).

Downstream of the profile, horizontal velocity measurements are made every 5 cm across the flow; the following results are obtained:

vertical position (cm)	horizontal speed u_2 ($\mathrm{m\,s^{-1}}$)
0	50
5	50
10	49
15	48
20	45
25	41
30	39
35	40
40	43
45	47
50	48
55	50
60	50

The width of the profile (perpendicular to the flow) is 50 cm. The airflow is incompressible ($\rho = 1{,}23\,\mathrm{kg\,m^{-3}}$) and the pressure is uniform across the measurement surface.

1. What is the drag applying on the profile?
2. How would the above calculation change if *vertical* speed measurements were also taken into account?

3.9 Moment on gas deflector

We revisit the exhaust gas deflector of exercise 3.2. Figure 3.14 shows the deflector viewed from the side. The midpoint of the inlet is 2 m above and 5 m behind the wheel labeled "**A**", while the midpoint of the outlet is 3,5 m above and 1,5 m behind it.

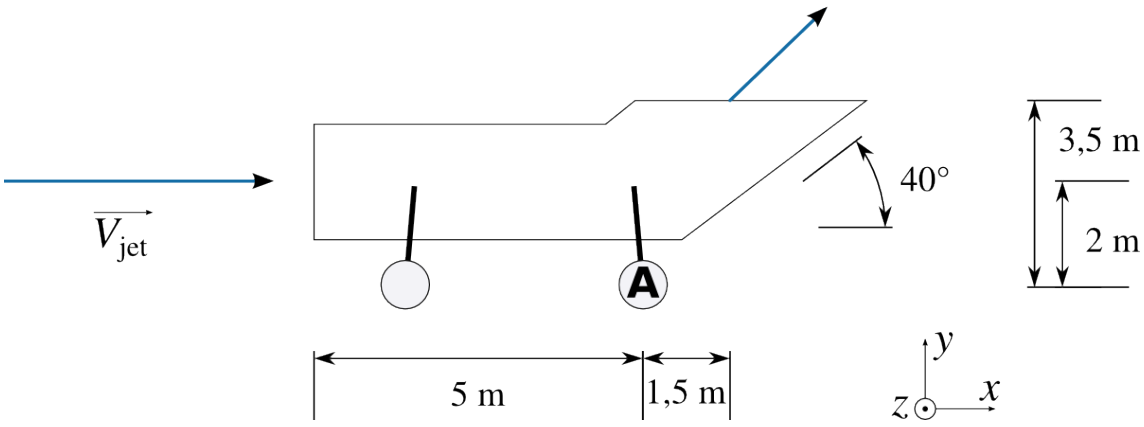

Figure 3.14 – Side view of the mobile exhaust gas deflector which was shown in fig. 3.7 p.64

Figure CC-0 o.c.

What is the moment generated by the gas flow about the axis of the wheel labeled "**A**"?

3.10 Helicopter tail moment

In a helicopter, the role of the tail is to counter exactly the moment exerted by the main rotor about the main rotor axis. This is usually done using a tail rotor which is rotating around a horizontal axis.

A helicopter, shown in figure 3.15, is designed to use a tail *without* a rotor, so as to reduce risks of accidents when landing and taking off. The tail is a long hollow cylindrical tube with two inlets and one outlet. To simplify calculations, we consider that pressure is atmospheric at every inlet and outlet.

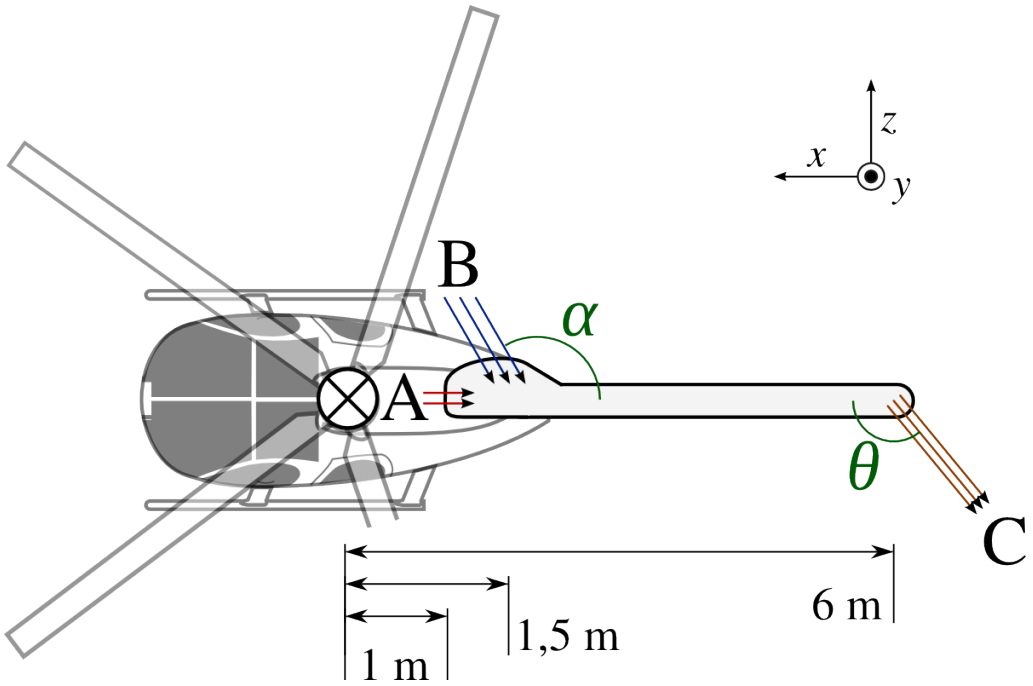

Figure 3.15 – Top-view of a helicopter using a rotor-less tail.

Figure derived from a figure CC-BY-SA *by Commons User:FOX 52*

- inlet A has a cross-section area of $0{,}2\,\mathrm{m}^2$. It contributes hot exhaust gases of density $0{,}8\,\mathrm{kg\,m^{-3}}$ and velocity $12\,\mathrm{m\,s^{-1}}$, aligned with the (x) axis of the tail;
- inlet B contributes $25\,\mathrm{kg\,s^{-1}}$ of atmospheric air incoming at an angle $\alpha = 130°$ relative to the axis of the tail, with a velocity of $3\,\mathrm{m\,s^{-1}}$.

The mix of exhaust gases and atmospheric air is rejected at the tip of the tail (outlet C) with a fixed velocity of $45\,\mathrm{m\,s^{-1}}$. The angle θ at which gases are rejected is controlled by the flight computer.

1. What is the rejection angle θ required so that the tail generates a moment of $+6\,\mathrm{kN\,m}$ around the main rotor (y) axis?
2. Propose and quantify a modification to the tail geometry or operating conditions that would allow the tail to produce no thrust (that is to say, zero force in the x-axis), while still generating the same moment.

Remark: this system is commercialized by MD Helicopters as the NOTAR*. The use of exhaust gases was abandoned, however, a clever use of air circulation around the tail pipe axis contributes to the generated moment; this effect is explored in chapter 8 (§8.6.2 p.167).*

3.11 Pressure losses in a pipe flow

Non-examinable. Based on White [9]

Water is circulated inside a cylindrical pipe with diameter 1 m (fig. 3.16).

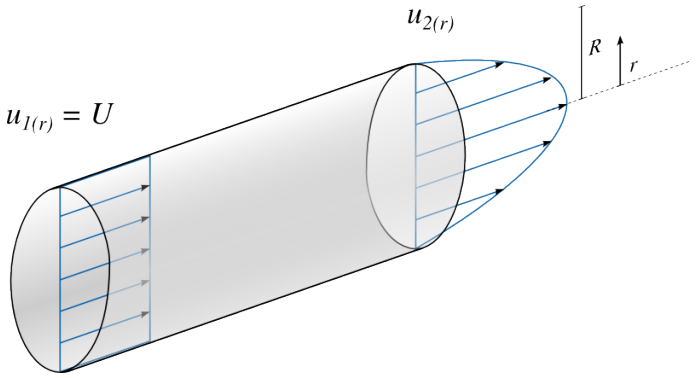

Figure 3.16 – Velocity profiles at the inlet and outlet of a circular pipe.

Figure CC-0 o.c.

At the entrance of the pipe, the speed is uniform: $u_1 = U_{\text{av.}} = 5\,\text{m}\,\text{s}^{-1}$.

At the outlet of the pipe, the velocity profile is not uniform. It can be modeled as a function of the radius with the relationship:

$$u_{2(r)} = U_{\text{center}} \left(1 - \frac{r}{R}\right)^{\frac{1}{7}} \tag{3/21}$$

The momentum flow at the exit may be described solely in terms of the average velocity $U_{\text{av.}}$ with the help of a *momentum flux correction factor* β, such that $\rho \int u_2^2 \, \mathrm{d}A = \beta \rho A U_{\text{av.}}^2$. When $u_2 = U_{\text{center}} \left(1 - \frac{r}{R}\right)^m$, it can be shown that $\beta = \frac{(1+m)^2(2+m)^2}{2(1+2m)(2+2m)}$, and so with $m = \frac{1}{7}$, we have $\beta \approx 1{,}02$.

[difficult question]

What is the net force applied on the water so that it may travel through the pipe?

3.12 Thrust reverser

non-examinable

A turbofan installed on a civilian aircraft is equipped with a thrust inverter system. When the inverters are deployed, the "cold" outer flow of the engine is deflected outside of the engine nacelle.

We accept that the following characteristics of the engine, when it is running at full power, and measured from a reference point moving with the engine, are independent of the aircraft speed and engine configuration:

Inlet diameter	$D_1 = 2{,}5\,\text{m}$
Inlet speed	$V_1 = 60\,\text{m}\,\text{s}^{-1}$
Inlet temperature	$T_1 = 288\,\text{K}$
Cold flow outlet velocity	$V_3 = 85\,\text{m}\,\text{s}^{-1}$
Cold flow temperature	$T_3 = 300\,\text{K}$
Hot flow outlet diameter	$D_4 = 0{,}5\,\text{m}$
Hot flow outlet velocity	$V_4 = 200\,\text{m}\,\text{s}^{-1}$
Hot flow outlet temperature	$T_4 = 400\,\text{K}$
Air pressure at all exits	$p_3 = p_4 = p_{\text{atm.}} = 1\,\text{bar}$
Bypass ratio	$\dot{m}_3/\dot{m}_4 = 6$

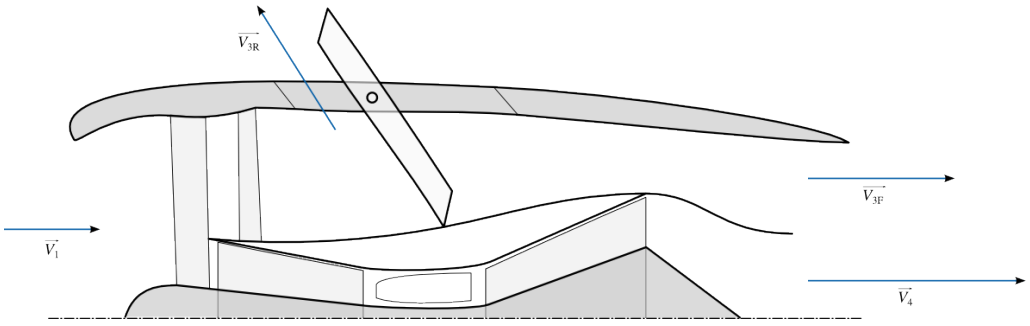

Figure 3.17 – Conceptual layout sketch of a turbofan. The airflow is from left to right.

Figure CC-BY-SA O.C.

We first study the engine in normal (forward thrust) configuration.

1. When mounted on a stationary test bench, what is the thrust provided by the engine?
2. In the approximation that the operating parameters remain unchanged, what is the thrust generated when the engine moves with a speed of $40\,\mathrm{m\,s^{-1}}$?

We now deploy the thrust reversers. They deflect the cold flow with a 75° angle relative to the aircraft longitudinal axis.

3. What is the net thrust developed when the aircraft velocity is $40\,\mathrm{m\,s^{-1}}$?
4. What is the net thrust developed when the aircraft is stationary?

Answers

3.1 1) $F_{\text{net sys.}} = -120\,\text{N}$; 2) $F_{\text{net sys.}} = -7{,}5\,\text{N}$, $\vec{V}_{\text{exit, absolute}} = (15; 5)$; $V_{\text{exit, absolute}} = 15{,}8\,\text{m s}^{-1}$.

3.2 1) $F_{\text{net } x} = -9{,}532\,\text{kN}$ & $F_{\text{net } y} = +1{,}479\,\text{kN}$: $F_{\text{net}} = 9{,}646\,\text{kN}$;
2) $F_{\text{net 2}} = 8{,}525\,\text{kN}$.

3.3 1) $F_{\text{net}} = -883{,}6\,\text{N}$; 2) $M_{\text{net}\,X} = |F_{\text{net}}|R = 883{,}6\,\text{N m}$;
3) $\dot{W}_{\text{rotor}} = 0\,\text{W}$; 4) $\omega = 143{,}2\,\text{rpm}$ ($F_{\text{net}} = 0\,\text{N}$);
5) $\dot{W}_{\text{rotor}} = 0\,\text{W}$ again;
6) $\dot{W}_{\text{rotor, max}} = 1{,}963\,\text{kW}$ @ $V_{\text{blade, optimal}} = \frac{1}{3}V_{\text{water jet}}$.

3.4 1) $\dot{m} = 2\,500\,\text{kg s}^{-1}$; $F_{\text{net } x} = +10{,}07\,\text{kN}$, $F_{\text{net } z} = +12{,}63\,\text{kN}$;
2) $\dot{W} = \vec{F}_{\text{net}} \cdot \vec{V}_{\text{plow}} = F_{\text{net}x}|V_1| = 69{,}94\,\text{kW}$

3.5 $\dot{m} = 222{,}4\,\text{kg s}^{-1}$, $h_2 = 0{,}1027\,\text{m}$: $M_{\text{net}X} = -2\,697\,\text{N m}$; $\dot{W} = \omega M_{\text{net}X} = 225{,}9\,\text{kW}$.

3.6 $F_{\text{net}x} = \rho L \int_{S2} \left(u_2^2 - U u_2\right)\,\text{d}y = -95{,}78\,\text{N}$.

3.7 $F_{\text{net}x} = \rho L \int_0^{\delta} \left(u_{(y)}^2 - U u_{(y)}\right)\,\text{d}y = -7{,}175 \cdot 10^{-2}\,\text{N}$: $\dot{W}_{\text{drag}} = U|F_{\text{net}x}| = 0{,}718\,\text{W}$.

3.8 $F_{\text{net}x} \approx \rho L \Sigma_y \left[\left(u_2^2 - U u_2\right)\delta y\right] = -64{,}8\,\text{N}$.

3.9 Re-use $\dot{m} = 67{,}76\,\text{kg s}^{-1}$, $V_1 = 166{,}7\,\text{m s}^{-1}$, $V_2 = 33{,}94\,\text{m s}^{-1}$ from ex.3.2. From trigonometry, find $R_{2\perp V_2} = 1{,}717\,\text{m}$. Then, plug in eq. 3/12 p.59: $M_{\text{net}} = -18{,}64\,\text{kN m}$ in z-direction.

3.10 1) Work eq. 3/11 down to scalar equation (in y-direction), solve for θ: $\theta = 125{,}6°$.
2) There are multiple solutions which allow both moment and force equations to be solved at the same time. r_{C} can be shortened, the flow in C can be split into forward and rearward components, or tilted downwards etc. Reductions in $\dot{m}_{\text{B}}$ or V_{C} are also possible, but quantifying them requires solving both equations at once.

3.11 $V_{\text{center}} = 1{,}2245U$; $F_{\text{net}} = +393\,\text{N}$ (positive!)

3.12 $\dot{m}_{\text{cold}} = 297\,\text{kg s}^{-1}$, $\dot{m}_{\text{hot}} = 59{,}4\,\text{kg s}^{-1}$; $F_{\text{cold flow, normal, bench \& runway}} = +74{,}25\,\text{kN}$, $F_{\text{hot flow, normal \& reverse, bench \& runway}} = +8{,}316\,\text{kN}$;
$F_{\text{cold flow, reverse, bench \& runway}} = -24{,}35\,\text{kN}$ and $F_{\text{hot flow, normal, bench \& runway}} = +8{,}316\,\text{kN}$.
Adding the net pressure force due to the (lossless) flow acceleration upstream of the inlet, we obtain, on the bench: $F_{\text{engine bench, normal}} = -93{,}26\,\text{kN}$, $F_{\text{engine bench, reverse}} = +5{,}344\,\text{kN}$; and on the runway: $F_{\text{engine runway, normal}} = -92{,}5\,\text{kN}$ and $F_{\text{engine bench, reverse}} = +6{,}094\,\text{kN}$.

Fluid Mechanics
Chapter 4 – Differential analysis of fluid flows

last edited May 14, 2016

These lecture notes are based on textbooks by White [9], Çengel & al.[12], and Munson & al.[14].

4.1 Motivation

In this chapter we assign ourselves the daunting task of describing the movement of fluids in an extensive manner. We wish to express formally and calculate the dynamics of fluids –the velocity field as a function of time— in any arbitrary situation.

Let us not shy away from the truth: the methods developed here are disproportionately complex in comparison to the solutions they allow us to derive by hand. Despite this, this chapter is extraordinarily important, for two reasons:

- derivative analysis allows us to formally *describe* and *relate* the key parameters that regulate fluid flow, and so is the key to developing an understanding of any fluid phenomenon, even when solutions cannot be derived;
- it is the backbone for *computational fluid dynamics* in which approximate solutions are obtained using numerical procedures.

4.2 Eulerian description of fluid flow

4.2.1 Problem description

From now on, we wish to describe the velocity and pressure fields of a fluid with the highest possible resolution. For this, we aim to predict and describe the trajectory of *fluid particles* (§0.2.2) as they travel.

Newton's second law allows us to quantify how the speed vector of a particle varies with time. If we know all of the forces to which one particle is

subjected, we can obtain a streak of velocity vectors $\vec{V}_{\text{particle}} = (u, v, w) = f(x, y, z, t)$ as the particle moves through our area of interest. This is a description of the velocity of *one* particle; we obtain a function of time which depends on where and when the particle started its travel: $\vec{V}_{\text{particle}} = f(x_0, y_0, z_0, t_0, t)$. This is the process used in solid mechanics when we wish to describe the movement of an object, for example, a single satellite in orbit.

This kind of description, however, is poorly suited to the description of fluid flow, for three reasons:

- Firstly, in order to describe a given fluid flow (e.g. air flow around a car external mirror), we would need a large number of initial points (x_0, y_0, z_0, t_0), and we would then obtain as many trajectories $\vec{V}_{\text{particle}}$. It then becomes very difficult to describe to study and describe a problem that is local in space (e.g. the wake immediately behind the car mirror), because this requires finding out where the particles of interest originated, and accounting for the trajectories of each of them.
- Secondly, the concept of a "fluid particle" is not well-suited to the drawing of trajectories. Indeed, particles can not only strain indefinitely, but also diffuse into the surrounding particles, "blurring" and blending themselves one into another.
- Finally, the speed and other properties of a given particle very strongly depend on the properties of the surrounding particles. We have to resolve *simultaneously* the movement equations of all of the particles. A space-based description of properties —one in which we describe properties at a chosen fixed point of coordinates $x_{\text{point}}, y_{\text{point}}, z_{\text{point}}, t_{\text{point}}$— is much more useful than a particle-based description which depends on departure points x_0, y_0, z_0, t_0. It is easier to determine the acceleration of a particle together with that of its current neighbors, than together with that of its initial (former) neighbors.

What we are looking for, therefore, is a description of the velocity fields that is expressed in terms of a fixed observation point $\vec{V}_{\text{point}} = (u, v, w) = f(x_{\text{point}}, y_{\text{point}}, z_{\text{point}}, t)$, through which particles of many different origins may be passing. This is termed a *Eulerian* flow description, as opposed to the particle-based *Lagrangian* description. Grouping all of the point velocities in our flow study zone, we will obtain a velocity field $\vec{V}_{\text{point}}$ that is a function of time.

4.2.2 Substantial derivative

Let us imagine a water canal flowing at constant and uniform speed $u = U_{\text{canal}}$ and filled with water whose temperature T_{water} is steady in time, but not homogeneous (fig. 4.1). We measure this temperature with a stationary probe, obtaining $T_{\text{probe}} = T_{\text{water}}$. Even though the temperature T_{water} is constant, at the probe, temperature will be changing with time:

$$\begin{cases} \frac{\mathrm{d}T_{\text{water}}}{\mathrm{d}t} &= 0 \\ \frac{\mathrm{d}T_{\text{probe}}}{\mathrm{d}t} &= \frac{\mathrm{d}T_{\text{water}}}{\mathrm{d}x}\, u_{\text{water}} \end{cases}$$

In the case where the water temperature is not simply heterogeneous, but also unsteady (varying in time with a rate $\frac{\partial T}{\partial t}$) then that rate will also affect

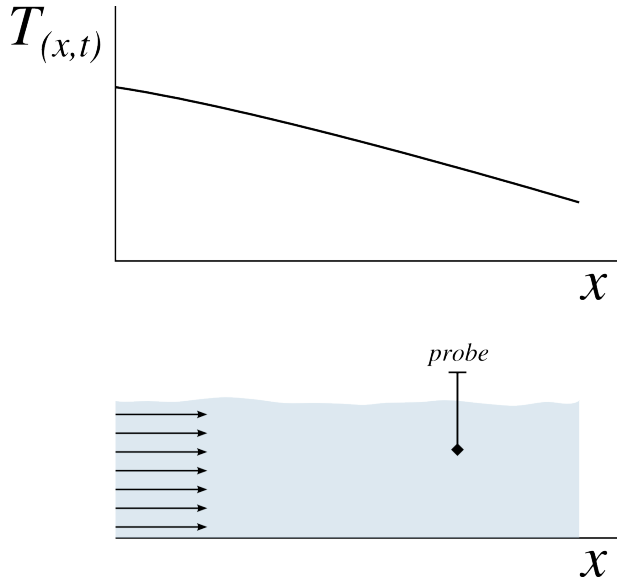

Figure 4.1 – A one-dimensional water flow, for example in a canal. The water has a non-uniform temperature, which, even if it is constant in time, translates in a temperature *time rate* change at the probe.

Figure CC-0 o.c.

the rate which is measured at the probe:

$$\begin{cases} \frac{\mathrm{d}T_{\text{water}}}{\mathrm{d}t} & \neq & 0 \\ \frac{\mathrm{d}T_{\text{probe}}}{\mathrm{d}t} & = & \frac{\partial T_{\text{water}}}{\partial t}\Big|_{\text{probe}} + \frac{\partial T_{\text{water}}}{\partial x} u_{\text{water}} \end{cases} \tag{4/1}$$

We keep in mind that the rate $\frac{\partial T}{\partial t}$ can itself be a function of time and space; in equation 4/1, it is its value at the position of the probe and at the time of measurement which is taken into account.

This line of thought can be generalized for three dimensions and for any property A of the fluid (including vector properties). The property A of one individual particle can vary as it is moving, so that it has a distribution $A = f(x,y,z,t)$ within the fluid. The time rate change of A measured at a point fixed in space is named the *total* or *substantial derivative* of A and written $\frac{\mathrm{D}A}{\mathrm{D}t}$:

$$\frac{\mathrm{D}}{\mathrm{D}t} \equiv \frac{\partial}{\partial t} + u\frac{\partial}{\partial x} + v\frac{\partial}{\partial y} + w\frac{\partial}{\partial z} \tag{4/2}$$

$$\frac{\mathrm{D}A}{\mathrm{D}t} = \frac{\partial A}{\partial t} + u\frac{\partial A}{\partial x} + v\frac{\partial A}{\partial y} + w\frac{\partial A}{\partial z} \tag{4/3}$$

$$\frac{\mathrm{D}\vec{A}}{\mathrm{D}t} = \frac{\partial \vec{A}}{\partial t} + u\frac{\partial \vec{A}}{\partial x} + v\frac{\partial \vec{A}}{\partial y} + w\frac{\partial \vec{A}}{\partial z} \tag{4/4}$$

$$= \begin{pmatrix} \frac{\partial A_x}{\partial t} + u\frac{\partial A_x}{\partial x} + v\frac{\partial A_x}{\partial y} + w\frac{\partial A_x}{\partial z} \\ \frac{\partial A_y}{\partial t} + u\frac{\partial A_y}{\partial x} + v\frac{\partial A_y}{\partial y} + w\frac{\partial A_y}{\partial z} \\ \frac{\partial A_z}{\partial t} + u\frac{\partial A_z}{\partial x} + v\frac{\partial A_z}{\partial y} + w\frac{\partial A_z}{\partial z} \end{pmatrix} \tag{4/5}$$

In eq. equation 4/3, we now wish to simplify the writing of the last three terms. We know the coordinates of the speed vector $\vec{V}$ (by definition) and of

the operator gradient $\vec{\nabla}$ (as defined in eq. 1/8 p. 26) are:

$$\vec{V} \equiv \vec{i}\, u + \vec{j}\, v + \vec{k}\, w$$
$$\vec{\nabla} \equiv \vec{i}\, \frac{\partial}{\partial x} + \vec{j}\, \frac{\partial}{\partial y} + \vec{k}\, \frac{\partial}{\partial z}$$

We thus define the *advective operator*, $(\vec{V} \cdot \vec{\nabla})$:

$$\vec{V} \cdot \vec{\nabla} = u\frac{\partial}{\partial x} + v\frac{\partial}{\partial y} + w\frac{\partial}{\partial z} \tag{4/6}$$

We can now rewrite eqs. 4/2 and 4/3 in a more concise way:

$$\frac{\mathrm{D}}{\mathrm{D}t} \equiv \frac{\partial}{\partial t} + (\vec{V} \cdot \vec{\nabla}) \tag{4/7}$$

$$\frac{\mathrm{D}A}{\mathrm{D}t} = \frac{\partial A}{\partial t} + (\vec{V} \cdot \vec{\nabla})A \tag{4/8}$$

The total time derivative is the tool that we were looking for. Now, as we solve for the fluid properties in a stationary reference frame, instead of in the reference frame of a moving particle, we will replace all the time derivatives $\frac{\mathrm{d}}{\mathrm{d}t}$ with *total* derivatives $\frac{\mathrm{D}}{\mathrm{D}t}$.

As we explored in equation 4/1, the substantial derivative of a property can be non-null even if the flow is perfectly steady; similarly, the substantial derivative of a property can be zero (e.g. when a stationary probe provides a constant measurement) even if the properties of the particles have a non-zero time change (e.g. a fluid with falling temperature, but with a non-uniform temperature).

4.3 Mass conservation

The first physical principle we wish to express in a derivative manner is the conservation of mass (eq. 0/13 p.13). Let us consider a fluid particle of volume $\mathrm{d}\mathcal{V}$, at a given instant in time (fig. 4.2). We can reproduce our analysis from chapter 3 by quantifying the time change of mass within an arbitrary volume.

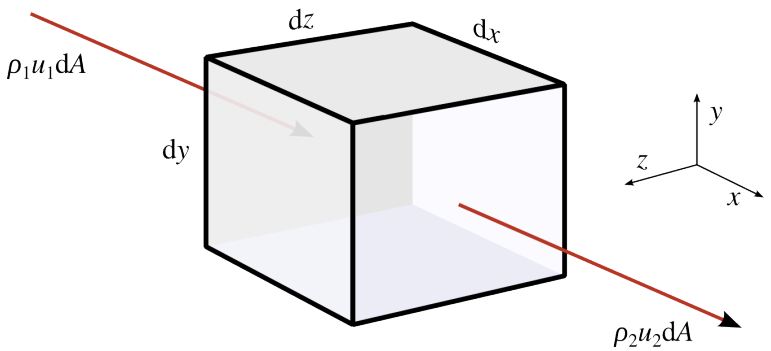

Figure 4.2 – Conservation of mass within a fluid particle. In the x-direction, a mass flow $\dot{m}_1 = \iint \rho_1 u_1 \, \mathrm{d}z \, \mathrm{d}y$ is flowing in, and a mass flow $\dot{m}_2 = \iint \rho_2 u_2 \, \mathrm{d}z \, \mathrm{d}y$ is flowing out. These two flows may not be equal, since mass may also flow in the y- and z-directions.

Figure CC-0 o.c.

In the present case, the control volume is stationary and the particle (our system) is flowing through it. We start with eq. 3/5 p.56:

$$\frac{\mathrm{d}m_{\text{particle}}}{\mathrm{d}t} = 0 = \frac{\mathrm{d}}{\mathrm{d}t}\iiint_{\text{CV}} \rho \,\mathrm{d}\mathcal{V} + \iint_{\text{CS}} \rho(\vec{V}_{\text{rel}} \cdot \vec{n}) \,\mathrm{d}A \tag{4/9}$$

The first of these two integrals can be rewritten using the Leibniz integral rule:

$$\begin{aligned}\frac{\mathrm{d}}{\mathrm{d}t}\iiint_{\text{CV}} \rho \,\mathrm{d}\mathcal{V} &= \iiint_{\text{CV}} \frac{\partial \rho}{\partial t} \,\mathrm{d}\mathcal{V} + \iint_{\text{CS}} \rho V_S \,\mathrm{d}A \\ &= \iiint_{\text{CV}} \frac{\partial \rho}{\partial t} \,\mathrm{d}\mathcal{V}\end{aligned} \tag{4/10}$$

where V_S is the speed of the control volume wall;
and where the term $\iint_{\text{CS}} \rho V_S \,\mathrm{d}A$ is simply zero because we chose a fixed control volume, such as a fixed computation grid[1].

Now we turn to the second term of equation 4/9, $\iint_{\text{CS}} \rho(\vec{V}_{\text{rel}} \cdot \vec{n}) \,\mathrm{d}A$, which represents the mass flow $\dot{m}_{\text{net}}$ flowing through the control volume.

In the direction x, the mass flow $\dot{m}_{\text{net } x}$ flowing through our control volume can be expressed as:

$$\begin{aligned}\dot{m}_{\text{net } x} &= \iint_{\text{CS}} -\rho_1 |u_1| \,\mathrm{d}z \,\mathrm{d}y + \iint_{\text{CS}} \rho_2 |u_2| \,\mathrm{d}z \,\mathrm{d}y \\ &= \iint_{\text{CS}} \int \frac{\partial}{\partial x}(\rho u) \,\mathrm{d}x \,\mathrm{d}z \,\mathrm{d}y \\ &= \iiint_{\text{CV}} \frac{\partial}{\partial x}(\rho u) \,\mathrm{d}\mathcal{V}\end{aligned} \tag{4/11}$$

The same applies for directions y and z, so that we can write:

$$\begin{aligned}\iint_{\text{CS}} \rho(\vec{V}_{\text{rel}} \cdot \vec{n}) \,\mathrm{d}A = \dot{m}_{\text{net}} &= \dot{m}_{\text{net } x} + \dot{m}_{\text{net } y} + \dot{m}_{\text{net } z} \\ &= \iiint_{\text{CV}} \left[\frac{\partial}{\partial x}(\rho u) + \frac{\partial}{\partial y}(\rho v) + \frac{\partial}{\partial z}(\rho w)\right] \mathrm{d}\mathcal{V} \\ &= \iiint_{\text{CV}} \vec{\nabla} \cdot (\rho \vec{V}) \;\mathrm{d}\mathcal{V}\end{aligned} \tag{4/12}$$

Now, with these two equations 4/10 and 4/12, we can come back to equation 4/9, which becomes:

$$\begin{aligned}\frac{\mathrm{d}m_{\text{particle}}}{\mathrm{d}t} = 0 &= \frac{\mathrm{d}}{\mathrm{d}t}\iiint_{\text{CV}} \rho \,\mathrm{d}\mathcal{V} + \iint_{\text{CS}} \rho(\vec{V}_{\text{rel}} \cdot \vec{n}) \,\mathrm{d}A \\ 0 &= \iiint_{\text{CV}} \frac{\partial \rho}{\partial t} \,\mathrm{d}\mathcal{V} \;+ \iiint_{\text{CV}} \vec{\nabla} \cdot (\rho \vec{V}) \;\mathrm{d}\mathcal{V}\end{aligned} \tag{4/13}$$

Since we are only concerned with a very small volume $\mathrm{d}\mathcal{V}$, we drop the integrals, obtaining:

[1] In a CFD calculation in which the grid is deforming, this term $\iint_{\text{CS}} \rho V_S \,\mathrm{d}A$ will have to be re-introduced in the continuity equation.

$$0 = \frac{\partial \rho}{\partial t} + \vec{\nabla} \cdot (\rho \vec{V}) \tag{4/14}$$

for all flows, with all fluids.

This equation 4/14 is named *continuity equation* and is of crucial importance in fluid mechanics. All fluid flows, in all conditions and at all times, obey this law.

Equation 4/14 is a scalar equation: it gives us no particular information about the orientation of $\vec{V}$ or about its change in time. In itself, this is insufficient to solve the majority of problems in fluid mechanics, and in practice it is used as a kinematic constraint to solutions used to evaluate their physicality or the quality of the approximations made to obtain them.

The most assiduous readers will have no difficulty reading the following equation,

$$\frac{\partial \rho}{\partial t} + \vec{\nabla} \cdot (\rho \vec{V}) = \frac{\partial \rho}{\partial t} + \vec{V} \cdot \vec{\nabla} \rho + \rho (\vec{\nabla} \cdot \vec{V}) = 0 \tag{4/15}$$

which allows us to re-write equation 4/14 like so:

$$\frac{1}{\rho} \frac{\mathrm{D}\rho}{\mathrm{D}t} + \vec{\nabla} \cdot \vec{V} = 0 \tag{4/16}$$

Therefore, we can see that for an incompressible flow, the divergent of velocity $\vec{\nabla} \cdot \vec{V}$ (sometimes called *volumetric dilatation rate*) is zero:

$$\vec{\nabla} \cdot \vec{V} = 0 \tag{4/17}$$

for any incompressible flow.

In three Cartesian coordinates, this is re-expressed as:

$$\frac{\partial u}{\partial x} + \frac{\partial v}{\partial y} + \frac{\partial w}{\partial z} = 0 \tag{4/18}$$

4.4 Change of linear momentum

Now that we have seen what mass conservation tells us about the dynamics of fluids, we turn to the momentum equation, hoping to express the velocity field to the forces that are applied on the fluid.

4.4.1 The Cauchy equation

We start by writing Newton's second law (eq. 0/14 p.14) as it applies to a fluid particle of mass m_{particle}, as shown in fig. 4.3. Fundamentally, the forces on a fluid particle are of only three kinds, namely weight, pressure, and shear:[1]

$$m_{\text{particle}} \frac{\mathrm{d}\vec{V}}{\mathrm{d}t} = \vec{F}_{\text{weight}} + \vec{F}_{\text{net, pressure}} + \vec{F}_{\text{net, shear}} \tag{4/19}$$

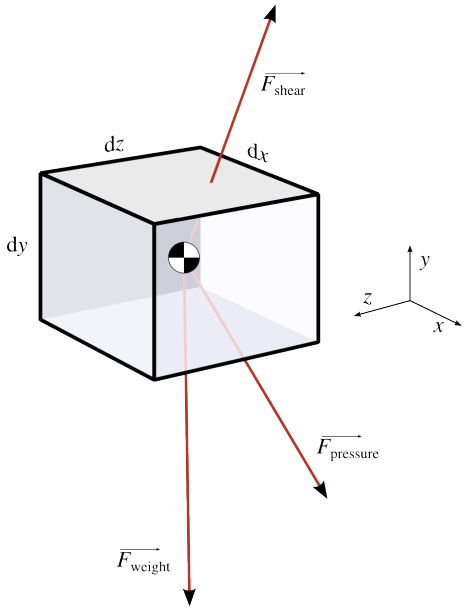

Figure 4.3 – In our study of fluid mechanics, we consider only forces due to gravity, shear, or pressure.

Figure CC-0 o.c.

We now apply this equation to a stationary cube of infinitesimal volume $\mathrm{d}\mathcal{V}$ which is traversed by fluid. Measuring the velocity from the reference frame of the cube, and thus using a Eulerian description, we obtain:

$$\begin{aligned} \frac{m_{\text{particle}}}{\mathrm{d}\mathcal{V}} \frac{\mathrm{D}\vec{V}}{\mathrm{D}t} &= \frac{m}{\mathrm{d}\mathcal{V}}\vec{g} + \frac{1}{\mathrm{d}\mathcal{V}}\vec{F}_{\text{net, pressure}} + \frac{1}{\mathrm{d}\mathcal{V}}\vec{F}_{\text{net, shear}} \\ \rho\frac{\mathrm{D}\vec{V}}{\mathrm{D}t} &= \rho\vec{g} + \frac{1}{\mathrm{d}\mathcal{V}}\vec{F}_{\text{net, pressure}} + \frac{1}{\mathrm{d}\mathcal{V}}\vec{F}_{\text{net, shear}} \end{aligned} \tag{4/20}$$

Let us now account for pressure and shear efforts applying on each of the faces of the fluid particle. For pressure, we obtain:

$$\begin{aligned} F_{\text{net, pressure},x} &= \mathrm{d}y\,\mathrm{d}z\,[p_1 - p_4] \\ &= \mathrm{d}y\,\mathrm{d}z\left[-\frac{\partial p}{\partial x}\,\mathrm{d}x\right] \end{aligned}$$

$$F_{\text{net, pressure},x} = \mathrm{d}\mathcal{V}\frac{-\partial p}{\partial x} \tag{4/21}$$

$$F_{\text{net, pressure},y} = \mathrm{d}\mathcal{V}\frac{-\partial p}{\partial y} \tag{4/22}$$

$$F_{\text{net, pressure},z} = \mathrm{d}\mathcal{V}\frac{-\partial p}{\partial z} \tag{4/23}$$

This pattern, we had seen in chapter 1 (with eq.1/8 p.26), can more elegantly be expressed with the gradient operator, allowing us to write:

$$\frac{1}{\mathrm{d}\mathcal{V}}\vec{F}_{\text{net, pressure}} = -\vec{\nabla}p \tag{4/24}$$

As for shear, we can put our work from chapter 2 to good use now. There, we had seen that the effect of shear on a volume had eighteen components,

[1] In some very special and rare applications, electromagnetic forces may also apply.

the careful examination of which allowed us to quantify the net and that the net *force* due to shear (which has only three components). In the x-direction, for example, we had seen (with eq.2/8 p.41, as illustrated in fig. 4.4) that the shear in the x-direction on each of the six faces contributed to the net shear force in the x-direction as:

$$\begin{aligned}\vec{F}_{\text{shear } x} = \; & \mathrm{d}x\,\mathrm{d}y(\vec{\tau}_{zx\ 3} - \vec{\tau}_{zx\ 6}) \\ & + \mathrm{d}x\,\mathrm{d}z(\vec{\tau}_{yx\ 2} - \vec{\tau}_{yx\ 5}) \\ & + \mathrm{d}z\,\mathrm{d}y(\vec{\tau}_{xx\ 1} - \vec{\tau}_{xx\ 4})\end{aligned}$$

This, in turn, was more elegantly expressed using the divergent operator (def. 2/10) as equation 2/13:

$$\vec{F}_{\text{shear } x} = \mathrm{d}\mathcal{V}\left(\frac{\partial\vec{\tau}_{zx}}{\partial z} + \frac{\partial\vec{\tau}_{yx}}{\partial y} + \frac{\partial\vec{\tau}_{xx}}{\partial x}\right) \tag{4/25}$$

$$= \mathrm{d}\mathcal{V}\;\vec{\nabla}\cdot\vec{\tau}_{ix} \tag{4/26}$$

Finally, we had assembled the components in all three directions into a single expression for the net shear force with eq. 2/14 p.42:

$$\vec{F}_{\text{shear}} = \mathrm{d}\mathcal{V}\;\vec{\nabla}\cdot\vec{\tau}_{ij} \tag{4/27}$$

Now, we can put together our findings, eq. 4/24 for the force due to pressure and eq. 4/27 for the force due to shear, back into equation 4/20, we obtain the *Cauchy equation*:

$$\rho\frac{\mathrm{D}\vec{V}}{\mathrm{D}t} = \rho\vec{g} - \vec{\nabla}p + \vec{\nabla}\cdot\vec{\tau}_{ij} \tag{4/28}$$

for all flows, with all fluids.

The Cauchy equation is an expression of Newton's second law applied to a fluid particle. It expresses the time change of the speed vector measured at a fixed point as a function of gravity, pressure and shear effects. This is quite a breakthrough. Within the chaos of an arbitrary flow, in which fluid particles are shoved, pressurized, squeezed, and distorted, we know precisely what we need to look for in order to quantify the time-change of velocity: the gradient of pressure, and the divergent of shear.

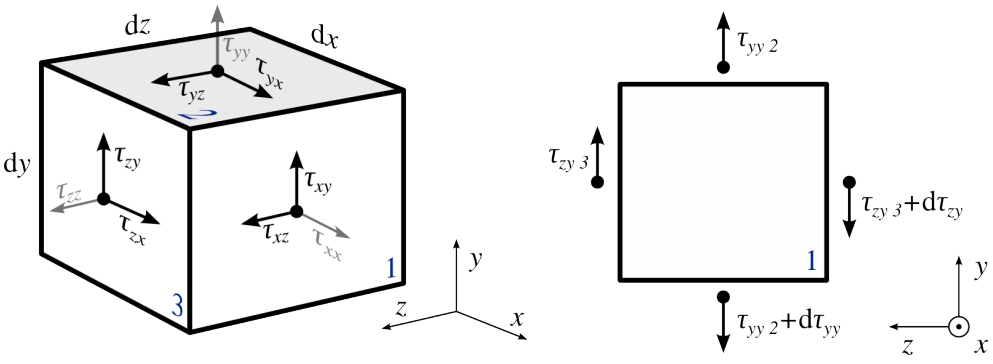

Figure 4.4 – Shear efforts on a cubic fluid particle (already represented in fig. 2.1 p.40).

Figure CC-0 o.c.

While it is an excellent start however, this equation isn't detailed enough for us. In our search for the velocity field $\vec{V}$, the changes in time and space of the shear tensor $\vec{\tau}_{ij}$ and pressure p are unknowns. Ideally, those two terms should be expressed solely as a function of the flow's other properties. Obtaining such an expression is what Claude-Louis Navier and Gabriel Stokes set themselves to in the 19th century: we follow their footsteps in the next paragraphs.

4.4.2 The Navier-Stokes equation for incompressible flow

The Navier-Stokes equation is the Cauchy equation (eq. 4/28) applied to Newtonian fluids. In Newtonian fluids, which we encountered in chapter 2 (§2.3.3 p.44), shear efforts are simply proportional to the rate of strain; thus, the shear component of eq. 4/28 can be re-expressed usefully.

We had seen with eq. 2/16 that the norm $||\vec{\tau}_{ij}||$ of shear component in direction j along a surface perpendicular to i can be expressed as:

$$||\vec{\tau}_{ij}|| = \mu \frac{\partial u_j}{\partial i}$$

Thus, in a Newtonian fluid, on each of the six faces of the infinitesimal cube from fig. 4.4, the shear in x-direction is proportional to the partial derivative of u (the component of velocity in the x-direction) with respect to the direction perpendicular to each face:

$$\begin{aligned}
\vec{\tau}_{xx1} &= \mu \left.\frac{\partial u}{\partial x}\right|_1 \vec{i} & \qquad \vec{\tau}_{xx4} &= -\mu \left.\frac{\partial u}{\partial x}\right|_4 \vec{i} \\
\vec{\tau}_{yx2} &= \mu \left.\frac{\partial u}{\partial y}\right|_2 \vec{i} & \qquad \vec{\tau}_{yx5} &= -\mu \left.\frac{\partial u}{\partial y}\right|_5 \vec{i} \\
\vec{\tau}_{zx3} &= \mu \left.\frac{\partial u}{\partial z}\right|_3 \vec{i} & \qquad \vec{\tau}_{zx6} &= -\mu \left.\frac{\partial u}{\partial z}\right|_6 \vec{i}
\end{aligned}$$

These are the six constituents of the x-direction shear tensor $\vec{\tau}_{ix}$. Their net effect is a vector expressed as the divergent $\vec{\nabla} \cdot \vec{\tau}_{ix}$, which, in incompressible flow[1], is expressed as:

$$\begin{aligned}
\vec{\nabla} \cdot \vec{\tau}_{ix} &= \frac{\partial \vec{\tau}_{xx}}{\partial x} + \frac{\partial \vec{\tau}_{yx}}{\partial y} + \frac{\partial \vec{\tau}_{zx}}{\partial z} \\
&= \frac{\partial \left(\mu \frac{\partial u}{\partial x} \vec{i}\right)}{\partial x} + \frac{\partial \left(\mu \frac{\partial u}{\partial y} \vec{i}\right)}{\partial y} + \frac{\partial \left(\mu \frac{\partial u}{\partial z} \vec{i}\right)}{\partial z} \\
&= \mu \left(\frac{\partial^2 u}{(\partial x)^2} + \frac{\partial^2 u}{(\partial y)^2} + \frac{\partial^2 u}{(\partial z)^2} \right) \vec{i}
\end{aligned} \tag{4/29}$$

[1] When the flow becomes compressible, normal stresses τ_{xx} will see an additional term related to the change in density within the particle. An additional term, $+\frac{1}{3}\mu \vec{\nabla} \left(\vec{\nabla} \cdot \vec{V}\right)$, would appear on the right side of eq. 4/37. This is well outside of the scope of this course.

Using the *Laplacian* operator to represent the spatial variation of the spatial variation of an object:

$$\vec{\nabla}^2 \equiv \vec{\nabla} \cdot \vec{\nabla} \tag{4/30}$$

$$\vec{\nabla}^2 A \equiv \vec{\nabla} \cdot \vec{\nabla} A \tag{4/31}$$

$$\vec{\nabla}^2 \vec{A} \equiv \begin{pmatrix} \vec{\nabla}^2 A_x \\ \vec{\nabla}^2 A_y \\ \vec{\nabla}^2 A_z \end{pmatrix} = \begin{pmatrix} \vec{\nabla} \cdot \vec{\nabla} A_x \\ \vec{\nabla} \cdot \vec{\nabla} A_y \\ \vec{\nabla} \cdot \vec{\nabla} A_z \end{pmatrix} \tag{4/32}$$

we can re-write eq. 4/29 more elegantly and generalize to three dimensions:

$$\vec{\nabla} \cdot \vec{\tau}_{ix} = \mu \vec{\nabla}^2 u \, \vec{i} = \mu \vec{\nabla}^2 \vec{u} \tag{4/33}$$

$$\vec{\nabla} \cdot \vec{\tau}_{iy} = \mu \vec{\nabla}^2 v \, \vec{j} = \mu \vec{\nabla}^2 \vec{v} \tag{4/34}$$

$$\vec{\nabla} \cdot \vec{\tau}_{iz} = \mu \vec{\nabla}^2 w \, \vec{k} = \mu \vec{\nabla}^2 \vec{w} \tag{4/35}$$

The three last equations are grouped together simply as

$$\vec{\nabla} \cdot \vec{\tau}_{ij} = \mu \vec{\nabla}^2 \vec{V} \tag{4/36}$$

With this new expression, we can come back to the Cauchy equation (eq. 4/28), in which we can replace the shear term with eq. 4/36. This produces the glorious *Navier-Stokes equation for incompressible flow*:

$$\rho \frac{\mathrm{D}\vec{V}}{\mathrm{D}t} = \rho \vec{g} - \vec{\nabla} p + \mu \vec{\nabla}^2 \vec{V} \tag{4/37}$$

for all incompressible flows of a Newtonian fluid.

This formidable equation describes the property fields of all incompressible flows of Newtonian fluids. The solutions we look for in equation 4/37 are the velocity (vector) field $\vec{V} = (u, v, w) = f_1(x, y, z, t)$ and the pressure field $p = f_2(x, y, z, t)$, given a set of constraints to represent the problem at hand. These constraints, called *boundary conditions*, may be expressed in terms of velocities (e.g. the presence of a fixed solid body is expressed as a region for which $\vec{V} = \vec{0}$) or pressure (e.g. a discharge into an open atmosphere may be expressed as a region of known constant pressure).

The combination of equations 4/37 and 4/14 (continuity & Navier-Stokes) may not be enough to predict the solution of a given problem, most especially if large energy transfers take place within the flow. In that case, the addition of an energy equation and an expression of the second law of thermodynamics, both in a form suitable for derivative analysis, may be needed to provide as many equations as there are unknowns.

Though it is without doubt charming, equation 4/37 should be remembered for what it is really: a three-dimensional system of coupled equations. In

Cartesian coordinates this complexity is more apparent:

$$\rho\left[\frac{\partial u}{\partial t}+u\frac{\partial u}{\partial x}+v\frac{\partial u}{\partial y}+w\frac{\partial u}{\partial z}\right]=\rho g_x-\frac{\partial p}{\partial x}+\mu\left[\frac{\partial^2 u}{(\partial x)^2}+\frac{\partial^2 u}{(\partial y)^2}+\frac{\partial^2 u}{(\partial z)^2}\right] \tag{4/38}$$

$$\rho\left[\frac{\partial v}{\partial t}+u\frac{\partial v}{\partial x}+v\frac{\partial v}{\partial y}+w\frac{\partial v}{\partial z}\right]=\rho g_y-\frac{\partial p}{\partial y}+\mu\left[\frac{\partial^2 v}{(\partial x)^2}+\frac{\partial^2 v}{(\partial y)^2}+\frac{\partial^2 v}{(\partial z)^2}\right] \tag{4/39}$$

$$\rho\left[\frac{\partial w}{\partial t}+u\frac{\partial w}{\partial x}+v\frac{\partial w}{\partial y}+w\frac{\partial w}{\partial z}\right]=\rho g_z-\frac{\partial p}{\partial z}+\mu\left[\frac{\partial^2 w}{(\partial x)^2}+\frac{\partial^2 w}{(\partial y)^2}+\frac{\partial^2 w}{(\partial z)^2}\right] \tag{4/40}$$

Indeed in the 150 years since it was first written, no general expression has been found for velocity or pressure fields that would solve this equation in the general case. Nevertheless, in this course we will use it directly:

- to understand and quantify the importance of key fluid flow parameters, in chapter 6;
- to find analytical solutions to flows in a few selected cases, in the other remaining chapters.

After this course, the reader might also engage into Computational Fluid Dynamics (CFD) a discipline entirely architectured around this equation, and to which it purposes to find solutions as fields of discrete values.

As a finishing remark, we note that when the flow is strictly two-dimensional, the Navier-Stokes equation is considerably simplified, shrinking down to the system:

$$\rho\left[\frac{\partial u}{\partial t}+u\frac{\partial u}{\partial x}+v\frac{\partial u}{\partial y}\right]=\rho g_x-\frac{\partial p}{\partial x}+\mu\left[\frac{\partial^2 u}{(\partial x)^2}+\frac{\partial^2 u}{(\partial y)^2}\right] \tag{4/41}$$

$$\rho\left[\frac{\partial v}{\partial t}+u\frac{\partial v}{\partial x}+v\frac{\partial v}{\partial y}\right]=\rho g_y-\frac{\partial p}{\partial y}+\mu\left[\frac{\partial^2 v}{(\partial x)^2}+\frac{\partial^2 v}{(\partial y)^2}\right] \tag{4/42}$$

Unfortunately, this simplification prevents us from accounting for turbulence, which is a strongly three-dimensional phenomenon.

4.5 Change of angular momentum

There is no differential equation for conservation of angular momentum in fluid flow. Indeed, as the size of our particle tends to zero, it loses its ability to possess (or exchange) angular momentum about its center of gravity. Infinitesimal fluid particles are not able to rotate about themselves, only about an external point. So, in this chapter, no analysis is carried out using the concept of angular momentum.

4.6 Energy conservation and increase in entropy

This topic is well covered in Anderson [6]

The last two key principles used in fluid flow analysis can be written together in a differential equation similar to the Navier-Stokes equation.

Once again, we start from the analysis of transfers on an infinitesimal control volume. We are going to relate three energy terms in the following form, naming them A, B and C for clarity:

$$\begin{array}{ccccc} \text{the rate of change} & & \text{the net flux} & & \text{the rate of work done} \\ \text{of energy inside} & = & \text{of heat into} & + & \text{on the element due to} \\ \text{the fluid element} & & \text{the element} & & \text{body and surface forces} \\ A & = & B & + & C \end{array} \tag{4/43}$$

Let us first evaluate term C. The rate of work done on the particle is the dot product of its velocity $\vec{V}$ and the net force $\vec{F}_{\text{net}}$ applying to it:

$$C = \vec{V} \cdot \left(\frac{\vec{F}_{\text{weight}}}{\mathrm{d}\mathcal{V}} + \frac{\vec{F}_{\text{net, pressure}}}{\mathrm{d}\mathcal{V}} + \frac{\vec{F}_{\text{net, shear}}}{\mathrm{d}\mathcal{V}} \right) \mathrm{d}\mathcal{V}$$
$$C = \vec{V} \cdot \left(\rho\vec{g} - \vec{\nabla}p + \vec{\nabla} \cdot \vec{\tau}_{ij} \right) \mathrm{d}\mathcal{V}$$

and for the case of a Newtonian fluid in an incompressible flow, this expression can be re-written as:

$$C = \vec{V} \cdot \left(\rho\vec{g} - \vec{\nabla}p + \mu\vec{\nabla}^2\vec{V} \right) \mathrm{d}\mathcal{V} \tag{4/44}$$

We now turn to term B, the net flux of heat into the element. We attribute this flux to two contributions, the first named $\dot{Q}_{\text{radiation}}$ from the emission or absorption of radiation, and the second, named $\dot{Q}_{\text{conduction}}$ to thermal conduction through the faces of the element. We make no attempt to quantify $\dot{Q}_{\text{radiation}}$, simply stating that

$$\dot{Q}_{\text{radiation}} = \rho\dot{q}_{\text{radiation}} \, \mathrm{d}\mathcal{V} \tag{4/45}$$

in which $\dot{q}_{\text{radiation}}$ is the local power per unit mass (in $\mathrm{W\,kg^{-1}}$) transfered to the element, to be determined from the boundary conditions and flow temperature distribution.

In the x-direction, thermal conduction through the faces of the element causes a net flow of heat $\dot{Q}_{\text{conduction},x}$ expressed as a function of the power per area q (in $\mathrm{W\,m^{-2}}$) through each of the two faces perpendicular to x:

$$\begin{aligned} \dot{Q}_{\text{conduction},x} &= \left[q_x - \left(q_x + \frac{\partial q_x}{\partial x} \mathrm{d}x \right) \right] \mathrm{d}y \, \mathrm{d}z \\ &= -\frac{\partial q_x}{\partial x} \mathrm{d}x \, \mathrm{d}y \, \mathrm{d}z \qquad (4/46) \\ &= -\frac{\partial q_x}{\partial x} \mathrm{d}\mathcal{V} \qquad (4/47) \end{aligned}$$

Summing contributions from all three directions, we obtain:

$$\begin{aligned} \dot{Q}_{\text{conduction}} &= \dot{Q}_{\text{conduction},x} + \dot{Q}_{\text{conduction},y} + \dot{Q}_{\text{conduction},z} \\ &= -\left[\frac{\partial q_x}{\partial x} + \frac{\partial q_y}{\partial y} + \frac{\partial q_z}{\partial z} \right] \mathrm{d}\mathcal{V} \end{aligned} \tag{4/48}$$

So we finally obtain an expression for B:

$$\begin{aligned} B &= \dot{Q}_{\text{radiation}} + \dot{Q}_{\text{conduction}} \\ &= \left(\rho\dot{q}_{\text{radiation}} - \left[\frac{\partial q_x}{\partial x} + \frac{\partial q_y}{\partial y} + \frac{\partial q_z}{\partial z}\right]\right) \mathrm{d}\mathcal{V} \end{aligned} \tag{4/49}$$

Finally, term A, the rate of change of energy inside the fluid element, can be expressed as a function of the specific kinetic energy e_k and specific internal energy i:

$$A = \rho\frac{\mathrm{D}}{\mathrm{D}t}\left(i + \frac{1}{2}V^2\right) \mathrm{d}\mathcal{V} \tag{4/50}$$

We are therefore able to relate the properties of a fluid particle to the principle of energy conservation as follows:

$$\rho\frac{\mathrm{D}}{\mathrm{D}t}\left(i + \frac{1}{2}V^2\right) = \left(\rho\dot{q}_{\text{radiation}} - \left[\frac{\partial q_x}{\partial x} + \frac{\partial q_y}{\partial y} + \frac{\partial q_z}{\partial z}\right]\right) + \vec{V}\cdot\left(\rho\vec{g} - \vec{\nabla}p + \mu\vec{\nabla}^2\vec{V}\right) \tag{4/51}$$

This is a scalar equation — it only has one dimension, and involves the length of the velocity vector, $V \equiv \left[u^2 + v^2 + w^2\right]^{\frac{1}{2}}$.

In an interesting hack, we are able to incorporate an expression for the *second* principle of thermodynamics in this equation simply by expressing the fluxes q_i as a function of the temperature gradients. Indeed, expressing a heat flux as the result of a difference in temperature according to the Fourier law,

$$q_i = -k\frac{\partial T}{\partial i} \tag{4/52}$$

we constrain the direction of the heat fluxes and thus ensure that all dissipative terms resulting in temperature increases cannot be fed back into other energy terms, thus increasing the overall entropy.

Equation 4/52 inserted into eq. 4/51 yields:

$$\rho\frac{\mathrm{D}}{\mathrm{D}t}\left(i + \frac{1}{2}V^2\right) = \left(\rho\dot{q}_{\text{radiation}} + k\left[\frac{\partial^2 T}{(\partial x)^2} + \frac{\partial^2 T}{(\partial y)^2} + \frac{\partial^2 T}{(\partial z)^2}\right]\right) + \vec{V}\cdot\left(\rho\vec{g} - \vec{\nabla}p + \mu\vec{\nabla}^2\vec{V}\right)$$

Making use of a Laplacian operator, we come to:

$$\rho\frac{\mathrm{D}}{\mathrm{D}t}\left(i + \frac{1}{2}V^2\right) = \left(\rho\dot{q}_{\text{radiation}} + k\vec{\nabla}^2 T\right) + \vec{V}\cdot\left(\rho\vec{g} - \vec{\nabla}p + \mu\vec{\nabla}^2\vec{V}\right) \tag{4/53}$$

This equation has several shortcomings, most importantly because the term $\dot{q}_{\text{radiation}}$ is not expressed in terms of fluid properties, and because μ is typically not independent of the temperature T. Nevertheless, it in principle brings closure to our system of continuity and momentum equations, and these two influences may be either neglected, or modeled numerically.

This topic is well covered in Versteeg & Malalasekera [8]

4.7.1 Principle

In our analysis of fluid flow from a derivative perspective, our five physical principles from §0.5 have been condensed into three equations (often loosely referred together to as the *Navier-Stokes equations*). Out of these, the first two, for conservation of mass (4/17) and linear momentum (4/37) in incompressible flows, are often enough to characterize most free flows, and should in principle be enough to find the primary unknown, which is the velocity field $\vec{V}$:

$$0 = \vec{\nabla} \cdot \vec{V}$$
$$\rho \frac{\mathrm{D}\vec{V}}{\mathrm{D}t} = \rho\vec{g} - \vec{\nabla}p + \mu\vec{\nabla}^2\vec{V}$$

We know of many individual analytical solutions to this mathematical problem: they apply to simple cases, and we shall describe several such flows in the upcoming chapters. However, we do not have one *general* solution: one that would encompass all of them. For example, in solid mechanics we have long understood that *all* pure free fall movements can be described with the solution $x = x_0 + u_0 t$ and $y = y_0 + v_0 t + \frac{1}{2}gt^2$, regardless of the particularities of each fall. In fluid mechanics, even though our analysis was carried out in the same manner, we have yet to find such one general solution — or even to prove that one exists at all.

It is therefore tempting to attack the above pair of equations from the numerical side, with a computer algorithm. If one discretizes space and time in small increments δx, δy, δz and δt, we could re-express the x-component of eq. 4/37 as:

$$\rho\left[\frac{\delta u|_t}{\delta t} + u\frac{\delta u|_x}{\delta x} + v\frac{\delta u|_y}{\delta y} + w\frac{\delta u|_z}{\delta z}\right] = \rho g_x - \frac{\delta p|_x}{\delta x} + \mu\left[\frac{\delta\left.\frac{\delta u|_x}{\delta x}\right|_x}{\delta x} + \frac{\delta\left.\frac{\delta u|_y}{\delta y}\right|_y}{\delta y} + \frac{\delta\left.\frac{\delta u|_z}{\delta z}\right|_z}{\delta z}\right] \tag{4/54}$$

If we start with a *known* (perhaps guessed) initial field for velocity and pressure, this equation 4/54 allows us to isolate and solve for $\delta u|_t$, and therefore predict what the u velocity field would look like after a time increment δt. The same can be done in the y- and z-directions. Repeating the process, we then proceed to the next time step and so on, *marching in time*, obtaining at every new time step the value of u, v and w at each position within our computation grid. This is the fundamental working principle for computational fluid dynamics (CFD) today.

4.7.2 Two problems with CFD

There are two flaws with the process described above.

The first flaw is easy to identify: while we may be able to *start* the calculation with a known pressure field, we do not have a mean to predict p (and thus

$\delta p/\delta x$ in eq. 4/54) at the next position in time ($t + \delta t$).
This is not a surprise. Going back to the Cauchy equation (eq. 4/28), we notice that we took care of the divergent of shear $\vec{\nabla} \cdot \vec{\tau}_{ij}$, but not of the gradient of pressure $\vec{\nabla} p$. We have neither an expression $p = f(\vec{V})$, nor an equation that would give us a value for $\partial p/\partial t$. CFD software packages deal with this problem in the most uncomfortable way: by guessing a pressure field $p_{(t+\delta t)}$, calculating the new velocity field $\vec{V}_{(t+\delta t)}$, and then correcting and re-iterating with the help of the continuity equation, until continuity errors are acceptably small. This scheme and its implementation are a great source of anguish amongst numerical fluid dynamicists.

The second flaw appears once we consider the effect of grid coarseness. Every decrease in the size of the grid cell and in the length of the time step increases the total number of equations to be solved by the algorithm. Halving each of δx, δy, δz and δt multiplies the total number of equations by 16, so that soon enough the experimenter will wish to know what maximum (coarsest) grid size is appropriate or tolerable. Furthermore, in many practical cases, we may not even be interested in an exhaustive description of the velocity field, and just wish to obtain a general, coarse description of the fluid flow.

Using a coarse grid and large time step, however, prevents us from resolving small variations in velocity: movements which are small enough to fit in between grid points, or short enough to happen in between time steps. Let us decompose the velocity field into two components: one is the *average* flow $(\overline{u}, \overline{v}, \overline{w})$, and the other the *instantaneous fluctuation* flow (u', v', w'), too fine to be captured by our grid:

$$u_i \equiv \overline{u}_i + u'_i \tag{4/55}$$

$$\overline{u}'_i \equiv 0 \tag{4/56}$$

With the use of definition 4/55, we re-formulate equation 4/38 as follows:

$$\rho \left[\frac{\partial(\overline{u} + u')}{\partial t} + (\overline{u} + u') \frac{\partial(\overline{u} + u')}{\partial x} + (\overline{v} + v') \frac{\partial(\overline{u} + u')}{\partial y} + (\overline{w} + w') \frac{\partial(\overline{u} + u')}{\partial z} \right]$$
$$= \rho g_x - \frac{\partial(\overline{p} + p')}{\partial x} + \mu \left[\frac{\partial^2(\overline{u} + u')}{(\partial x)^2} + \frac{\partial^2(\overline{u} + u')}{(\partial y)^2} + \frac{\partial^2(\overline{u} + u')}{(\partial z)^2} \right]$$

Taking the *average* of this equation —thus expressing the dynamics of the flow as we calculate them with a finite, coarse grid— yields, after some intimidating but easily conquerable algebra:

$$\rho \left[\frac{\partial \overline{u}}{\partial t} + \overline{u} \frac{\partial \overline{u}}{\partial x} + \overline{v} \frac{\partial \overline{u}}{\partial y} + \overline{w} \frac{\partial \overline{u}}{\partial z} \right] + \rho \left[\overline{u' \frac{\partial u'}{\partial x}} + \overline{v' \frac{\partial u'}{\partial y}} + \overline{w' \frac{\partial u'}{\partial z}} \right]$$
$$= \rho g_x - \frac{\partial \overline{p}}{\partial x} + \mu \left[\frac{\partial^2 \overline{u}}{(\partial x)^2} + \frac{\partial^2 \overline{u}}{(\partial y)^2} + \frac{\partial^2 \overline{u}}{(\partial z)^2} \right] \tag{4/57}$$

Equation 4/57 is the x-component of the *Reynolds-averaged Navier-Stokes equation* (RANS). It shows that when one observes the flow in terms of the sum of an average and an instantaneous component, the dynamics cannot be expressed solely according to the average component. Comparing eqs. 4/57 and 4/38 we find that an additional term has appeared on the left side. This term, called the *Reynolds stress*, is often re-written as $\rho \, \partial \overline{u'_i u'_j}/\partial j$; it is *not zero* since we observe in practice that the instantaneous fluctuations of velocity are strongly correlated.

The difference between eqs. 4/57 and 4/38 can perhaps be expressed differently: the time-average of a real flow cannot be calculated by solving for the time-average velocities. Or, more bluntly: *the average of the solution cannot be obtained with only the average of the flow.* This is a tremendous burden in computational fluid dynamics, where limits on the available computational power prevent us in practice from solving for these fluctuations. In the overwhelming majority of computations, the Reynolds stress has to be approximated in bulk with schemes named *turbulence models*.

Diving into the intricacies of CFD is beyond the scope of our study. Nevertheless, the remarks in this last section should hopefully hint at the fact that an understanding of the *mathematical nature* of the differential conservation equations is of great practical importance in fluid dynamics. It is for that reason that we shall dedicate the exercises of this chapter solely to playing with the mathematics of our two main equations.

Fluid Mechanics
Exercise sheet 4 – Differential analysis

last edited May 13, 2016

These lecture notes are based on textbooks by White [9], Çengel & al.[12], and Munson & al.[14].

Except otherwise indicated, we assume that fluids are Newtonian, and that:
$\rho_{\text{water}} = 1\,000\,\text{kg m}^{-3}$; $p_{\text{atm.}} = 1\,\text{bar}$; $\rho_{\text{atm.}} = 1{,}225\,\text{kg m}^{-3}$; $T_{\text{atm.}} = 11{,}3\,^{\circ}\text{C}$; $\mu_{\text{atm.}} = 1{,}5 \cdot 10^{-5}\,\text{N s m}^{-2}$;
$g = 9{,}81\,\text{m s}^{-2}$. Air is modeled as a perfect gas ($R_{\text{air}} = 287\,\text{J K}^{-1}\,\text{kg}^{-1}$; $\gamma_{\text{air}} = 1{,}4$; $c_{p\text{air}} = 1\,005\,\text{J kg}^{-1}\,\text{K}^{-1}$).

Continuity equation:

$$\frac{1}{\rho}\frac{\mathrm{D}\rho}{\mathrm{D}t} + \vec{\nabla}\cdot\vec{V} = 0 \tag{4/16}$$

Navier-Stokes equation for incompressible flow:

$$\rho\frac{\mathrm{D}\vec{V}}{\mathrm{D}t} = \rho\vec{g} - \vec{\nabla}p + \mu\vec{\nabla}^2\vec{V} \tag{4/37}$$

4.1 Revision questions

For the continuity equation (eq. 4/16), and then for the incompressible Navier-Stokes equation (eq. 4/37),

1. Write out the equation in its fully-developed form in three Cartesian coordinates;
2. State in which flow conditions the equation applies.

Also, in order to revise the notion of substantial (or total) derivative:

3. Describe a situation in which the substantial derivative of a property is non-zero although the fluid property is independent of time.
4. Describe a situation in which the substantial derivative of a property is zero although the time rate of change of this property is non-zero.

4.2 Acceleration field

Çengel & al. [12] E4-3

A flow is described with the velocity field $\vec{V} = (0{,}5 + 0{,}8x)\vec{i} + (1{,}5 - 0{,}8y)\vec{j}$ (in SI units).

What is the acceleration measured by a probe positioned at $(2; 2; 2)$ at $t = 3\,\text{s}$?

4.3 Volumetric dilatation rate

der. Munson & al. [14] 6.4

A flow is described by the following field (in SI units):

$$u = x^3 + y^2 + z$$
$$v = xy + yz + z^3$$
$$w = -4x^2z - z^2 + 4$$

What is the volumetric dilatation rate field? What is the value of this rate at {2;2;2}?

4.4 Incompressibility

Çengel & al. [12] 9-28

Does the vector field $\vec{V} = (1{,}6 + 1{,}8x)\vec{i} + (1{,}5 - 1{,}8y)\vec{j}$ satisfy the continuity equation for two-dimensional incompressible flow?

4.5 Missing components

Munson & al. [14] E6.2 + Çengel & al. [12] 9-4

Two flows are described by the following fields:

$$u_1 = x^2 + y^2 + z^2$$
$$v_1 = xy + yz + z$$
$$w_1 = ?$$

$$u_2 = ax^2 + by^2 + cz^2$$
$$v_2 = ?$$
$$w_2 = axz + byz^2$$

What must w_1 and v_2 be so that these flows be incompressible?

4.6 Another acceleration field

White [9] E4.1

Given the velocity field $\vec{V} = (3t)\vec{i} + (xz)\vec{j} + (ty^2)\vec{k}$ (SI units), what is the acceleration field, and what is the value measured at {2;4;6} and $t = 5$ s?

4.7 Vortex

Çengel & al. [12] 9.27

A vortex is modeled with the following two-dimensional flow:

$$u = C\frac{y}{x^2 + y^2}$$
$$v = -C\frac{x}{x^2 + y^2}$$

Verify that this field satisfies the continuity equation for incompressible flow.

4.8 Pressure fields

Çengel & al. [12] E9-13, White [9] 4.32 & 4.34

We consider the four (separate and independent) incompressible flows below:

$$\vec{V}_1 = (ax + b)\vec{i} + (-ay + cx)\vec{j}$$
$$\vec{V}_2 = (2y)\vec{i} + (8x)\vec{j}$$
$$\vec{V}_3 = (ax + bt)\vec{i} + (cx^2 + ey)\vec{j}$$
$$\vec{V}_4 = U_0\left(1 + \frac{x}{L}\right)\vec{i} - U_0\frac{y}{L}\vec{j}$$

The influence of gravity is neglected on the first three fields.

Does a function exist to describe the pressure field of each of these flows, and if so, what is it?

Answers

4.1 1) For continuity, use eqs. 4/2 and 1/8 in equation 4/16. For Navier-Stokes, see eqs. 4/38, 4/39 and 4/40 p. 85; 2) Read §4.3 p. 78 for continuity, and §4.4.2 p.83 for Navier-Stokes; 3) and 4) see §4.2.2 p. 76.

4.2 $\frac{\mathrm{D}\vec{V}}{\mathrm{D}t} = (0{,}4 + 0{,}64x)\vec{i} + (-1{,}2 + 0{,}64y)\vec{j}$. At the probe it takes the value $1{,}68\vec{i} + 0{,}08\vec{j}$ (length $1{,}682\,\mathrm{m\,s^{-2}}$).

4.3 $\vec{\nabla} \cdot \vec{V} = -x^2 + x - z$; thus at the probe it takes the value $\left(\vec{\nabla} \cdot \vec{V}\right)_{\text{probe}} = -4\,\mathrm{s^{-1}}$.

4.4 Apply equation 4/18 p.80 to $\vec{V}$: the answer is yes.

4.5 1) Applying equation 4/18: $w_1 = -3xz - \frac{1}{2}z^2 + f_{(x,y,t)}$;
2) idem, $v_2 = -3axy - bzy^2 + f_{(x,z,t)}$.

4.6 $\frac{\mathrm{D}\vec{V}}{\mathrm{D}t} = (3)\vec{i} + (3z + y^2x)t\vec{j} + (y^2 + 2xyzt)\vec{k}$. At the probe it takes the value $3\vec{i} + 250\vec{j} + 496\vec{k}$.

4.7 Apply equation 4/18 to $\vec{V}$ to verify incompressibility.

4.8 Note: the constant (initial) value p_0 is sometimes implicitly written in the unknown functions f.
1) $p = -\rho\left[abx + \frac{1}{2}a^2x^2 + bcy + \frac{1}{2}a^2y^2\right] + p_0 + f_{(t)}$;
2) $p = -\rho\left(8x^2 + 8y^2\right) + p_0 + f_{(t)}$; 3) $\frac{\partial}{\partial x}\left(\frac{\partial p}{\partial y}\right) \neq \frac{\partial}{\partial y}\left(\frac{\partial p}{\partial x}\right)$, thus we cannot describe the pressure with a mathematical function;
4) $p = -\rho\left[\frac{U_0^2}{L}\left(x + \frac{x^2}{2L} + \frac{y^2}{2L}\right) - g_x x - g_y y\right] + p_0 + f_{(t)}$.

Fluid Mechanics
Chapter 5 – Duct flow

last edited May 28, 2016

These lecture notes are based on textbooks by White [9], Çengel & al.[12], and Munson & al.[14].

5.1 Motivation

In this chapter we focus on fluid flow within ducts and pipes. This topic allows us to explore several important phenomena with only very modest mathematical complexity. In particular, we are trying to answer two questions:

1. How can be describe steady fluid flow in a duct?
2. How can we quantify pressure losses in ducts and the power necessary to overcome them?

5.2 Inviscid flow in ducts

We begin with the simplest possible ducted flow case: a purely hypothetical fully-inviscid, incompressible, steady fluid flow in a one-dimensional pipe. Since there are no viscous effects, the velocity profile across the duct remains uniform (flat) all along the flow (fig. 5.1).

If the cross-sectional area A is changed, then the principle of mass conservation (eqs. 0/13, 3/5) is enough to allow us to compute the change in velocity $u = V$:

$$\rho V_1 A_1 = \rho V_2 A_2 \tag{5/1}$$

in laminar inviscid straight pipe flow.

This information, in turn allows us to compute the pressure change between two sections of different areas by using the principel of energy conservation.

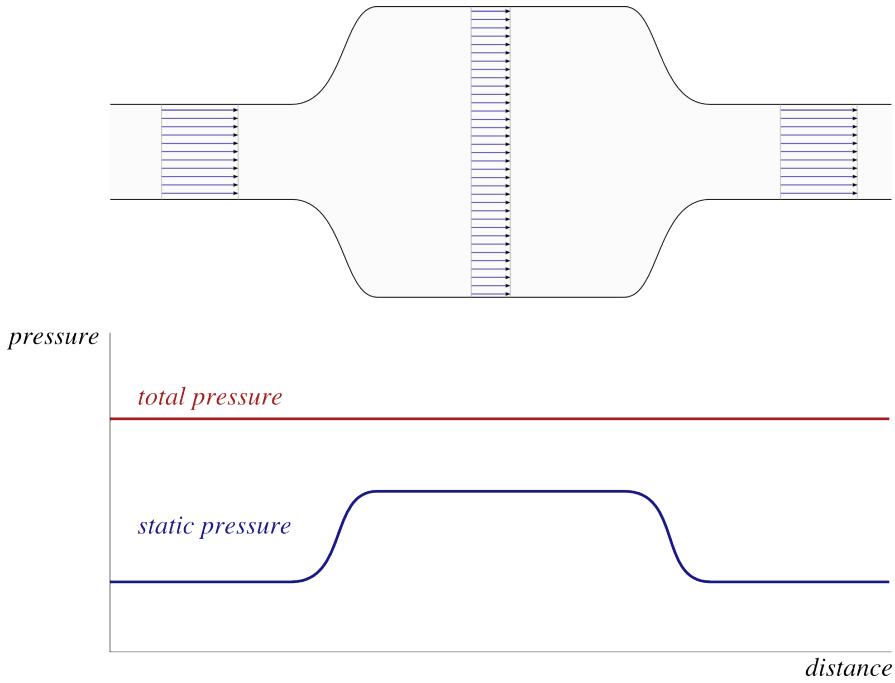

Figure 5.1 – Inviscid fluid flow in a one-dimensional duct. In this purely hypothetical case, the velocity distribution is uniform across a cross-section of the duct. The average velocity and pressure change with cross-section area, but the total pressure $p_0 = p + \frac{1}{2}\rho V_{\text{av.}}^2$ remains constant.

Figure CC-0 o.c.

We notice that the flow is so simple that the five conditions associated with the use of the Bernoulli equation (§3.7) are fulfilled: the flow is steady, incompressible, one-dimensional, has known trajectory, and does not feature friction or energy transfer. A simple application of eq. 3/18 p. 61 yields:

$$p_2 - p_1 = \frac{1}{2}\rho\left[V_2^2 - V_1^2 + g(z_2 - z_1)\right] \tag{5/2}$$

in laminar inviscid pipe flow.

Thus, in this kind of flow pressure increases everywhere the velocity decreases, and vice-versa.

Another way of writing this equation is by stating that at constant altitude, the *total* or *dynamic pressure* $p_{\text{total}} \equiv p_0 \equiv p + \frac{1}{2}\rho V^2$ remains constant:

$$p_0 = \text{cst.} \tag{5/3}$$

at constant altitude, in laminar inviscid straight pipe flow.

We shall, of course, turn immediately to more realistic flows. With viscous effects, one key assumption of the Bernoulli equation breaks down, and additional pressure losses $\Delta p_{\text{friction}}$ will occur, which we would like to quantify.

5.3 Viscous laminar flow in ducts

5.3.1 The entry zone

Let us observe the velocity profile at the entrance of a symmetrical duct in a steady, laminar, viscous flow (fig. 5.2).

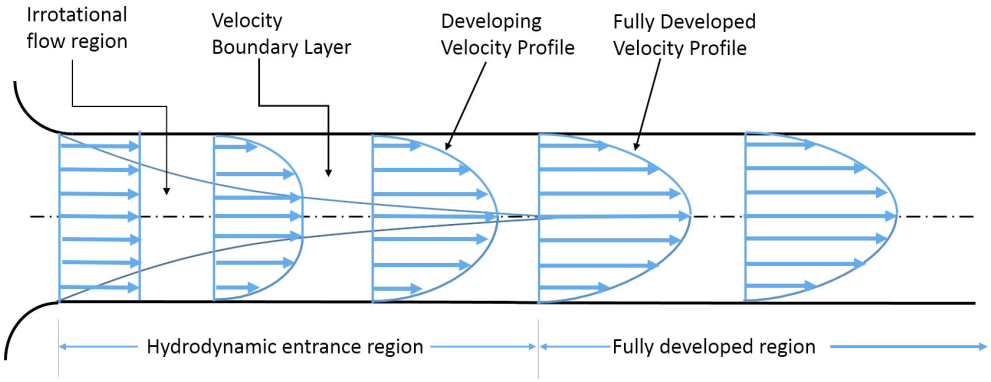

Figure 5.2 – Fluid flow velocity distributions at the entrance of a duct.

Diagram CC-BY-SA *by Wikimedia Commons user:Devender Kumar5908*

The fluid enters the duct with a uniform (flat) velocity profile. Because of the no-slip condition at the wall (§2.3.1 p.42), the particles in contact with the duct walls are immediately stopped. Through viscosity, shear stress effects propagate progressively inwards. A layer appears in which viscosity effects are predominant, which we name *boundary layer*; this layer grows until it reaches the center of the duct. Past this point, the flow is entirely dictated by viscous effects and the velocity profile does not change with distance.
All throughout the entrance region, the core region of the flow is accelerated, and the outer region decelerated, even though the flow itself is steady.

5.3.2 Laminar viscous flow in a one-dimensional duct

Once the flow is fully-developed (but still steady and laminar), how can we describe the velocity and pressure distribution in our one-dimensional horizontal duct? We can start with a qualitative description. With the no-slip condition at the walls, the velocity distribution cannot be uniform (fig. 5.3). Shear will then occur, which translates into a pressure decrease along the flow. The greater the average velocity, and the greater the cross-sectional gradient of velocity. Thus, shear within the flow, and the resulting pressure loss, both increase when the cross-sectional area is decreased.

How can we now describe *quantitatively* the velocity profile and the pressure loss? We need a powerful, extensive tool to describe the flow — and we turn to the Navier-Stokes equation which we derived in the previous chapter as eq. 4/37 p.84:

$$\rho \frac{\mathrm{D}\vec{V}}{\mathrm{D}t} = \rho\vec{g} - \vec{\nabla}p + \mu\vec{\nabla}^2\vec{V} \tag{5/4}$$

Since we are applying this tool to the simple case of fully-developed, two-dimensional incompressible fluid flow between two parallel plates (fig. 5.4), we need only two Cartesian coordinates, reproducing eqs. 4/41 & 4/42:

$$\rho\left[\frac{\partial u}{\partial t} + u\frac{\partial u}{\partial x} + v\frac{\partial u}{\partial y}\right] = \rho g_x - \frac{\partial p}{\partial x} + \mu\left[\frac{\partial^2 u}{(\partial x)^2} + \frac{\partial^2 u}{(\partial y)^2}\right] \tag{5/5}$$

$$\rho\left[\frac{\partial v}{\partial t} + u\frac{\partial v}{\partial x} + v\frac{\partial v}{\partial y}\right] = \rho g_y - \frac{\partial p}{\partial y} + \mu\left[\frac{\partial^2 v}{(\partial x)^2} + \frac{\partial^2 v}{(\partial y)^2}\right] \tag{5/6}$$

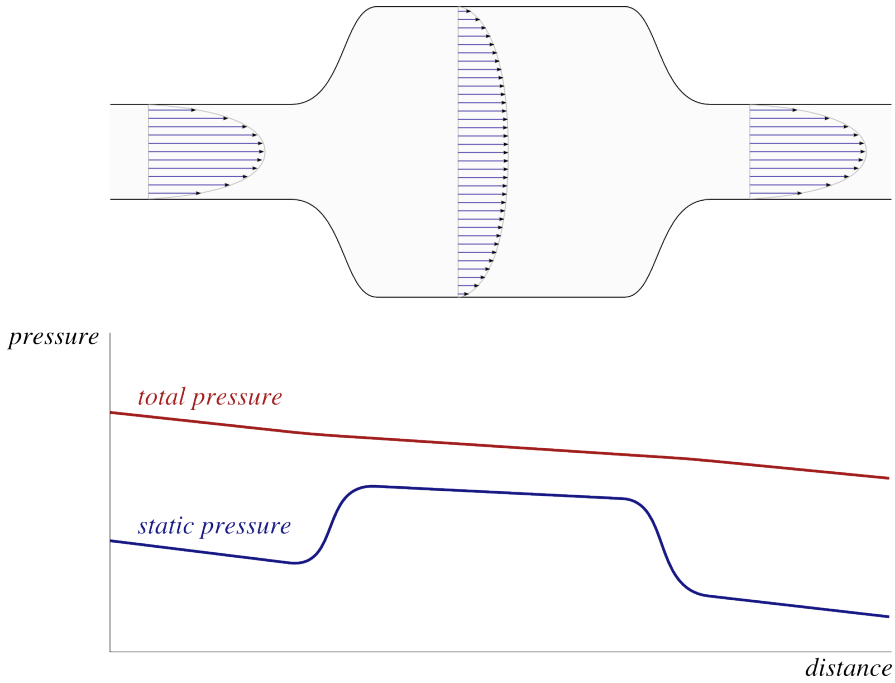

Figure 5.3 – Viscous laminar fluid flow in a one-dimensional pipe. This time, the no-slip condition at the wall creates a viscosity gradient across the duct cross-section. This in turn translates into pressure loss. Sudden duct geometry changes such as represented here would also disturb the flow further, but the effect was neglected here.

Figure CC-0 o.c.

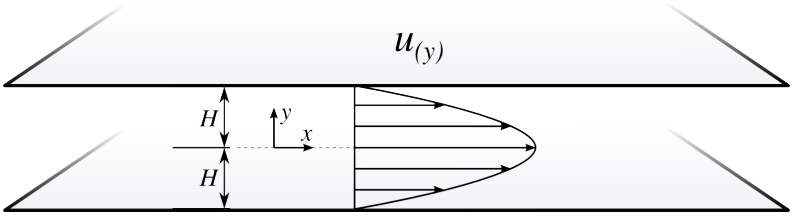

Figure 5.4 – Two-dimensional laminar flow between two plates, also called *Couette flow*. We already studied this flow case in fig. 2.4 p.47; this time, we wish to derive an expression for the velocity distribution.

Figure CC-0 o.c.

Here, we have restricted ourselves to a fully-steady ($\frac{\mathrm{d}}{\mathrm{d}t} = 0$), horizontal ($g = g_y$), one-directional flow ($v = 0$). When the flow is fully developed, $\frac{\partial u}{\partial x} = 0$ and $\frac{\partial^2 u}{(\partial x)^2} = 0$, and the system above shrinks down to:

$$0 = -\frac{\partial p}{\partial x} + \mu \left[\frac{\partial^2 u}{(\partial y)^2} \right] \tag{5/7}$$

$$0 = \rho g - \frac{\partial p}{\partial y} \tag{5/8}$$

We only have to integrate equation 5/7 twice to come to the velocity profile across two plates separated by a height $2H$:

$$u = \frac{1}{2\mu} \left(\frac{\partial p}{\partial x} \right) (y^2 - H^2) \tag{5/9}$$

Now, the longitudinal pressure gradient $\frac{\partial p}{\partial x}$ can be evaluated by working out the volume flow rate $\dot{\mathcal{V}}$ for any given depth z (length across the document plane) with one further integration of equation 5/9:

$$\begin{aligned} \frac{\dot{\mathcal{V}}}{z} &= \frac{1}{z}\int_0^H uz\,\mathrm{d}y = -\frac{2H^3}{3\mu}\left(\frac{\partial p}{\partial x}\right) \\ \frac{\partial p}{\partial x} &= -\frac{3}{2}\frac{\mu}{zH^3}\dot{\mathcal{V}} \end{aligned} \tag{5/10}$$

In this section, the overall process is more important than the result: by starting with the Navier-Stokes equations, and adding known constraints that describe the flow of interest, we can predict analytically all of the characteristics of a laminar flow.

5.4 Viscous laminar flow in cylindrical pipes

We now turn to studying flow in *cylindrical* pipes, which are widely used; first considering laminar flow, and then expanding to turbulent flow.

5.4.1 Principle

The process is identical to above, only applied to cylindrical instead of Cartesian coordinates. We focus on the fully-developed laminar flow of a fluid in a horizontal cylindrical pipe (fig. 5.5).

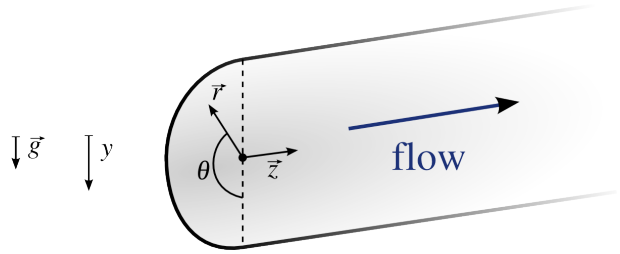

Figure 5.5 – A cylindrical coordinate system to study laminar flow in a horizontal cylindrical duct.

Figure CC-0 o.c.

For this flow, we wish to work out the velocity profile and calculate the pressure loss related to the flow.

5.4.2 Velocity profile

We once again start from the Navier-Stokes vector equation, choosing this time to develop it using *cylindrical* coordinates:

$$\rho\left[\frac{\partial v_r}{\partial t}+v_r\frac{\partial v_r}{\partial r}+\frac{v_\theta}{r}\frac{\partial v_r}{\partial \theta}-\frac{v_\theta^2}{r}+v_z\frac{\partial v_r}{\partial z}\right] = \rho g_r-\frac{\partial p}{\partial r}+\mu\left[\frac{1}{r}\frac{\partial}{\partial r}\left(r\frac{\partial v_r}{\partial r}\right)-\frac{v_r}{r^2}+\frac{1}{r^2}\frac{\partial^2 v_r}{(\partial\theta)^2}-\frac{2}{r^2}\frac{\partial v_\theta}{\partial\theta}+\frac{\partial^2 v_r}{(\partial z)^2}\right] \tag{5/11}$$

$$\rho\left[\frac{\partial v_\theta}{\partial t}+v_r\frac{\partial v_\theta}{\partial r}+\frac{v_\theta}{r}\frac{\partial v_\theta}{\partial \theta}+\frac{v_r v_\theta}{r}+v_z\frac{\partial v_\theta}{\partial z}\right] = \rho g_\theta-\frac{1}{r}\frac{\partial p}{\partial\theta}+\mu\left[\frac{1}{r}\frac{\partial}{\partial r}\left(r\frac{\partial v_\theta}{\partial r}\right)-\frac{v_\theta}{r^2}+\frac{1}{r^2}\frac{\partial^2 v_\theta}{(\partial\theta)^2}+\frac{2}{r^2}\frac{\partial v_r}{\partial\theta}+\frac{\partial^2 v_\theta}{(\partial z)^2}\right] \tag{5/12}$$

$$\rho\left[\frac{\partial v_z}{\partial t}+v_r\frac{\partial v_z}{\partial r}+\frac{v_\theta}{r}\frac{\partial v_r}{\partial \theta}+v_z\frac{\partial v_z}{\partial z}\right] = \rho g_z-\frac{\partial p}{\partial z}+\mu\left[\frac{1}{r}\frac{\partial}{\partial r}\left(r\frac{\partial v_z}{\partial r}\right)+\frac{1}{r^2}\frac{\partial^2 v_z}{(\partial\theta)^2}+\frac{\partial^2 v_z}{(\partial z)^2}\right] \tag{5/13}$$

This mathematical arsenal does not frighten us, for the simplicity of the flow we are studying allows us to bring in numerous simplifications. Firstly, we have $v_r = 0$ and $v_\theta = 0$ everywhere. Thus, by continuity, $\partial v_z/\partial z = 0$. Furthermore, since our flow is symmetrical, v_z is independent from θ. With these two conditions, the above system shrinks down to:

$$0 = \rho g_r-\frac{\partial p}{\partial r} \tag{5/14}$$

$$0 = \rho g_\theta-\frac{1}{r}\frac{\partial p}{\partial\theta} \tag{5/15}$$

$$0 = -\frac{\partial p}{\partial z}+\mu\left[\frac{1}{r}\frac{\partial}{\partial r}\left(r\frac{\partial v_z}{\partial r}\right)\right] \tag{5/16}$$

Equations (5/14) and (5/15) hold the key to describing pressure:

$$p = -\rho g y + f_{(z)} \tag{5/17}$$

this expresses the (unsurprising) fact that the pressure distribution within a cross-section of the pipe perpendicular to the flow is simply the result of a hydrostatic gradient.

Now, with equation 5/16, we work towards obtaining an expression for v_z by integrating twice our expression for $\partial v_z/\partial r$:

$$\begin{aligned}\frac{\partial}{\partial r}\left(r\frac{\partial v_z}{\partial r}\right) &= \frac{r}{\mu}\frac{\partial p}{\partial z}\\ \left(r\frac{\partial v_z}{\partial r}\right) &= \frac{r^2}{2\,\mu}\left(\frac{\partial p}{\partial z}\right)+k_1\\ v_z &= \frac{r^2}{4\,\mu}\left(\frac{\partial p}{\partial z}\right)+k_1\ln r+k_2\end{aligned} \tag{5/18}$$

We have to use boundary conditions so as to unburden ourselves from integration constants k_1 and k_2.

By setting $v_{z\ (r=0)}$ as finite, we deduce that $k_1 = 0$ (because $\ln(0) \to -\infty$).
By setting $v_{z\ (r=R)} = 0$ (no-slip condition), we obtain $k_2 = -\frac{R^2}{4\,\mu}\frac{\partial p}{\partial z}$.
This simplifies eq. (5/18) and brings us to our objective, an extensive expression for the velocity profile across a pipe of radius R when the flow is laminar:

$$v_z = u_{(r)} = -\frac{1}{4\mu}\left(\frac{\partial p}{\partial z}\right)(R^2 - r^2) \tag{5/19}$$

This equation is parabolic (fig. 5.6). It tells us that in a pipe of given length L and radius R, a given velocity profile will be achieved which is a function only of the ratio $\Delta p/\mu$.

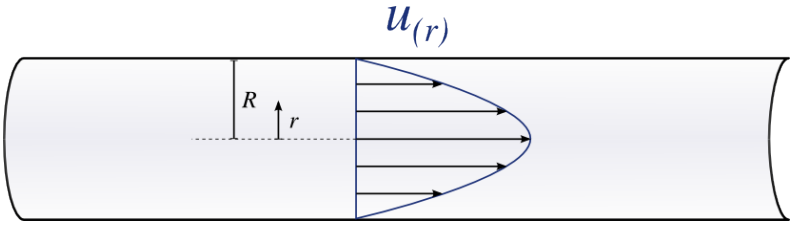

Figure 5.6 – The velocity profile across a cylindrical pipe featuring laminar viscous flow.

Figure CC-0 o.c.

In the same way we proceeded before, we can express the pressure gradient in the pipe as a function of the volume flow rate, which itself is obtained through integration:

$$\dot{\mathcal{V}} = \int_0^R v_z(2\pi r)\,\mathrm{d}r = -\frac{\pi D^4}{128\,\mu}\left(\frac{\partial p}{\partial x}\right)$$
$$\frac{\partial p}{\partial x} = \frac{\Delta p_{\text{friction}}}{L} = -\frac{128}{\pi}\frac{\mu}{D^4}\dot{\mathcal{V}} \tag{5/20}$$

This equation is interesting in several respects. For a given pipe length L and pressure drop $\Delta p_{\text{friction}}$, the volume flow $\dot{\mathcal{V}}$ increases with the power 4 of the diameter D. In other words, the volume flow is multiplied by 16 every time the diameter is doubled.

We also notice that the pipe wall roughness does not appear in equation 5/20. In a laminar flow, increasing the pipe roughness has no effect on the velocity of the fluid layers at the center of the pipe.

When the pipe is inclined relative to the horizontal with an angle α, eqs. (5/19) and (5/20) remain valid except for the pressure drop term Δp which is simply replaced by $(\Delta p_{\text{friction}} + \rho g L \sin\alpha)$, since gravity then contributes to the longitudinal change in pressure.

5.4.3 Quantification of losses

Hydraulics was the first sub-discipline of fluid dynamics which yielded practical engineering results; the conventions used in the industry to measure key parameters related to liquid flows borrow from this history and may not always seem self-evident. The most widely-used parameters for quantifying losses due to friction in a duct are the following (hereon $\Delta p_{\text{friction}}$ is simply written Δp):

The elevation loss noted $|\Delta e|$ is defined as

$$|\Delta e| \equiv \frac{|\Delta p|}{\rho g} \tag{5/21}$$

It represents the hydrostatic height loss (with a positive number) caused by the fluid flow in the duct, and is measured in meters. It is often written Δh (without bars, but as a positive number), but in this document we reserve h to denote enthalpy (as in eq. 3/17 p.60).

The Darcy friction factor noted f is defined as

$$f \equiv \frac{|\Delta p|}{\frac{L}{D}\frac{1}{2}\rho V_{\text{av.}}^2} \tag{5/22}$$

where $V_{\text{av.}}$ is the average flow velocity in the pipe.

This dimensionless term is widely used in the industry because it permits the quantification of losses independently of scale effects (L/D) and inflow conditions ($\rho V_{\text{av.}}^2$).

The loss coefficient noted K_L is defined as

$$K_L \equiv \frac{|\Delta p|}{\frac{1}{2}\rho V_{\text{av.}}^2} \tag{5/23}$$

It is simply equivalent to a Darcy coefficient in which no value of D/L can be measured, and it is used mostly in order to describe losses in single components found in pipe systems, such as bends, filter screens, or valves.

For a laminar flow in a cylindrical duct, for example, we can easily compute f, inserting equation 5/20 into the definition 5/22:

$$f_{\text{laminar cylinder flow}} = \frac{32 V_{\text{av.}} \mu L}{\frac{L}{D}\frac{1}{2}\rho V_{\text{av.}}^2 D^2} = 64 \frac{\mu}{\rho V_{\text{av.}}\, D} \tag{5/24}$$

in which we inserted the average velocity $V_{\text{av.}} = \frac{\dot{\mathcal{V}}}{\pi R^2} = -\frac{\Delta p\, D^2}{32 \mu L}$.

5.5 Viscous turbulent flow in cylindrical pipes

5.5.1 Predicting the occurrence of turbulence

It has long been observed that pipe flow can have different *regimes*. In some conditions, the flow is unable to remain laminar (one-directional, fully-steady); it becomes *turbulent*. Although the flow is steady when it is averaged over a time period of a few seconds, it is subject to constant, small-scale, chaotic and spontaneous velocity field changes in all directions.

In 1883, Osborne Reynolds published the results of a meticulous investigation into the conditions in which the flow is able, or not, to remain laminar (figs. 5.7 and 5.8). He showed that they could be predicted using a single non-dimensional parameter, later named *Reynolds number*, which can be expressed as:

$$[\text{Re}]_D \equiv \frac{\rho\, V_{\text{av.}}\, D}{\mu} \tag{5/25}$$

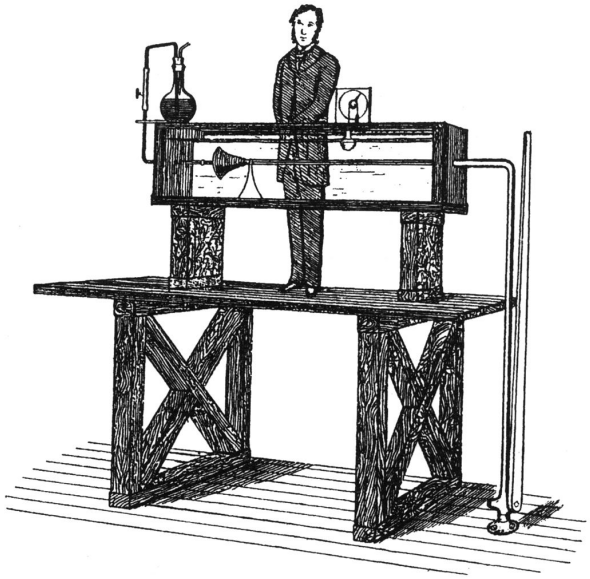

Figure 5.7 – Illustrations published by Reynolds in 1883 showing the installation he set up to investigate the onset of turbulence. Water flows from a transparent rectangular tank down into a transparent drain pipe, to the right of the picture. Colored die is injected at the center of the pipe water flow, allowing for the visualization of the flow regime.

Image by Osborne Reynolds (1883, public domain)

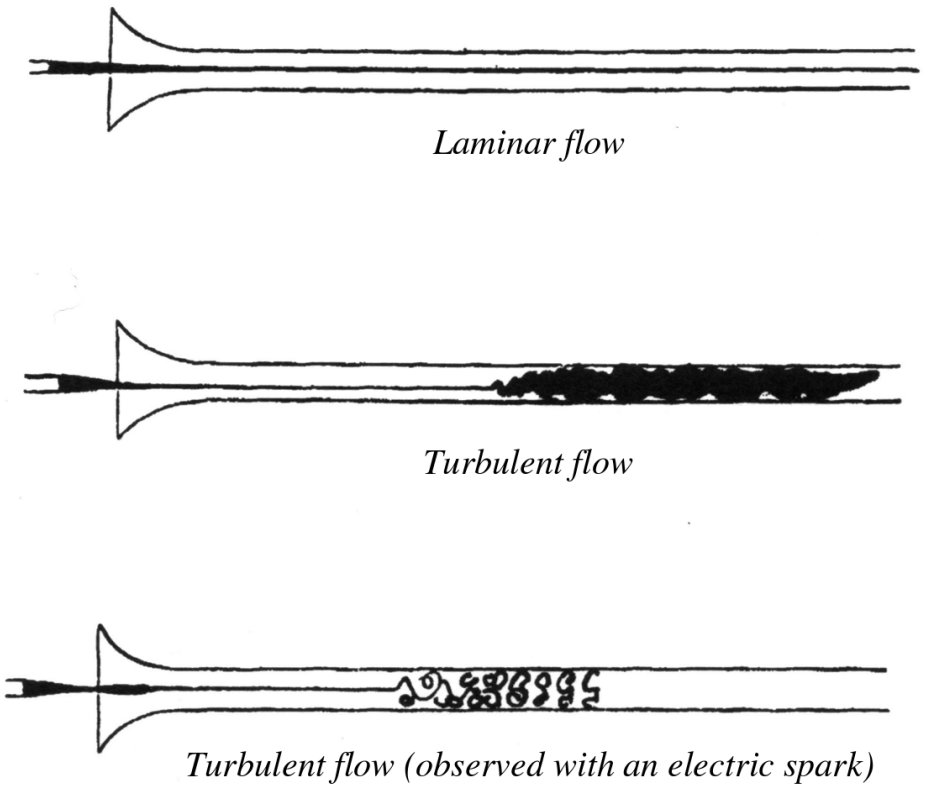

Figure 5.8 – Illustrations published by Reynolds in 1883 showing two different flow regimes observed in the installation from fig. 5.7.

Image by Osborne Reynolds (1883, public domain)

where $V_{\text{av.}}$ is the average velocity in the pipe ($\mathrm{m\,s^{-1}}$),
and D is the pipe diameter (m).

The occurrence of turbulence is very well documented (although it is still not well-predicted by purely-theoretical models). The following values are now widely accepted:

- Pipe flow is laminar for $[\mathrm{Re}]_D \lesssim 2\,300$;
- Pipe flow is turbulent for $[\mathrm{Re}]_D \gtrsim 4\,000$.

The significance of the Reynolds number extends far beyond pipe flow; we shall explore this in chapter 6 (pp.122 & 127).

5.5.2 Characteristics of turbulent flow

This topic is well covered in Tennekes & Lumley [2]

Turbulence is a complex topic which is still not fully described analytically today. Although it may display steadiness when time-averaged, a turbulent flow is highly three-dimensional, unsteady, and chaotic in the sense that the description of its velocity field is carried out with statistical, instead of analytic, methods.

In the scope of our study of fluid dynamics, the most important characteristics associated with turbulence are the following:

- A strong increase in mass and energy transfer within the flow. Slow and rapid fluid particles have much more interaction (especially momentum transfer) than within laminar flow;
- A strong increase in losses due to friction (typically by a factor 2). The increase in momentum exchange within the flow creates strong dissipation through viscous effects and thus transfer, as heat, of kinetic and pressure energy (at a macroscopic scale) towards internal energy (agitation at a microscopic scale);
- Internal flow movements appear to be chaotic (though not merely *random*, as would be white noise), and we do not have mathematical tools to describe them analytically.

Consequently, solving a turbulent flow requires taking account of flow in all three dimensions even for one-directional flow!

5.5.3 Velocity profile in turbulent pipe flow

In order to deal with the vastly-increased complexity of turbulent flow in pipes, we split each velocity component v_i in two parts, a time-averaged component $\overline{v_i}$ and an instantaneous fluctuation v_i':

$$v_r = \overline{v_r} + v_r' \tag{5/26}$$
$$v_\theta = \overline{v_\theta} + v_\theta' \tag{5/27}$$
$$v_z = \overline{v_z} + v_z' \tag{5/28}$$

In our case, $\overline{v_r}$ and $\overline{v_\theta}$ are both zero, but the fluctuations v'_r and v'_θ are not, and will cause v_z to differ from the laminar flow case. The extent of turbulence is often measured with the concept of *turbulence intensity* I:

$$I \equiv \frac{\left[\overline{v_i'^2}\right]^{\frac{1}{2}}}{\overline{v_i}} \tag{5/29}$$

Regrettably, we have not found a general analytical solution to turbulent pipe flow — note that if we did, it would likely exhibit complexity in proportion to that of such flows. A widely-accepted average velocity profile constructed from experimental observations is:

$$\overline{u}_{(r)} = \overline{v_z} = \overline{v_{z\,\max}}\left(1 - \frac{r}{R}\right)^{\frac{1}{7}} \tag{5/30}$$

While it closely and neatly matches experimental observations, this model is nowhere as potent as an analytical one and must be seen only as an approximation. For example, it does not allow us to predict internal energy dissipation rates (because it describes only time-averaged velocity), or even wall shear stress (because it yields $(\partial\overline{u}/\partial r)_{r=R} = \infty$, which is not physical).

The following points summarize the most important characteristics of turbulent velocity profiles:

- They continuously fluctuate in time and we have no means to predict them extensively;
- They are much "flatter" than laminar profiles (fig. 5.9);
- They depend on the wall roughness;
- They result in shear and dissipation rates that are markedly higher than laminar profiles.

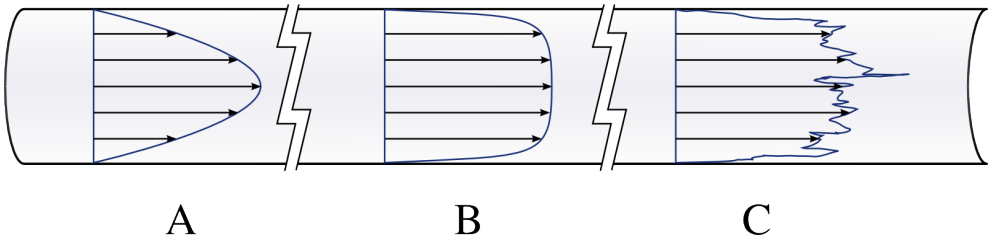

Figure 5.9 – Velocity profiles for laminar (A), and turbulent (B and C) flows in a cylindrical pipe. B represents the time-averaged velocity distribution, while C represents an arbitrary instantaneous distribution. Turbulent flow in a pipe also features velocities in the radial and angular directions, which are not shown here.

Figure CC-0 o.c.

5.5.4 Pressure losses in turbulent pipe flow

Losses caused by turbulent flow depend on the wall roughness ϵ and on the diameter-based Reynolds number $[\mathrm{Re}]_D$.

For lack of an analytical solution, we are not able to predict the value of the friction factor f anymore. Several empirical models can be built to obtain f,

the most important of which is known as the *Colebrook equation* expressed as:

$$\frac{1}{\sqrt{f}} = -2\log\left(\frac{1}{3{,}7}\frac{\epsilon}{D} + \frac{2{,}51}{[\mathrm{Re}]_D\sqrt{f}}\right) \tag{5/31}$$

The structure of this equation makes it inconvenient to solve for f. To circumvent this difficulty, equation 5/31 can be solved graphically on the *Moody diagram*, fig. 5.10. This classic document allows us to obtain numerical values for f (and thus predict the pressure losses $\Delta p_{\text{friction}}$) if we know the diameter-based Reynolds number $[\mathrm{Re}]_D$ and the relative roughness ϵ/D.

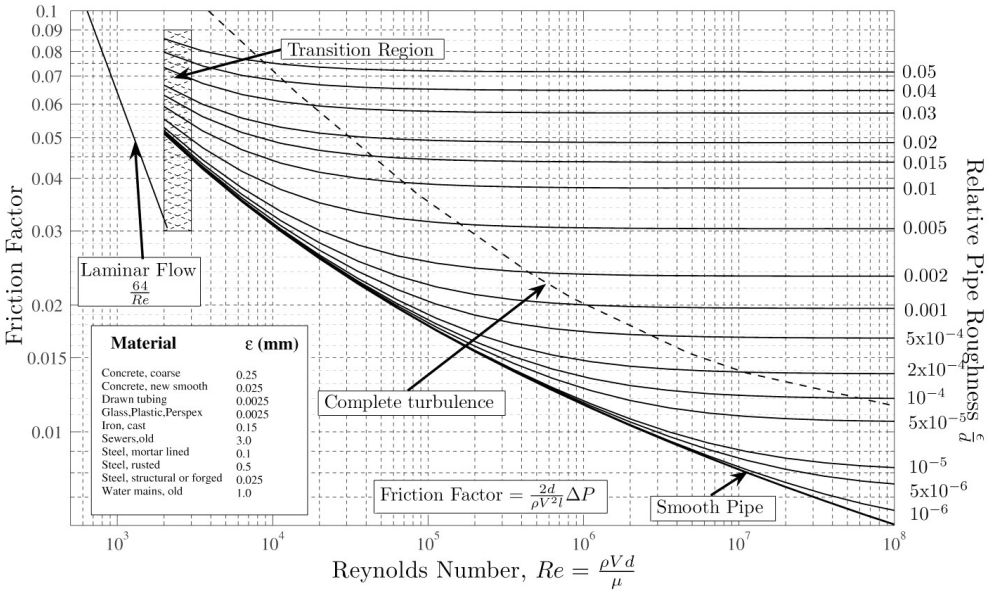

Figure 5.10 – A Moody diagram, which presents values for f measured experimentally, as a function of the diameter-based Reynolds number $[\mathrm{Re}]_D$, for different values of the relative roughness ϵ/D. This figure is reproduced with a larger scale as figure 5.12 p.108.

Diagram CC-BY-SA *S Beck and R Collins, University of Sheffield*

Fluid Mechanics
Exercise sheet 5 – Duct flow

last edited May 29, 2016

These lecture notes are based on textbooks by White [9], Çengel & al.[12], and Munson & al.[14].

Except otherwise indicated, we assume that fluids are Newtonian, and that:
$\rho_{\text{water}} = 1\,000\,\text{kg m}^{-3}$; $p_{\text{atm.}} = 1\,\text{bar}$; $\rho_{\text{atm.}} = 1{,}225\,\text{kg m}^{-3}$; $T_{\text{atm.}} = 11{,}3\,^{\circ}\text{C}$; $\mu_{\text{atm.}} = 1{,}5 \cdot 10^{-5}\,\text{N s m}^{-2}$;
$g = 9{,}81\,\text{m s}^{-2}$. Air is modeled as a perfect gas ($R_{\text{air}} = 287\,\text{J K}^{-1}\,\text{kg}^{-1}$; $\gamma_{\text{air}} = 1{,}4$; $c_{p\text{air}} = 1\,005\,\text{J kg}^{-1}\,\text{K}^{-1}$).

In cylindrical pipe flow, we accept the flow is always laminar for $[\text{Re}]_D \lesssim 2\,300$, and always turbulent for $[\text{Re}]_D \gtrsim 4\,000$. The Darcy friction factor f is defined as:

$$f \equiv \frac{|\Delta p|}{\frac{L}{D}\frac{1}{2}\rho V_{\text{av.}}^2} \tag{5/22}$$

The loss coefficient K_L is defined as:

$$K_L \equiv \frac{|\Delta p|}{\frac{1}{2}\rho V_{\text{av.}}^2} \tag{5/23}$$

Viscosities of various fluids are given in fig. 5.11. Pressure losses in cylindrical pipes can be calculated with the help of the Moody diagram presented in fig. 5.12.

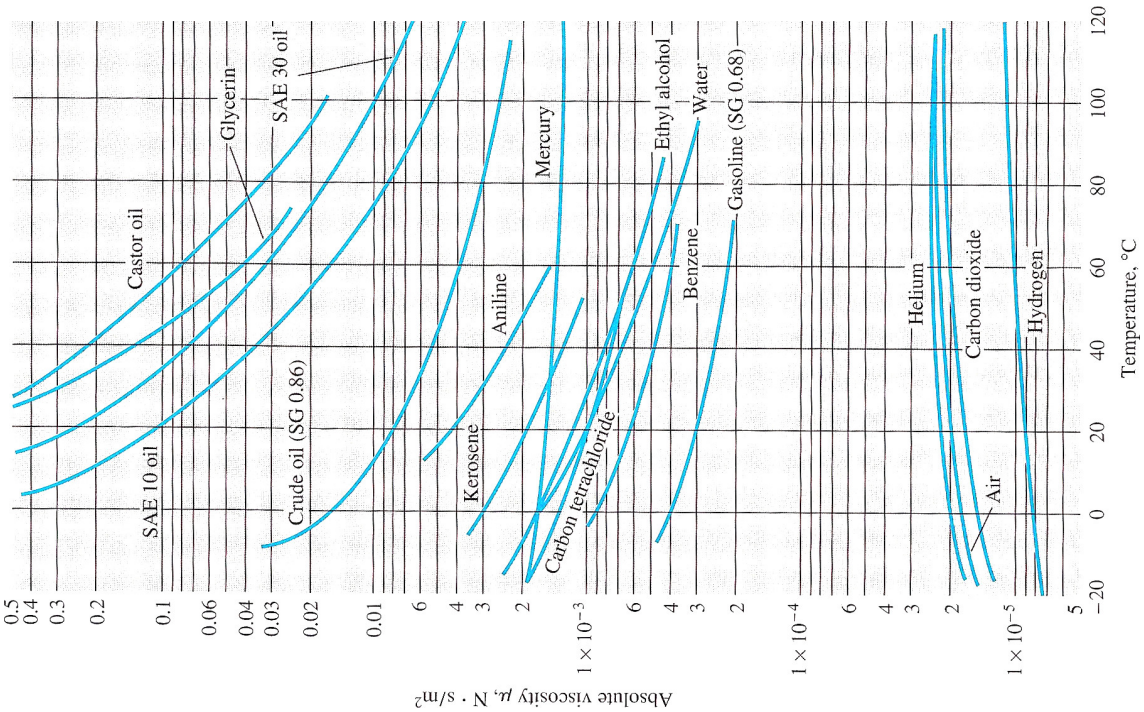

Figure 5.11 – Viscosity of various fluids at a pressure of 1 bar (in practice viscosity is almost independent of pressure).

Figure © White 2008 [9]

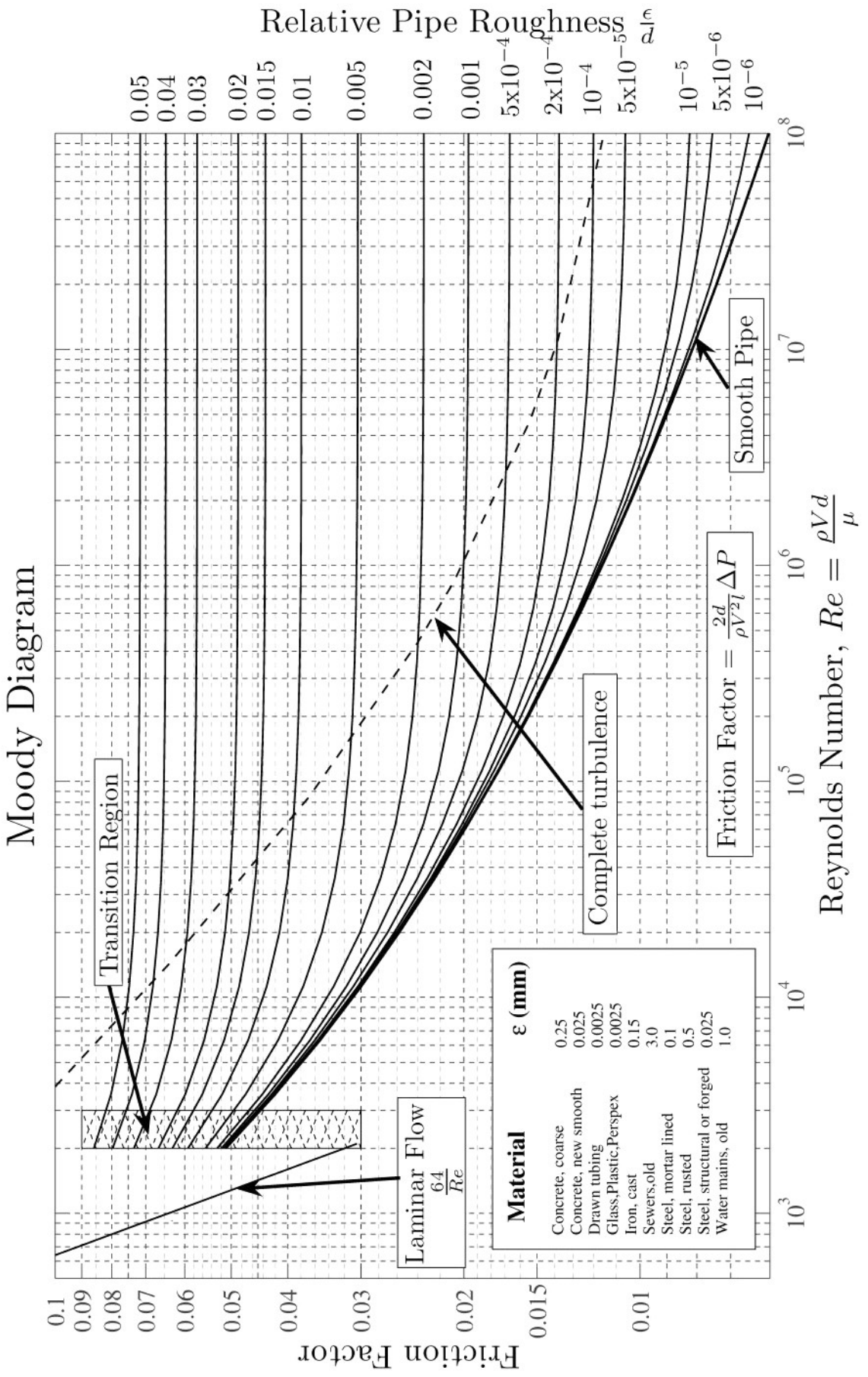

Figure 5.12 – A Moody diagram, which presents values for f measured experimentally, as a function of the diameter-based Reynolds number $[\mathrm{Re}]_D$, for different relative roughness values.

Diagram CC-BY-SA *S Beck and R Collins, University of Sheffield*

5.1 Revision questions

non-examinable

The Moody diagram (fig. 5.12) is simple to use, yet it takes practice to understand it fully… here are three questions to guide your exploration. They can perhaps be answered as you work through the other examples.

1. Why is there no zero on the diagram?
2. Why are the curves sloped downwards — should friction losses not instead *increase* with increasing Reynolds number?
3. Why can the pressure losses Δp be calculated given the volume flow $\dot{\mathcal{V}}$, but not the other way around?

5.2 Air flow in a small pipe

Munson & al. [14] E8.5

A machine designed to assemble micro-components uses an air jet. This air is driven through a 10 cm-long cylindrical pipe with a 4 mm diameter, roughness 0,0025 mm, at an average speed of 50 $\mathrm{m\,s^{-1}}$.

The inlet air pressure and temperature are 1,2 bar and 20 °C; the air viscosity is quantified in fig. 5.11 p. 107.

1. What is the pressure loss caused by the flow through the pipe?
2. Although that is not possible in practice, what would the loss in the case where laminar flow could be maintained throughout the pipe?

5.3 Couette flow

CC-0 o.c.

We consider the laminar flow of a fluid between two parallel plates (named *Couette flow*), as shown in fig. 5.13.

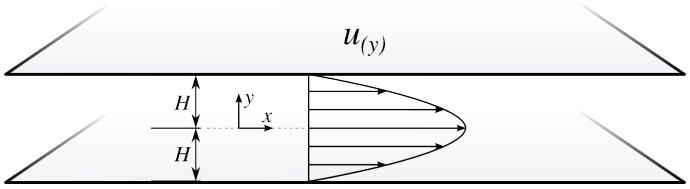

Figure 5.13 – Two-dimensional laminar flow between two plates, also called *Couette flow*.

Figure CC-0 o.c.

1. Starting from the Navier-Stokes equations for incompressible, two-dimensional flow,

$$\rho\left[\frac{\partial u}{\partial t}+u\frac{\partial u}{\partial x}+v\frac{\partial u}{\partial y}\right]=\rho g_x-\frac{\partial p}{\partial x}+\mu\left[\frac{\partial^2 u}{(\partial x)^2}+\frac{\partial^2 u}{(\partial y)^2}\right] \tag{4/41}$$

$$\rho\left[\frac{\partial v}{\partial t}+u\frac{\partial v}{\partial x}+v\frac{\partial v}{\partial y}\right]=\rho g_y-\frac{\partial p}{\partial y}+\mu\left[\frac{\partial^2 v}{(\partial x)^2}+\frac{\partial^2 v}{(\partial y)^2}\right] \tag{4/42}$$

show that the velocity profile in a horizontal, laminar, fully-developed flow between two horizontal plates separated by a gap of height $2H$ is:

$$u = \frac{1}{2\mu}\left(\frac{\partial p}{\partial x}\right)(y^2 - H^2) \tag{5/9}$$

2. Why would this equation fail to describe turbulent flow?

5.4 Kugel fountain

Munson & al. [14] 6.91

A *Kugel fountain* is erected to entertain students of fluid mechanics (figs. 5.14 and 5.15). A granite block ($2\,700\,\mathrm{kg\,m^{-3}}$) is sculpted into a very smooth sphere of diameter 1,8 m. The sphere is laid on a cylindrical concrete stand of internal diameter 1,2 m, whose edges are also smoothed out.

The stand is filled with water, and a pump creates a flow which lifts the sphere to make a decorative fountain. Water flows between the stand and the sphere along a length of 10 cm, with a thickness of 0,13 mm.

What is the power required to drive the fountain?

Hints: you may assume that the flow is laminar, and that a *Couette flow* in between two parallel plates of width z separated by a height $2H$ can be modeled with the velocity distribution $u_{(y)}$ and longitudinal pressure gradient $\frac{\partial p}{\partial x}$ described as:

$$u = \frac{1}{2\mu}\left(\frac{\partial p}{\partial x}\right)(y^2 - H^2) \tag{5/9}$$

$$\frac{\partial p}{\partial x} = -\frac{3}{2}\frac{\mu}{zH^3}\dot{\mathcal{V}} \tag{5/10}$$

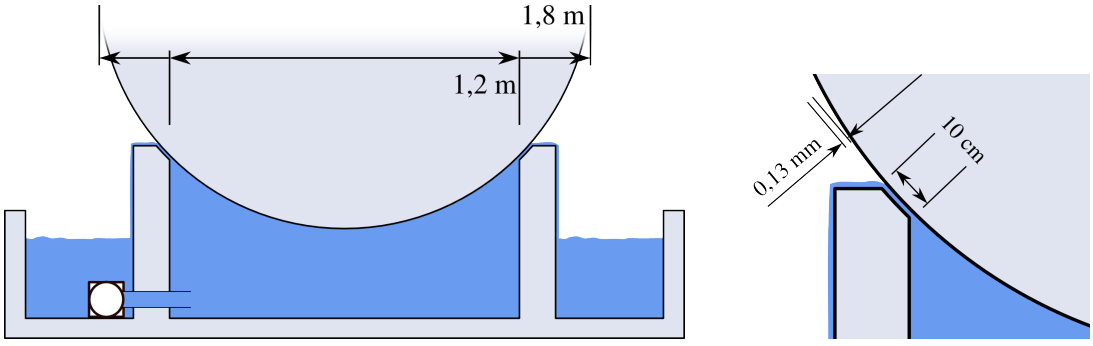

Figure 5.14 – Schematic layout for a *Kugel fountain*. A pump (bottom left) increases the water pressure to a value high enough that it can support the weight of the sphere. A thin strip of water flows between the concrete foundation and the sphere.

Figure CC-0 o.c.

Figure 5.15 – A *Kugel fountain*, in which a granite sphere is supported by the flow of water between the sphere and a solid strip of concrete.

Photo CC-BY-SA *by Commons User:Atamari*

5.5 Water piping

CC-0 o.c.

A long pipe is installed to carry water from one large reservoir to another (fig. 5.16). The total length of the pipe is 10 km, its diameter is 0,5 m, and its roughness is $\epsilon = 0{,}5$ mm. It must climb over a hill, so that the altitude changes along with distance.

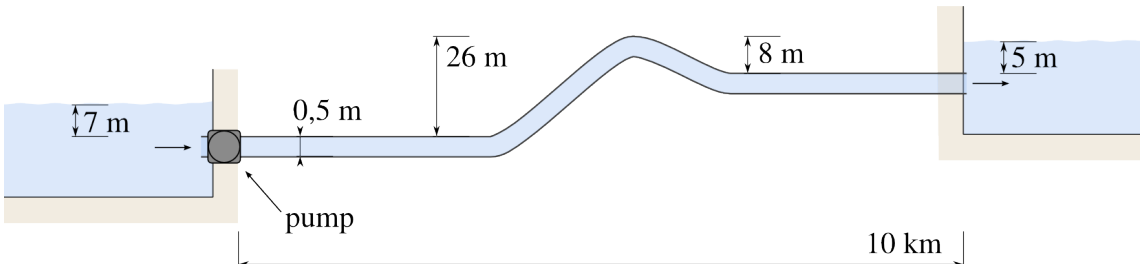

Figure 5.16 – Layout of the water pipe. For clarity, the vertical scale is greatly exaggerated. The diameter of the pipe is also exaggerated.

Figure CC-0 o.c.

The pump must be powerful enough to push 1 $m^3\ s^{-1}$ of water at 20 °C.

Figure 5.11 quantifies the viscosity of various fluids, and fig. 5.12 quantifies losses in cylindrical pipes.

1. Will the flow in the water pipe be turbulent?
2. What is the pressure drop generated by the water flow?
3. What is the pumping power required to meet the design requirements?
4. What would be the power required for the same volume flow if the pipe diameter was doubled?

5.6 Pipeline

CC-0 o.c.

The *Trans-Alaska Pipeline System* is a cylindrical smooth steel duct with 1,22 m diameter, average roughness $\epsilon = 0{,}15\,\mathrm{mm}$, and length 1 200 km. Approximately 700 thousand barrels of oil (110 000 m^3) transit through the pipe each day.

The density of crude oil is approximately 900 $\mathrm{kg\,m^{-3}}$ and its viscosity is quantified in fig. 5.11. The average temperature of the oil during the transit is 60 °C. In industrial pumps, oil starts to cavitate (change state, a very undesirable behavior) when its pressure falls below 0,7 bar.

The pipeline is designed to withstand ground deformations due to seismic movements in several key zones, and crosses a mountain range with a total altitude variation of 1 400 m.

1. How much time does an oil particle need to travel across the line?
2. Propose a pumping station arrangement, and calculate the power required for each pump.
3. How would the pumping power change if the speed was increased?

5.7 Pump with pipe expansion

A pump is used to carry a volume flow of 200 $\mathrm{L\,s^{-1}}$ from one large water reservoir to another (fig. 5.17). The altitude of the water surface in both reservoirs is the same.

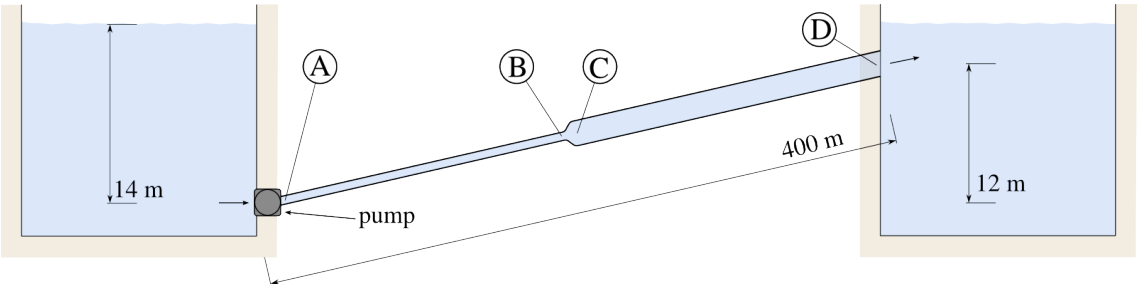

Figure 5.17 – Layout of the water pipe. For clarity, the diameter of the pipe and the vertical scale are exaggerated.

Figure CC-0 o.c.

The pipe connecting the reservoirs is made of concrete ($\epsilon = 0{,}25\,\mathrm{mm}$); it has a diameter of 50 cm on the first half, and 100 cm on the second half. In the middle, the conical expansion element induces a loss coefficient of 0,8.

The inlet is 14 m below the surface. The total pipe length is 400 m; the altitude change between inlet and outlet is 12 m.

1. Represent qualitatively (that is to say, showing the main trends, but without displaying accurate values) the water pressure as a function of pipe distance, when the pump is turned off.
2. On the same graph, represent qualitatively the water pressure when the pump is switched on.
3. What is the water pressure at points A, B, C and D?

5.8 A more complex ducted flow

non-examinable. From institute archives

A more complicated laminar flow case can be studied with the following case.

In the middle of a vertical container of width $2h$ filled with oil (fig. 5.18), a plate of width b (perpendicular to the plane) and length L with negligible thickness is sinking at constant velocity v_p.

Under the assumption that the flow is laminar everywhere, steady and fully developed, give an analytical expression for the friction force applied on the plate.

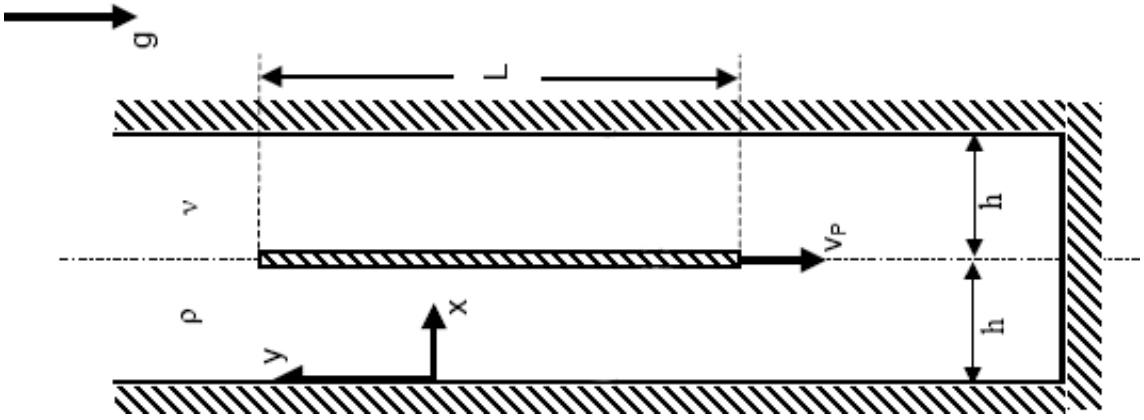

Figure 5.18 – The hypothetical case of a plate sinking vertically in an oil reservoir.

5.9 Wind tunnel

non-examinable

Describe the main characteristics of a wind tunnel that could be installed and operated in the room you are standing in.

In order to do this:

- Start by proposing key characteristics for the test section;
- From these dimensions, draw approximately an air circuit to feed the test section (while attempting to minimize the size of the fan, whose cost increases exponentially with diameter).
- Quantify the static and stagnation pressures along the air circuit, by estimating the losses generated by wall shear and in the bends (you may use data from fig. 5.19);
- Quantify the minimum power required to generate your chosen test section flow characteristics.

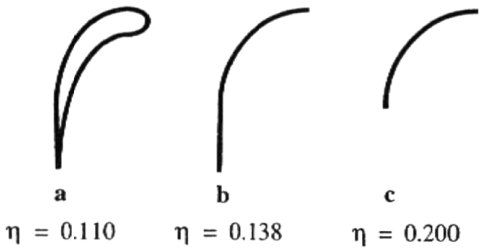

Filter screen: $\eta = 0{,}05$

Figure 5.19 – Loss coefficients K_L (here noted η) generated by the use of various components within wind tunnel ducts.

Figure © Barlow, Rae & Pope 1999 [7]

5.10 Politically incorrect fluid mechanics

non-examinable

In spite of the advice of their instructor, a group of students attempts to apply fluid mechanics to incommendable activities. Their objective is to construct a drinking straw piping system that can mix a drink of vodka and tonic water in the correct proportions (fig. 5.20). They use a "*Strawz*" kit of connected drinking straws, two bottles, and a glass full of ice and liquid water to cool the mix.

For simplicity, the following information is assumed about the setup:

- Vodka is modeled as 40 % pure alcohol (ethanol) with 60 % water by volume;
- Ethanol density is 0,8 $\mathrm{kg\,m^{-3}}$;
- Tonic water is modeled as pure water;
- The viscosity of water and alcohol mixes is described in table 5.1 (use the nearest relevant value);
- The pipe bends induce a loss coefficient factor $K_{L\mathrm{bend}} = 0{,}5$ each;
- The pipe T-junction induces a loss coefficient factor $K_L = 0{,}3$ in the line direction and 1 in the branching flow;

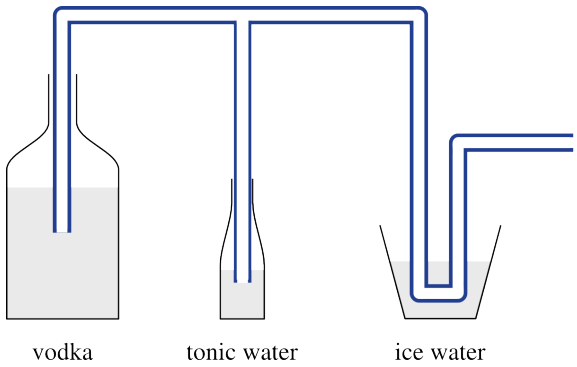

Figure 5.20 – Conceptual sketch of a student experiment.

Figure CC-0 o.c.

Percentage of alcohol by weight	Viscosity in centipoise
0	1,005
10	1,538
20	2,183
30	2,71
40	2,91
50	2,87
60	2,67
70	2,37
80	2,008
90	1,61
100	1,2

Table 5.1 – Viscosity of a mix of ethanol and water at 20 °C.

data from Bingham, Trans. Chem. Soc, 1902, 81, 179.

- The pipe has inner diameter $D = 3\,\text{mm}$ and roughness $\eta = 0{,}0025\,\text{mm}$.

The students wish to obtain the correct mix: one quarter vodka, three quarters tonic water. For given levels of liquid in the bottles, is there a straw pipe network configuration that will yield the correct mix, and if so, what is it?

Answers

5.2 1) Calculating inlet density with the perfect gas model, $[\mathrm{Re}]_D = 14\,263$ (turbulent), a Moody diagram read gives $f \approx 0{,}029$, so $\Delta p_{\text{friction}} = -1\,292{,}6\,\mathrm{Pa} = -0{,}0129\,\mathrm{bar}$.
2) If the flow were (magically) kept laminar, with equation 5/24, $\Delta p_{\text{friction}} = 200\,\mathrm{Pa}$.

5.3 The structure is given in the derivation of equation 5/9 p. 99, and more details about the math are given in the derivation of the (very similar) equation 5/19 p. 101.

5.4 $\Delta p = \frac{F_{W\,\text{sphere}}}{A_{\text{basin}}} = 71{,}51\,\mathrm{kPa}$. Then $\dot{\mathcal{V}} = 0{,}494\,\mathrm{L\,s^{-1}}$ which enables us to obtain $\dot{W}_{\text{pump}} = 35{,}3\,\mathrm{W}$.

5.5 $|\Delta p_{\text{alt.}}| = \rho g(26-8+5-7) = 1{,}57\,\mathrm{bar}$ and $|\Delta p_{\text{friction}}| = 51{,}87\,\mathrm{bar}$: $\dot{W}_{\text{pump}} = 5{,}345\,\mathrm{MW}$.

5.6 The total pumping power is $\dot{W} = 10\,\mathrm{MW}$ (!). Be careful not to cavitate the oil in the ascending sections, and not to burst the pipe in the descending sections!

5.7 Pressure losses to friction are $-3\,735\,\mathrm{Pa}$ in the first half, $+71\,\mathrm{Pa}$ in the throat, $-117\,\mathrm{Pa}$ in the second half. Add hydrostatic pressure to obtain final result.

5.8 Calculate the velocity distribution in the same way as for equation 5/9 p.99. Evaluate the pressure gradient $\frac{\partial p}{\partial y}$ using mass conservation (total cross-section mass flow is zero). With the full velocity distribution, derivate v with respect to x to obtain $F_\tau = \rho S g h + \frac{2\mu S}{h} v_{\text{p}}$.

5.9 This is a fun (and quick) exercise, but the results strongly depend on your proposed design! Get help during office hours.

5.10 The author cannot remember which exercise you are referring to.

Fluid Mechanics
Chapter 6 – Scale effects

last edited May 23, 2016

These lecture notes are based on textbooks by White [9], Çengel & al.[12], and Munson & al.[14].

6.1 Motivation

In this chapter, we use the tools we derived in chapters 3 and 4 to analyze scale effects in fluid mechanics. This study should allow us to answer two questions:

- How can a flow be adequately reproduced in a smaller or larger scale?
- How do forces and powers change when the flow is scaled?

6.2 Scaling forces

6.2.1 Force coefficients

Let us begin as a designer working for an automobile manufacturer. We wish to investigate the air flow around a full-size car, using a small model in a wind tunnel. The question we seek to answer is: if we succeed in "reproducing the exact real flow" in the wind tunnel, how large (or small) will the aerodynamic forces be on the model?

For this, we wish to have a sense of how flow-induced forces scale when fluid flows are scaled. A look back on chapter 3, and in particular eq. 3/8 p.57, reminds us that for a steady flow through a given control volume, the net force induced on the fluid is expressed by:

$$\vec{F}_{\text{net}} = \iint_{\text{CS}} \rho \vec{V} \, (\vec{V}_{\text{rel}} \cdot \vec{n}) \, \mathrm{d}A = \sum_{\text{net}} \left\{ (\rho |V_{\perp}| A) \vec{V} \right\} \tag{6/1}$$

This equation tells us that the norm of the force vector $\vec{F}_{\text{net}}$ is directly related to the norm of the vector $\Sigma\ \rho|V_\perp|\vec{AV}$. In the selection of a scale by which to measure F_{net}, it is therefore sensible to include a term proportional to the the density ρ, a term proportional to the area A, and a term proportional to the square of velocity V. This "scale of fluid-induced force" is conventionally measured using the *force coefficient* C_F:

$$C_F \equiv \frac{F}{\frac{1}{2}\rho S V^2} \tag{6/2}$$

where F is the considered fluid-induced force (N);
ρ is a reference fluid density ($\mathrm{kg\,m^{-3}}$);
S is a reference surface area ($\mathrm{m^2}$);
and V is a reference velocity ($\mathrm{m\,s^{-1}}$).

In effect, the force coefficient relates the magnitude of the force exerted by the fluid on an object (F) to the amount of fluid momentum available to the object ($\rho S V^2$).

It is worth making a few remarks about this equation. First, it is important to realize that eq. 6/2 is a *definition*: while the choice of terms is guided by physical principles, it is not a physical law in itself, and there are no reasons to expect C_F (which has no dimension, and thus no unit) to reach any particular value in any given case. The choice of terms is also worth commenting:

- F can be any fluid-induced force; generally we are interested in quantifying either the *drag* F_{D} (the force component parallel to the free-stream velocity) or the *lift* F_{L} (force component perpendicular to the free-stream velocity);
- the reference area S is chosen arbitrarily. It matters only that this area grow and shrink in proportion to the studied flow case. In the automobile industry, it is customary to choose the vehicle frontal area as a reference, while in the aeronautical industry the top-view wing area is customarily used. The square of a convenient reference length L can also be chosen instead;
- the choice of reference velocity V and density ρ is also arbitrary, since both these properties may vary in time and space within the studied fluid flow case. It matters merely that the chosen reference values are representative of the case; typically the free-stream (faraway) conditions V_∞ and ρ_∞ are used;
- the term 1/2 in the denominator is a purely arbitrary and conventional value.

Force coefficients are meaningful criteria to compare and relate what is going on in the wind tunnel and on the full-size object: in each case, we scale the measured force according to the relevant local flow conditions.

6.2.2 Power coefficient, and other coefficients

During our investigation of the flow using a small-scale model, we may be interested in measuring not only forces, but also other quantities such as power — this would be an important parameter, for example, when studying a pump, an aircraft engine, or a wind turbine.

Going back once again to chapter 3, and in particular eq. 3/15 p.60, we recall that power gained or lost by a fluid flowing steadily through a control volume could be expressed as:

$$\frac{\mathrm{d}E_{\mathrm{sys}}}{\mathrm{d}t} = \iint_{\mathrm{CS}} \rho\, e\, (\vec{V}_{\mathrm{rel}} \cdot \vec{n})\, \mathrm{d}A = \sum_{\mathrm{net}} \{(\rho |V_\perp| A) e\} \tag{6/3}$$

in which the specific energy e grows proportionally to $\frac{1}{2}V^2$.

Thus, the power gained or lost by the fluid is directly related to the magnitude of the scalar $\Sigma\ \rho |V_\perp| A V^2$. A meaningful "scale" for the power of a machine can therefore be the amount of energy in the fluid that is made available to it every second, a quantity that grows proportionally to $\rho A V^3$.

This "scale of fluid flow-related power" is conventionally measured using the *power coefficient* C_{P}:

$$C_{\mathrm{P}} \equiv \frac{\dot{W}}{\frac{1}{2}\rho S V^3} \tag{6/4}$$

where $\dot{W}$ is the power added to or subtracted from the fluid (W).

Other quantities related to fluid flow, such as pressure loss or shear friction, are measured using similarly-defined coefficients. We have already used the *pressure loss coefficient* $K_L \equiv |\Delta p| / \frac{1}{2}\rho V_{\mathrm{av.}}^2$ in chapter 5 (eq. 5/23 p.102), and we shall soon use the *shear coefficient* c_f in the coming chapter (eq. 7/5 p.139).

6.2.3 Physical similarity

In the paragraphs above, we have already hinted that under certain conditions, the force and power coefficients in experiments of differing scales may have the same value. This happens when we have attained *physical similarity*. Several levels of similarity may be achieved between two experiments:

- geometrical similarity (usually an obvious requirement), by which we ensure similarity of shape between the solid boundaries, which are then all related by a scale factor r;
- kinematic similarity, by which we ensure that the motion of all solid and fluid particles is reproduced to scale — thus that for a given time scale ratio r_t the relative positions are scaled by r, the relative velocities by r/r_t and the relative accelerations by $(r/r_t)^2$;
- dynamic similarity, by which we ensure that not only the movement, but also the *forces* are all scaled by the same factor.

In more complex cases, we may want to observe other types of similarity, such as thermal or chemical similarity (for which ratios of temperature or concentrations become important).

The general rule that we follow is that *the measurements in two experiments can be meaningfully compared if the experiments are physically similar.* A direct consequence for our study of fluid mechanics is that *in two different experiments, the force and power coefficients will be the same if the flows are physically similar.*

In the design of experiments in fluid mechanics, considerable effort is spent to attain at least partial physical similarity. Once this is done, measurements can

easily be extrapolated from one case to the other because all forces, velocities, powers, pressure differences etc. can be connected using coefficients.

For example, a flow case around a car A may be studied using a model B. *If dynamic similarity is maintained* (and that is by no means an easy task!), then the flow dynamics will be identical. The drag force $F_{\mathrm{D\,B}}$ measured on the model can then be compared to the force $F_{\mathrm{D\,A}}$ on the real car, using coefficients: since $C_{F_{\mathrm{D\,B}}} = C_{F_{\mathrm{D\,A}}}$ we have:

$$\begin{aligned} F_{\mathrm{D\,A}} &= C_{F_{\mathrm{D\,A}}} \frac{1}{2} \rho_A S_{\mathrm{A}} V_{\mathrm{A}}^2 = C_{F_{\mathrm{D\,B}}} \frac{1}{2} \rho_A S_{\mathrm{A}} V_{\mathrm{A}}^2 = \frac{F_{\mathrm{D\,B}}}{\frac{1}{2}\rho_B S_{\mathrm{B}} V_{\mathrm{B}}^2} \frac{1}{2} \rho_A S_{\mathrm{A}} V_{\mathrm{A}}^2 \\ &= \left(\frac{\rho_A}{\rho_B} \frac{S_{\mathrm{A}}}{S_{\mathrm{B}}} \frac{V_{\mathrm{A}}^2}{V_{\mathrm{B}}^2} \right) F_{\mathrm{D\,B}} \end{aligned}$$

It should be noted that even when perfect dynamic similarity is achieved, fluid-induced forces do not scale with other types of forces. For example, if the length of model B is 1/10th that of car A, then $S_{\mathrm{B}} = 0{,}1^2 S_{\mathrm{A}}$ and at identical fluid density and velocity, we would have $F_{\mathrm{D\,B}} = 0{,}1^2 F_{\mathrm{D\,A}}$. Nevertheless, the *weight* $F_{\mathrm{W\,B}}$ of model B would not be one hundredth of the weight of car A. If the same materials were used to produce the model, weight would stay proportional to *volume*, not surface, and we would have $F_{\mathrm{W\,B}} = 0{,}1^3 F_{\mathrm{W\,A}}$. This has important consequences when weight has to be balanced by flow-induced forces such as aerodynamic lift on an airplane. It is also the reason why large birds such as condors or swans do not look like, and cannot fly as slowly as mosquitoes and bugs![1]

6.3 Scaling flows

We have just seen that when two flows are dynamically similar, their comparison is made very easy, as measurements made in one case can be transposed to the other with the use of coefficients. This naturally raises the question: how can we *ensure* that two flows are flows are dynamically similar? The answer comes from a careful re-writing of the Navier-Stokes equation: two flows are dynamically similar when all the relevant *flow coefficients* have the same value.

6.3.1 The non-dimensional Navier-Stokes equation

In this section we wish to obtain an expression for the Navier-Stokes equation for incompressible flow that allows for an easy comparison of its constituents. We start with the original equation, which we derived in chapter 4 as eq. 4/37 (p.84):

$$\rho \frac{\partial \vec{V}}{\partial t} + \rho(\vec{V} \cdot \vec{\nabla})\vec{V} = \rho \vec{g} - \vec{\nabla} p + \mu \vec{\nabla}^2 \vec{V} \qquad (6/5)$$

What we would now like to do is *separate the geometry from the scalars* in this equation. This is akin to re-expressing each vector $\vec{A}$ as the multiple of its length A and a *non-dimensional* vector $\vec{A}^*$, which has the same direction as $\vec{A}$ but only unit length.

[1] These ideas are beautifully and smartly explored in Tennekes [5, 10].

In order to achieve this, we introduce a series of non-dimensional physical terms, starting with non-dimensional time t^*, defined as time t multiplied by the frequency f at which the flow repeats itself:

$$t^* \equiv f\,t \tag{6/6}$$

A flow with a very high frequency is highly unsteady, and the changes in time of the velocity field will be relatively important. On the other hand, flows with very low frequencies are quasi-steady. In all cases, as we observe the flow, non-dimensional time t^* progresses from 0 to 1, after which the solution is repeated.

We then introduce non-dimensional speed $\vec{V}^*$, a unit vector field equal to the speed vector field divided by its own (scalar field) length V:

$$\vec{V}^* \equiv \frac{\vec{V}}{V} \tag{6/7}$$

Pressure p is non-dimensionalized differently, since in fluid mechanics, it is the pressure *changes* across a field, not their absolute value, that influence the velocity field. For example, in eq. 6/5 $\vec{\nabla}p$ can be replaced by $\vec{\nabla}(p - p_\infty)$ (in which p_∞ can be any constant faraway pressure). Now, the pressure field $p - p_\infty$ is non-dimensionalized by dividing it by a reference pressure difference $p_0 - p_\infty$, obtaining:

$$p^* \equiv \frac{p - p_\infty}{p_0 - p_\infty} \tag{6/8}$$

If p_0 is taken to be the maximum pressure in the studied field, then p^* is a scalar field whose values can only vary between 0 and 1.

Non-dimensional gravity $\vec{g}^*$ is simply a unit vector equal to the gravity vector $\vec{g}$ divided by its own length g:

$$\vec{g}^* \equiv \frac{\vec{g}}{g} \tag{6/9}$$

And finally, we define a new operator, the *non-dimensional del* $\vec{\nabla}^*$,

$$\vec{\nabla}^* \equiv L\,\vec{\nabla} \tag{6/10}$$

which ensures that vector fields obtained with a non-dimensional gradient, and the scalar fields obtained with a non-dimensional divergent, are "scaled" by a reference length L.

These new terms allow us to replace the constituents of equation 6/5 each by a non-dimensional "unit" term multiplied by a scalar term representing its length or value:

$$\begin{aligned} t &= \frac{t^*}{f} \\ \vec{V} &= V\,\vec{V}^* \\ p - p_\infty &= p^*\,(p_0 - p_\infty) \\ \vec{g} &= g\,\vec{g}^* \\ \vec{\nabla} &= \frac{1}{L}\vec{\nabla}^* \end{aligned}$$

Now, inserting these in equation 6/5, and re-arranging, we obtain:

$$\rho\frac{\partial}{\partial\frac{1}{f}t^*}\left(V\vec{V}^*\right)+\rho\left(V\vec{V}^*\cdot\frac{1}{L}\vec{\nabla}^*\right)\left(V\vec{V}^*\right)=\rho g\,\vec{g}^*-\frac{1}{L}\vec{\nabla}^*\left[p^*\left(p_0-p_\infty\right)+p_\infty\right]+\mu\frac{\vec{\nabla}^{*2}}{L^2}\left(V\vec{V}^*\right)$$

$$\rho Vf\frac{\partial\vec{V}^*}{\partial t^*}+\rho VV\frac{1}{L}\left(\vec{V}^*\cdot\vec{\nabla}^*\right)\vec{V}^*=\rho g\,\vec{g}^*-\frac{1}{L}\vec{\nabla}^*\left[p^*\left(p_0-p_\infty\right)\right]+\mu V\frac{1}{L^2}\vec{\nabla}^{*2}\vec{V}^*$$

$$[\rho Vf]\;\frac{\partial\vec{V}^*}{\partial t^*}+\left[\frac{\rho V^2}{L}\right]\;\left(\vec{V}^*\cdot\vec{\nabla}^*\right)\vec{V}^*=[\rho g]\;\vec{g}^*-\left[\frac{p_0-p_\infty}{L}\right]\;\vec{\nabla}^*p^*+\left[\frac{\mu V}{L^2}\right]\;\vec{\nabla}^{*2}\vec{V}^* \tag{6/11}$$

In equation 6/11, the terms in brackets each appear in front of non-dimensional (unit) vectors. These bracketed terms all have the same dimension, i.e. $\mathrm{kg\,m^{-2}\,s^{-2}}$. Multiplying each by $\frac{L}{\rho V^2}$ (of dimension $\mathrm{m^2\,s^2\,kg^{-1}}$), we obtain a purely non-dimensional equation:

$$\left[\frac{fL}{V}\right]\;\frac{\partial\vec{V}^*}{\partial t^*}+[1]\;\left(\vec{V}^*\cdot\vec{\nabla}^*\right)\vec{V}^*=\left[\frac{gL}{V^2}\right]\;\vec{g}^*-\left[\frac{p_0-p_\infty}{\rho V^2}\right]\;\vec{\nabla}^*p^*+\left[\frac{\mu}{\rho VL}\right]\;\vec{\nabla}^{*2}\vec{V}^* \tag{6/12}$$

Equation 6/12 does not bring any information on top of the original incompressible Navier-Stokes equation (eq. 6/5). Instead, it merely separates it into two distinct parts: one is a scalar field (purely numbers, and noted in brackets); while the other is a unit vector field (a field of oscillating vectors, all of length one, and noted with stars). In this form, we can more easily observe and quantify the weight of the different terms relative to one another. This is the role of the flow parameters.

6.3.2 The flow parameters of Navier-Stokes

From here on, we convene to call the terms written in brackets in eq. 6/12 *flow parameters*, and label them with the following definitions:

$$[\mathrm{St}]\equiv\frac{f\,L}{V} \tag{6/13}$$

$$[\mathrm{Eu}]\equiv\frac{p_0-p_\infty}{\rho\,V^2} \tag{6/14}$$

$$[\mathrm{Fr}]\equiv\frac{V}{\sqrt{g\,L}} \tag{6/15}$$

$$[\mathrm{Re}]\equiv\frac{\rho\,V\,L}{\mu} \tag{6/16}$$

This allows us to re-write eq. 6/12 as:

$$[\mathrm{St}]\;\frac{\partial\vec{V}^*}{\partial t^*}+[1]\;\vec{V}^*\cdot\vec{\nabla}^*\vec{V}^*=\left[\frac{1}{\mathrm{Fr}^2}\right]\;\vec{g}^*-[\mathrm{Eu}]\;\vec{\nabla}^*p^*+\left[\frac{1}{\mathrm{Re}}\right]\;\vec{\nabla}^{*2}\vec{V}^*$$

And finally, we arrive at the simple, elegant and formidable *non-dimensional incompressible Navier-Stokes equation* expressed with flow parameters:

$$[\mathrm{St}]\,\frac{\partial \vec{V}^*}{\partial t^*} + [1]\,\vec{V}^* \cdot \vec{\nabla}^* \vec{V}^* = \frac{1}{[\mathrm{Fr}]^2}\,\vec{g}^* - [\mathrm{Eu}]\,\vec{\nabla}^* p^* + \frac{1}{[\mathrm{Re}]}\,\vec{\nabla}^{*2} \vec{V}^* \tag{6/17}$$

Equation 6/17 is an incredibly potent tool in the study of fluid mechanics, for two reasons:

1. It allows us to quantify the **relative weight** of the different terms in a given flow.
   In this way, it serves as a compass, helping us determine which terms can safely be neglected in our attempts to find a particular flow solution, merely by quantifying the four parameters [St], [Eu], [Fr], and [Re].

2. It allows us to obtain **dynamic similarity** between two flows at different scales (fig. 6.1).
   In order that a fluid flow be representative of another flow (for example in order to simulate airflow around an aircraft with a model in a wind tunnel), it must generate the same vector field $\vec{V}^*$. In order to do this, we must generate an incoming flow with the same four parameters [St], [Eu], [Fr], and [Re].

Let us therefore take the time to explore the signification of these four parameters.

The Strouhal number $[\mathrm{St}] \equiv \frac{f\,L}{V}$ (eq. 6/13) quantifies the relative importance of the representative frequency f at which the flow pattern repeats itself. If the frequency is very low, [St] is very small; the flow is then quasi-steady and it can be solved at a given moment in time as if it was entirely steady.

The Euler number $[\mathrm{Eu}] \equiv \frac{p_0 - p_\infty}{\rho\,V^2}$ (eq. 6/14) quantifies the relative importance of the pressure gradient field, represented by $p_0 - p_\infty$, within the flow field. The greater [Eu] is, and the more the changes in the velocity field $\vec{V}$ are likely to be caused by pressure gradients rather than viscosity, convection or unsteadiness.

The Froude number $[\mathrm{Fr}] \equiv \frac{V}{\sqrt{g\,L}}$ (eq. 6/15) quantifies the relative importance of gravity effects. In practice, gravity effects only play an important role in free surface flows, such as waves on the surface of a water reservoir. In most other cases, gravity contributes only to a hydrostatic effect, which has little influence over the velocity field.

The Reynolds number $[\mathrm{Re}] \equiv \frac{\rho\,V\,L}{\mu}$ (eq. 6/16) quantifies the importance of viscous effects relative to inertial effects. When [Re] is very large, viscosity plays a negligible role and the velocity field is mostly dictated by the inertia of the fluid. We return to the significance in §6.5 below.

The Mach number $[\mathrm{Ma}] \equiv V/a$ (eq. 0/4) compares the flow velocity V with that of the molecules within the fluid particles (the speed of sound a). [Ma] does not appear in equation 6/17 because from the start in chapter 4, we chose to restrict ourselves to non-compressible flows. If we hadn't, an additional term would exist on the right-hand side, $+\frac{1}{3}\mu\vec{\nabla}\left(\vec{\nabla}\cdot\vec{V}\right)$, which is null when the divergent of velocity $\vec{\nabla}\cdot\vec{V}$ is zero

(which is always so at low to moderate flow speeds).
We shall explore the significance of the Mach number in chapter 9.

These five flow parameters should be thought of *scalar fields* within the studied flow domain: there is one distinct Reynolds number, one Mach number etc. for each point in space and time. Nevertheless, when describing fluid flows, the custom is to choose for each parameter *a single representative value* for the whole flow. For example, when describing pipe flow, it is customary to quantify a representative Reynolds number $[\mathrm{Re}]_D$ based on the average flow velocity $V_{\mathrm{av.}}$ and the pipe diameter D (as we have seen with eq. 5/25 p. 102), while the representative Reynolds number for flow over an aircraft wing is often based on the free-stream velocity V_∞ and the wing chord length c. Similarly, the flight Mach number $[\mathrm{Ma}]_\infty$ displayed on an aircraft cockpit instrument is computed using the relative free-stream air speed V_∞ and the free-stream speed of sound a_∞, rather than particular values measured closer to the aircraft.

6.3.3 Scaling flows

Although the above mathematical treatment may be intimidating, it leads us to a rather simple and useful conclusion, which can be summarized as follows.
When studying one particular fluid flow around or within an object, it may be useful to construct a model that allows for less expensive or more comfortable measurements (fig. 6.1). In that case, we need to make sure that the fluid flow on the model is representative of the real case. This can be achieved only if the relevant flow parameters have the same value in both cases. If this can be achieved —although in practice this can rarely be achieved exactly!— then the force and power coefficients also keep the same value. The scale effects are then fully-controlled and the model measurements are easily extrapolated to the real case.

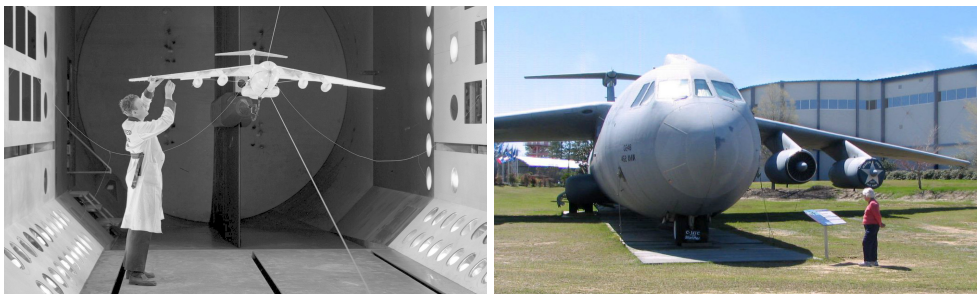

Figure 6.1 – In order for the flow around a wind tunnel model to be representative of the flow around the real-size aircraft (here, a 48 m-wide Lockheed C-141 Starlifter), dynamic similarity must be obtained. The value of all flow parameters must be kept identical. This is not always feasible in practice.

Wind tunnel photo by NASA (public domain)
Full-size aircraft photo CC-BY *by Peter Long*

6.4 Flow parameters as force ratios

This topic is well covered in Massey [3]

Instead of the above mathematical approach, the concept of flow parameter can be approached by *comparing forces* in fluid flows.

Fundamentally, understanding the movement of fluids requires applying Newton's second law of motion: the sum of forces which act upon a fluid particle is equal to its mass times its acceleration. We have done this in an aggregated manner with integral analysis (in chapter 3, eq. 3/8 p.57), and then in a precise and all-encompassing way with differential analysis (in chapter 4, eq. 4/37 p.84). With the latter method, we obtain complex mathematics suitable for numerical implementation, but it remains difficult to obtain rapidly a quantitative measure for what is happening in any given flow.

In order to obtain this, an engineer or scientist can use force ratios. This involves comparing the magnitude of a type of force (pressure, viscous, gravity) either with another type of force, or with the mass-times-acceleration which a fluid particle is subjected to as it travels. We are not interested in the absolute value of the resulting ratios, but rather, in having a measure of the parameters that influence them, and being able to compare them across experiments.

6.4.1 Acceleration vs. viscous forces: the Reynolds number

The net sum of forces acting on a particle is equal to its mass times its acceleration. If a representative length for the particle is L, the particle mass grows proportionally to the product of its density ρ and its volume L^3. Meanwhile, its acceleration relates how much its velocity V will change over a time interval Δt: it may be expressed as a ratio $\Delta V/\Delta t$. In turn, the time interval Δt may be expressed as the representative length L divided by the velocity V, so that the acceleration may be represented as proportional to the ratio $V\Delta V/L$. Thus we obtain:

$$\begin{aligned} |\text{net force}| = |\text{mass} \times \text{acceleration}| &\sim \rho L^3 \frac{V\Delta V}{L} \\ |\vec{F}_{\text{net}}| &\sim \rho L^2 V \Delta V \end{aligned}$$

We now observe the viscous force acting on a particle: it is proportional to the the shear effort and a representative acting surface L^2. The shear can be modeled as proportional to the viscosity μ and the rate of strain, which will grow proportionally to $\Delta V/L$. We thus obtain a crude measure for the magnitude of the shear force:

$$\begin{aligned} |\text{viscous force}| &\sim \mu \frac{\Delta V}{L} L^2 \\ |\vec{F}_{\text{viscous}}| &\sim \mu \Delta V L \end{aligned}$$

The magnitude of the viscous force can now be compared to the net force:

$$\frac{|\text{net force}|}{|\text{viscous force}|} \sim \frac{\rho L^2 V \Delta V}{\mu \Delta V L} = \frac{\rho V L}{\mu} = [\text{Re}] \qquad (6/18)$$

and we recognize the ratio as the Reynolds number (6/16). We thus see that the Reynolds number can be interpreted as the inverse of the influence of viscosity. The larger [Re] is, and the smaller the influence of the viscous forces will be on the trajectory of fluid particles.

6.4.2 Acceleration vs. gravity force: the Froude number

The weight of a fluid particle is equal to its mass, which grows with ρL^3, multiplied by gravity g:

$$|\text{weight force}| = |\vec{F}_\text{W}| \sim \rho L^3 g$$

The magnitude of this force can now be compared to the net force:

$$\frac{|\text{net force}|}{|\text{weight force}|} \sim \frac{\rho L^2 V^2}{\rho L^3 g} = \frac{V^2}{Lg} = [\text{Fr}]^2 \tag{6/19}$$

and here we recognize the square of the Froude number (6/15). We thus see that the Froude number can be interpreted as the inverse of the influence of weight on the flow. The larger [Fr] is, and the smaller the influence of gravity will be on the trajectory of fluid particles.

6.4.3 Acceleration vs. elastic forces: the Mach number

In some flows called *compressible flows* the fluid can perform work on itself, and and the fluid particles then store and retrieve energy in the form of changes in their own volume. In such cases, fluid particles are subject to an *elastic force* in addition to the other forces. We can model the pressure resulting from this force as proportional to the bulk modulus of elasticity K of the fluid (formally defined as $K \equiv \rho\, \partial p/\partial \rho$); the elastic force can therefore be modeled as proportional to KL^2:

$$|\text{elasticity force}| = |\vec{F}_\text{elastic}| \sim KL^2$$

The magnitude of this force can now be compared to the net force:

$$\frac{|\text{net force}|}{|\text{elasticity force}|} \sim \frac{\rho L^2 V^2}{KL^2} = \frac{\rho V^2}{K}$$

This ratio is known as the Cauchy number; it is not immediately useful because the value of K in a given fluid varies considerably not only according to temperature, but also according to the type of compression undergone by the fluid: for example, it grows strongly during brutal compressions.

During isentropic compressions and expansions (isentropic meaning that the process is fully reversible, i.e. without losses to friction, and adiabatic, i.e. without heat transfer), we will show in chapter 9 (with eq. 9/7 p.183) that the bulk modulus of elasticity is proportional to the square of the speed of sound a:

$$K|_\text{reversible} = a^2 \rho \tag{6/20}$$

The Cauchy number calibrated for isentropic evolutions is then

$$\frac{|\text{net force}|}{|\text{elasticity force}|_{\text{reversible}}} \sim \frac{\rho V^2}{K} = \frac{V^2}{a^2} = [\text{Ma}]^2 \tag{6/21}$$

and here we recognize the square of the Mach number (0/4). We thus see that the Mach number can be interpreted as the influence of elasticity on the flow. The larger [Ma] is, and the smaller the influence of elastic forces will be on the trajectory of fluid particles.

6.4.4 Other force ratios

The same method can be applied to reach the definitions for the Strouhal and Euler numbers given in §6.3. Other numbers can also be used which relate forces that we have ignored in our study of fluid mechanics. For example, the relative importance of surface tension forces or of electromagnetic forces are quantified using similarly-constructed flow parameters.
In some applications featuring rotative motion, such as flows in centrifugal pumps or planetary-scale atmospheric weather, it may be convenient to apply Newton's second law in a rotating reference frame. This results in the appearance of new reference-frame forces, such as the Coriolis or centrifugal forces; their influence can then be studied using additional flow parameters.

In none of those cases can flow parameters give enough information to predict solutions. They do, however, provide quantitative data to indicate which forces are relevant in which places: this not only helps us understand the mechanisms at work, but also distinguish the negligible from the influential, a key characteristic of efficient scientific and engineering work.

6.5 The Reynolds number in practice

Among the five non-dimensional parameters described above, the *Reynolds number* [Re] is by far the most relevant in the study of most fluid flows, and it deserves a few additional remarks. As we have seen, the Reynolds number is a measure of how little effect the viscosity has on the time-change of the velocity vector field:

- With low [Re], the viscosity μ plays an overwhelmingly large role, and the velocity of fluid particles is largely determined by that of their own neighbors;
- With high [Re], the momentum ρV of the fluid particles plays a more important role than the viscosity μ, and the inertia of fluid particles affects their trajectory much more than the velocity of their neighbors.

In turn, this gives the Reynolds number a new role in characterization of flows: it can be thought of as **the likeliness of the flow being turbulent over the length** L. Indeed, from a cinematic point of view, viscous effects are highly stabilizing: they tend to harmonize the velocity field and smooth out disturbances. On the contrary, when these effects are overwhelmed by inertial effects, velocity non-uniformities have much less opportunity to dissipate, and at the slightest disturbance the flow will become and remain turbulent (fig. 6.2). This is the reason why the quantification of a representative Reynolds number is often the first step taken in the study of a fluid flow.

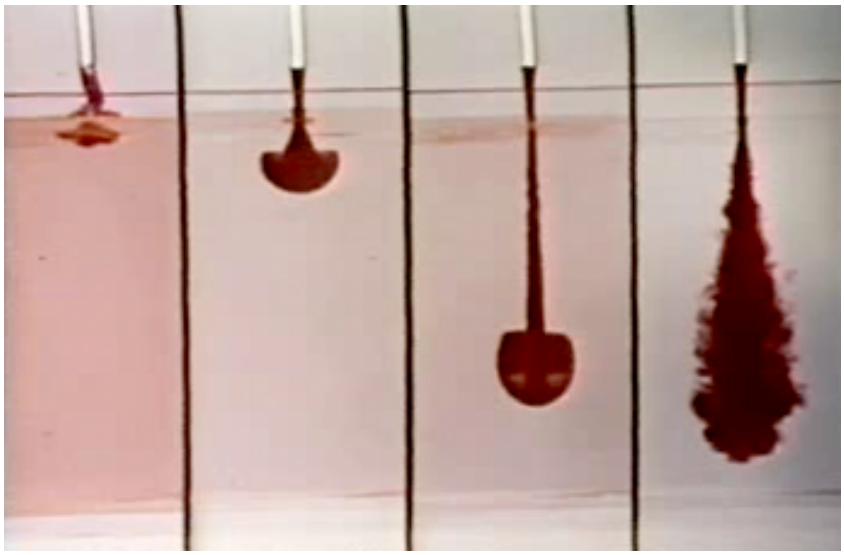

Figure 6.2 – A viscous opaque fluid is dropped into a clearer receiving static fluid with identical viscosity. The image shows four different experiments photographed after the same amount of time has elapsed. The viscosity is decreased from left to right, yielding Reynolds numbers of 0,05, 10, 200 and 3 000 respectively.
As described in eq. 6/18, low Reynolds number indicate that viscous effects dominate the change in time of the flow field. As the Reynolds number increases, the nature of the velocity field changes until it becomes clearly turbulent.

Fluid Mechanics
Exercise sheet 6 – Scale effects

last edited May 28, 2016

Except otherwise indicated, we assume that fluids are Newtonian, and that:
$\rho_{\text{water}} = 1\,000\,\text{kg m}^{-3}$; $p_{\text{atm.}} = 1\,\text{bar}$; $\rho_{\text{atm.}} = 1{,}225\,\text{kg m}^{-3}$; $T_{\text{atm.}} = 11{,}3\,^{\circ}\text{C}$; $\mu_{\text{atm.}} = 1{,}5 \cdot 10^{-5}\,\text{N s m}^{-2}$;
$g = 9{,}81\,\text{m s}^{-2}$. Air is modeled as a perfect gas ($R_{\text{air}} = 287\,\text{J K}^{-1}\,\text{kg}^{-1}$; $\gamma_{\text{air}} = 1{,}4$; $c_{p\text{air}} = 1\,005\,\text{J kg}^{-1}\,\text{K}^{-1}$).

Non-dimensional incompressible Navier-Stokes equation:

$$[\text{St}]\,\frac{\partial \vec{V}^*}{\partial t^*} + [1]\,\vec{V}^* \cdot \vec{\nabla}^* \vec{V}^* = \frac{1}{[\text{Fr}]^2}\,\vec{g}^* - [\text{Eu}]\,\vec{\nabla}^* p^* + \frac{1}{[\text{Re}]}\,\vec{\nabla}^{*2} \vec{V}^* \qquad (6/17)$$

in which $[\text{St}] \equiv \frac{f\,L}{V}$, $[\text{Eu}] \equiv \frac{p_0 - p_\infty}{\rho\,V^2}$, $[\text{Fr}] \equiv \frac{V}{\sqrt{g\,L}}$ and $[\text{Re}] \equiv \frac{\rho\,V\,L}{\mu}$.

The force coefficient C_F and power coefficient C_P are defined as:

$$C_F \equiv \frac{F}{\frac{1}{2}\rho S V^2} \qquad C_\text{P} \equiv \frac{\dot{W}}{\frac{1}{2}\rho S V^3} \qquad (6/4)$$

The speed of sound a in air is modeled as:

$$a = \sqrt{\gamma R T} \qquad (0/5)$$

Figure 6.3 quantifies the viscosity of various fluids as a function of temperature.

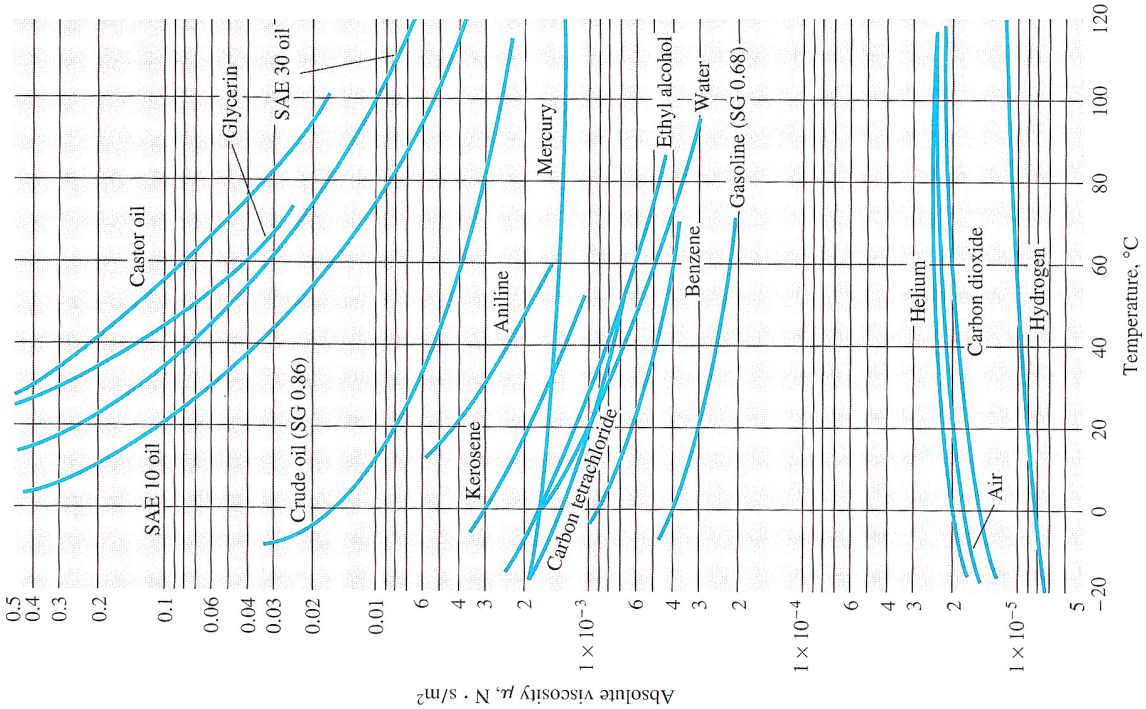

Figure 6.3 – Viscosity of various fluids at a pressure of 1 bar (in practice viscosity is almost independent of pressure).

Figure repeated from fig. 5.11 p.107; © White 2008 [9]

6.1 Scaling with the Reynolds number

1. Give the definition of the Reynolds number, indicating the SI units for each term.
2. What is the consequence on the velocity field of having a low Reynolds number? A high Reynolds number?
3. Give an example of a high Reynolds number flow, and of a low Reynolds number flow.

The standard golf ball has a diameter of 42,67 mm and a mass of 45,93 g. A typical maximum velocity for such balls is 200 $\mathrm{km\,h^{-1}}$.

A student wishes to investigate the flow over a golf ball using a model in a wind tunnel. S/he prints an enlarged model with a diameter of 50 cm.

4. If the atmospheric conditions are identical, what flow velocity needs to be generated during the experiment in order to reproduce the flow patterns around the real ball?
5. Would the Mach number for the real ball then be reproduced?
6. Would this velocity need to be adjusted if the experiment was run on a very hot summer day?
7. If the model was made of the same material as the real ball, how heavy would it be?

6.2 Fluid mechanics of a giant airliner

non-examinable,

In this exercise, we consider that that viscosity is entirely independent from pressure and density (this is a reasonable first approximation).

An Airbus A380 airliner has an 80 m-wingspan and is designed to cruise at [Ma] = 0,85 where the air temperature and pressure are −40 °C and 0,25 bar.

A group of students wishes to study the flow field around the aircraft, with a wind tunnel whose test section has a diameter of 1 m (in which, obviously, the model has to fit!).

1. If the temperature inside the tunnel is maintained at $T_{\text{tunnel}} = 20\,^{\circ}\mathrm{C}$, propose a combination of wind tunnel velocity and pressure which would enable the team to adequately model the effects of viscosity.
2. Which flow conditions would be required in a *water* tunnel with the same dimensions?

Shocked by their answers to the above questions, the group of students decides instead to study the effect of compressibility (while accepting that viscous effects may not be adequately modeled).

3. If the maximum velocity attainable in the wind tunnel is 80 $\mathrm{m\,s^{-1}}$, which air temperature is required for compressibility effects to be modeled?

6.3 Scale effects on a dragonfly

A dragonfly (sketched in fig. 6.4) has a 10 cm wingspan, a mass of 80 mg, and cruises at 4 $\mathrm{m\,s^{-1}}$, beating its four wings 20 times per second.

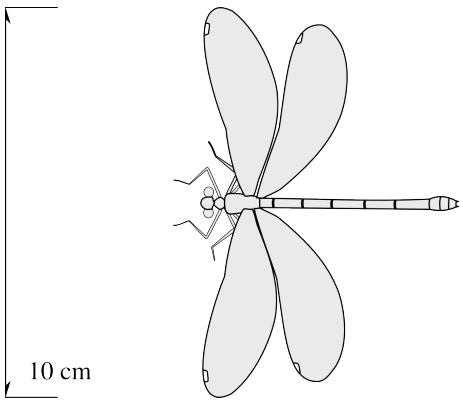

Figure 6.4 – Plan view of a dragonfly

Figure by o.c., *A. Plank, Drury, Dru, Westwood, J. O. (*CC-0*)*

You are tasked with the investigation of the flight performance of the dragonfly, and have access to a wind tunnel with a test section of diameter 1 m.

1. Which model size and flow velocity would you use for this experiment?
2. How many wing beats per second would then be required on the model?
3. What would be the lift developed by the model during the experiment?
4. How much mechanical power would the model require, compared to the real dragonfly?

6.4 Formula One testing

You are leading the Aerodynamics team in a successful Formula One racing team. Your team races a car that is 5,1 m long, 1,8 m wide, has a 610 kW power plant, and a mass of 750 kg. The car can reach a top speed of 310 $\mathrm{km\,h^{-1}}$, at which speed the drag force is 7,1 kN.

In order to test different aerodynamic configurations for the car, your team invests in a 50-million euro wind tunnel in which you will run tests on a model. You currently have the choice between two possible model sizes: a 60 % model and a (smaller) 50 % model.

1. What would be the frontal area of each model, in proportion to the frontal area of the real car?
2. What would be the volume of each model, compared to the volume of the real car?
3. How much less weight would the 50 % model have than the 60 % model?

In the end, the regulations for the Formula One racing change, and your team is forced to opt for a 50 % car model.

4. If the ambient atmospheric conditions cannot be changed, which flow speed in the wind tunnel is required, so that the air flow around the real car is reproduced around the model?

In practice the regulations change once again, and the maximum speed authorized in wind tunnel tests is now $50\,\mathrm{m\,s^{-1}}$.

5. Your team considers modifying the air temperature to compensate for the limit in the air speed. If the temperature in the tunnel can be controlled between $-10\,^{\circ}\mathrm{C}$ and $40\,^{\circ}\mathrm{C}$, but the pressure remains atmospheric, what is the maximum race-track speed that can be reproduced in the wind tunnel?

6. In that case, by which factor should the model drag force measurements be multiplied in order to correspond to the real car?

7. *[non-examinable question]* The wind tunnel has a $2\,\mathrm{m}$ by $2\,\mathrm{m}$ square test cross-section. What is the power required to bring atmospheric air ($T_{\mathrm{atm.}} = 15\,^{\circ}\mathrm{C}$, $V_{\mathrm{atm.}} = 0\,\mathrm{m\,s^{-1}}$) to the desired speed and temperature in the test section?

NB: this exercise is inspired by an informative and entertaining video by the Sauber F1 team about their wind tunnel testing, which the reader is encouraged to watch at https://www.youtube.com/watch?v=KC0E0wU6inU.

Answers

6.1 1) See equation 6/16 and subsequent comments;
2) See §6.5, in practice this can be summarized in two or three sentences;
3) High-Re: air flow around an airliner in cruise; Low-Re: air flow around a dust particle falling to the ground. 4) Match [Re]: $V_2 = 4{,}74\,\mathrm{m\,s^{-1}}$
5) No, but it is very low anyway (no compressibility effects to be reproduced)
6) Yes! (discuss in class) 7) $m_2 = 73{,}9\,\mathrm{kg}$

6.2 1) With a half-aircraft model of half-length $\frac{L_2}{2} = 80\,\mathrm{cm}$, at identical speed, we would need an air density $\rho_2 = 24{,}9\,\mathrm{kg\,m^{-3}}$. At ambient temperature, this requires a pressure $p_2 = 20{,}9\,\mathrm{bar}$! 2) In water, the density cannot be reasonably controlled, and we need a velocity $V_3 = 418\,\mathrm{m\,s^{-1}}$!
3) In air, at $V_4 = 80\,\mathrm{m\,s^{-1}}$, Mach number can be reproduced at $T_4 = -251\,^\circ\mathrm{C}$ (although the Reynolds number is off). Wind tunnels used to investigate compressible flow around aircraft have very powerful coolers.

6.3 1) With e.g. a model of span 60 cm, match the Reynolds number: $V_2 = 0{,}67\,\mathrm{m\,s^{-1}}$;
2) Match the Strouhal number: $f_2 = 0{,}56\,\mathrm{Hz}$. Mach, Froude and Euler numbers will have no effect here; 3) and 4) are left as a surprise for the student.

6.4 3) The third model would have 42 % less mass than the second;
4) Maintaining [Re] requires $V_3 = 172{,}2\,\mathrm{m\,s^{-1}}$ (fast!);
5) Now the fastest track speed that can be studied is $24{,}23\,\mathrm{m\,s^{-1}}$;
6) Multiply force measurements by 1,19 to scale up to reality;
7) One needs powerful coolers!

Fluid Mechanics
Chapter 7 – The boundary layer

last edited June 26, 2016

These lecture notes are based on textbooks by White [9], Çengel & al.[12], and Munson & al.[14].

7.1 Motivation

In this chapter, we focus on fluid flow in the close proximity of solid walls. In these regions, fluid flow is dominated by viscous effects. This study should allow us to answer two questions:

- How can we quantify shear-induced friction on solid walls?
- How can we describe and predict flow separation?

7.2 Describing the boundary layer

7.2.1 Concept

At the very beginning of the 20th century, Ludwig Prandtl observed that for most ordinary fluid flows, viscous effects played almost no role outside of a very small layer of fluid along solid surfaces. In this area, shear between the zero-velocity solid wall and the outer flow dominates the flow structure. He named this zone the *boundary layer*.

We indeed observe that around any solid object within a fluid flow, there exists a thin zone which is significantly slowed down because of the object's presence. This deceleration can be visualized by measuring the velocity profile (fig. 7.1).

The boundary layer is a *concept*, a thin invisible layer whose upper limit (termed δ, as we will see in §7.2.3) is defined as the distance where the fluid velocity in direction parallel to the wall is 99 % of the outer (undisturbed) flow velocity.

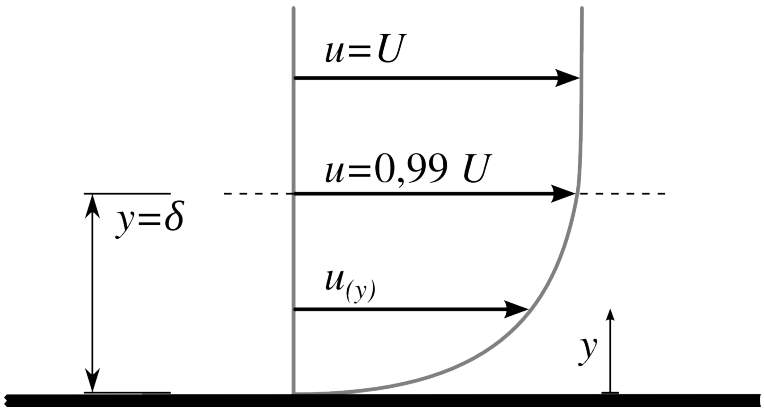

Figure 7.1 – A typical velocity profile in a boundary layer. Only the horizontal component of velocity ($V_x = u$) is represented.

Figure CC-BY *Olivier Cleynen*

Upon investigation, we observe that the boundary layer thickness depends strongly on the main flow characteristics. In particular, it *decreases* when speed increases or when viscosity is decreased (fig. 7.2).

As we travel downstream along a boundary layer, we observe experimentally that the flow regime is always laminar at first. Then, at some distance downstream which we name *transition point*, the boundary layer becomes turbulent. The flow-wise position of the transition point depends on the flow properties and is somewhat predictable. Further downstream, the boundary layer becomes fully turbulent. It has larger thickness than in the laminar regime, and grows at a faster rate. Like all turbulent flows, it then features strong energy dissipation and its analytical description becomes much more difficult.

The flow within the boundary layer, and the main external flow (outside of it) affect one another, but may be very different in nature. A laminar boundary layer may exist within a turbulent main flow; while turbulent boundary layers are commonplace in laminar flows.

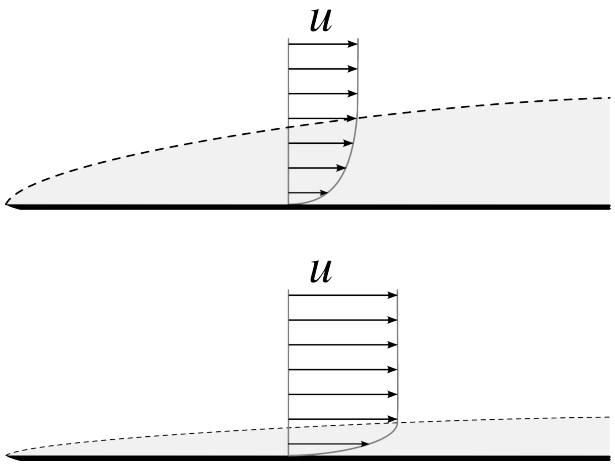

Figure 7.2 – The thickness of the boundary layer depends strongly on the faraway incoming flow velocity U_∞.

Figure CC-BY-SA *Olivier Cleynen & Commons User:F l a n k e r*

7.2.2 Why do we study the boundary layer?

Expending our energy on solving such a minuscule area of the flow may seem counter-productive, yet three great stakes are at play here:

- First, a good description allows us to **avoid having to solve the Navier-Stokes equations in the whole flow**.
  Indeed, outside of the boundary layer and of the wake areas, viscous effects can be safely neglected. Fluid flow can then be described with $\rho\frac{\mathrm{D}\vec{V}}{\mathrm{D}t} = -\vec{\nabla}p$ (the Euler equation, which we will introduce as eq. 8/8 in the next chapter) with acceptably low inaccuracy. As we will see in the next chapter, this allows us to find many interesting solutions, all within reach of human comprehension and easily obtained with computers. Unfortunately, they cannot account for shear on walls.
  Thus, solving the flow within the boundary layer, whether analytically or experimentally, allows us to solve the rest of the flow in a simplified manner (fig. 7.3).

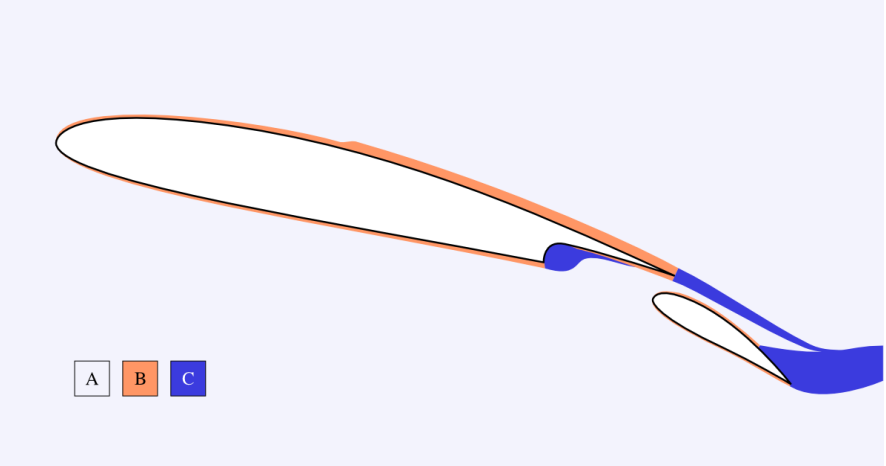

Figure 7.3 – Fluid flow around a wing profile. When analyzing the flow, whether analytically or within a computational fluid dynamics (CFD) simulation, the flow domain is frequently split into three distinct areas. In the boundary layer (B), fluid flow is dominated by viscosity. Outside of the boundary layer (A), viscous effects are very small, and the flow can be approximately solved using the Euler equation. Lastly, in the turbulent wake (C), characterization of the flow is very difficult and typically necessitates experimental investigations.

Figure CC-BY-SA *Olivier Cleynen*

- Secondly, the boundary layer is the key to **quantifying friction**. A good resolution of the boundary layer allows us to precisely quantify the shear forces generated by a fluid on an object.
- Finally, a good understanding of the mechanisms at hand within the boundary layer allows us to predict **flow separation**, which is the divergence of streamlines relative to the object. Control of the boundary layer is key to ensuring that a flow will follow a desired trajectory!

7.2.3 Characterization of the boundary layer

Three different parameters are typically used to quantify how thick a boundary layer is at any given position.

The first is the *thickness* δ,

$$\delta \equiv (y)_{u=0{,}99U} \tag{7/1}$$

which is, as we have seen above, equal to the distance away from the wall where the speed u is 99 % of U.

The second is the *displacement thickness* δ^*, which corresponds to the length of the vertical displacement of streamlines outside of the boundary layer. This vertical "shifting" of the flow occurs because the inner fluid is slowed down near the wall, creating some blockage in the process for the outer flow, which then proceeds to avoid it partially by deviating outwards (fig. 7.4).

A review of the concepts we studied in chapter 3 allows us to see that:

$$\delta^* \equiv \int_0^\infty \left(1 - \frac{u}{U}\right) \mathrm{d}y \tag{7/2}$$

In practice, this integral can be calculated on a finite interval (instead of using the ∞ limit), as long as the upper limit exceeds the boundary layer thickness.

The third and last parameter is the *momentum thickness* θ, which corresponds to the thickness of the fluid at velocity U which possesses the same amount of momentum as the boundary layer. The momentum thickness can be seen as the thickness of the fluid that would need to be entirely stopped (for example by pumping it outside of the main flow) in order to generate the same drag as the local boundary layer.

A review of the concepts of chapter 3 (e.g. in exercises 3.6 to 3.8) allows us to write:

$$\theta \equiv \int_0^\delta \frac{u}{U}\left(1 - \frac{u}{U}\right) \mathrm{d}y \tag{7/3}$$

with the same remark regarding the upper limit. The momentum thickness, in particular when compared to the displacement thickness, is a key parameter used in prediction models for boundary layer separation.

Once these three thicknesses have been quantified, we are generally looking for a quantification of the shear term τ_{wall}. Since we are working with the hypothesis that the fluid is Newtonian, we merely have to know $u_{(y)}$ to quantify shear according to equation 2/16 (p.43):

$$\tau_{\text{wall } yx} = \mu \frac{\partial u}{\partial y} \tag{7/4}$$

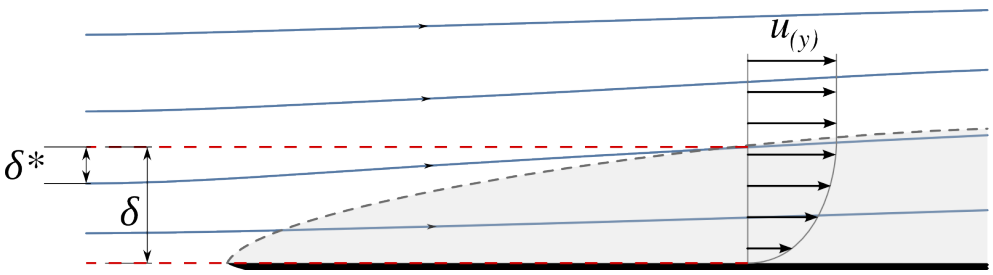

Figure 7.4 – Thickness δ and displacement thickness δ^* of a boundary layer. It is important to understand that the boundary layer is not a closed zone: streamlines (drawn blue) penetrate it and the vertical velocity v, although very small compared to u, is not zero.

Figure CC-BY-SA *Olivier Cleynen & Commons User:F l a n k e r*

this expression is a function of x, and typically τ_{wall} decreases with increasing distance inside a laminar boundary layer.

The wall shear exerted by the boundary layer is typically non-dimensionalized with the *shear coefficient* c_f,

$$c_{f_{(x)}} \equiv \frac{\tau_{\text{wall}}}{\frac{1}{2}\rho U^2} \tag{7/5}$$

where U is the outer-layer (free-stream) velocity.

The shear coefficient, just like the shear, remains a function of x.

Once these parameters are known, the wall shear force is simply obtained by integrating τ over the entire surface S:

$$F_{\text{shear}yx} = \int_S \tau_{\text{wall}yx}\, \mathrm{d}x\, \mathrm{d}z \tag{7/6}$$

7.3 The laminar boundary layer

7.3.1 Governing equations

What is happening inside a laminar, steady boundary layer? We begin by writing out the Navier-Stokes for incompressible isothermal flow in two Cartesian coordinates (eqs. 4/41 & 4/42 p.85):

$$\rho\left[\frac{\partial u}{\partial t} + u\frac{\partial u}{\partial x} + v\frac{\partial u}{\partial y}\right] = \rho g_x - \frac{\partial p}{\partial x} + \mu\left[\frac{\partial^2 u}{(\partial x)^2} + \frac{\partial^2 u}{(\partial y)^2}\right] \tag{7/7}$$

$$\rho\left[\frac{\partial v}{\partial t} + u\frac{\partial v}{\partial x} + v\frac{\partial v}{\partial y}\right] = \rho g_y - \frac{\partial p}{\partial y} + \mu\left[\frac{\partial^2 v}{(\partial x)^2} + \frac{\partial^2 v}{(\partial y)^2}\right] \tag{7/8}$$

Building from these two equations, we are going to add **three simplifications**, which are hypothesis based on experimental observation of fluid flow in boundary layers:

1. Gravity plays a negligible role;
2. The component of velocity perpendicular to the wall (in our convention, v) is very small ($v \ll u$).
   Thus, its stream-wise spatial variations can also be neglected: $\frac{\partial v}{\partial x} \approx 0$ and $\frac{\partial^2 v}{(\partial x)^2} \approx 0$. The same goes for the derivatives in the y-direction: $\frac{\partial v}{\partial y} \approx 0$ and $\frac{\partial^2 v}{(\partial y)^2} \approx 0$.
3. The component of velocity parallel to the wall (in our convention, u) varies much more strongly in the y-direction than in the x-direction: $\frac{\partial^2 u}{(\partial x)^2} \ll \frac{\partial^2 u}{(\partial y)^2}$.

With all of these simplifications, equation 7/8 shrinks down to

$$\frac{\partial p}{\partial y} \approx 0 \tag{7/9}$$

which tells us that pressure is a function of x only ($\frac{\partial p}{\partial x} = \frac{\mathrm{d}p}{\mathrm{d}x}$).

We now turn to equation 7/7, first to obtain an expression for pressure by applying it outside of the boundary layer where $u = U$:

$$\frac{\mathrm{d}p}{\mathrm{d}x} = -\rho U \frac{\mathrm{d}U}{\mathrm{d}x} \tag{7/10}$$

and secondly to obtain an expression for the velocity profile:

$$\begin{aligned} u\frac{\partial u}{\partial x} + v\frac{\partial u}{\partial y} &= -\frac{1}{\rho}\frac{\partial p}{\partial x} + \frac{\mu}{\rho}\frac{\partial^2 u}{(\partial y)^2} \\ &= U\frac{\mathrm{d}U}{\mathrm{d}x} + \frac{\mu}{\rho}\frac{\partial^2 u}{(\partial y)^2} \end{aligned} \tag{7/11}$$

Thus, the velocity field $\vec{V} = (u; v) = f(x, y)$ in a steady laminar boundary layer is driven by the two following equations, answering to Newton's second law and continuity:

$$u\frac{\partial u}{\partial x} + v\frac{\partial u}{\partial y} = U\frac{\mathrm{d}U}{\mathrm{d}x} + \frac{\mu}{\rho}\frac{\partial^2 u}{(\partial y)^2} \tag{7/12}$$

$$\frac{\partial u}{\partial x} + \frac{\partial v}{\partial y} = 0 \tag{7/13}$$

The main unknown in this system is the longitudinal speed profile across the layer, $u_{(x,y)}$. Unfortunately, over a century after it has been written, we still have not found an analytical solution to it.

7.3.2 Blasius' solution

Heinrich Blasius undertook a PhD thesis under the guidance of Prandtl, in which he focused on the characterization of laminar boundary layers. As part of his work, he showed that the geometry of the velocity profile (i.e. the velocity distribution) within such a layer is *always the same*, and that regardless of the flow velocity or the position, u can be simply expressed as a function of non-dimensionalized distance away from the wall termed η:

$$\eta \equiv y\sqrt{\frac{\rho U}{\mu x}} \tag{7/14}$$

Blasius was able to show that u is a function such that $\frac{u}{U} = f'_{(\eta)}$, with $f''' + \frac{1}{2}ff'' = 0$ — unfortunately, no known analytical solution to this equation is known. However, it has now long been possible to obtain numerical values for f' at selected positions η. Those are plotted in fig. 7.5.

Based on this work, it can be shown that for a laminar boundary layer flowing along a smooth wall, the four parameters about which we are interested are

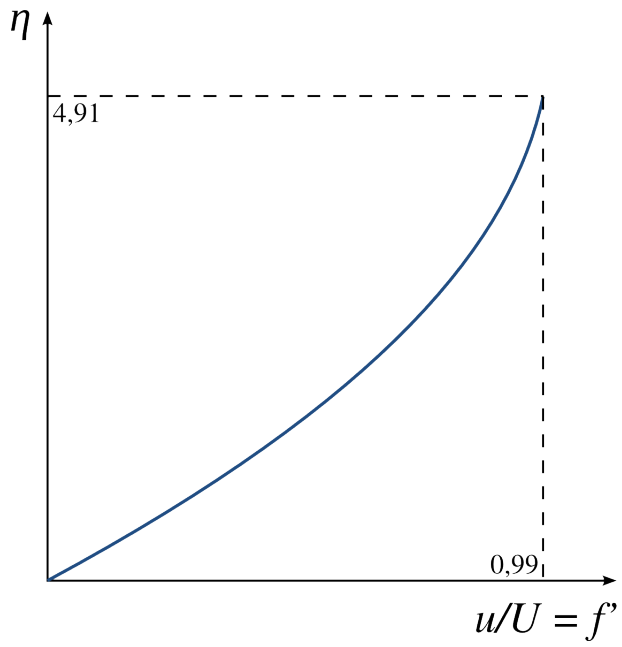

Figure 7.5 – The velocity profile obtained by Blasius (an exact solution to the Navier-Stokes equations simplified with laminar boundary-layer hypothesis).

Figure CC-0 o.c.

solely function of the distance-based Reynolds number $[\mathrm{Re}]_x$:

$$\frac{\delta}{x} = \frac{4{,}91}{\sqrt{[\mathrm{Re}]_x}} \tag{7/14a}$$

$$\frac{\delta^*}{x} = \frac{1{,}72}{\sqrt{[\mathrm{Re}]_x}} \tag{7/14b}$$

$$\frac{\theta}{x} = \frac{0{,}664}{\sqrt{[\mathrm{Re}]_x}} \tag{7/14c}$$

$$c_{f_{(x)}} = \frac{0{,}664}{\sqrt{[\mathrm{Re}]_x}} \tag{7/14d}$$

7.3.3 Pohlhausen's model

Contrary to Blasius who was searching for an exact solution, Ernst Pohlhausen made an attempt at modeling the velocity profile in the boundary layer with a *simple* equation. He imagined an equation of the form:

$$\frac{u}{U} = g_{(Y)} = aY + bY^2 + cY^3 + dY^4 \tag{7/15}$$

in which $Y \equiv y/\delta$ represents the distance away from the wall, and he then set to find values for the four coefficients a, b, c and d that would match the conditions we set in eqs. (7/12) and (7/13).

In order to obtain these coefficients, Blasius simply calibrated his model using known boundary conditions at the edges of the boundary layer:

- for $y = 0$ (meaning $Y = 0$), we have both $u = 0$ and $v = 0$. Equation 7/12 becomes:

$$0 = U\frac{\mathrm{d}U}{\mathrm{d}x} + \frac{\mu}{\rho}g''_{(0)} \tag{7/16}$$

- for $y = \delta$ (meaning $Y = 1$) we have $u = U$, $\partial u/\partial y = 0$ and $\partial^2 u/(\partial y)^2 = 0$. These values allow us to evaluate three properties of function g :

$$u = U = U g_{(1)} \tag{7/17}$$

$$\frac{\partial u}{\partial y} = 0 = \frac{U}{\delta} g'_{(1)} \tag{7/18}$$

$$\frac{\partial^2 u}{(\partial y)^2} = 0 = \frac{U}{\delta^2} g''_{(1)} \tag{7/19}$$

This system of four equations allowed Pohlhausen to evaluate the four terms a, b, c and d. He introduced the variable Λ, a non-dimensional measure of the outer velocity flow-wise gradient:

$$\Lambda \equiv \delta^2 \frac{\rho}{\mu} \frac{\mathrm{d}U}{\mathrm{d}x} \tag{7/20}$$

and he then showed that his velocity model in the smooth-surface laminar boundary layer, equation 7/15, had finally become:

$$\frac{u}{U} = 1 - (1 + Y)(1 - Y)^3 + \Lambda \frac{Y}{6}(1 - Y^3) \tag{7/21}$$

Pohlhausen's model is remarkably close to the exact solution described by Blasius (fig. 7.6). We thus have an approximate model for $u_{(x,y)}$ within the boundary layer, as a function of $U_{(x)}$.

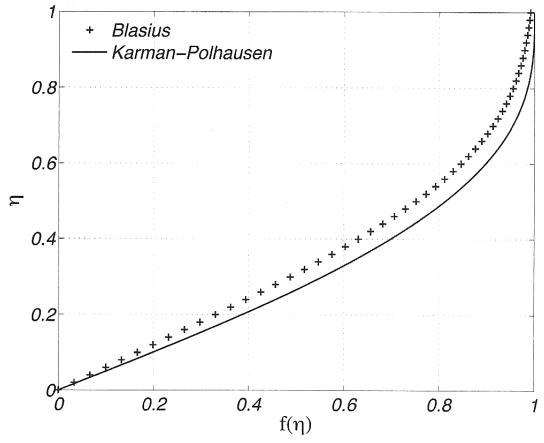

Figure 7.6 – Velocity profiles in the Pohlhausen and Blasius boundary layer profiles.
Figure © from Richecœeur 2012 [13]

It can be seen now that neither Blasius nor Pohlhausen's models are fully satisfactory. The first is drawn from a handful of realistic, known boundary conditions, but we fail to find an analytical solution to match them. The second is drawn from the hypothesis that the analytical solution is simple, but it is not very accurate. And we have not even considered yet the case for turbulent flow!
Here, it is the process which matters to us. Both of those methods are frequently-attempted, sensible approaches to solving problems in modern fluid dynamics research, where, just as here, one often has to contend with approximate solutions.

7.4 Transition

After it has traveled a certain length along the wall, the boundary layer becomes very unstable and it transits rapidly from a laminar to a turbulent regime (fig. 7.7). We have already briefly described the characteristics of a turbulent flow in chapter 5; the same apply to turbulence within the boundary layer. Again, we stress that the boundary layer may be turbulent in a globally laminar flow (it may conversely be laminar in a globally turbulent flow): that is commonly the case around aircraft in flight, for example.

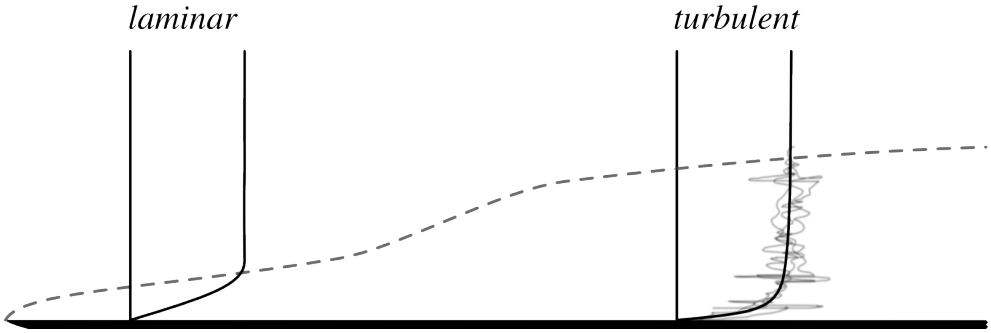

Figure 7.7 – Transition of a boundary layer from laminar to turbulent regime.

Figure CC-BY *Olivier Cleynen*

We observe that the distance $x_{\text{transition}}$ at which the boundary layer changes regime is reduced when the velocity is increased, or when the viscosity is decreased. In practice this distance depends on the distance-based Reynolds number $[\text{Re}]_x \equiv \frac{\rho U x}{\mu}$. The most commonly accepted prediction for the transition position is:

$$[\text{Re}]_{x\ \text{transition}} \approx 5 \cdot 10^5 \tag{7/22}$$

Transition can be generated earlier if the surface roughness is increased, or if obstacles (e.g. turbulators, vortex generators, trip wires) are positioned within the boundary layer. Conversely, a very smooth surface and a very steady, uniform incoming flow will result in delayed transition.

7.5 The turbulent boundary layer

The extensive description of turbulent flows remains an unsolved problem. As we have seen when studying duct flows, by contrast with laminar counterparts turbulent flows result in

- increased mass, energy and momentum exchange;
- increased losses to friction;
- apparently chaotic internal movements.

Instead of resolving the entire time-dependent flow in the boundary layer, we satisfy ourselves with describing the average component of the longitudinal speed, $\overline{u}$. A widely-accepted velocity model is:

$$\frac{\overline{u}}{U} \approx \left(\frac{y}{\delta}\right)^{\frac{1}{7}} \tag{7/23}$$

This profile has a much flatter geometry near the wall than its laminar counterpart (fig. 7.8).

In the same way that we have worked with the laminar boundary layer profiles, we can derive models for our characteristics of interest from this velocity profile:

$$\frac{\delta}{x} \approx \frac{0{,}16}{[\mathrm{Re}]_x^{\frac{1}{7}}} \tag{7/23a}$$

$$\frac{\delta^*}{x} \approx \frac{0{,}02}{[\mathrm{Re}]_x^{\frac{1}{7}}} \tag{7/23b}$$

$$\frac{\theta}{x} \approx \frac{0{,}016}{[\mathrm{Re}]_x^{\frac{1}{7}}} \tag{7/23c}$$

$$c_{f_{(x)}} \approx \frac{0{,}027}{[\mathrm{Re}]_x^{\frac{1}{7}}} \tag{7/23d}$$

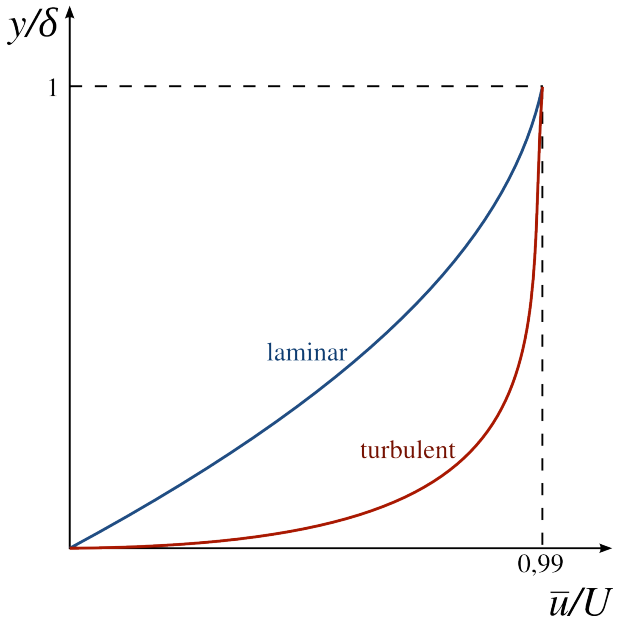

Figure 7.8 – Comparison of laminar and turbulent boundary layer profiles, both scaled to the same size. It is important to remember that in practice turbulent boundary layers are much thicker than laminar ones, and that $\overline{u}$ is only a time-average velocity.

Figure CC-0 o.c.

7.6.1 Principle

Under certain conditions, fluid flow separates from the wall. The boundary layer then disintegrates and we observe the appearance of a turbulent wake near the wall. Separation is often an undesirable phenomenon in fluid mechanics: it may be thought of as the point where we fail to impart a desired trajectory to the fluid.

When the main flow speed U along the wall is varied, we observe that the geometry of the boundary layer changes. The greater the longitudinal speed gradient ($\mathrm{d}U/\mathrm{d}x > 0$), and the flatter the profile becomes. Conversely, when the longitudinal speed gradient is negative, the boundary layer velocity profile straightens up. When it becomes perfectly vertical at the wall, it is such that streamlines separate from the wall: this is called *separation* (fig. 7.9).

The occurrence of separation can be predicted if we have a robust model for the velocity profile inside the boundary layer. For this, we go back to fundamentals, stating that **at the separation point, the shear effort on the surface must be zero**:

$$\tau_{\text{wall at separation}} = 0 = \mu \left(\frac{\partial u}{\partial y} \right)_{y=0} \tag{7/24}$$

At the wall surface ($u = 0$ and $v = 0$), equation 7/12 becomes:

$$\mu \left(\frac{\partial^2 u}{(\partial y)^2} \right)_{y=0} = \frac{\mathrm{d}p}{\mathrm{d}x} = -\rho U \frac{\mathrm{d}U}{\mathrm{d}x} \tag{7/25}$$

Thus, as we progressively increase the term $\mathrm{d}p/\mathrm{d}x$, the term $\frac{\partial^2 u}{(\partial y)^2}$ reaches higher (positive) values on the wall surface. Nevertheless, we know that it *must* take a negative value at the exterior boundary of the boundary layer.

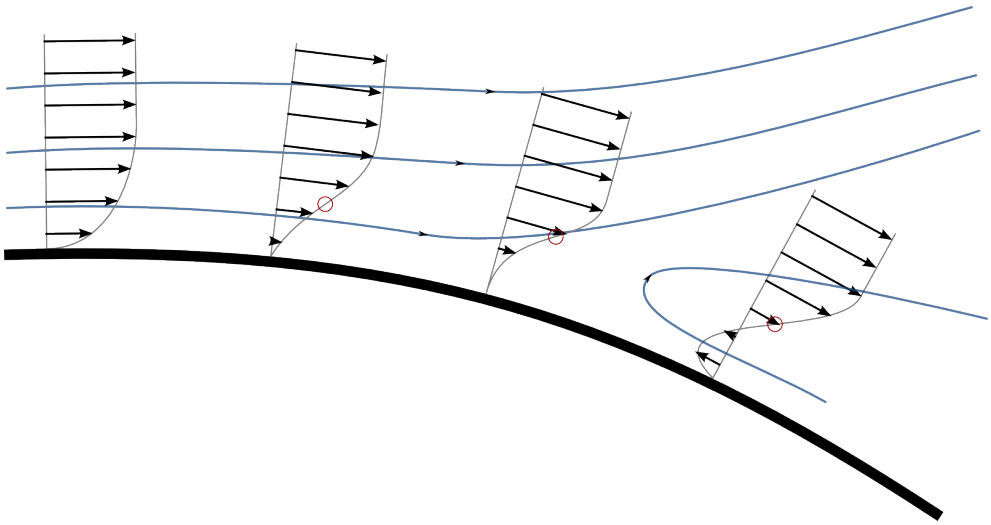

Figure 7.9 – Separation of the boundary layer. The main flow is from left to right, and flowing towards a region of increasing pressure. For clarity, the y-scale is greatly exaggerated.

Figure CC-BY *Olivier Cleynen*

Therefore, it must change sign somewhere in the boundary. This point where $\frac{\partial^2 u}{(\partial y)^2}$ changes sign is called *inflexion point*.

The existence of the inflection point within the boundary layer tells us that the term $\frac{\partial u}{\partial y}$ tends towards a smaller and smaller value at the wall. Given enough distance x, it will reach zero value, and the boundary layer will separate (fig. 7.10). Therefore, the longitudinal pressure gradient, which in practice determines the longitudinal velocity gradient, is the key factor in the analytical prediction of separation.

We shall remember two crucial points regarding the separation of boundary layers:

1. **Separation occurs in the presence of a positive pressure gradient**, which is sometimes named *adverse pressure gradient*.
   Separation points along a wall (e.g. a car bodywork, an aircraft wing, rooftops, mountains) are always situated in regions where pressure increases (positive $\mathrm{d}p/\mathrm{d}x$ or negative $\mathrm{d}U/\mathrm{d}x$). If pressure remains constant, or if it decreases, then the boundary layer cannot separate.

2. **Laminar boundary layers are much more sensitive to separation** than turbulent boundary layers (fig. 7.11).
   A widely-used technique to reduce or delay the occurrence of separation is to make boundary layers turbulent, using low-height artificial obstacles positioned in the flow. By doing so, we compromise shear-based friction (which increases with turbulence) and resistance to stall.

Predicting in practice the position of a separation point is difficult, because an intimate knowledge of the boundary layer profile and of the (external-flow-generated) pressure field are required — but as the flow separates, these are no longer independent. Resorting to experimental measurements, in this case, is often a wise idea!

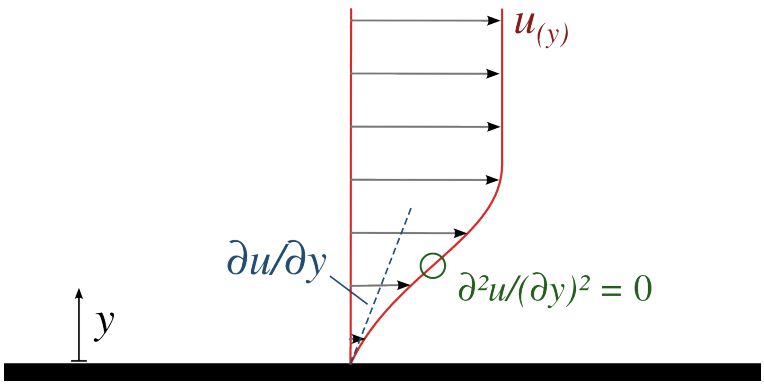

Figure 7.10 – The inflection point within a boundary layer about to separate.

Figure CC-BY *Olivier Cleynen*

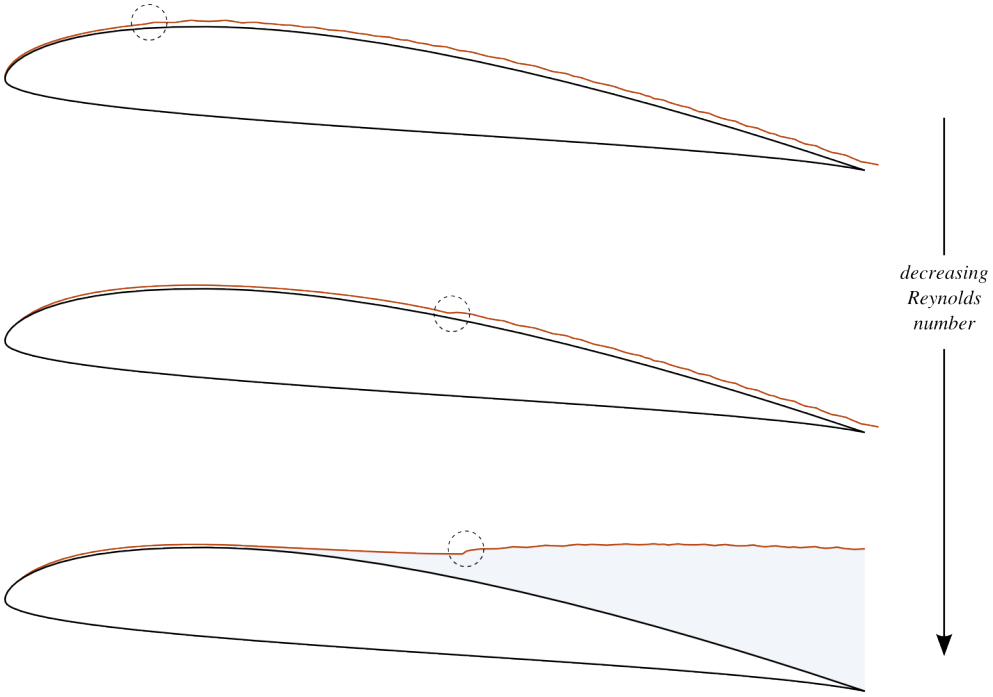

Figure 7.11 – The effect of decreasing Reynolds number on flow attachment over an airfoil at constant angle of attack, with the transition point highlighted. Laminar boundary layers are much more prone to separation than turbulent boundary layers.

Figure CC-BY-SA *Olivier Cleynen, based on Barlow & Pope 1999 [7]*

7.6.2 Separation according to Pohlhausen

In the case of a laminar flow along a smooth surface, Pohlhausen's model allows for interesting results. Indeed, at the separation point, $\tau_{\text{wall}} = 0$, thus:

$$\begin{aligned} \tau_{\text{wall}} = 0 = \mu \left(\frac{\partial u}{\partial y} \right)_{y=0} &= \mu \left(\frac{U}{\delta} g' \right)_{Y=0} \\ 0 = g'_{Y=0} &= a \\ \Lambda = -12 & \end{aligned} \tag{7/26}$$

$$\delta^2 \frac{\rho}{\mu} \frac{\mathrm{d}U}{\mathrm{d}x} = -12 \tag{7/27}$$

This equation allows us to predict the thickness of the boundary layer at the point where separation occurs, and therefore its position, if the velocity gradient $\mathrm{d}U/\mathrm{d}x$ is known.

We can see here that once we have obtained an extensive description of the flow within the boundary layer, we can generate a large amount of useful information regarding the general flow around the object.

Unfortunately, Pohlhausen's model's agreement with experimental measurements is not very good, and it can only usefully predict the position of the separation point in a few simple cases. Nevertheless, the overall thought process, i.e.

intuition of a simple model
↓
non-dimensionalization
↓
correlation with known boundary conditions

↓
exploitation of the model to predict flow behavior

is what should be remembered here, for it is typical of the research process in fluid dynamics.

Fluid Mechanics
Exercise sheet 7 – The boundary layer

last edited June 12, 2016

These lecture notes are based on textbooks by White [9], Çengel & al.[12], and Munson & al.[14].

Except otherwise indicated, we assume that fluids are Newtonian, and that:
$\rho_{\text{water}} = 1\,000\,\text{kg m}^{-3}$; $p_{\text{atm.}} = 1\,\text{bar}$; $\rho_{\text{atm.}} = 1{,}225\,\text{kg m}^{-3}$; $T_{\text{atm.}} = 11{,}3\,^{\circ}\text{C}$; $\mu_{\text{atm.}} = 1{,}5 \cdot 10^{-5}\,\text{N s m}^{-2}$;
$g = 9{,}81\,\text{m s}^{-2}$. Air is modeled as a perfect gas ($R_{\text{air}} = 287\,\text{J K}^{-1}\,\text{kg}^{-1}$; $\gamma_{\text{air}} = 1{,}4$; $c_{p\text{air}} = 1\,005\,\text{J kg}^{-1}\,\text{K}^{-1}$).

In boundary layer flow, we accept that transition occurs at $[\text{Re}]_x \gtrsim 5 \cdot 10^5$.

The wall shear coefficient c_f, a function of distance x,
is defined based on the free-stream flow velocity U:

$$c_{f_{(x)}} \equiv \frac{\tau_{\text{wall}}}{\frac{1}{2}\rho U^2} \tag{7/5}$$

Exact solutions to the laminar boundary layer along a smooth surface yield:

$$\frac{\delta}{x} = \frac{4{,}91}{\sqrt{[\text{Re}]_x}} \qquad \frac{\delta^*}{x} = \frac{1{,}72}{\sqrt{[\text{Re}]_x}} \tag{7/14b}$$

$$\frac{\theta}{x} = \frac{0{,}664}{\sqrt{[\text{Re}]_x}} \qquad c_{f_{(x)}} = \frac{0{,}664}{\sqrt{[\text{Re}]_x}} \tag{7/14d}$$

Solutions to the turbulent boundary layer along a smooth surface yield the following time-averaged characteristics:

$$\frac{\delta}{x} \approx \frac{0{,}16}{[\text{Re}]_x^{\frac{1}{7}}} \qquad \frac{\delta^*}{x} \approx \frac{0{,}02}{[\text{Re}]_x^{\frac{1}{7}}} \tag{7/23b}$$

$$\frac{\theta}{x} \approx \frac{0{,}016}{[\text{Re}]_x^{\frac{1}{7}}} \qquad c_{f_{(x)}} \approx \frac{0{,}027}{[\text{Re}]_x^{\frac{1}{7}}} \tag{7/23d}$$

Figure 7.12 quantifies the viscosity of various fluids as a function of temperature.

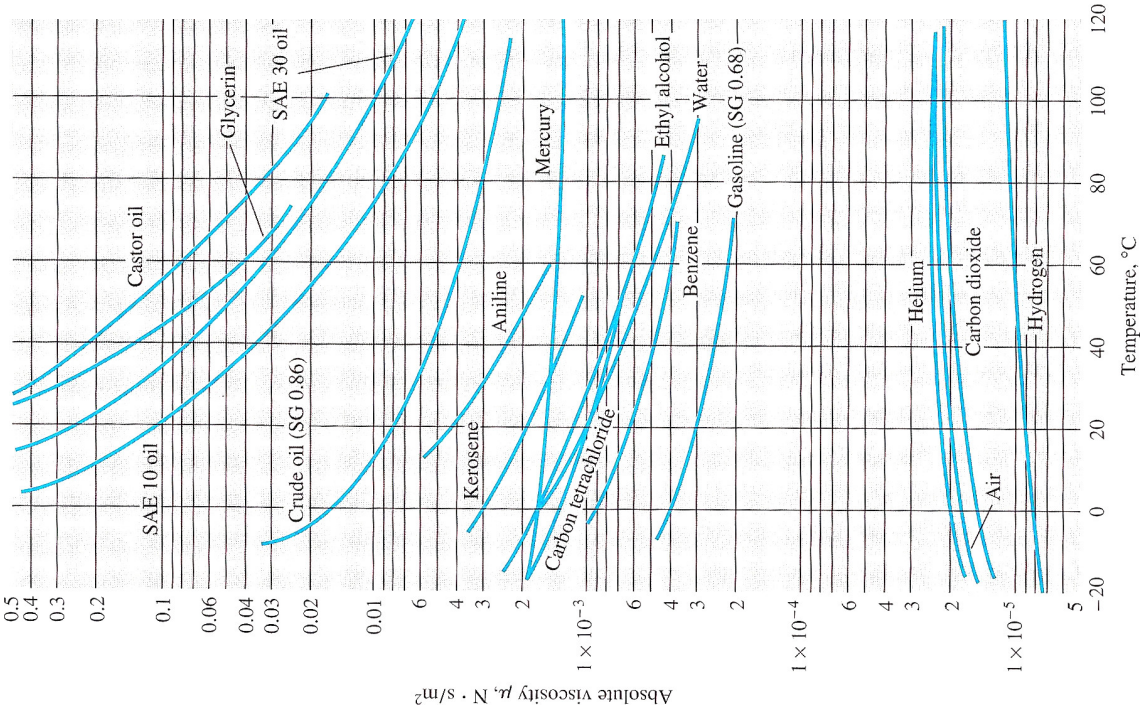

Figure 7.12 – Viscosity of various fluids at a pressure of 1 bar (in practice viscosity is almost independent of pressure).

Figure repeated from fig. 5.11 p.107; © White 2008 [9]

7.1 Water and air flow

White [9] E7.2

A flat plate of length 0,3 m is placed parallel to a uniform flow with speed 0,3 $\mathrm{m\,s^{-1}}$. How thick can the boundary layer become:

1. if the fluid is air at 1 bar and 20 °C?
2. if the fluid is water at 20 °C?

7.2 Boundary layer sketches

CC-0 o.c.

A thin and long horizontal plate is moved horizontally through a stationary fluid.

1. Sketch the velocity profile of the fluid:
   - at the leading edge;
   - at a point where the boundary layer is laminar;
   - and at a point further downstream where the boundary layer is turbulent.
2. Draw a few streamlines, indicate the boundary layer thickness δ, and the displacement thickness δ^*.
3. Explain shortly (e.g. in 30 words or less) how the transition to turbulent regime can be triggered.
4. Explain shortly (e.g. in 30 words or less) how the transition to turbulent regime could instead be delayed.

7.3 Shear force due to boundary layer

White [9] E7.3

A thin and smooth plate of dimensions $0{,}5 \times 3\,\mathrm{m}$ is placed with a zero angle of attack in a flow incoming at $1{,}25\,\mathrm{m\,s^{-1}}$, as shown in fig. 7.13.

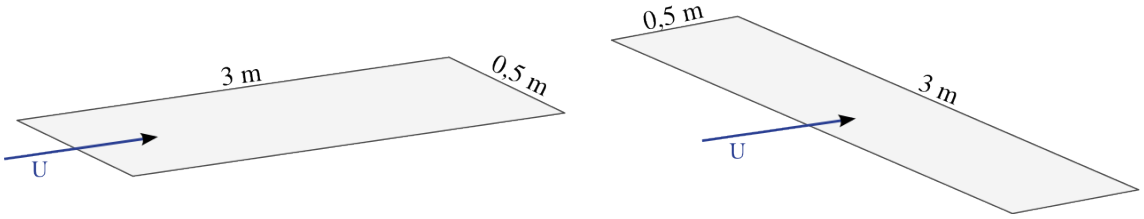

Figure 7.13 – A thin plate positioned parallel to an incoming uniform flow. Two configurations are studied in this exercise.

Figure CC-0 o.c.

1. What is the shear force exerted on the plate for each of the two configurations shown in fig. 7.13, when the fluid is air of viscosity $1{,}5 \cdot 10^{-5}\,\mathrm{Pa\,s}$?
2. What are the shear forces when the fluid is water of viscosity $1 \cdot 10^{-3}\,\mathrm{Pa\,s}$?
3. *[difficult question]* How would these shear efforts evolve if the plate was tilted with an angle of 20° relative to the flow?

7.4 Wright Flyer I

CC-0 o.c.

The Wright Flyer I, the first airplane capable of sustained controlled flight (1903), was a biplane with a 12 m wingspan (fig. 7.14). It had two wings of chord length 3,92 m stacked one on top of the other.[1] The wing profile was extremely thin and it could only fly at very low angles of attack. Its flight speed was approximately $40\,\mathrm{km\,h^{-1}}$.

Figure 7.14 – The Wright Flyer I, first modern airplane in history. Built with meticulous care and impeccable engineering methodology by two bicycle makers, it made history in December 1903.

Figure by Orville Wright, 1908 (public domain)

1. If the flow over the wings can be treated as if they were flat plates, what is the power necessary to compensate the shear exerted by the airflow on the wings during flight?
2. What other forms of drag would also be found on the aircraft?

[1] As can be seen in fig. 7.14, the chord length given here is obviously erroneous. This error is temporarily left as-is so as not to cause confusion (at time of writing this exercise is worked upon by a class of 80).

7.5 Power lost to shear on an airliner fuselage

CC-0 o.c.

An Airbus A340-600 is cruising at $M = 0{,}82$ at an altitude of 10 000 m (viscosity $1{,}457 \cdot 10^{-5}\,\mathrm{N\,s\,m^{-2}}$, temperature 220 K, density $0{,}4\,\mathrm{kg\,m^{-3}}$).

1. Estimate the power dissipated to friction on the cylindrical part of the fuselage, which has diameter 5,6 m and length 65 m.
2. In practice, in which circumstances could flow separation occur on the fuselage skin?

7.6 Separation according to Pohlhausen

non-examinable, based on Richecœur 2012 [13]

Air at 1 bar and 20 °C flows along a smooth surface, and decelerates slowly, with a constant rate of $-0{,}25\,\mathrm{m\,s^{-1}\,m^{-1}}$.

According to the Pohlhausen model (eq. 7/21 p.142), at which distance downstream will separation occur? Is the boundary layer still laminar then?

How could one generate such a deceleration in practice?

7.7 Separation mechanism

non-examinable, CC-0 o.c.

Sketch the velocity profile of a laminar or turbulent boundary layer shortly upstream of, and at a separation point.

The two equations below describe flow in laminar boundary layer:

$$u\frac{\partial u}{\partial x} + v\frac{\partial u}{\partial y} = U\frac{\mathrm{d}U}{\mathrm{d}x} + \frac{\mu}{\rho}\frac{\partial^2 u}{(\partial y)^2} \tag{7/12}$$

$$\frac{\partial u}{\partial x} + \frac{\partial v}{\partial y} = 0 \tag{7/13}$$

Identify these two equations, list the conditions in which they apply, and explain shortly (e.g. in 30 words or less) why a boundary layer cannot separate when a favorable pressure gradient is applied along the wall.

7.8 Laminar wing profile

non-examinable. Based on a diagram from Bertin et al. 2010 [11]

The characteristics of a so-called “laminar” wing profile are compared in figs. 7.15 to 7.17 with those of an ordinary profile.

On the graph representing the pressure coefficient $C_p \equiv \frac{p-p_\infty}{\frac{1}{2}\rho V^2}$, identify the curve corresponding to each profile.

What advantages and disadvantages does the laminar wing profile have, and how can they be explained? In which applications will it be most useful?

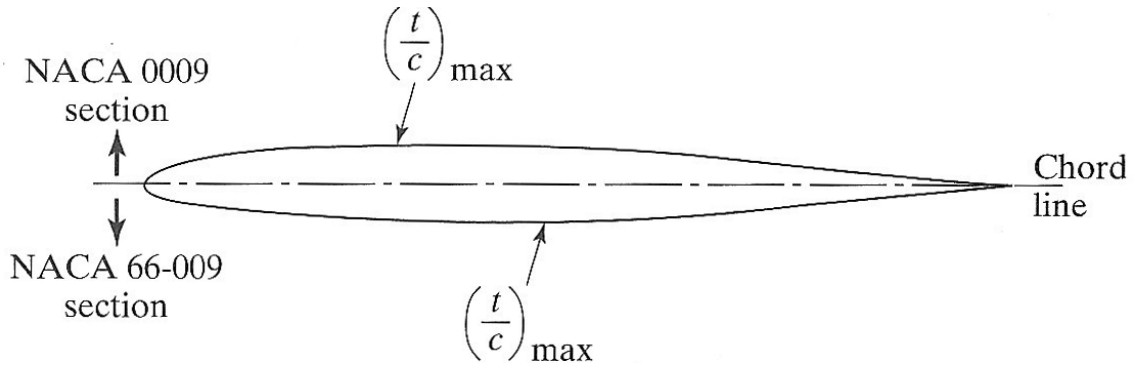

Figure 7.15 – Comparison of the thickness distribution of two uncambered wing profiles: an ordinary medium-speed NACA 0009 profile, and a "laminar" NACA 66-009 profile.

Figure © Bertin & Cummings 2010 [11]

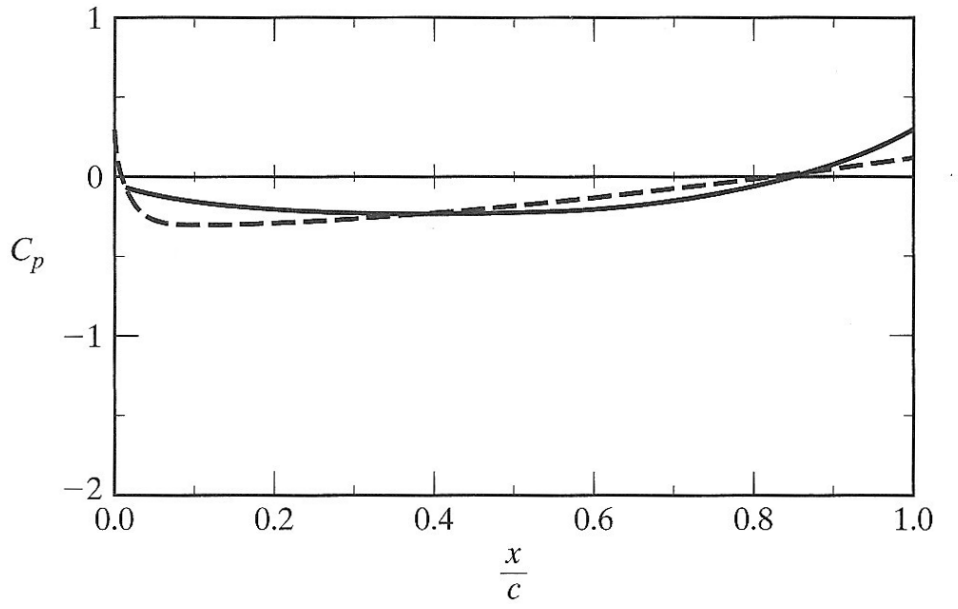

Figure 7.16 – Static pressure distribution (represented as a the local non-dimensional *pressure coefficient* $C_p \equiv \frac{p-p_\infty}{\frac{1}{2}\rho V^2}$) as a function of distance x (non-dimensionalized with the chord c) over the surface of the two airfoils shown in fig. 7.15.

Figure © Bertin & Cummings 2010 [11]

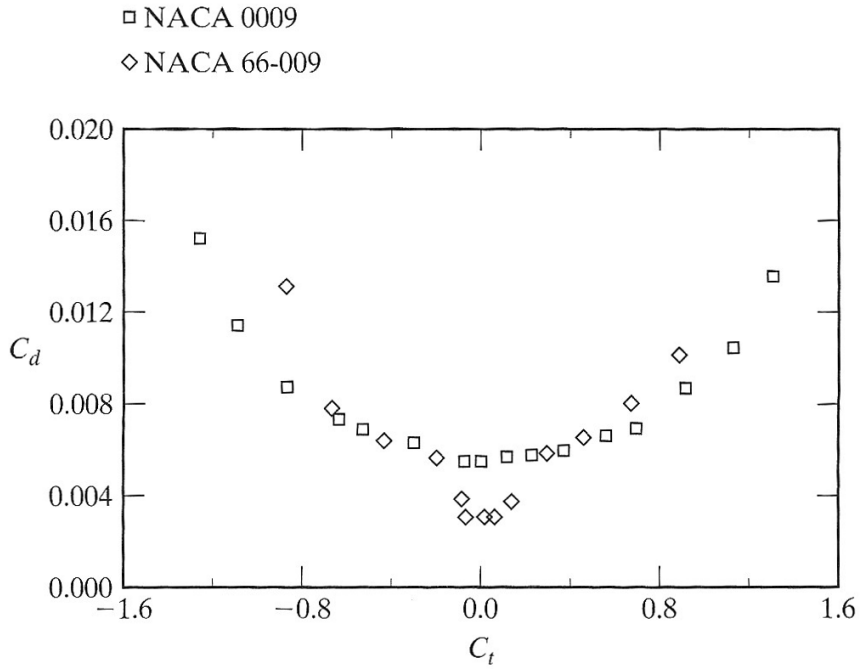

Figure 7.17 – Values of the section drag coefficient $C_d \equiv \frac{d}{\frac{1}{2}c\rho V^2}$ as a function of the section lift coefficient $C_l \equiv \frac{l}{\frac{1}{2}c\rho V^2}$ for both airfoils presented in fig. 7.15.

Figure © Bertin & Cummings 2010 [11], based on data by Abott & Von Doenhoff 1949 [1]

7.9 Thwaites' separation model

non-examinable, from White [9] E7.5

In 1949, Bryan Thwaites explored the limits of the Pohlhausen separation model. He proposed a different model to describe the laminar boundary layer velocity profile, which is articulated upon an expression for the momentum thickness θ and is more accurate than the Reynolds-number based descriptions that we have studied. Thwaites proposed the model:

$$\theta^2 = \theta_0^2 \left(\frac{U_0}{U}\right)^6 + 0{,}45\frac{\mu}{\rho}\frac{1}{U^6}\int_0^x U^5 \,\mathrm{d}x \tag{7/28}$$

in which the 0-subscripts denote initial conditions (usually $\theta_0 = 0$)

Thwaites also defined a non-dimensional momentum thickness λ_θ:

$$\lambda_\theta \equiv \theta^2 \frac{\rho}{\mu}\frac{\mathrm{d}U}{\mathrm{d}x} \tag{7/29}$$

and then went on to show that for the model above, separation ($c_f = 0$) occurs when $\lambda_\theta = -0{,}09$.

A classical model for flow deceleration is the Howarth longitudinal velocity profile $U_{(x)} = U_0\left(1 - \frac{x}{L}\right)$, in which L is a reference length of choice. In this velocity distribution with linear deceleration, what is the distance at which the Thwaites model predicts the boundary layer separation?

Answers

7.1 1) At trailing edge $[\mathrm{Re}]_x = 5\,348$ thus the layer is laminar everywhere. δ will grow from 0 to 2,01 cm (eq. 7/14a p.141); 2) For water: $\delta_{\text{trailing edge}} = 4{,}91\,\text{mm}$.

7.2 1) See fig. 7.7 p.143. At the leading-edge the velocity is uniform. Note that the y-direction is greatly exaggerated, and that the outer velocity U is identical for both regimes; 2) See fig. 7.4 p.138. Note that streamlines penetrate the boundary layer; 3) and 4) See §7.4 p. 143.

7.3 $x_{\text{transition, air}} = 4{,}898\,\text{m}$ and $x_{\text{transition, water}} = 0{,}4\,\text{m}$. In a laminar boundary layer, inserting equation 7/14d into equation 7/5 into equation 7/6 yields $F_\tau = 0{,}664 L U^{1{,}5} \sqrt{\rho\mu} \left[\sqrt{x} \right]_0^{x_{\text{transition}}}$.
In a turbulent boundary layer, we use equation 7/23d instead and get $F_\tau = 0{,}01575 L \rho^{\frac{6}{7}} U^{\frac{13}{7}} \mu^{\frac{1}{7}} \left[x^{\frac{6}{7}} \right]_{x_{\text{transition}}}^{x_{\text{trailing edge}}}$. These expressions allow the calculation of the forces below:
1) (air) First case: $F = 3{,}445 \cdot 10^{-3}\,\text{N}$; second case $F = 8{,}438 \cdot 10^{-3}\,\text{N}$ (who would have thought eh?);
2) (water) First case: $F = 3{,}7849\,\text{N}$; second case $F = 2{,}7156\,\text{N}$.

7.4 Using the expressions developed in exercise 7.3, $\dot{W}_{\text{friction}} \approx 510\,\text{W}$.

7.5 1) $x_{\text{transition}} = 7{,}47\,\text{cm}$ (the laminar part is negligible). With the equations developed in exercise 7.3, we get $F = 24{,}979\,\text{kN}$ and $\dot{W} = 6{,}09\,\text{MW}$. Quite a jump from the Wright Flyer I!
2) When the longitudinal pressure gradient is zero, the boundary layer cannot separate. Thus separation from the fuselage skin can only happen if the fuselage is flown at an angle relative to the flight direction (e.g. during a low-speed maneuver).

7.9 Once the puzzle pieces are put together, this is an algebra exercise: $\left(\frac{x}{L}\right)_{\text{separation}} = 0{,}1231$. Bryan beats Ernst!

Fluid Mechanics
Chapter 8 – Creeping and inviscid flows

last edited June 18, 2016

These lecture notes are based on textbooks by White [9], Çengel & al.[12], and Munson & al.[14].

8.1 Motivation

This exploratory chapter is not a critical component of fluid dynamics; instead, it is meant as a brief overview of two extreme cases: flows for which viscous effects are dominant, and flows for which they play no role. This exploration should allow us to answer two questions:

- What are the key characteristics of highly-viscous flows?
- Which aspects of inviscid flows are relevant for the engineer?

8.2 Creeping flow

Fluid flow in which viscosity is dominant is called *creeping* or *Stokes flow*. Looking back on the non-dimensional Navier-Stokes equation for incompressible flow derived as eq. 6/17 p.123,

$$[\mathrm{St}]\,\frac{\partial \vec{V}^*}{\partial t^*} + [1]\,\vec{V}^* \cdot \vec{\nabla}^* \vec{V}^* = \frac{1}{[\mathrm{Fr}]^2}\,\vec{g}^* - [\mathrm{Eu}]\,\vec{\nabla}^* p^* + \frac{1}{[\mathrm{Re}]}\,\vec{\nabla}^{*2}\vec{V}^* \qquad (8/1)$$

we see that creeping flow will occur when the Reynolds number is much smaller than 1. The relative weight of the term $\frac{1}{[\mathrm{Re}]}\,\vec{\nabla}^{*2}\vec{V}^*$ then becomes overwhelming.

In addition to cases where $[\mathrm{Re}] \ll 1$, we restrict ourselves to flows for which

- gravitational effects have negligible influence over the velocity field;
- the frequency is extremely low (quasi-steady flow).

With these characteristics, the Strouhal and Froude numbers become very small with respect to the other terms, and our non-dimensionalized Navier-Stokes equation (eq. 8/1) is approximately reduced to:

$$\vec{0} \approx -[\mathrm{Eu}]\ \vec{\nabla}^* p^* + \frac{1}{[\mathrm{Re}]}\ \vec{\nabla}^{*2}\vec{V}^* \tag{8/2}$$

We can now come back to dimensionalized equations, concluding that for a fluid flow dominated by viscosity, the pressure and velocity fields are linked together by the approximate relation:

$$\vec{\nabla} p = \mu \vec{\nabla}^2 \vec{V} \tag{8/3}$$

In this type of flow, the pressure field is entirely dictated by the laplacian of velocity, and the fluid density has no importance. Micro-organisms, for which the representative length L is very small, spend their lives in such flows (fig. 8.1). At the human scale, we can visualize the effects of these flows by moving an object slowly in highly-viscous fluids (e.g. a spoon in honey), or by swimming in a pool filled with plastic balls. The inertial effects are almost inexistent, drag is extremely important, and the object geometry has comparatively small influence.

In 1851, George Gabriel Stokes worked through equation 8/3 for flow around a sphere, and obtained an analytical solution for the flow field. This allowed him to show that the drag $F_{\mathrm{D\ sphere}}$ applying on a sphere of diameter D in creeping flow (fig. 8.2) is:

$$F_{\mathrm{D\ sphere}} = 3\pi\mu V_\infty D \tag{8/4}$$

Inserting this equation 8/4 into the definition of the drag coefficient $C_{FD} \equiv F_\mathrm{D}/\frac{1}{2}\rho S_{\mathrm{frontal}} V_\infty^2$ (from eq. 6/2 p.118) then yields:

$$C_{FD} = \frac{F_{\mathrm{D\ sphere}}}{\frac{1}{2}\rho V_\infty^2 \frac{\pi}{4} D^2} = \frac{24\mu}{\rho\, UD} = \frac{24}{[\mathrm{Re}]_D} \tag{8/5}$$

These equations are specific to flow around spheres, but the trends they describe apply well to most bodies evolving in highly-viscous flows, such as dust or liquid particles traveling through the atmosphere. Drag is only

Figure 8.1 – Micro-organisms carry themselves through fluids at extremely low Reynolds numbers, since their scale L is very small. For them, viscosity effects are dominant over inertial effects

Photo by Yutaka Tsutsumi, M.D., Fujita Health University School of Medicine

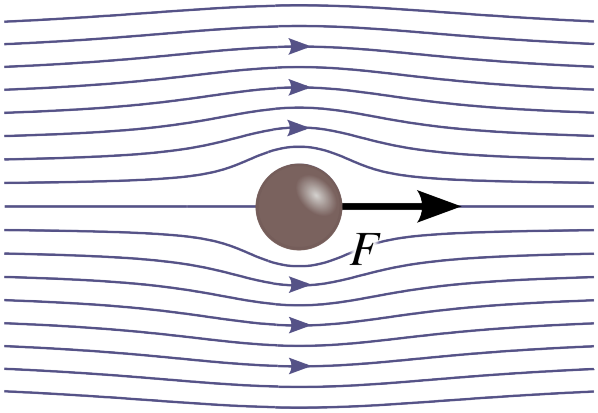

Figure 8.2 – Flow at very low Reynolds numbers around a sphere. In this regime, the drag force is proportional to the velocity.

Figure CC-BY-SA *by Olivier Cleynen& Commons User:Kraaiennest*

proportional to the speed (as opposed to low-viscosity flows in which it grows with velocity *squared*), and it does not depend on fluid density.

8.3 Inviscid incompressible flow

At the complete opposite of the spectrum of flows in fluid dynamics are *inviscid flows*, where viscosity plays no role at all. We propose to explore them just as briefly as we did with creeping flows.

8.3.1 Why study inviscid flow?

It is commonly observed that far away from solid walls, the influence of viscosity in fluid flow is very small. This is an opportunity to simplify the governing flow equations and attempt to describe these flows extensively. If successful, this process should allow us to calculate the pressure field around a solid object in a fluid flow.

Thus, if we can obtain a satisfactory description of inviscid flow, we will be in a position to complete the analysis we started in chapter 7 (summarized in figure 7.3 p.137). A study of the boundary layer will allow us to quantify shear and separation; while a study of far-field inviscid flow will allow us to quantify pressure (which is needed together with shear in order to compute body forces such as lift and drag).

Developing a method for solving any arbitrary inviscid flow is beyond the scope of this chapter; we shall instead satisfy ourselves with the modeling of a key phenomenon: *lift*.

8.3.2 The Euler equation

We define *inviscid flow* as one in which viscous effects do not influence the velocity field. Once again, we start from our beloved non-dimensional Navier-Stokes equation for incompressible flow derived as eq. 6/17 p.123,

$$[\mathrm{St}]\,\frac{\partial \vec{V}^*}{\partial t^*} + [1]\,\vec{V}^* \cdot \vec{\nabla}^* \vec{V}^* = \frac{1}{[\mathrm{Fr}]^2}\,\vec{g}^* - [\mathrm{Eu}]\,\vec{\nabla}^* p^* + \frac{1}{[\mathrm{Re}]}\,\vec{\nabla}^{*2} \vec{V}^* \tag{8/6}$$

in which we see that when the Reynolds number [Re] is very large, the last term becomes negligible relative to the other four terms. Thus, our governing equation can be reduced as follows:

$$[\mathrm{St}]\ \frac{\partial \vec{V}^*}{\partial t^*} + [1]\ \vec{V}^* \cdot \vec{\nabla}^* \vec{V}^* \approx \frac{1}{[\mathrm{Fr}]^2}\ \vec{g}^* - [\mathrm{Eu}]\ \vec{\nabla}^* p^* \tag{8/7}$$

It is worth mentioning that the only requirement for inviscid flow is for the Reynolds number $[\mathrm{Re}] \equiv \rho V L/\mu$ to be very large; thus even fluids with high viscosity may evolve in inviscid flows if their velocity, the representative scale and their density are sufficiently high.

Now, converting eq. 8/7 back to dimensional terms, our governing momentum equation for inviscid flow becomes:

$$\rho \frac{\mathrm{D}\vec{V}}{\mathrm{D}t} = \rho \vec{g} - \vec{\nabla} p \tag{8/8}$$

This simplified version of the Navier-Stokes equation, which describes incompressible inviscid flow, is named *Euler equation*. It stipulates that time-changes in the velocity field are due only to gravity and the pressure field.

What are the solutions to this equation? Unfortunately, as we have seen in chapter 6, the absence of viscous effects facilitates the occurrence of turbulence and makes for much more chaotic flows. Although the removal of shear from the Navier-Stokes equation simplifies the governing equation, the *solutions* to this new equation are even harder to find and describe.

8.4 Two-dimensional laminar incompressible potential flow

8.4.1 Rationale

Even though it does away with shear effects, the Euler equation is far too complex to be solved analytically.

Nevertheless, for a long time there has been a desire to describe simple flows analytically. In particular, it is tempting to draw an object (a square, a circle) on a sheet of paper and then trying to *calculate the simplest possible streamlines* for fluid flow around it. Such a flow would be:

- two-dimensional;
- fully-steady (laminar)
- inviscid;
- incompressible;
- and without gravitational effects.

This would allow to develop *some* understanding of fluid flow, and calculate basic parameters from solutions, such as pressure forces. Indeed, when one follows a streamline in a fully-steady inviscid flow, five particular conditions are met: steady, incompressible, constant-energy, friction-less flow with a known trajectory. These are, of course, the five criteria which we set forth

in chapter 3 for using the Bernoulli equation. Thus, along a streamline in a steady inviscid flow, Euler's equation reduces to eq. 3/18 (p.61):

$$\frac{p_1}{\rho} + \frac{1}{2}V_1^2 + gz_1 = \frac{p_2}{\rho} + \frac{1}{2}V_2^2 + gz_2 = \text{cst.} \tag{8/9}$$

along a streamline in a steady incompressible inviscid flow.

and so it follows that if the solution to an inviscid flow is known, the forces due to pressure can be calculated with relative ease.

8.4.2 Potential flows

In the early 19th century, when searching for solutions to the above problem, it was found that many interesting flow patterns could be obtained by superposing solutions for simple flows called *elementary flows*. In this process, we *start from known flow solutions* and then hope to obtain flow patterns that are relevant to our study, thus, this is clearly not an efficient methodology if one wishes to study a particular flow! Nevertheless, the flow patterns obtained by superposition not only give insight onto the mechanics of inviscid flow, but more importantly they have resulted in an extraordinary result regarding the understanding and the modeling of lift.

A category of flows that corresponds to the conditions listed above is that of *two-dimensional, laminar, incompressible, potential flows*.

We now introduce a new mathematical operator $\vec{\nabla}\times$ named *curl*:

$$\vec{\nabla}\times\vec{A} \equiv \begin{vmatrix} \vec{i} & \vec{j} & \vec{k} \\ \frac{\partial}{\partial x} & \frac{\partial}{\partial y} & \frac{\partial}{\partial z} \\ A_x & A_y & A_z \end{vmatrix} = \left(\frac{\partial A_z}{\partial y} - \frac{\partial A_y}{\partial z}\right)\vec{i} \;+\; \left(-\frac{\partial A_z}{\partial x} + \frac{\partial A_x}{\partial z}\right)\vec{j} \;+\; \left(\frac{\partial A_y}{\partial x} - \frac{\partial A_x}{\partial y}\right)\vec{k} \tag{8/10}$$

With this definition, we consider the curl of velocity field as the following vector field:

$$\vec{\nabla}\times\vec{V} = \begin{vmatrix} \vec{i} & \vec{j} & \vec{k} \\ \frac{\partial}{\partial x} & \frac{\partial}{\partial y} & \frac{\partial}{\partial z} \\ u & v & w \end{vmatrix} = \left(\frac{\partial w}{\partial y} - \frac{\partial v}{\partial z}\right)\vec{i} \;+\; \left(-\frac{\partial w}{\partial x} + \frac{\partial u}{\partial z}\right)\vec{j} \;+\; \left(\frac{\partial v}{\partial x} - \frac{\partial u}{\partial y}\right)\vec{k} \tag{8/11}$$

A *potential* (also called *irrotational*) flow, by definition, is one for which the curl of velocity is always null:

$$\vec{\nabla}\times\vec{V} = \vec{0} \tag{8/12}$$

by definition, for a potential flow.

Let us now attempt to *draw* a flow field for a simple steady two-dimensional flow, such as flow around a cylinder. There exists an acceptably simple method to ensure that a couple of functions $u = f_1(x,y)$ and $v = f_2(x,y)$ does indeed meet the conditions dictated above. It involves evaluating two functions ψ and ϕ.

The stream function written ψ (psi), expresses the fact that mass must be conserved ($\vec{\nabla}\cdot\vec{V} = \frac{\partial u}{\partial x} + \frac{\partial v}{\partial y} = 0$, eq. 4/17 p.80). For any incompressible

flow, we have, by definition:

$$\frac{\partial \psi}{\partial y} \equiv u \tag{8/13}$$

$$-\frac{\partial \psi}{\partial x} \equiv v \tag{8/14}$$

It is possible to show that when traced out, lines of of constant ψ value are *streamlines* – in other words, as they travel along, fluid particles follow paths of constant ψ value.

the potential function written ϕ (phi), expresses the fact that the flow is irrotational. It can be shown that in an irrotational flow the velocity vector field is the gradient of a function ϕ which is such that:

$$\vec{\nabla}\phi \equiv \vec{V} \tag{8/15}$$

When traced out, lines of constant ϕ (named *potential lines*) are always perpendicular to the streamlines.

This shift from looking for u and v, to looking for ψ and ϕ, is an interesting mathematical trick, which we exploit in the next section. If these functions are know, then the velocity components can be obtained easily either in Cartesian coordinates,

$$u = \frac{\partial \phi}{\partial x} = \frac{\partial \psi}{\partial y} \tag{8/16}$$

$$v = \frac{\partial \phi}{\partial y} = -\frac{\partial \psi}{\partial x} \tag{8/17}$$

or angular coordinates:

$$v_r = \frac{\partial \phi}{\partial r} = \frac{1}{r}\frac{\partial \psi}{\partial \theta} \tag{8/18}$$

$$v_\theta = \frac{1}{r}\frac{\partial \phi}{\partial \theta} = -\frac{\partial \psi}{\partial r} \tag{8/19}$$

8.5 Elementary potential flows

In this section, we briefly go over elementary potential flows. These will serve as basic ingredients which will be added or subtracted to produce more interesting flows in the upcoming sections.

8.5.1 Linear uniform flow

A simple flow with a uniform velocity field $\vec{V}$, such as described in fig. 8.3, can be described with the two components:

$$u = U \cos \alpha \tag{8/20}$$

$$v = U \sin \alpha \tag{8/21}$$

in which α is the angle between $\vec{V}$ and the x-axis.

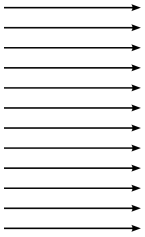

Figure 8.3 – A simple uniform steady flow.

figure CC-0 o.c.

The flow functions corresponding to this flow are:

$$\phi = U(x\cos\alpha + y\sin\alpha) \tag{8/22}$$
$$\psi = U(y\cos\alpha - x\sin\alpha) \tag{8/23}$$

In polar coordinates (r, θ), these two systems become:

$$u = u_r\cos\theta - u_\theta\sin\theta \tag{8/24}$$
$$v = u_r\sin\theta + u_\theta\cos\theta \tag{8/25}$$

and, most relevantly,

$$\phi = U\ r\cos\theta \tag{8/26}$$
$$\psi = U\ r\sin\theta \tag{8/27}$$

8.5.2 Sources and sinks

A source (fig. 8.4) is associated with the appearance of a volume flow rate $\dot{\mathcal{V}}$ from a single point in the flow. Conversely, a sink is associated with the removal of this flow rate (negative $\dot{\mathcal{V}}$) from the flow at a single point. Both source and sink can be described by the flow functions:

$$\phi = \frac{\dot{\mathcal{V}}}{2\pi}\ln r \tag{8/28}$$
$$\psi = \frac{\dot{\mathcal{V}}}{2\pi}\theta \tag{8/29}$$

In turn, these functions produce the vector field:

$$v_r = \frac{\dot{\mathcal{V}}}{2\pi r} \tag{8/30}$$
$$v_\theta = 0 \tag{8/31}$$

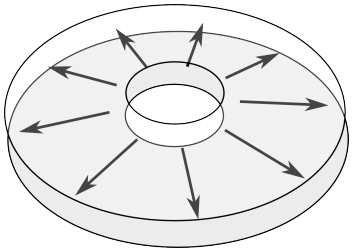

Figure 8.4 – Concept of a source inside a two-dimensional potential flow. A sink would display exactly opposed velocities.

Figure CC-BY-SA *Commons User:Nicoguaro*

8.5.3 Irrotational vortices

A *vortex* (plural: *vortices* is a pattern of rotation within a fluid flow. All vortices impart a rotational velocity $v_\theta = f(r, \theta)$ on the flow, in addition to which there may exist a radial component v_r. An *irrotational vortex* (fig. 8.5) is quite particular: its velocity field is such that $\vec{\nabla} \times \vec{V}$ is everywhere null. In other words, an object dropped inside an irrotational vortex will circle around the center of the vortex without ever rotating upon itself.

Figure 8.5 – Conceptual illustration of a two-dimensional vortex flow, with two leaves dropped on the surface of a whirlpool.
Left: reference position of the two leaves.
Center: in a *rotational vortex*, the leaves rotate around the center of the vortex, and about themselves in the process.
Right: in an *irrotational vortex*, the leaves also rotate around the center of the vortex, but they keep the same orientation when doing so.

Figures 1, 2 and 3 CC-BY-SA *en:Wikipedia User:Cayte*

An irrotational vortex is described by the two functions:

$$\phi = \frac{\Gamma}{2\pi}\theta \tag{8/32}$$

$$\psi = -\frac{\Gamma}{2\pi}\ln r \tag{8/33}$$

where Γ is the *circulation* (measured in s^{-1}) and represents the "strength" of the vortex.

These two functions produce the velocity field

$$v_r = 0 \tag{8/34}$$

$$v_\theta = \frac{\Gamma}{2\pi r} \tag{8/35}$$

Now that we have gathered a few essential "ingredients", we can start assembling them to construct interesting flow patterns.

8.6.1 Cylinder in a uniform flow

If we position a source and a sink of equal volume flow rate extremely close one to another, we obtain a potential flow named *doublet*. It can be shown that a doublet combined with a uniform flow produces a field described by the stream function:

$$\begin{aligned}\psi &= U\, r \sin\theta - U\, R^2 \frac{\sin\theta}{r} \\ &= U \sin\theta \left(r - \frac{R^2}{r}\right)\end{aligned} \tag{8/36}$$

in which R is a constant proportional to the source/sink volume flow rate $\dot{\mathcal{V}}$.

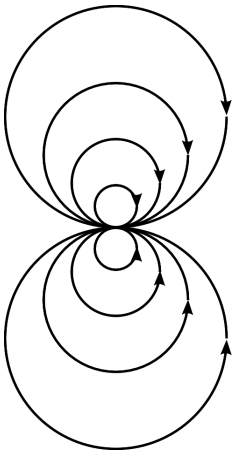

Figure 8.6 – When a source and a sink are brought very close one to another, the resulting flow is called a *doublet*.

Figure CC-0 o.c.

This function allows us to obtain the velocity field:

$$u_r = \frac{1}{r}\frac{\partial\psi}{\partial\theta} = U\cos\theta\left(1 - \frac{R^2}{r^2}\right) \tag{8/37}$$

$$u_\theta = -\frac{\partial\psi}{\partial r} = -U\sin\theta\left(1 + \frac{R^2}{r^2}\right) \tag{8/38}$$

When this field is plotted out, as in fig. 8.7, we find out that it corresponds to two-dimensional laminar inviscid incompressible flow around a cylinder!

In particular, along the cylinder wall, $r = R$ and

$$u_r|_{r=R} = 0 \tag{8/39}$$

$$u_\theta|_{r=R} = -2U\sin\theta \tag{8/40}$$

This velocity fields describes frictionless flow around a circular section. The fluid flows past along the surface without any shear, and has a purely symmetrical flow field.

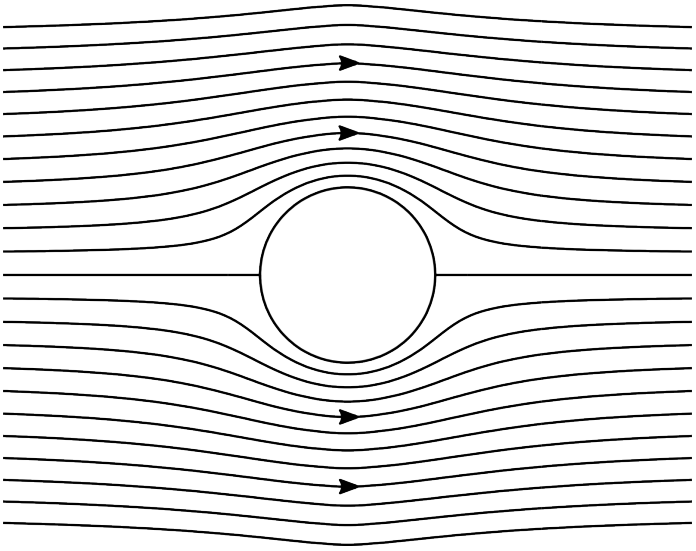

Figure 8.7 – The addition of a *doublet* and a *uniform flow* produces streamlines for an (idealized) flow around a cylinder.

Figure CC-BY-SA *by Commons User:Kraaiennest*

Since the Bernoulli equation can be applied along any streamline in inviscid incompressible steady irrotational potential flow, we can express the pressure p_s on the cylinder surface as a function of θ:

$$p_\infty + \frac{1}{2}\rho U^2 = p_s + \frac{1}{2}\rho v_\theta^2 \tag{8/41}$$

$$p_{s\ (\theta)} = p_\infty + \frac{1}{2}\rho\left(U^2 - v_\theta^2\right) \tag{8/42}$$

Now a simple integration yields the net forces exerted by the fluid on the cylinder per unit width L, in each of the two directions x and y:

$$\frac{F_{\text{net},x}}{L} = -\int_0^{2\pi} p_s\ \cos\theta\ R\,\mathrm{d}\theta = 0 \tag{8/43}$$

$$\frac{F_{\text{net},y}}{L} = -\int_0^{2\pi} p_s\ \sin\theta\ R\,\mathrm{d}\theta = 0 \tag{8/44}$$

The results are devastating: both lift and drag are null. This absence of friction, which was predicted far before the notion of viscosity was formalized (1768), is often called the *d'Alembert paradox*. The pressure distribution on the cylinder surface can be represented graphically (fig. 8.8). Good agreement is obtained with measurements on the leading edge of the cylinder; but as the pressure gradient becomes unfavorable, in practice the boundary layer separates – a phenomenon that cannot be described with inviscid flow.

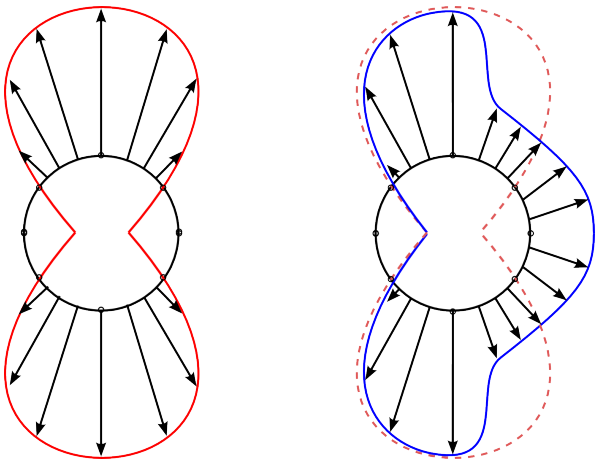

Figure 8.8 – Pressure distribution (relative to the far-flow pressure) on the surface of a cylinder, with flow from left to right. On the left is the potential flow case, purely symmetrical. On the right (in blue) is a measurement made at a high Reynolds number. Boundary layer separation occurs on the second half of the cylinder, which prevents the recovery of leading-edge pressure values, and increases drag.

Figure CC-BY-SA *Commons User:BoH & Olivier Cleynen*

8.6.2 Circulating cylinder

We now proceed to an extraordinary hack on the previous flow by adding to it an irrotational vortex of stream function $\psi = -\frac{\Gamma}{2\pi} \ln r$. The overall flow field becomes:

$$\psi = U \sin\theta \left(r - \frac{R^2}{r} \right) - \frac{\Gamma}{2\pi} \ln r \tag{8/45}$$

With this function, several key characteristics of the flow field can be obtained.

The first is the velocity field at the cylinder surface:

$$u_r|_{r=R} = 0 \tag{8/46}$$

$$u_\theta|_{r=R} = -2U \sin\theta + \frac{\Gamma}{2\pi R} \tag{8/47}$$

and we immediately notice that the velocity distribution is no longer symmetrical with respect to the horizontal axis (fig. 8.9): the fluid is deflected, and so there will be a net force on the cylinder.

The position of the stagnation points can be determined by setting $u_\theta = 0$ in eq. 8/47:

$$\theta_{\text{stagnation}} = \sin^{-1}\left(\frac{\Gamma}{4\pi R\, U} \right) \tag{8/48}$$

This time, the net pressure forces on the cylinder have changed:

$$\frac{F_{\text{net},x}}{L} = -\int_0^{2\pi} p_s \cos\theta \, R \, \mathrm{d}\theta = 0 \tag{8/49}$$

$$\frac{F_{\text{net},y}}{L} = -\int_0^{2\pi} p_s \sin\theta \, R \, \mathrm{d}\theta = -\rho \, U \, \Gamma \tag{8/50}$$

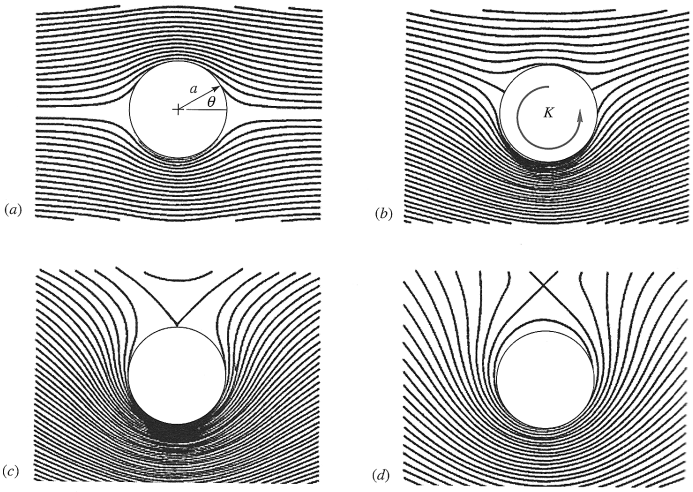

Figure 8.9 – The addition of an irrotational vortex on top of the cylinder flow described in fig. 8.7 distorts the flow field and it becomes asymmetrical: a lift force is developed, which depends directly on the circulation Γ.

Figure © White 2008 [9]

We thus find out that **the drag is once again zero** —as for any potential flow— but that **lift occurs** which is proportional to the free-stream velocity U and to the circulation Γ.

In practice, such a flow can be generated by spinning a cylindrical part in a uniform flow. A lateral force is then obtained, which can be used as a propulsive or sustaining force. Several boats and even an aircraft have been used in practice to demonstrate this principle. Naturally, flow separation from the cylinder profile and the high shear efforts generated on the surface cause real flows to differ from the ideal case described here, and it turns out that rotating cylinders are a horribly uneconomical and unpractical way of generating lift.

8.7 Modeling lift with circulation

Fluid flow around cylinders may have little appeal for the modern student of fluid mechanics, but the methodology above has been taken much further. With further mathematical manipulation called *conformal mapping*, potential flow can be used to described flow around geometrical shapes such as airfoils (fig. 8.10). Because the flow around such streamlined bodies usually does not feature boundary layer separation, the predicted flow fields everywhere but in the close vicinity of the solid surface are accurately predicted.

There again, it is observed that regardless of the constructed geometry, no lift can be modeled unless circulation is also added within the flow. The amount of circulation needed so that results may correspond to experimental observations is found by increasing it progressively until the the rear stagnation point reaches the rear trailing edge of the airfoil, a condition known as the *Kutta condition*. Regardless of the amount of circulation added, potential flow remains entirely reversible, both in a cinematic and a thermodynamic sense: thus care must be taken in the model set-up to make sure the model is realistic (fig. 8.11).

It is then observed in general that *any* dynamic lift generation can be modeled as the superposition of a free-stream flow and a circulation effect (fig. 8.12).

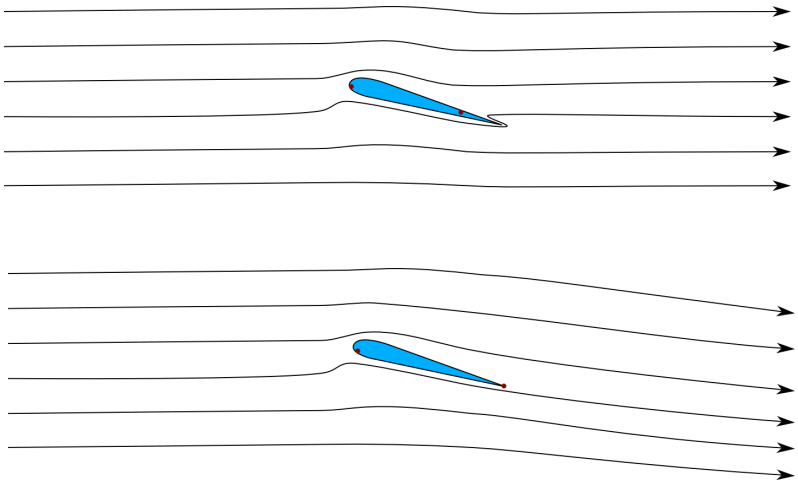

Figure 8.10 – Potential flow around an airfoil without (top) and with (bottom) circulation. Much like potential flow around a cylinder, potential flow around an airfoil can only result in a net vertical force if an irrotational vortex (with circulation Γ) is added on top of the flow. Only one value for Γ will generate a realistic flow, with the rear stagnation point coinciding with the trailing edge, a occurrence named *Kutta condition*.

Figure CC-0 o.c.

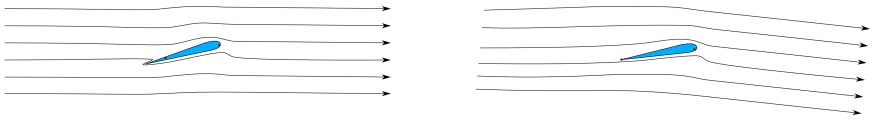

Figure 8.11 – Potential flow allows all velocities to be inverted without any change in the flow geometry. Here the flow around an airfoil is reversed, displaying unphysical behavior.

Figure CC-0 o.c.

With such a tool, potential flow becomes an extremely useful tool, mathematically and computationally inexpensive, in order to model and understand the cause and effect of dynamic lift in fluid mechanics. In particular, it has been paramount in the description of aerodynamic lift distribution over aircraft wing surfaces (fig. 8.13), with a concept called the Lifting-line theory.

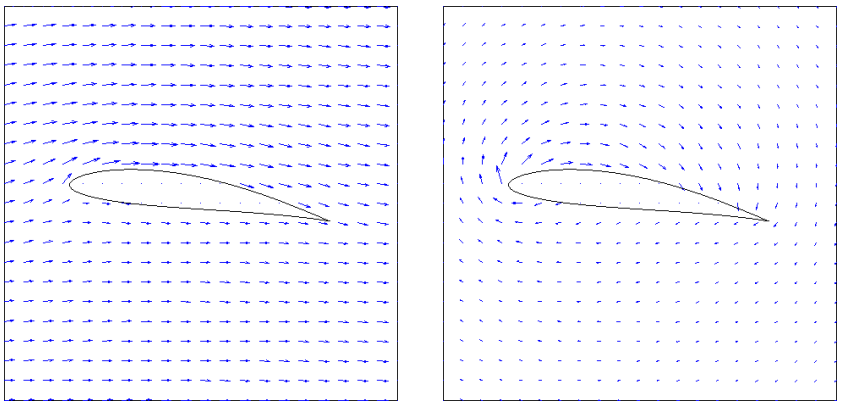

Figure 8.12 – A numerical model of flow around an airfoil. In the left figure, the velocity vectors are represented relative to a stationary background. In the right figure, the velocity of the free-stream flow has been subtracted from each vector, bringing the circulation phenomenon into evidence.

Figures 1 & 2 CC-BY-SA *by en:Wikipedia User:Crowsnest*

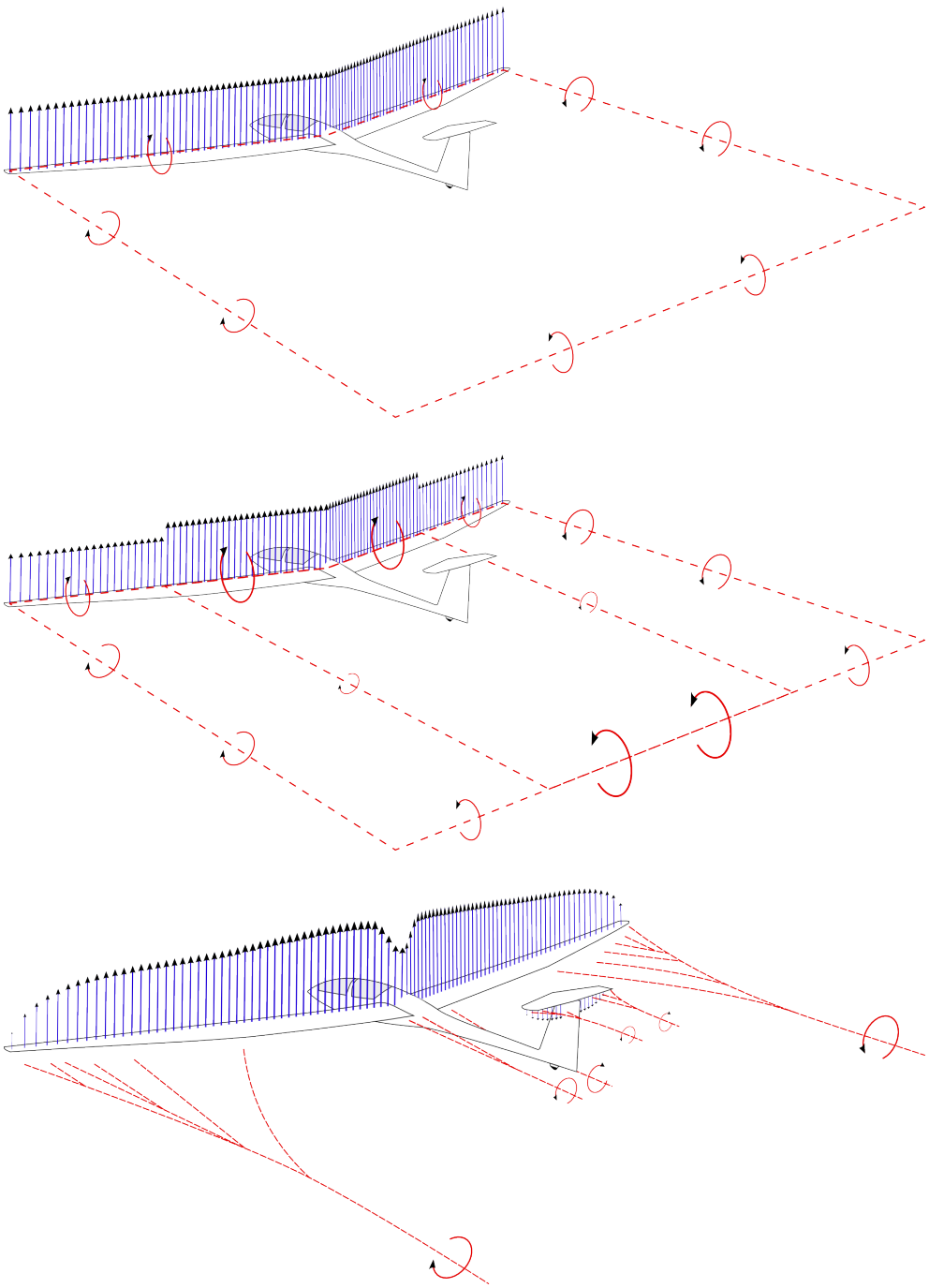

Figure 8.13 – From top to bottom, the lift distribution over the wings of a glider is modeled with increasingly complex (and accurate) lift and circulation distributions along the span. The Lifting-line theory is a method associating each element of lift with a certain amount of circulation. The effect of each span-wise change of circulation is then mapped onto the flow field as a trailing vortex.

Figures 1, 2 & 3 CC-BY-SA *Olivier Cleynen*

Fluid Mechanics
Exercise sheet 8 – Creeping and inviscid flows

last edited June 12, 2016

These lecture notes are based on textbooks by White [9], Çengel & al.[12], and Munson & al.[14].

Except otherwise indicated, we assume that fluids are Newtonian, and that:
$\rho_{\text{water}} = 1\,000\,\text{kg m}^{-3}$; $p_{\text{atm.}} = 1\,\text{bar}$; $\rho_{\text{atm.}} = 1{,}225\,\text{kg m}^{-3}$; $T_{\text{atm.}} = 11{,}3\,^{\circ}\text{C}$; $\mu_{\text{atm.}} = 1{,}5 \cdot 10^{-5}\,\text{N s m}^{-2}$;
$g = 9{,}81\,\text{m s}^{-2}$. Air is modeled as a perfect gas ($R_{\text{air}} = 287\,\text{J K}^{-1}\,\text{kg}^{-1}$; $\gamma_{\text{air}} = 1{,}4$; $c_{p\text{air}} = 1\,005\,\text{J kg}^{-1}\,\text{K}^{-1}$).

In a highly-viscous (creeping) steady flow, the drag F_{D} exerted on a spherical body of diameter D at by flow at velocity V_∞ is quantified as:

$$F_{\text{D sphere}} = 3\pi\mu V_\infty D \tag{8/4}$$

8.1 Volcanic ash from the Eyjafjallajökull

Çengel & al. [12] E10.2

In 2010, a volcano with a complicated name and unpredictable mood decided to ground the entire European airline industry for five days.

We consider a microscopic ash particle released at very high altitude ($-50\,^{\circ}\text{C}$, 0,55 bar, $1{,}474 \cdot 10^{-5}\,\text{N s m}^{-2}$). We model it as a sphere with 50 µm diameter. The density of volcanic ash is $1\,240\,\text{kg m}^{-3}$.

1. What is the terminal velocity of the particle?
2. Will this terminal velocity increase or decrease as the particle progresses towards the ground? (give a brief, qualitative answer)

8.2 Water drop

Çengel & al. [12] 10-21

A rainy day provides yet another opportunity for exploring fluid dynamics (fig. 8.14). A water drop with diameter 42,4 µm is falling through air at 25 °C and 1 bar.

1. Which terminal velocity will it reach?
2. Which velocity will it reach once its diameter will have doubled?

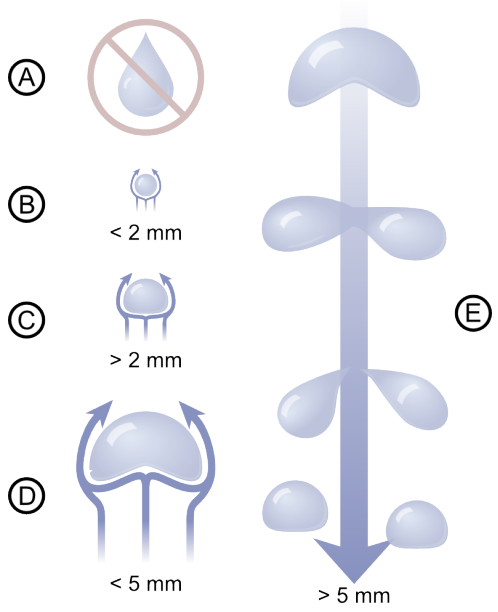

Figure 8.14 – A sketched diagram showing the geometry of water drops of various sizes in free fall. When their diameter is lower than 2 mm, water drops are approximately spherical (B). As they grow beyond this size, their shape changes and they eventually break-up (C-E). They never display the "classical" shape displayed in A, which is caused only by surface tension effects when they drip from solid surfaces.

Figure CC-BY-SA *by Ryan Wilson*

8.3 Hangar roof

based on White [9] P8.54

Certain flows in which both compressibility and viscosity effects are negligible can be described using the potential flow assumption (the hypothesis that the flow is everywhere irrotational). If we compute the two-dimensional laminar steady fluid flow around a cylinder profile, we obtain the velocities in polar coordinates as:

$$u_r = \frac{1}{r}\frac{\partial \psi}{\partial \theta} = U\cos\theta\left(1 - \frac{R^2}{r^2}\right) \tag{8/37}$$

$$u_\theta = -\frac{\partial \psi}{\partial r} = -U\sin\theta\left(1 + \frac{R^2}{r^2}\right) \tag{8/38}$$

where the origin ($r = 0$) is at the center of the cylinder profile;
θ is measured relative to the free-stream velocity vector;
U is the incoming free-stream velocity;
and R is the (fixed) cylinder radius.

Based on this model, in this exercise, we study the flow over a hangar roof.

Wind with a nearly-uniform velocity $U = 100\,\mathrm{km\,h^{-1}}$ is blowing across a 50 m-long hangar with a semi-cylindrical geometry, as shown in fig. 8.15. The radius of the hangar is $R = 20\,\mathrm{m}$.

1. If the pressure inside the hangar is the same as the pressure of the faraway atmosphere, and if the wind closely follows the hangar roof geometry (without any flow separation), what is the total lift force on the hangar?
(hint: we accept that $\int \sin^3 x\,\mathrm{d}x = \frac{1}{3}\cos^3 x - \cos x + k$).

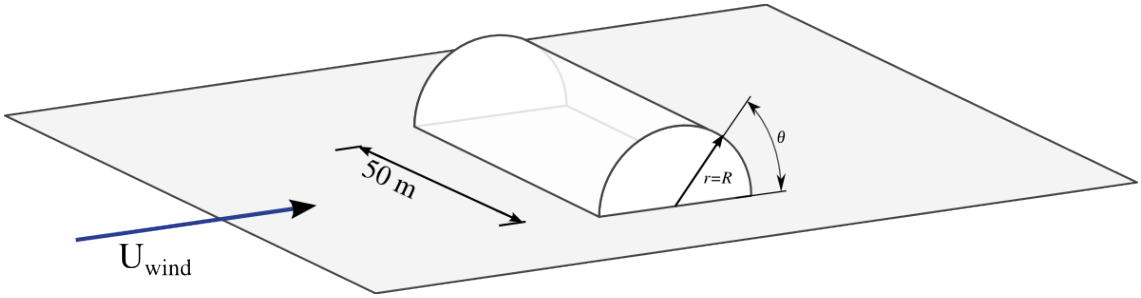

Figure 8.15 – A semi-cylindrical hangar roof. Wind with uniform velocity U flows perpendicular to the cylinder axis.

Figure CC-0 o.c.

2. At which position on the roof could we drill a hole to negate the aerodynamic lift force?

3. Propose two reasons why the aerodynamic force measured in practice on the hangar roof may be lower than calculated with this model.

8.4 Cabling of the Wright Flyer

derived from Munson & al. [14] 9.106

The *Wright Flyer I*, the first powered and controlled aircraft in history, was subjected to multiple types of drag. We have already studied viscous friction on its thin wings in exercise 7.4. The data in figure 8.16 provides the opportunity to quantify drag due to pressure.

A network of metal cables with diameter 1,27 mm criss-crossed the aircraft in order to provide structural rigidity. They were positioned perpendicularly to the air flow, which came at 40 $\mathrm{km\,h^{-1}}$. The total cable length was approximately 60 m.

What was the drag generated by the cables?

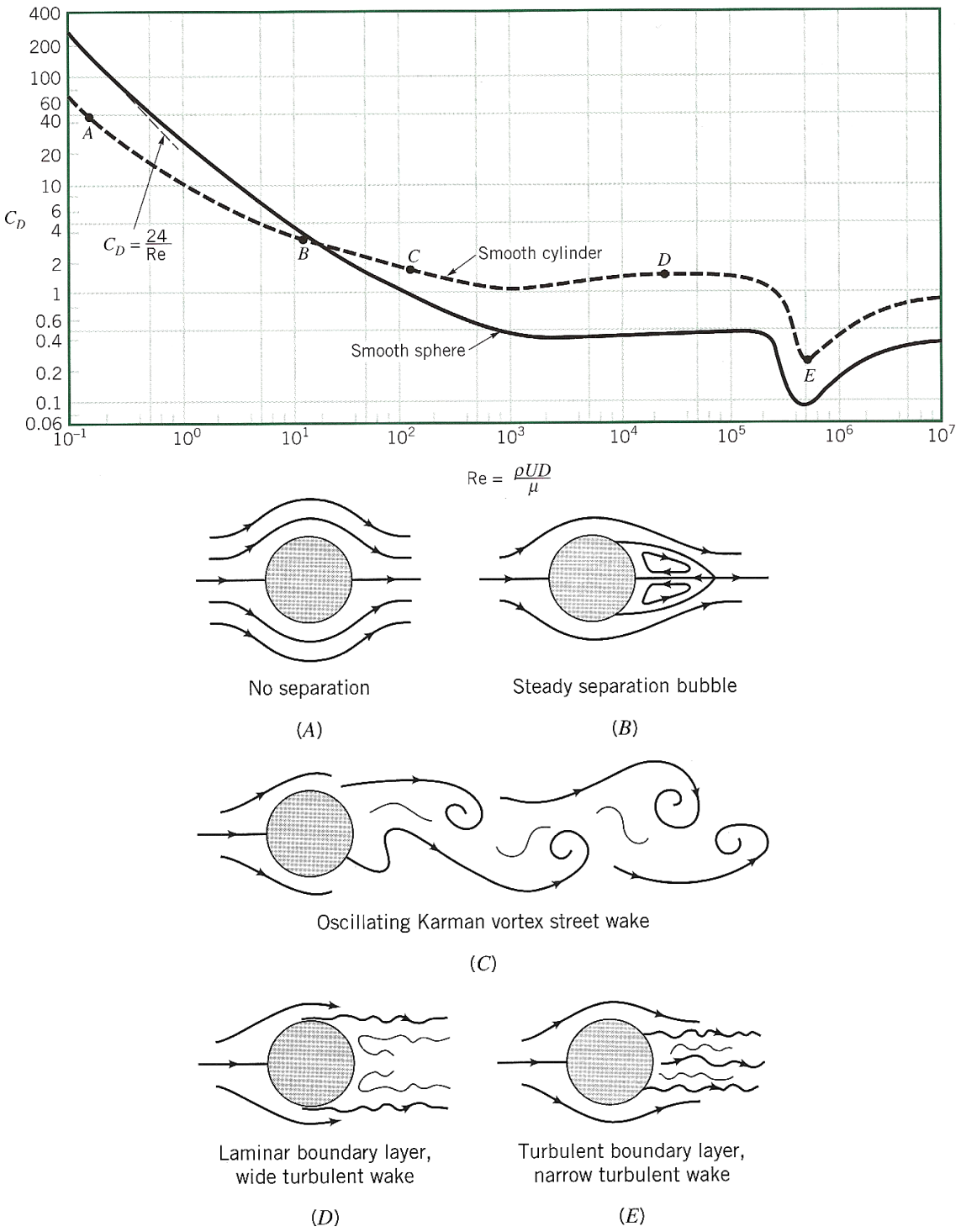

Figure 8.16 – Experimental measurements of the drag coefficient applying to a cylinder and to a sphere as a function of the diameter-based Reynolds number $[\mathrm{Re}]_D$, shown together with schematic depictions of the flow around the cylinder. By convention, the *drag coefficient* $C_\mathrm{D} \equiv C_{F\,\mathrm{D}} \equiv \frac{F_\mathrm{D}}{\frac{1}{2}\rho S U^2}$ (eq. 6/2 p.118) compares the drag force F_D with the frontal area S.

Both figures © from Munson & al.[14]

8.5 Ping pong ball

Munson & al. [14] E9.16

A series of experiments is conducted in a wind tunnel on a large cast iron ball with a smooth surface; the results are shown in fig. 8.17. These measurement data are used to predict the behavior of a ping ping ball. Table tennis regulations constrain the mass of the ball to 2,7 g and its diameter to 40 mm.

1. Is it possible for a ball thrown at a speed of 50 $\mathrm{km\,h^{-1}}$ to have a perfectly horizontal trajectory?
2. If so, what would be its deceleration?
3. How would the drag and lift applying on the ball evolve if the air viscosity was progressively decreased to zero?

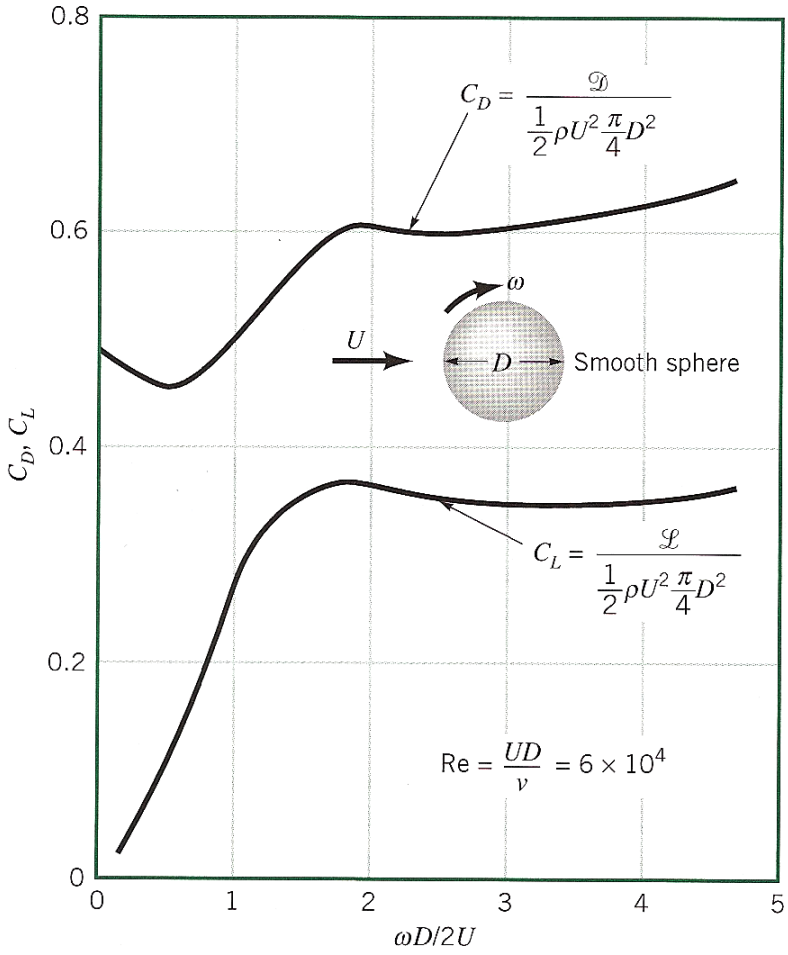

Figure 8.17 – Experimental measurements of the lift and drag coefficients applying on a rotating sphere in an steady uniform flow.

Figure © from Munson & al.[14]

8.6 Lift on a symmetrical object

non-examinable

Briefly explain (e.g. with answers 30 words or less) how lift can be generated on a sphere or a cylinder,

- with differential control boundary layer control;
- with the effect of rotation.

Draw a few streamlines in a two-dimensional sketch of the phenomenon.

8.7 Air flow over a wing profile

Non-examinable. From Munson & al. [14] 9.109

The characteristics of a thin, flat-bottomed airfoil are examined by a group of students in a wind tunnel. The first investigations focus on the boundary layer, and the research group evaluate the boundary layer thickness and make sure that it is fully attached.

Once this is done, the group proceeds with speed measurements all around the airfoil. Measurements of the longitudinal speed u just above the boundary layer on the top surface are tabulated below:

x/c (%)	y/c (%)	u/U
0	0	0
2,5	3,72	0,971
5	5,3	1,232
7,5	6,48	1,273
10	7,43	1,271
20	9,92	1,276
30	11,14	1,295
40	10,49	1,307
50	10,45	1,308
60	9,11	1,195
70	6,46	1,065
80	3,62	0,945
90	1,26	0,856
100	0	0,807

On the bottom surface, the speed is measured as being constant ($u = U$) to within experimental error.

What is the lift coefficient on the airfoil?

8.8 Flow field of a tornado

Non-examinable. From Çengel & al. [12] E9-5, E9-14 & E10-3

The continuity and Navier-Stokes equations for incompressible flow written in cylindrical coordinates are as follows:

$$\rho\left[\frac{\partial v_r}{\partial t}+v_r\frac{\partial v_r}{\partial r}+\frac{v_\theta}{r}\frac{\partial v_r}{\partial \theta}-\frac{v_\theta^2}{r}+v_z\frac{\partial v_r}{\partial z}\right] = \rho g_r-\frac{\partial p}{\partial r}+\mu\left[\frac{1}{r}\frac{\partial}{\partial r}\left(r\frac{\partial v_r}{\partial r}\right)-\frac{v_r}{r^2}+\frac{1}{r^2}\frac{\partial^2 v_r}{(\partial\theta)^2}-\frac{2}{r^2}\frac{\partial v_\theta}{\partial\theta}+\frac{\partial^2 v_r}{(\partial z)^2}\right] \tag{8/51}$$

$$\rho\left[\frac{\partial v_\theta}{\partial t}+v_r\frac{\partial v_\theta}{\partial r}+\frac{v_\theta}{r}\frac{\partial v_\theta}{\partial \theta}+\frac{v_r v_\theta}{r}+v_z\frac{\partial v_\theta}{\partial z}\right] = \rho g_\theta-\frac{1}{r}\frac{\partial p}{\partial\theta}+\mu\left[\frac{1}{r}\frac{\partial}{\partial r}\left(r\frac{\partial v_\theta}{\partial r}\right)-\frac{v_\theta}{r^2}+\frac{1}{r^2}\frac{\partial^2 v_\theta}{(\partial\theta)^2}+\frac{2}{r^2}\frac{\partial v_r}{\partial\theta}+\frac{\partial^2 v_\theta}{(\partial z)^2}\right] \tag{8/52}$$

$$\rho\left[\frac{\partial v_z}{\partial t}+v_r\frac{\partial v_z}{\partial r}+\frac{v_\theta}{r}\frac{\partial v_r}{\partial \theta}+v_z\frac{\partial v_z}{\partial z}\right] = \rho g_z-\frac{\partial p}{\partial z}+\mu\left[\frac{1}{r}\frac{\partial}{\partial r}\left(r\frac{\partial v_z}{\partial r}\right)+\frac{1}{r^2}\frac{\partial^2 v_z}{(\partial\theta)^2}+\frac{\partial^2 v_z}{(\partial z)^2}\right] \tag{8/53}$$

$$\frac{1}{r}\frac{\partial r u_r}{\partial r}+\frac{1}{r}\frac{\partial u_\theta}{\partial\theta}+\frac{\partial u_z}{\partial z}=0 \tag{8/54}$$

In this exercise, we are interested in solving the pressure field in a simplified description of a tornado. For this, we consider only a horizontal layer of the flow, and we consider that all properties are independent of the altitude z and of the time t.

We start by modeling the tornado as a vortex imparting an angular velocity such that:

$$u_\theta=\frac{\Gamma}{2\pi r} \tag{8/55}$$

in which Γ is the *circulation* (measured in s^{-1}) and remains constant everywhere.

1. What form must the radial velocity u_r take in order to satisfy continuity?

Among all the possibilities for u_r, we choose the simplest in our study, so that:

$$u_r=0 \tag{8/56}$$

all throughout the tornado flow field.

2. What is the pressure field throughout the horizontal layer of the tornado?

The flow field described above becomes unphysical in the very center of the tornado vortex. Indeed, our model for u_θ is typical of an *irrotational vortex*, which, like all irrotational flows, is constructed under the premise that the flow is inviscid. However, in the center of the vortex, we are confronted with high velocity gradients over very small distances: viscous effects can no longer be neglected and our model breaks down.

It is observed that in most such vortices, a *vortex core* region forms that rotates just like a solid cylindrical body. This flow is *rotational* and its governing equations result in a realistic pressure distribution.

3. What is the pressure field within the rotational core of the tornado?
   Make a simple sketch showing the pressure distribution as a function of radius throughout the entire tornado flow field.

4. *[An opening question for curious students]*
   What is the basic mechanism of *vortex stretching*? How would it modify the flow field described here?

Answers

8.1 1) At terminal velocity, the weight of the sphere equals the drag. This allows us to obtain $U = g\rho_{\text{sphere}}\frac{D^2}{18\mu} = 0{,}1146\,\mathrm{m\,s^{-1}}$: unbearably slow when you are stuck in an airport! With U, check that the Reynolds number indeed corresponds to creeping flow: $[\mathrm{Re}]_D = 0{,}334$.

8.2 Same as previous exercise: $U_1 = 4{,}578 \cdot 10^{-2}\,\mathrm{m\,s^{-1}}$ and $U_2 = 0{,}183\,\mathrm{m\,s^{-1}}$, with Reynolds numbers of 0,113 and 0,906 respectively (thus creeping flow hypothesis valid).

8.3 1) express roof pressure as a function of θ using eq. 8/42 p.166 on eq. 8/38, then integrate the vertical component of force due to pressure: $F_{\text{L roof}} = 1{,}575\,\mathrm{MN}$.
2) $\theta|_{F=0} = 54{,}7^\circ$

8.4 A simple reading gives $F_{\text{D}} = 6{,}9\,\mathrm{N}$, $\dot{W} = 76\,\mathrm{W}$.

8.5 Yes — a reading gives $\omega = 83\,\mathrm{rev/s}$.

Fluid Mechanics
Chapter 9 – Compressible flow

last edited June 20, 2016

These lecture notes are based on textbooks by White [9], Çengel & al.[12], and Munson & al.[14].

9.1 Motivation

In this chapter we begin the exploration of compressible flow: those in which density varies significantly. This study should allow us to answer two questions:

- What are the mechanisms behind reversible compressible flow?
- What is a shock wave, and how does it influence a flow?

9.2 Compressibility and its consequences

9.2.1 Problem description

Ever since we have begun describing fluid flow in an extensive manner in chapter 4, we have restricted ourselves to incompressible flows — those in which the fluid density ρ is uniform and constant. Now, ρ becomes one additional unknown property field.

In cases where we wish to calculate e.g. water temperature in a heat transfer case, or species concentration in a reacting flow, it is possible to first solve for the flow, and then solve for those particular property fields within the solution; thus the additional unknowns are solved separately with additional equations.

The mathematical treatment of density, however, is much worse, because ρ appears in the momentum and mass conservation equations. Density directly affects the velocity fields, and so we have solve for ρ, p and $\vec{V}$ *simultaneously*.

From a physical point of view, compressibility brings two new effects:

- Density changes in fluids translate into large changes in fluid mechanical energy; these can be come very large in comparison to other forms of fluid energy, in particular kinetic energy. When ρ varies, fluids "perform work upon themselves", storing and spending this work energy in terms of kinetic energy changes, and irreversible losses as heat transfer.
- When density is allowed to vary, pressure travels at *finite velocity* within the fluid — one could say that the fluid becomes appreciably "squishy". The delay resulting from this finite pressure propagation velocity becomes very significant if the fluid velocity is high, and it may even prevent the upstream propagation of pressure waves altogether.

In this chapter, we wish to quantify both of those effects. By now, after eight chapters already where ρ was just an input constant, the reader should readily agree we have no hope of coming up with a general solution to compressible flow. Nevertheless, it is possible to reproduce and quantify the most important aspects of compressibility effects with relatively simple, one-dimensional air flow cases — and this will suffice for us in this last exploratory chapter.

9.2.2 The speed of pressure

We start by focusing on the *speed of pressure*. In compressible fluids, pressure changes propagate with a velocity that increases with the magnitude of the pressure change. When this magnitude tends to zero (and the pressure wave reduces to that of a weak sound wave, with fully-reversible fluid compression and expansion) then the velocity tends to a given velocity which we name *speed of sound* and note a. At ambient conditions, this velocity is approximately 1 000 km/h in air and roughly 5 000 km/h in water.

Let us create a small pressure change inside a static fluid, and then travel along with the pressure wave. As we follow the wave, traveling from right to left, we perceive fluid movement from left to right (fig. 9.1). We construct a small control volume encompassing and moving with the wave — at the speed of sound a.

Control volume fluid flow analysis does not frighten us anymore. From mass conservation (eq. 3/5 p.56) we write:

$$\rho a A = (\rho + \mathrm{d}\rho)(a - \mathrm{d}V)A \tag{9/1}$$

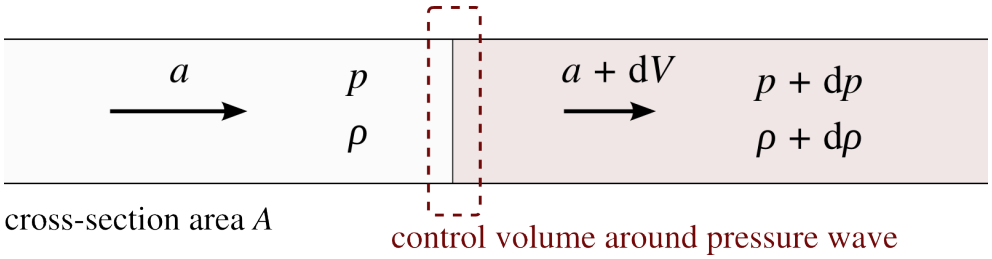

Figure 9.1 – An infinitesimal pressure-difference wave is represented traveling from right to left inside a stationary fluid, in a one-dimensional tube. From the point of view of a control volume attached to (and traveling with) the wave, the flow is from left to right.

Figure CC-0 o.c.

This equation 9/1 relates the density change across the wave to the velocity change between inlet and outlet. Re-arranging, and focusing only on the case where the pressure wave is extremely weak (as are sound waves in practice), we see the product $\mathrm{d}\rho\,\mathrm{d}V$ vanish and obtain:

$$\begin{aligned} \rho a &= \rho a - \rho\,\mathrm{d}V + a\,\mathrm{d}\rho - \mathrm{d}\rho\,\mathrm{d}V \\ \rho\,\mathrm{d}V &= a\,\mathrm{d}\rho \end{aligned} \tag{9/2}$$

In equation 9/2, which relates the speed of sound a to the density ρ, we would now like to eliminate the $\mathrm{d}V$ term. For this, we turn to the control volume momentum equation (eq: 3/8 p.57):

$$\begin{aligned} F_{\text{net}} &= -\dot{m}_{\text{in}} V_{\text{in}} + \dot{m}_{\text{out}} V_{\text{out}} \\ pA - (p + \mathrm{d}p)A &= -\rho a A a + (\rho - \mathrm{d}\rho)(a - \mathrm{d}V)A(a - \mathrm{d}V) \\ -\mathrm{d}pA &= \rho a A\,[-a + (a - \mathrm{d}V)] \\ \frac{\mathrm{d}p}{a} &= \rho\,\mathrm{d}V \end{aligned} \tag{9/3}$$

We can now combine eqs. (9/2) and (9/3) to obtain:

$$a = \sqrt{\frac{\mathrm{d}p}{\mathrm{d}\rho}} \tag{9/4}$$

This can be generalized for any pressure wave, and we state that

$$a = \sqrt{\left.\frac{\partial p}{\partial \rho}\right|_{s=\text{cst.}}} \tag{9/5}$$

where the s = cst. subscript indicates that entropy s is constant.

So now, we see that in a fluid the speed of sound –the velocity of pressure waves when they travel in a reversible (constant-entropy) manner— is the square root of the derivative of pressure with respect to density. This allows us to compare it to another term, the *bulk modulus of elasticity* K, which represents the differential amount of pressure that one has to apply on a body to see its density increase by a certain percentage:

$$K \equiv \frac{\mathrm{d}p}{\frac{\mathrm{d}\rho}{\rho}} \tag{9/6}$$

where K is expressed in Pa.

Inserting eq. 9/6 into eq. 9/5, we obtain a relationship which we had introduced already in chapter 6 (as eq. 6/20 p.126):

$$a = \sqrt{\frac{K_{s=\text{cst.}}}{\rho}} \tag{9/7}$$

With this equation 9/7 we see that in any fluid, the square of the speed of sound increases inversely proportionally to the density and proportionally to the modulus of elasticity (the “hardness”) of the fluid.

9.2.3 The measure of compressibility

The most useful measure of compressibility in fluid mechanics is the Mach number, which we already defined (with eq. 0/4 p.11) as:

$$[\mathrm{Ma}] \equiv \frac{V}{a} \tag{9/8}$$

As we saw in chapter 6 (§6.4.3 p.126), $[\mathrm{Ma}]^2$ is proportional to the ratio of net force to elastic force on fluid particles: at high Mach numbers the forces related to the compression and expansion of the fluid dominate its dynamics.

Not all compressible flows feature high Mach numbers. In large-scale atmospheric weather for example, air flows mush slower than the speed of sound yet large density changes can occur because of the vertical (static) pressure gradient. The same is true in low-speed centrifugal machines because of centrifugal pressure gradients. In this chapter, we choose to focus on the simplest of compressible flows: one-directional gas flows with Mach numbers approaching or exceeding 1.

9.3 Thermodynamics of isentropic flow for a perfect gas

9.3.1 Principle

When a gas is compressed or expanded, its pressure and temperature vary together with its density. Before we consider the *dynamics* of such phenomena, we need a robust model to relate those properties. This is the realm of *Thermodynamics*.

In short, from a macroscopic point of view, a gas behaves as a mechanical spring (fig. 9.2): energy as work is needed to compress it, and energy as work is recovered when it expands. Three important points must be made regarding these compressions and expansions:

1. When gases are heated, the work transfers are increased; conversely they are decreased when the gas is cooled (fig. 9.4). Cases where no heat transfer occurs are called *adiabatic*;
2. The temperature of gases tends to increase when they are compressed, and tends to decrease when they expand, *even when no heat transfer occurs* (fig. 9.3);

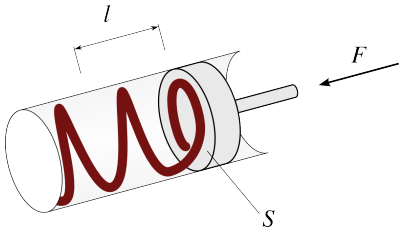

Figure 9.2 – When they are compressed or expanded, the behavior of fluids can be modeled as if they were “fragile” mechanical springs: extra energy is lost during compressions, and less energy is recovered during expansions, when those evolutions are sudden.

Figure CC-BY-SA *Olivier Cleynen*

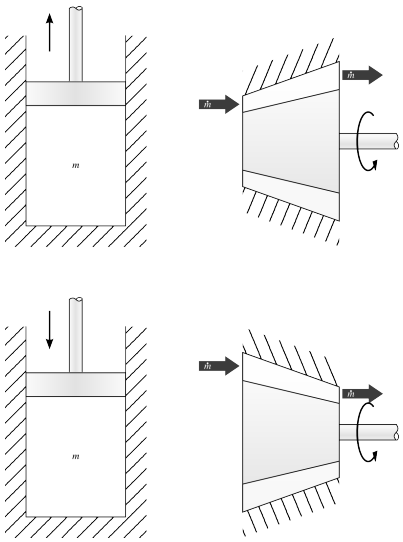

Figure 9.3 – When no heat transfer occurs, the a compression or expansion is said to be *adiabatic*. The temperature of fluids can still vary significantly because of the compression or expansion. When adiabatic evolutions are infinitely smooth, they are termed *isentropic*.

Figure CC-0 *Olivier Cleynen*

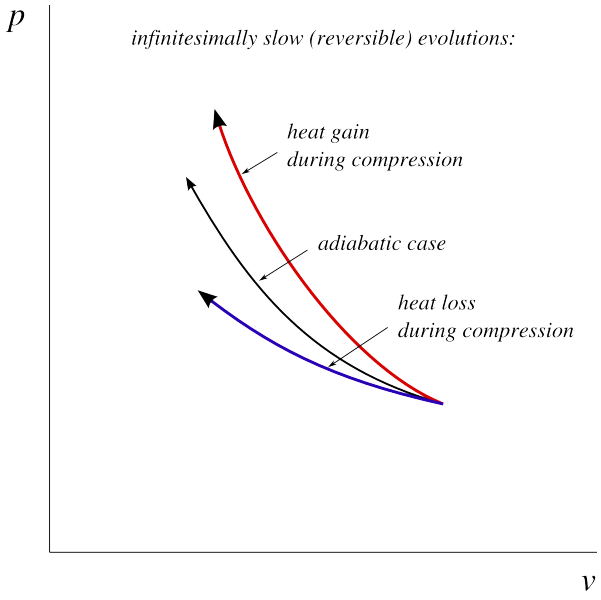

Figure 9.4 – Pressure-volume diagram of a perfect gas during a compression. When the fluid is heated up, more work is required; when it is cooled, less work is required. Opposite trends are observed during expansions.

Figure CC-0 *Olivier Cleynen*

3. A gas behaves as a "fragile" spring: the faster a compression occurs, and the more work is required to perform it. Conversely, the faster an expansion occurs, and the less work is recovered from it. Cases where evolutions occur infinitely slowly are used as a reference for comparison: such cases are termed *reversible*. Cases where the evolution is both adiabatic and reversible are named *isentropic* (*iso-entropic*, because they occur at constant entropy).

9.3.2 Pressure, temperature, density and the speed of sound

The quantitative relations between pressure, temperature and density of perfect gas during isentropic evolutions are classical results in the study of thermodynamics. In this section, we wish to re-write them with particular focus placed on the speed of sound and the Mach number. The goal is to arrive to eqs. equation 9/20 to equation 9/22, which we need in the upcoming sections to describe supersonic flow of gases.

Let us then focus on the isentropic evolutions of a perfect gas. It is known from the study of thermodynamics that in isentropic flow from a point 1 to a point 2, the properties of a perfect gas are related one to another by the relations:

$$\left(\frac{T_1}{T_2}\right) = \left(\frac{v_2}{v_1}\right)^{\gamma-1} \tag{9/9}$$

$$\left(\frac{T_1}{T_2}\right) = \left(\frac{p_1}{p_2}\right)^{\frac{\gamma-1}{\gamma}} \tag{9/10}$$

$$\left(\frac{p_1}{p_2}\right) = \left(\frac{v_2}{v_1}\right)^{\gamma} \tag{9/11}$$

for a perfect gas, during an isentropic (constant-entropy) evolution.

It follows from eq. 9/11 that in an isentropic evolution, a perfect gas behaves such that $p\rho^{-\gamma} = k = \text{cst.}$, which enables us to re-write equation 9/5 for a perfect gas as:

$$a = \sqrt{\left.\frac{\partial p}{\partial \rho}\right|_{s=\text{cst.}}} = \sqrt{k\gamma\rho^{\gamma-1}} = \sqrt{p\rho^{-\gamma}\gamma\rho^{\gamma-1}} = \sqrt{\gamma p\rho^{-1}}$$

The speed of sound in a perfect gas can therefore be expressed as:

$$a = \sqrt{\gamma RT} \tag{9/12}$$

$$[\text{Ma}] = \frac{V}{\sqrt{\gamma RT}} \tag{9/13}$$

for any evolution in a perfect gas.

Thus, in a perfect gas, the speed of sound depends only on the local temperature.

We now introduce the concept of *stagnation* or *total properties*, a measure of the total amount of specific energy possessed by a fluid particle at a given instant. They are the properties that the fluid would have if it was brought to

rest in an isentropic manner:

$$h_0 \equiv h + \frac{1}{2}V^2 \tag{9/14}$$

$$T_0 \equiv T + \frac{1}{c_p}\frac{1}{2}V^2 \tag{9/15}$$

$$h_0 = c_p T_0 \tag{9/16}$$

Using equation 9/13, we can re-write eq. (9/15) as:

$$\begin{aligned}\frac{T_0}{T} &= 1 + \frac{1}{c_p T}\frac{1}{2}V^2 = 1 + \frac{1}{\frac{\gamma R}{\gamma - 1}T}\frac{1}{2}V^2 \\ &= 1 + \left(\frac{\gamma - 1}{2}\right)\frac{V^2}{a^2} = 1 + \left(\frac{\gamma - 1}{2}\right)[\mathrm{Ma}]^2\end{aligned}$$

Eqs. (9/9) to (9/11) can thus be re-written to express the transition from flow condition to stagnation condition:

$$\left(\frac{T_0}{T}\right) = 1 + \left(\frac{\gamma - 1}{2}\right)[\mathrm{Ma}]^2 \tag{9/17}$$

$$\left(\frac{p_0}{p}\right) = \left[1 + \left(\frac{\gamma - 1}{2}\right)[\mathrm{Ma}]^2\right]^{\frac{\gamma}{\gamma - 1}} \tag{9/18}$$

$$\left(\frac{\rho_0}{\rho}\right) = \left[1 + \left(\frac{\gamma - 1}{2}\right)[\mathrm{Ma}]^2\right]^{\frac{1}{\gamma - 1}} \tag{9/19}$$

These three equations (9/17) to (9/19) relate, for any point inside the flow of a perfect gas, the local Mach number [Ma] as a function of the ratio of the local (current) property (T, p or ρ) to the local *total* property (T_0, p_0, ρ_0). These ratios are always inferior or equal to one, by definition.

Now, if now we define *critical conditions* as those that would occur if the fluid was exactly at [Ma] = 1, noting them with an asterisk, we can re-write eqs. (9/17) to (9/19) comparing stagnation properties to critical properties:

$$\left(\frac{T^*}{T_0}\right) = \frac{2}{\gamma + 1} \tag{9/20}$$

$$\left(\frac{p^*}{p_0}\right) = \left[\frac{2}{\gamma + 1}\right]^{\frac{\gamma}{\gamma - 1}} \tag{9/21}$$

$$\left(\frac{\rho^*}{\rho_0}\right) = \left[\frac{2}{\gamma + 1}\right]^{\frac{1}{\gamma - 1}} \tag{9/22}$$

Here, we compare the local total property (e.g. the total temperature T_0) to the value the property needs to have for the flow to be at sonic speed (e.g. the critical temperature T^*). This ratio does not depend at all on the fluid flow: it is merely a function of the (invariant) characteristics of the gas.

This is it! It is important to understand that nothing in this section describes a particular flow movement. We have merely derived a convenient tool expressing flow properties as a function of their stagnation properties and the local Mach number, which we shall put to good use further down.

9.4 Speed and cross-sectional area

Let us now go back to fluid dynamics. The last time we considered frictionless pipe flow, in chapter 5, we situation was rather simple. From the one-dimensional mass conservation equation, eq. 5/1:

$$\rho_1 V_1 A_1 = \rho_2 V_2 A_2 \tag{9/23}$$

it was possible to relate cross-sectional area A and velocity V easily. Now that ρ is also allowed to vary, the situation is decidedly more interesting.

We wish to let static, pressurized air accelerate as fast as possible: letting V increase at a cost of a decease in ρ according to the rules of an isentropic, steady expansion. We know however, that according to mass conservation, $\rho V A$ has to remain constant all along the acceleration, so that only one given nozzle geometry ($A = f(p,T)$) will permit the desired acceleration. How can we find this geometry?

We start from the conservation of mass inside our isentropic acceleration nozzle, and differentiating the terms:

$$\begin{aligned} \rho A V &= \text{cst.} \\ \ln\rho + \ln A + \ln V &= \text{cst.} \\ \frac{\mathrm{d}\rho}{\rho} + \frac{\mathrm{d}A}{A} + \frac{\mathrm{d}V}{V} &= 0 \end{aligned}$$

for any steady flow.

Let us set this equation 9/24 aside for a moment. During our isentropic expansion, the total energy of the fluid remains constant, thus the total specific enthalpy h_0 is constant,

$$h + \frac{V^2}{2} = \text{cst.}$$

and here also we differentiate, obtaining:

$$\mathrm{d}h + V\,\mathrm{d}V = 0 \tag{9/24}$$

In last relation, since the process is reversible and without external energy input, we can write the first term as $\mathrm{d}h = \mathrm{d}p/\rho$, yielding:

$$\begin{aligned} \frac{1}{\rho}\,\mathrm{d}p + V\,\mathrm{d}V &= 0 \\ \rho &= -\frac{\mathrm{d}p}{V\,\mathrm{d}V} \end{aligned} \tag{9/25}$$

for isentropic gas flow.

This expression of ρ is the relation we were after. Now, coming back to equation 9/24 and inserting eq. (9/25), we get:

$$\begin{aligned} \frac{\mathrm{d}\rho}{\rho} + \frac{\mathrm{d}A}{A} - \frac{\mathrm{d}\rho}{\mathrm{d}p} V\,\mathrm{d}V &= 0 \\ \frac{\mathrm{d}V}{V}\left[1 - \frac{\mathrm{d}\rho}{\mathrm{d}p}V^2\right] + \frac{\mathrm{d}A}{A} &= 0 \end{aligned}$$

In this last relation, since we are in an isentropic flow, we can insert an expression for the speed of sound, $a^2 = \left.\frac{\partial p}{\partial \rho}\right|_s$ derived from equation 9/5,

obtaining:

$$\frac{\mathrm{d}V}{V}\left[1-\frac{1}{a^2}V^2\right]+\frac{\mathrm{d}A}{A}=0$$
$$\frac{\mathrm{d}V}{V}\left[1-[\mathrm{Ma}]^2\right]+\frac{\mathrm{d}A}{A}=0$$

This leads us to the following equation relating area change and speed change in compressible gas flow:

$$\frac{\mathrm{d}V}{V}=\frac{\mathrm{d}A}{A}\frac{1}{[\mathrm{Ma}]^2-1} \qquad (9/26)$$

for isentropic, one-dimensional gas flow.

This equation 9/26 is one of the most stunning equations of fluid dynamics. It relates the change in flow cross-section area, $\mathrm{d}A$, to the change in speed $\mathrm{d}V$, for lossless flow. Let us examine how these two terms relate one to another, as displayed in figure 9.5:

- When $[\mathrm{Ma}] < 1$, the term $1/([\mathrm{Ma}]^2-1)$ is negative, and $\mathrm{d}A$ and $\mathrm{d}V$ are always of opposite sign: an increase in area amounts to a decrease in speed, and a decrease in area amounts to an increase in speed.
- When $[\mathrm{Ma}] > 1$, $\mathrm{d}A$ and $\mathrm{d}V$ have the same sign, which —perhaps disturbingly— means that an increase in area amounts to an *increase* in speed, and a decrease in area amounts to a decrease in speed.

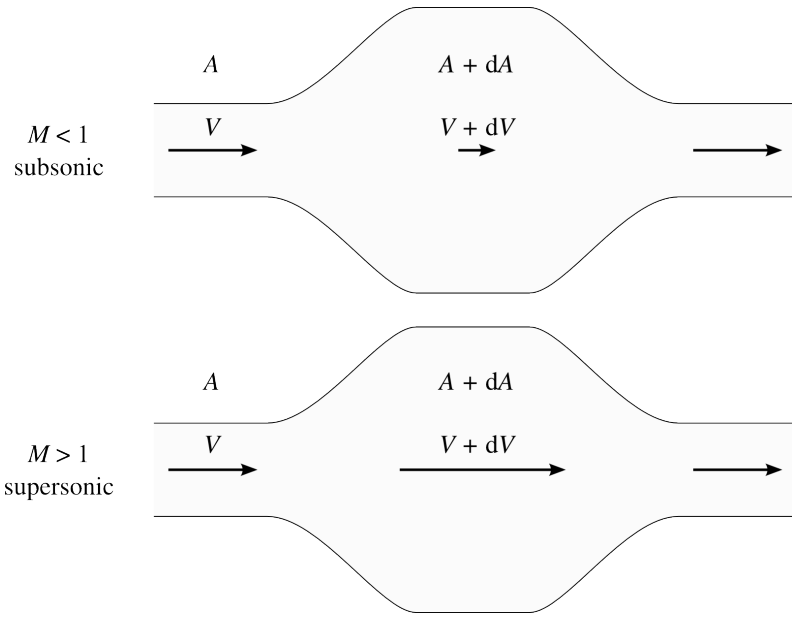

Figure 9.5 – Changes in nozzle cross-section area have opposite effects when the Mach number [Ma] is lower or greater than 1.
Note that because temperature changes as the gas compresses and expands, the local Mach number varies as the flow changes speed. It is thus possible for the flow to go from one regime to another during an expansion or compression. These effects are studied further down and described in figure 9.7 p.191.

Figure CC-0 o.c.

Thus, if we want to let a static, compressed fluid accelerate as fast as possible, we need a converging nozzle up to $[\mathrm{Ma}] = 1$, and a diverging nozzle onwards.

9.5 Isentropic flow in converging and diverging nozzles

The change of between the subsonic and supersonic flow regimes, by definition, occurs at Mach one. When the flow is isentropic, equation 9/26 above tells us that the [Ma] = 1 case *can only occur at a minimum area*.

Of course, there is no guarantee that a pipe flow will be able to become supersonic (fig. 9.6). For this, very large pressure ratios between inlet and outlet are required. Nevertheless, whichever the pressure ratio, according to eq. 9/26, a converging nozzle will only let an expanding fluid accelerate to Mach one (critical conditions). Changing the nozzle outlet area itself will not permit further acceleration unless an increase in nozzle area is generated beyond the critical point.

This is a surprising behavior. In a converging-only nozzle, increasing the inlet pressure increases the outlet velocity only up until [Ma] = 1 is reached at the outlet. From there on, further increases in inlet pressure have *no effect* on the outlet pressure, which remains fixed at $p_{\text{outlet}} = p^*$. The flow then reaches a maximum mass flow rate $\dot{m}_{\text{max}}$. This condition is called *choked flow*.

Once the flow is choked, adding a diverging section further down the nozzle may enable further acceleration, if the pressure ratio allows for it. Nevertheless, the pressure $p_{\text{T}} \equiv p_{\text{throat}}$ at the throat remains constant at $p_{\text{T}} = p^*$: from this point onwards, downstream conditions (in particular the pressure) are not propagated upstream anymore: the gas travels faster than the pressure waves inside it. With p_{T} still equal to the critical pressure p^*, the mass flow through the nozzle cannot exceed $\dot{m}_{\text{max}}$.

We can see, therefore, that it follows from equation 9/26 that *there exists a maximum mass flow for any duct*, which depends only on the stagnation properties of the fluid.

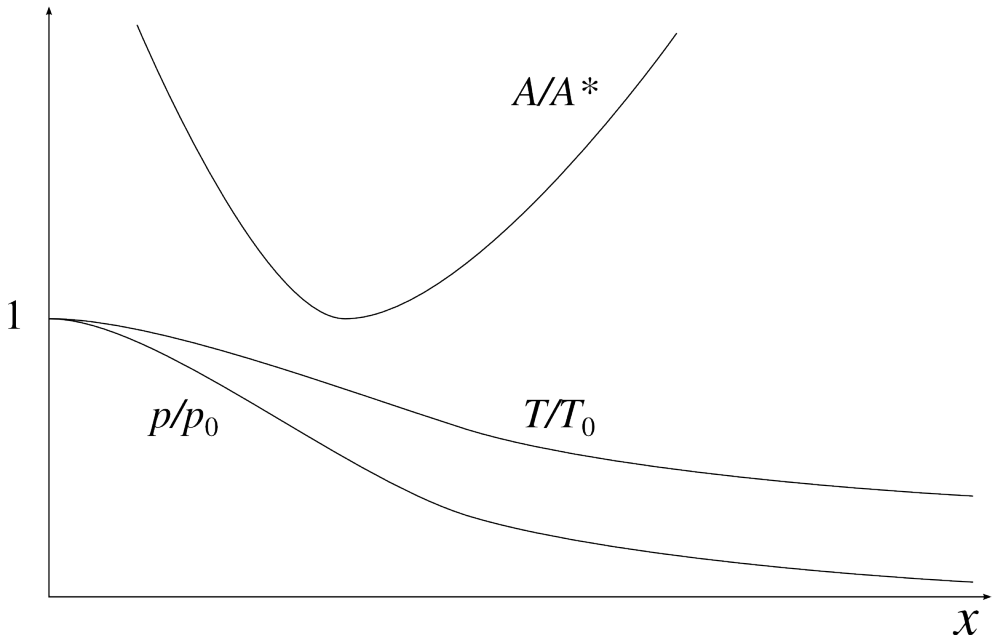

Figure 9.6 – Non-dimensionalized properties of a gas undergoing an isentropic (i.e. shock-less) expansion through a converging-diverging nozzle.

Figure CC-0 o.c.

The mass flow, which at any point in the duct has value:

$$\begin{aligned}\dot{m} &= \rho a A[\mathrm{Ma}] \\ &= \frac{p}{RT}\sqrt{\gamma RT}A[\mathrm{Ma}] \\ \dot{m} &= A[\mathrm{Ma}]p_0\sqrt{\frac{\gamma}{RT_0}}\left[1+\frac{(\gamma-1)[\mathrm{Ma}]^2}{2}\right]^{\frac{-\gamma-1}{2(\gamma-1)}} \qquad (9/27)\end{aligned}$$

and $\dot{m}$ will now reach a maximum when the flow is choked, i.e. reaches $[\mathrm{Ma}] = 1$ at the throat, where its properties will be $p^* = p_\mathrm{T}$, $T^* = T_\mathrm{T}$, and the area $A^* = A_\mathrm{T}$:

$$\dot{m}_{\max} = \left[\frac{2}{\gamma+1}\right]^{\frac{\gamma+1}{2(\gamma-1)}} A^* p_0\sqrt{\frac{\gamma}{RT_0}} \qquad (9/28)$$

A general description of the properties of a perfect gas flowing through a converging-diverging duct is given in figs. 9.6 and 9.7.

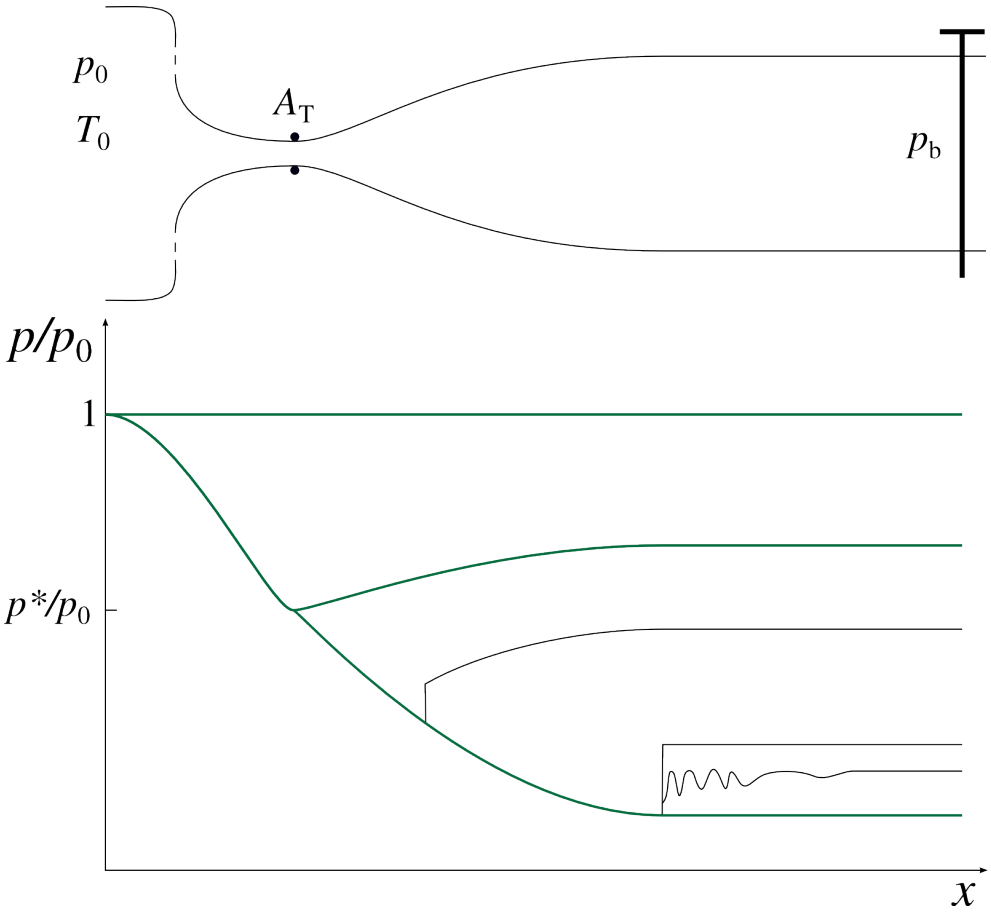

Figure 9.7 – The pressure of a gas attempting an isentropic expansion through a converging-diverging duct, represented as a function of distance for different values of outlet pressure p_b. The green curves show the reversible evolutions.
As long as the back pressure p_b is low enough, the flow is subsonic everywhere, and it remains reversible everywhere. When p_T reaches p^*, the flow downstream of the throat becomes supersonic. In that case, if the back pressure is low enough, a fully-reversible expansion will occur. If not, then a shock wave will occur and the flow will return to subsonic regime downstream of the shock.

9.6 The perpendicular shock wave

The movement of an object at supersonic speeds –or the supersonic flow over a stationary object, which produces the same effects– provokes pressure field changes that cannot propagate upstream. Thus, if a direction change or a pressure increase is required to flow past an obstacle, fluid particles will be subjected to very sudden changes. These localized changes are called *shock waves*.

The design of bodies moving at supersonic speeds usually focuses on ensuring pressure and direction changes that are very gradual, and at the limit (e.g. far away from a supersonic aircraft) these are very small.
The limiting case at the other side of the spectrum is that of the *normal shock wave*, the most loss-inducing (and simple!) type of shock wave. This will typically occur in front of a blunt supersonic body.

A perpendicular shock wave (fig. 9.8) is studied with the following hypothesis:

- It is a *constant energy* process;
- It it a *one-dimensional* process (i.e. the streamlines are all parallel to one another and perpendicular to the shock wave).

With these two hypothesis, we can compare the flow conditions upstream and downstream of a shock wave occurring in a tube using the continuity equation, which we wrote above as eq. 9/23:

$$\rho_1 A_1 V_1 = \rho_2 A_2 V_2 \tag{9/29}$$

The energy equation in this case shrinks down to:

$$T_{01} = T_{02} \tag{9/30}$$

Since, from equation 9/17, we have:

$$\frac{T_{01}}{T_1} = 1 + \left(\frac{\gamma - 1}{2}\right) [\mathrm{Ma}]_1^2$$
$$\frac{T_{02}}{T_2} = 1 + \left(\frac{\gamma - 1}{2}\right) [\mathrm{Ma}]_2^2$$

and given that $T_{01} = T_{02}$, dividing one by the other yields:

$$\frac{T_2}{T_1} = \frac{1 + \frac{\gamma-1}{2}[\mathrm{Ma}]_1^2}{1 + \frac{\gamma-1}{2}[\mathrm{Ma}]_2^2} \tag{9/31}$$

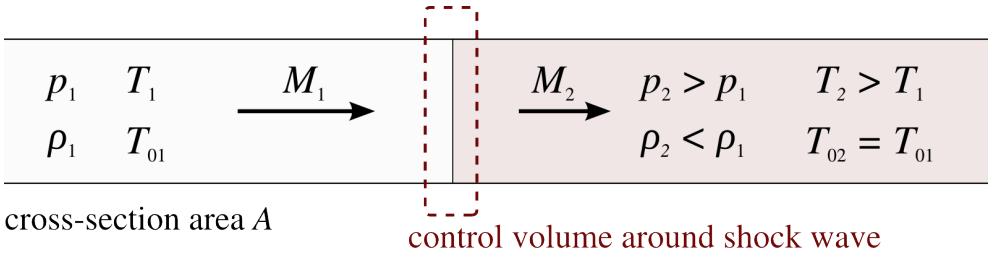

Figure 9.8 – A normal shock wave occurring in a constant-section duct. All properties change except for the total temperature T_0, which, since the transformation is at constant energy, remain constant.

Figure CC-0 o.c.

In a similar fashion, we can obtain:

$$\frac{p_2}{p_1} = \frac{1 + \gamma [\mathrm{Ma}]_1^2}{1 + \gamma [\mathrm{Ma}]_2^2} \tag{9/32}$$

Let us set aside these two equations 9/31 and 9/32 and compare conditions upstream and downstream starting with mass conservation, and re-writing it as a function of the Mach number:

$$\begin{aligned} \rho_1 V_1 &= \rho_2 V_2 \\ \frac{\rho_2}{\rho_1} &= \frac{V_2}{V_1} = \frac{[\mathrm{Ma}]_2 a_2}{[\mathrm{Ma}]_1 a_1} \\ &= \frac{[\mathrm{Ma}]_2 \sqrt{\gamma R T_1}}{[\mathrm{Ma}]_1 \sqrt{\gamma R T_2}} \\ \frac{[\mathrm{Ma}]_1}{[\mathrm{Ma}]_2} &= \frac{p_2}{p_1} \left(\frac{T_1}{T_2} \right)^{\frac{1}{2}} \end{aligned} \tag{9/33}$$

So far, we have not obtained anything spectacular, but now, inserting both equations 9/31 and 9/32 into this last equation 9/33, we obtain the staggering result:

$$\frac{[\mathrm{Ma}]_1}{[\mathrm{Ma}]_2} = \frac{1 + \gamma [\mathrm{Ma}]_1^2}{1 + \gamma [\mathrm{Ma}]_2^2} \left(\frac{1 + \frac{\gamma - 1}{2} [\mathrm{Ma}]_1^2}{1 + \frac{\gamma - 1}{2} [\mathrm{Ma}]_2^2} \right)^{\frac{1}{2}} \tag{9/34}$$

This equation is not interesting because of its mathematical properties, but because of its contents: the ratio $[\mathrm{Ma}]_1/[\mathrm{Ma}]_2$ depends only on $[\mathrm{Ma}]_1$ and $[\mathrm{Ma}]_2$! In other words, if the shock wave is perpendicular, **there is only one possible post-shock Mach number for any given upstream Mach number**.

After some algebra, $[\mathrm{Ma}]_2$ can be expressed as

$$[\mathrm{Ma}]_2^2 = \frac{[\mathrm{Ma}]_1^2 + \frac{2}{\gamma - 1}}{2 [\mathrm{Ma}]_1^2 \frac{\gamma}{\gamma - 1} - 1} \tag{9/35}$$

Values for $[\mathrm{Ma}]_2$ as a function of $[\mathrm{Ma}]_1$ according to equation 9/35 for particular values of γ can be tabulated or represented graphically, allowing us to predict properties of the flow across a shock wave. We can therefore quantify the pressure and temperature increases, and velocity decrease, that occur though a perpendicular shock wave.

9.7 Compressible flow beyond frictionless pipe flow

In this chapter, we have restricted ourselves to one-directional steady flow, i.e. flows inside a pipe; within these flows, we have neglected all losses but those which occur in perpendicular shock waves. This is enough to describe and understand the most important phenomena in compressible flow.

Of course, in reality most compressible flows are much more complex than that. Like other flows, compressible flows have boundary layers, feature laminarity and turbulence, heat transfer, unsteadiness, and more. Shock waves

occur not just perpendicularly to flow direction, but also in oblique patterns, reflecting against walls and interacting with boundary layers. Temperature variations in compressible flow are often high enough to provoke phase changes, which complicates the calculation of thermodynamic properties as well as flow dynamics and may result in spectacular visual patterns.

All those phenomena are beyond the scope of this study, but the reader can hopefully climb up to more advanced topics such as high-speed aerodynamics, or rocket engine and turbomachine design, where they are prominently featured and can surely make for some exciting learning opportunities.

Fluid Mechanics
Exercise sheet 9 – Compressible flow

last edited June 26, 2016

These lecture notes are based on textbooks by White [9], Çengel & al.[12], and Munson & al.[14].

Except otherwise indicated, we assume that fluids are Newtonian, and that:
$\rho_{water} = 1\,000\,\mathrm{kg\,m^{-3}}$; $p_{atm.} = 1\,\mathrm{bar}$; $\rho_{atm.} = 1{,}225\,\mathrm{kg\,m^{-3}}$; $T_{atm.} = 11{,}3\,^{\circ}\mathrm{C}$; $\mu_{atm.} = 1{,}5 \cdot 10^{-5}\,\mathrm{N\,s\,m^{-2}}$;
$g = 9{,}81\,\mathrm{m\,s^{-2}}$. Air is modeled as a perfect gas ($R_{air} = 287\,\mathrm{J\,K^{-1}\,kg^{-1}}$; $\gamma_{air} = 1{,}4$; $c_{p\,air} = 1\,005\,\mathrm{J\,kg^{-1}\,K^{-1}}$).

The speed of sound a in a perfect gas is a local property expressed as:

$$a = \sqrt{\gamma R T} \tag{9/12}$$

In isentropic, one-dimensional flow, we accept that the mass flow $\dot{m}$ is quantified as:

$$\dot{m} = A[\mathrm{Ma}]p_0\sqrt{\frac{\gamma}{RT_0}}\left[1 + \frac{(\gamma-1)[\mathrm{Ma}]^2}{2}\right]^{\frac{-\gamma-1}{2(\gamma-1)}} \tag{9/27}$$

This expression reaches a maximum $\dot{m}_{max}$ when the flow is choked:

$$\dot{m}_{max} = \left[\frac{2}{\gamma+1}\right]^{\frac{\gamma+1}{2(\gamma-1)}} A^* p_0\sqrt{\frac{\gamma}{RT_0}} \tag{9/28}$$

The properties of air flowing through a converging-diverging nozzle are described in fig. 9.9, and fig. 9.10 describes air property changes through a perpendicular shock wave.

TABLE A–13

One-dimensional isentropic compressible flow functions for an ideal gas with $k = 1.4$

Ma	Ma*	A/A^*	P/P_0	ρ/ρ_0	T/T_0
0	0	∞	1.0000	1.0000	1.0000
0.1	0.1094	5.8218	0.9930	0.9950	0.9980
0.2	0.2182	2.9635	0.9725	0.9803	0.9921
0.3	0.3257	2.0351	0.9395	0.9564	0.9823
0.4	0.4313	1.5901	0.8956	0.9243	0.9690
0.5	0.5345	1.3398	0.8430	0.8852	0.9524
0.6	0.6348	1.1882	0.7840	0.8405	0.9328
0.7	0.7318	1.0944	0.7209	0.7916	0.9107
0.8	0.8251	1.0382	0.6560	0.7400	0.8865
0.9	0.9146	1.0089	0.5913	0.6870	0.8606
1.0	1.0000	1.0000	0.5283	0.6339	0.8333
1.2	1.1583	1.0304	0.4124	0.5311	0.7764
1.4	1.2999	1.1149	0.3142	0.4374	0.7184
1.6	1.4254	1.2502	0.2353	0.3557	0.6614
1.8	1.5360	1.4390	0.1740	0.2868	0.6068
2.0	1.6330	1.6875	0.1278	0.2300	0.5556
2.2	1.7179	2.0050	0.0935	0.1841	0.5081
2.4	1.7922	2.4031	0.0684	0.1472	0.4647
2.6	1.8571	2.8960	0.0501	0.1179	0.4252
2.8	1.9140	3.5001	0.0368	0.0946	0.3894
3.0	1.9640	4.2346	0.0272	0.0760	0.3571
5.0	2.2361	25.000	0.0019	0.0113	0.1667
∝	2.2495	∝	0	0	0

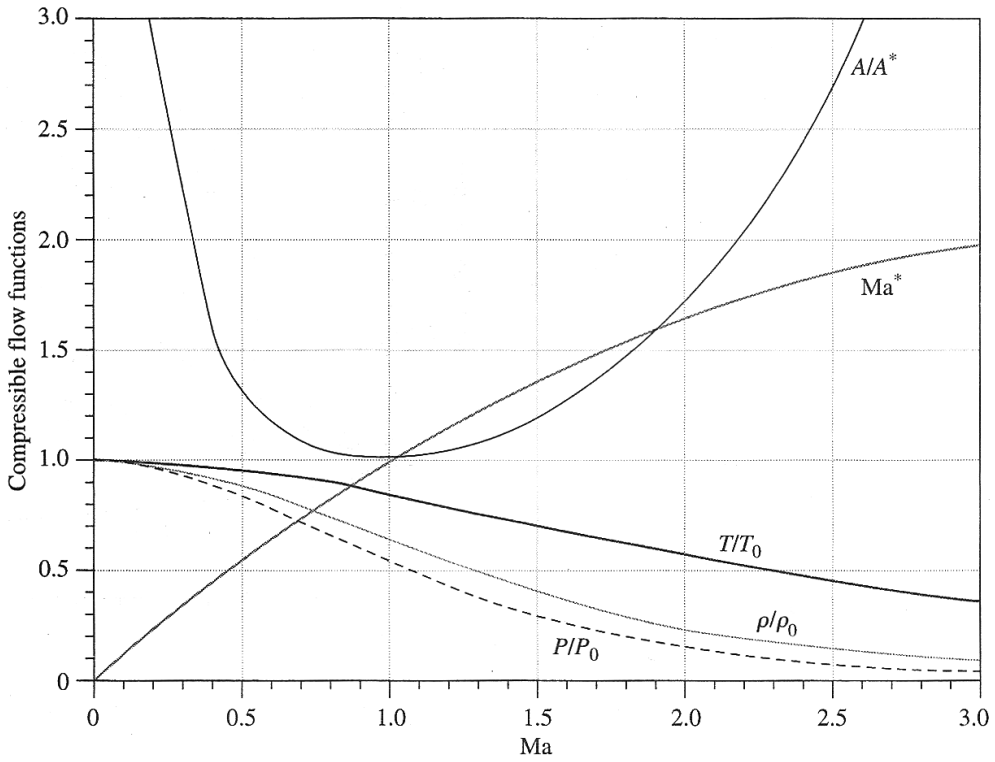

Figure 9.9 – Properties of air (modeled as a perfect gas) as it expands through a converging-diverging nozzle.
These are numerical values for equations (9/17) to (9/19). In this figure, the perfect gas parameter γ is noted k. Data also includes the parameter $[\text{Ma}]^* \equiv V/a^*$ (speed non-dimensionalized relative to the speed of sound at the throat).

TABLE A–14

One-dimensional normal shock functions for an ideal gas with $k = 1.4$

Ma_1	Ma_2	P_2/P_1	ρ_2/ρ_1	T_2/T_1	P_{02}/P_{01}	P_{02}/P_1
1.0	1.0000	1.0000	1.0000	1.0000	1.0000	1.8929
1.1	0.9118	1.2450	1.1691	1.0649	0.9989	2.1328
1.2	0.8422	1.5133	1.3416	1.1280	0.9928	2.4075
1.3	0.7860	1.8050	1.5157	1.1909	0.9794	2.7136
1.4	0.7397	2.1200	1.6897	1.2547	0.9582	3.0492
1.5	0.7011	2.4583	1.8621	1.3202	0.9298	3.4133
1.6	0.6684	2.8200	2.0317	1.3880	0.8952	3.8050
1.7	0.6405	3.2050	2.1977	1.4583	0.8557	4.2238
1.8	0.6165	3.6133	2.3592	1.5316	0.8127	4.6695
1.9	0.5956	4.0450	2.5157	1.6079	0.7674	5.1418
2.0	0.5774	4.5000	2.6667	1.6875	0.7209	5.6404
2.1	0.5613	4.9783	2.8119	1.7705	0.6742	6.1654
2.2	0.5471	5.4800	2.9512	1.8569	0.6281	6.7165
2.3	0.5344	6.0050	3.0845	1.9468	0.5833	7.2937
2.4	0.5231	6.5533	3.2119	2.0403	0.5401	7.8969
2.5	0.5130	7.1250	3.3333	2.1375	0.4990	8.5261
2.6	0.5039	7.7200	3.4490	2.2383	0.4601	9.1813
2.7	0.4956	8.3383	3.5590	2.3429	0.4236	9.8624
2.8	0.4882	8.9800	3.6636	2.4512	0.3895	10.5694
2.9	0.4814	9.6450	3.7629	2.5632	0.3577	11.3022
3.0	0.4752	10.3333	3.8571	2.6790	0.3283	12.0610
4.0	0.4350	18.5000	4.5714	4.0469	0.1388	21.0681
5.0	0.4152	29.000	5.0000	5.8000	0.0617	32.6335
∞	0.3780	∞	6.0000	∞	0	∞

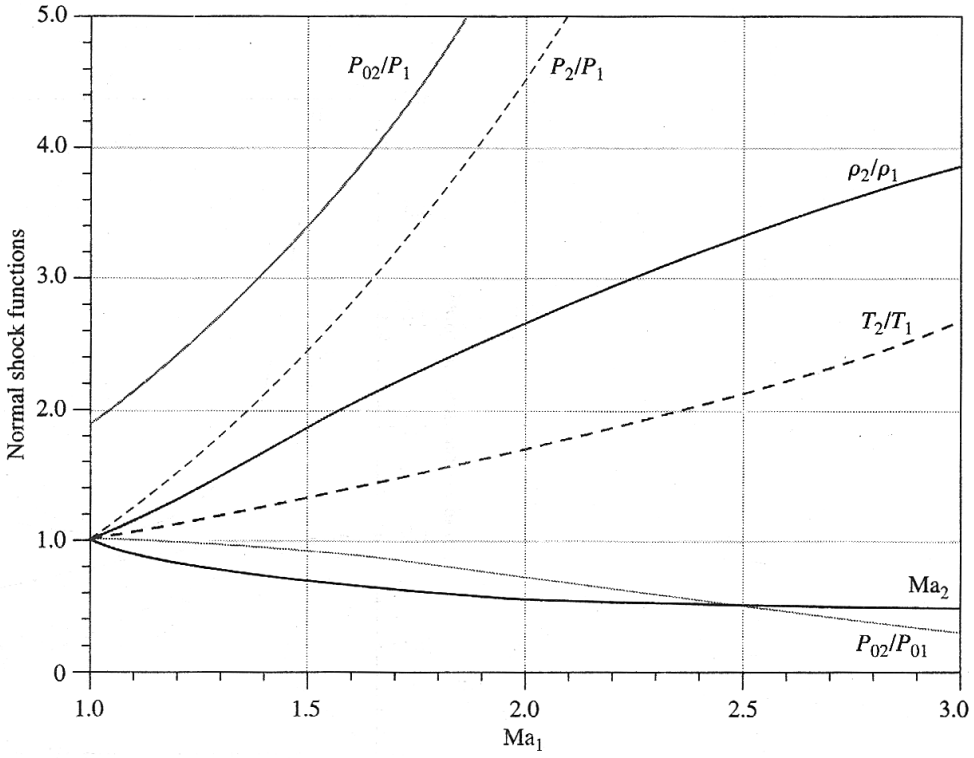

Figure 9.10 – Properties of air (modeled as a perfect gas) as it passes through a perpendicular shock wave.
These are numerical values calculated based on equation 9/35. In this figure the perfect gas parameter γ is noted k.

Figure © Çengel & Cimbala 2010 [12]

9.1 Flow in a converging nozzle

Çengel & al. [12] E12-5

Air from a 4 mm hole in a car tire leaks into the atmosphere. The pressure and temperature in the tire are 314 kPa and 25 °C. The exterior air conditions are 94 kPa and 16 °C.

If the flow can be approximated as isentropic, what is the air flow rate?

9.2 Flow in a converging-diverging nozzle

Exam WS2015-16, see also White [9] E9.4

An experiment is conducted where compressed air from a large reservoir is expanded and accelerated through a nozzle (figure 9.11). There is no external work transfer to or from the air, and the expansion can satisfactorily be modeled as a one-dimensional isentropic process (isentropic meaning that the process is fully reversible, i.e. without losses to friction, and adiabatic, i.e. without heat transfer).

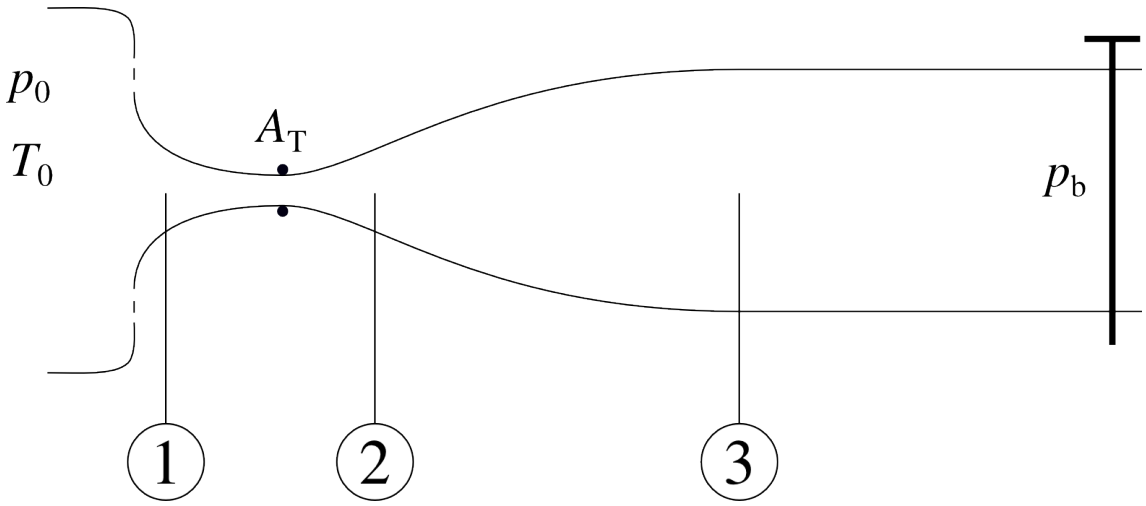

Figure 9.11 – A nozzle in which compressed air in a reservoir (left) is expanded as it accelerates towards the right. The back pressure p_b is controlled by a valve (represented on the right). The flow conditions of interest in this exercise are labeled 1, 2 and 3.

The air ($c_{p\text{air}} = 1\,005\,\mathrm{J\,kg^{-1}\,K^{-1}}$) flows through a converging-diverging nozzle. The entrance conditions into the nozzle are $A_1 = 0{,}15\,\mathrm{m^2}$, $p_1 = 620\,\mathrm{kPa}$, $V_1 = 180\,\mathrm{m\,s^{-1}}$, and $T_1 = 430\,\mathrm{K}$.

In the expanding section of the nozzle, we wish to know the conditions at a point 2 of cross-sectional area $A_2 = A_1 = 0{,}15\,\mathrm{m^2}$.

1. What is the mass flow through the nozzle?
2. If we wish the flow to become sonic (i.e. reach [Ma] = 1), what is approximately the required throat area A_T?
3. Which two flow regimes can be generated at section 2? What is approximately the pressure p_2 required for each?

The nozzle is now operated so that the flow becomes sonic at the throat, and accelerates to supersonic speeds in the expanding section of the nozzle.

The nozzle cross-sectional area increases further downstream of point 2, up until it reaches an area $A_3 = 0{,}33\,\mathrm{m^2}$. Downstream of point 3, the duct is of constant area and the back pressure p_b is set to $p_b = p_3 = p_2$.

4. Describe qualitatively (i.e. without numerical data) the pressure distribution throughout the nozzle.

Finally, we wish to expand the air with a fully-isentropic process, expanding the air from the reservoir to point 3 without a shock wave.

5. Propose and quantify one modification to the experimental set-up that would allow an isentropic, supersonic expansion of the flow into the outlet of area A_3.

9.3 Capsule re-entry

A *Soyuz* capsule incoming from the international space station is passing through Mach 3,5 at a pressure of 0,2 bar and temperature of −50 °C. A bow shock wave is generated in front of the bottom surface of the capsule, which is approximately normal to the flow for the particles directly in the path of the capsule.

What are the conditions (temperature, velocity, density and pressure) in between the shock wave and the capsule shield?

9.4 Explosion shock wave

In an unfortunate coincidence, on the morning following the fluid dynamics exam, the red Tesla S of the lecturer explodes on a parking lot (fortunately, no one was hurt). The explosion creates an spherical shock wave propagating radially into still air.

At a given moment, the pressure inside the spherical bubble is 1 380 kPa. The ambient atmospheric conditions are 17 °C.

At what speed does the shock wave propagate, and what is the air speed immediately behind the wave?

9.5 Home-made supersonic tunnel

A PhD student is thinking about constructing his/her own supersonic wind tunnel. To this purpose, s/he designs a converging-diverging tube with variable square cross-section. The throat T is 0,1 × 0,1 m; the tunnel expands progressively to an outlet nozzle of 0,13 × 0,13 m cross-section. The outlet exits directly in the ambient atmosphere. On the inlet side of the tunnel, the student hopes to install a very large concrete reservoir (fig. 9.12).

1. What is the maximum reservoir pressure for which the flow in the tunnel is subsonic everywhere?
2. What reservoir pressure would be required to generate a shock-less expansion to supersonic flow in the tunnel?
3. If the outlet temperature was to be ambient (11,3 °C), what would the outlet velocity be?
4. Which mass flow rate would then be passing in the tunnel?
5. Describe qualitatively (i.e. without numerical data) the pressure distribution throughout the nozzle for both flow cases above.

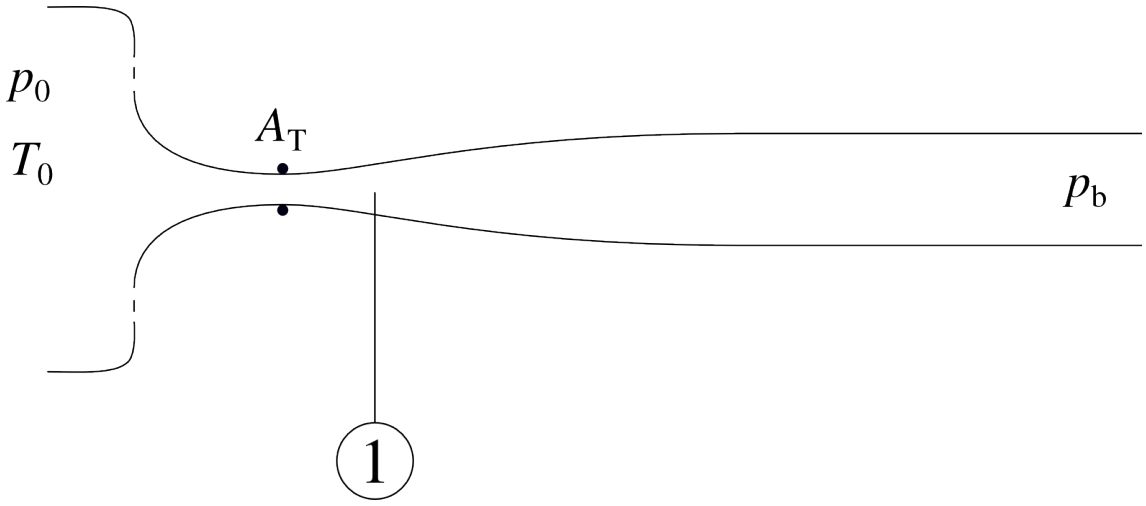

Figure 9.12 – A nozzle in which compressed air in a reservoir (left) is expanded as it accelerates towards the right. The back (outlet) pressure p_b is always atmospheric.

In order to impress his/her friends, the PhD student wishes to generate a perpendicular shock wave inside the tunnel at exactly one desired position (labeled 1 in fig. 9.12 above). At this position, the cross-section area is 0,01439 m^2.

6. Describe qualitatively (i.e. without numerical data) the pressure distribution throughout the nozzle for this case, along the two other pressure distributions.

7. *[difficult question]* What reservoir pressure would be required to generate the shock wave at exactly the desired position?

8. What would the outlet velocity approximately be?

Answers

9.1 Since $p_2/p_0 < 0{,}5283$, the flow is choked. Since there is no nozzle expansion, the flow cannot accelerate beyond [Ma] = 1 and it will exit the hole with excess pressure. With equation 9/28 we obtain $\dot{m} = 9{,}232\,\mathrm{kg\,s^{-1}}$ ($0{,}55\,\mathrm{kg\,min^{-1}}$).

9.2 1) $\dot{m} = \dot{m}_1 = \rho_1 V_1 A_1 = 135{,}6\,\mathrm{kg\,s^{-1}}$;
2) To position point 1 in fig. 9.9 we can either calculate $[\mathrm{Ma}]_1 = V_1/a_1 = 0{,}433$ or $T_1/T_0 = T_1/\left(T_1 + \frac{1}{2}\frac{1}{c_p}V_1^2\right) = 0{,}9639$. Either way we read $A_1/A^* \approx 1{,}5901$, which gets us the throat area required for sonic flow: $A^* = 9{,}433 \cdot 10^{-2}\,\mathrm{m^2}$;
3) We know the flow is isentropic, so at 2 we can have either $p_2 = p_1$ (flow subsonic everywhere), or $p_2 \approx 1{,}0446 \cdot 10^5\,\mathrm{Pa}$ (flow becomes supersonic, p_2 obtained from fig. 9.9 after inputing A_2/A^*);
4) This would be the third case in fig. 9.7 p. 191;
5) The easiest answer is to propose lowering p_3 to $0{,}0368p_0$. But we could also decrease A_T so that $A^* = A_3/3{,}5$ or increase p_0 to $1/0{,}0368p_3$.

9.3 All of the answers are listed in fig. 9.10. In 1-D flow, there is only one possible downstream solution. Interpolating between $[\mathrm{Ma}]_1 = 3$ and $[\mathrm{Ma}]_1 = 4$, we get $[\mathrm{Ma}]_2 = 0{,}4551$, $p_2 = 2{,}883\,\mathrm{bar}$ (!!), $\rho_2 = 1{,}316\,\mathrm{kg\,m^{-3}}$, $T_2 = 750{,}4\,\mathrm{K}$ (477 °C!) and V_2 a mere $249{,}9\,\mathrm{m\,s^{-1}}$ ($900\,\mathrm{km\,h^{-1}}$), down from $V_1 = 1\,048\,\mathrm{m\,s^{-1}}$. Re-entering from space flight is tough!

9.5 1) Flow subsonic everywhere: $p_0 = 1{,}103\,\mathrm{bar}$;
2) Flow supersonic in diverging section: $p_0 = 7{,}8247\,\mathrm{bar}$;
3) We would have $[\mathrm{Ma}]_\mathrm{b} = 2$ and $V_\mathrm{b} = 676{,}1\,\mathrm{m\,s^{-1}}$;
4) $\dot{m} = 13{,}98\,\mathrm{kg\,s^{-1}}$;
7) Before shock, $[\mathrm{Ma}]_1 = 1{,}8$; after it, $[\mathrm{Ma}]_2 = 0{,}6165$. Now, expand the post-shock flow subsonically to outlet condition to find $p_\mathrm{b}/p_{02} \approx 0{,}843$. From p_{02}, go back upstream through the shock: $p_{01} = p_\mathrm{tank} = 1{,}4596\,\mathrm{bar}$;
8) From T_0, find T_1 (isentropic expansion), then T_2 (through shock), then T_b (subsonic isentropic expansion): $T_\mathrm{b} \approx 487{,}4\,\mathrm{K}$. Now, $V_\mathrm{b} = [\mathrm{Ma}]_\mathrm{b}\sqrt{\gamma R T_\mathrm{b}} \approx 221{,}3\,\mathrm{m\,s^{-1}}$.

Appendix

A1 Notation

≡ By definition. The ≡ symbol sets the definition of the term on its left (which does not depend on previous equations).

· (dot above symbol) Time rate: $\dot{} \equiv \frac{\mathrm{d}}{\mathrm{d}t}$. For example, $\dot{Q}$ is the rate of heat (in watts) representing a heat quantity Q (in joules) every second.

- (bar above symbol) Time-average: $\overline{A} \equiv \mathrm{avg}(A) = \mathrm{avg}(\overline{A}+A')$. The prime symbol indicates the instantaneous fluctuation around the average.

Δ Indicates a net difference between two values: $(\Delta X)_{\mathrm{A}\to\mathrm{B}} \equiv X_\mathrm{B} - X_\mathrm{A}$. Can be negative.

italics Physical properties (e.g. mass m, temperature T).

straight subscripts Points in space or in time (temperature T_A at point A). Subscripts "cst" indicate a constant property, "in" indicates "incoming" and "out" is "outgoing".
Subscribt "av." indicates "average".

lowercase symbols Specific values: property per unit mass. For example, $b \equiv B/m$.

operators Differential d, partial differential ∂, finite differential δ, total (alt.: subtantial) derivative $\mathrm{D}/\mathrm{D}t$ (def. eq. 4/7 p.78), exponential $\exp x \equiv e^x$, natural logarithm $\ln x \equiv \log_e x$.

vectors Vectors are always written with an arrow. Velocity is $\vec{V} \equiv (u, v, w)$, alternatively written $u_i \equiv (u, v, w)$. The norm of a vector $\vec{A}$ (positive or negative) is $|\vec{A}|$, its length (always positive) is $||\vec{A}||$.

vector calculus Dot product $\vec{A} \cdot \vec{B}$; cross product $\vec{A} \wedge \vec{B}$; gradient $\vec{\nabla} A$ (def. eq. 1/8 p. 26); divergent $\vec{\nabla} \cdot \vec{A}$ (def. eq. 2/10 p.42); Laplacian $\vec{\nabla}^2 \vec{A}$ (def. eq. 4/30 p.84); curl $\vec{\nabla} \times \vec{A}$ (def. eq. 8/10 p.161).

units Units are typed in roman (normal) font and colored gray (1 kg). In sentences units are fully-spelled and conjugated (one hundred watts). The liter is noted L to increase readablility ($1\,\mathrm{L} \equiv 10^{-3}\,\mathrm{m}^3$). Units in equations are those from *système international* (SI) unless otherwise indicated.

numbers The decimal separator is a comma, the decimal exponent is preceded by a dot, integers are written in groups of three ($1{,}234 \cdot 10^3 = 1\,234$). Numbers are rounded up as late as possible and never in series. Leading and trailing zeroes are never indicated.

A2 List of references

These lecture notes are based on textbooks by White [9], Çengel & al.[12], and Munson & al.[14].

[1] Ira Herbert Abbott and Albert Edward Von Doenhoff. *Theory of wing sections, including a summary of airfoil data*. Courier, 1959.

[2] Hendrik Tennekes and John Leask Lumley. *A first course in turbulence*. MIT press, 1972. ISBN: 978-0262200196.

[3] Bernard Stanford Massey. *Mechanics of fluids*. 5th ed. Van Nostrand Reinhold, 1983. ISBN: 0442305524.

[4] Phillip M. Gerhart and Richard J. Gross. *Fundamentals of Fluid Dynamics*. 1st ed. Addison-Wesley, 1985. ISBN: 0201114100.

[5] Hendrik Tennekes. *The Simple Science of Flight. From Insects to Jumbo Jets*. 1st ed. MIT Press, 1992. ISBN: 0262201054.

[6] John David Anderson. *Computational Fluid Dynamics*. McGraw-Hill, 1995. ISBN: 0071132104.

[7] Jewel B. Barlow, William H. Jr. Rae, and Alan Pope. *Low-speed Wind Tunnel Testing*. 3rd ed. Wiley & Sons, 1999. ISBN: 0471557749.

[8] Henk Kaarle Versteeg and Weeratunge Malalasekera. *An introduction to computational fluid dynamics: the finite volume method*. 2nd ed. Pearson Education, 2007. ISBN: 9780131274983.

[9] Frank M. White. *Fluid Mechanics*. 7th ed. McGraw-Hill, 2008. ISBN: 9780071311212.

[10] Hendrik Tennekes. *The Simple Science of Flight. From Insects to Jumbo Jets*. 2nd ed. MIT Press, 2009. ISBN: 9780262513135.

[11] J.J Bertin and R.M. Cummings. *Aerodynamics for Engineers*. 5th ed. Pearson/Prentice Hall, 2010. ISBN: 978-0132272681.

[12] Yunus A. Çengel and John M. Cimbala. *Fluid Mechanics. Fundamentals and Applications*. 2nd ed. McGraw-Hill, 2010. ISBN: 9780070700345.

[13] Franck Richecœur. *Aérodynamique. Équations générales, écoulements laminaires et turbulents autour d'un profil, couche limite*. French. Technosup. Ellipses, 2012. ISBN: 9782729877958.

[14] Bruce R. Munson, Theodore H. Okiishi, Wade W. Huebsch, and Alric P. Rothmayer. *Fluid Mechanics*. 7th ed. Wiley, 2013. ISBN: 9781118318676.